University of Strathclyde

QOQMS
Department of Physics

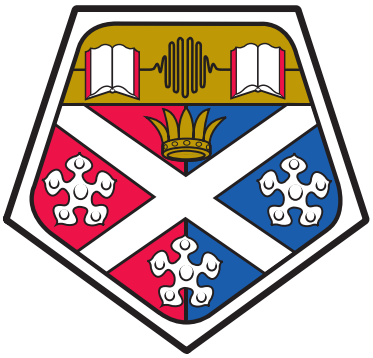

Quantum Correlations and Exchange Symmetry

Doctoral Thesis

Author:
Enrico Sindici

Supervisor:
Prof. Andrew Daley

PhD
2019

Declaration of Authorship

This thesis is the result of the author's original research. It has been composed by the author and has not been previously submitted for examination which has led to the award of a degree.

Signed:

_____

Date:

_____

Abstract

Many of the advantages that the flourishing fields of quantum technologies and quantum information theory achieve over their classical counterparts rely on quantum correlations. Such correlations represent a valuable resource and their characterization and quantification is a key theoretical task.

We study the quantum correlations for systems which are symmetric under the exchange of any two particles for two main reasons. Firstly, exchange symmetry constrains the set of possible states for the system and reduces the degrees of freedom required to describe them, simplifying the characterization of quantum correlations. Furthermore, systems that exhibit exchange symmetry have notable physical properties that make them well-suited for quantum information tasks and quantum simulation.

In this thesis we investigate how exchange symmetry affects the mathematical description, as well as the physical realization and measurement, of quantum correlations. To begin with, we address the open problem of quantifying identical-particle entanglement. We introduce a novel entanglement measure accounting for the wavefunction (anti)symmetrization in the first quantised picture of systems of fermions and bosons. This measure, which may be evaluated by means of semidefinite programming, is sensitive to quantum correlations originating from interactions and other entanglement generating dynamical processes, rather than the kinematic effect of (anti)symmetrization. We apply our novel measure to estimate entanglement based on measurements of a system of two ultracold fermionic atoms in an optical trap.

Exchange symmetry is not only a property of identical-particle states, but can pertain also to distinguishable subsystems. Based on the properties of subspaces of states which are symmetric or antisymmetric under particle exchange, we introduce a novel class of exchange-symmetric *bound entangled* states. We provide a simple parametrization that makes it possible to obtain states which are bound entangled in terms of a convex combination of well-studied exchange-symmetric states.

Finally, we study the quantum correlations of a family of states with exchange symmetry in the multipartite device-independent scenario. We evaluate the noise robustness of the task of entanglement certification for varying numbers of uncharacterised measurement devices for the states of the family. The resulting structure enables us to establish a hierarchy of quantum correlations in the tripartite case.

Acknowledgements

Four years are a sizeable chunk of one's life and any accomplishment achieved over such a long period is the result of countless factors and the help of more people than one could mention in a single page. In the case of this thesis, I am especially grateful for the guidance, patience and friendship of Marco Piani and Andrew Daley, whom I thank for having been excellent teachers and wonderful persons.

I would have not been able to even embark on the journey my PhD has been if it wasn't for the constant support and love of my family, which has always reached me through a whole continent.

I thank Amanda, for always bringing me sunshine even in the (many) rainy days. I thank all my office friends, who have made my time in the department an absolute pleasure, and my out-of-office ones, who haven't let me have any dull days. I thank all of the physicists I have talked to in our department or at conferences for the precious insight and feedback. A special mention in this sense goes to our collaborators at the Ultracold Quantum Gases group in Heidelberg University.

With sincere apologies to any non-inanimate individual that was not represented in the previous acknowledgements, I also owe a thank you to my car Gianni, my bike Gertrude and my uni laptop for their legendary resilience and for never letting me down.

Finally, I am thankful to the city of Glasgow for having become my second home.

Introduction

In recent years the technologies inspired by the physics of quantum information have begun to be transferred from the laboratory to high-tech industry. With an escalation in public interest and investment in the many ground-breaking quantum-based technologies (QT) [1, 2], it is looking increasingly likely that some instances of QT will make their way into our everyday lives in the near future. Indeed, at present anyone using a GPS system is benefiting from an example of QT, atomic clocks, which play an important role in the global positioning technology. Quantum cryptographic schemes are already commercially available [3] and numerous other technologies are being developed. Quantum-enhanced metrology is being applied to commercial magnetometers [4–6], gravimeters [7] and, more recently, accelerometers [8]. Quantum imaging [9] is sparking interest in applications ranging from hazardous gas detection [10] to microscopic biological imaging [11]. Private companies have developed quantum annealers [12–14], a scale up of which will enable the simulation of systems that are classically intractable [15]. Finally, although still at an early stage, the technological implications of realising scalable quantum computers are revolutionary [16, 17].

With the approach of the quantum information technology era it is of ever-increasing interest and importance to have a deep understanding of the fundamental physical principles underlying such potentially world-changing technologies. This has motivated extensive joint theoretical and experimental efforts in detecting and controlling quantum resources. The most notable of such resources is the type of quantum correlation called *entanglement*. Entanglement can be understood as the lack of a description in terms of factorised, or uncorrelated, single-subsystem states. While entanglement theory is a well-developed field of quantum information theory, there remain a number of open questions, one of which is given by the characterisation and quantification of entanglement of identical-particle systems.

One of the defining features of quantum systems is the quantization of observable quantities, or in other words, the existence of minimum discrete units (*quanta*, or *quantum numbers*) for physical properties in a given system. In quantum mechanics, when particles have the same quantum numbers, they are not only operationally, but also intrinsically indistinguishable. Quantum mechanical *spin*, or intrinsic angular momentum,

is one such physical property possessed by all physical systems, which may be classified according to their spin quantum number. In particular, in particle physics, objects with integer values of spin are called *bosonic*, whereas those with half-integer spin are called *fermionic* and such distinction reflects in their wavefunction representation. The wavefunctions describing systems of multiple bosons are necessarily symmetric under the exchange of any two particles, whereas fermionic systems are antisymmetric under particle exchange [18].

The particle-exchange symmetry intrinsic to such physical systems constrains the set of allowed physical states and affects the entanglement properties therein [19]. The main difficulties are connected with the wave-function (anti)symmetrization of systems of identical (fermions)bosons, bringing about correlations in play which have kinematic rather than dynamical origin. Entanglement, which is often inferred by analysing correlation functions, is however typically generated by dynamical processes, such as interactions. It is therefore of great interest to unravel the structure of correlations in identical-particle systems.

Entanglement of identical particles Several approaches to identical-particle entanglement characterization [20–29] and quantification [30,31] have been put forward in the last two decades, but a general consensus on the topic has still not been reached. In this thesis I address the issue in terms of a mathematical tool which has been applied extensively to quantum information theory in recent years, semidefinite programming [32]. Semidefinite programs are special cases of convex optimization instances suitable for imposing constraints over density matrices and quantum operations [33], which have been applied for multipartite entanglement detection [34], device-independent entanglement certification [35], quantum complexity theory [36] and nonlocal games [37].

Based on well-established identical-particle entanglement criteria [21], in Chapter 2 we introduce an entanglement measure for systems with exchange symmetry expressed as a semidefinite program. Our novel measure takes into account the symmetry of identical-particle states and quantifies the correlations present in a composite system which are not due to the exchange symmetry, but only to entanglement-generating processes, such as interactions or global operations acting on multiple subsystems. Furthermore, in Chapter 3 we prove the usefulness of our measure for entanglement estimation based on measurements of correlation functions in systems of interacting identical fermions. Even when the state of the system may not be fully recovered by measurements, the information extracted from the correlation functions may be imposed as a constraint in the optimization algorithm in terms of which our measure is evaluated.

We therefore obtain lower bounds on the entanglement due to interactions that are consistent with the incomplete information about the system.

Bound entanglement and exchange symmetry Exchange symmetry is not a property pertaining only to identical-particle systems. Permutation invariance is a property of several physical systems and fundamental forces [38] and has been studied to exploit the rich structure it enforces. Permutation-symmetric systems are of aid in the study of condensed matter theory [39], quantum error correction [40], decoherence-free (noiseless) subspaces [41] and entanglement theory [42]. The mathematical properties of permutation-symmetric subspaces may therefore bring about new insight into physical systems. Specifically, the symmetry constrains the number of independent degrees of freedom in complex systems, allowing a simpler mathematical description and a better unraveling and control of their properties. One such property is *bound entanglement*, an attribute of statistical mixtures of entangled states which may not be used, even by taking many copies of them, to generate a maximally-entangled state by means of local operations and classical communication [43]. Bound-entangled states are of great theoretical and experimental interest, but they are difficult to characterize and have proven challenging to realize in laboratories [34, 44, 45]. By looking into the properties of the exchange-symmetric and antisymmetric subspaces, in Chapter 4 we identify a novel class of states with a simple parametrization and amenable to experimental realization. We derive both analytical results and numerical recipes, based on semidefinite programming, to deterministically and randomly generate bound-entangled states of any bipartite system.

Furthermore, exchange symmetry plays an important role in preserving entanglement from degradation due to interaction with a noisy environment [41]. In particular, distinguishable-particle states which are antisymmetric under particle exchange are necessarily entangled and have proven to be a most valuable resource in terms of resistance to decoherence [46]. Despite the fact that it may be engineered to obtain advantages [47], noise is the main adversary in the realization of quantum systems. Noise reduction and error-correction in quantum information tasks are well-developed research areas, however noise may never be entirely removed from a real physical system. Robustness to noise is therefore a valuable property of entangled states, particularly for schemes relying on entanglement certification.

Device-independent entanglement certification A general and interdisciplinary problem in quantum information processing is the certification of entanglement shared between a number of parties under different assumptions. In quantum communication

protocols, such as quantum key distribution (QKD), quantum cryptography and state sharing it is a key requirement to benchmark the performance of the protocol when a number of measurement devices, or the parties manipulating them, are untrusted. More specifically, the need to assess quantum-enabled performance enhancements under such assumptions has prompted the development of the theory of *device-independent entanglement certification* (DIEC) [48].

The typical scenario for device-independent quantum information processing involves an unknown multipartite quantum state shared between a number of distant parties. When a number of the parties are untrusted, the *trusted* parties may interpret the conditional states resulting from the untrusted parties' measurements by assuming that the latter's measurement devices are uncharacterised. If the trusted parties, possessing a full characterization of their own measurements, are able to certify the presence of entanglement from the available conditional states, the composite system is said to demonstrate steering [35]. Entanglement is a necessary condition for steering, but the converse is not true. Steering may thus be considered a *stronger* type of quantum correlation than entanglement and its study is relevant to the benchmarking of quantum communication protocols in presence of adversary parties [48, 49].

A stronger condition than the steering one may be enforced, regarding all measurements by all parties on the quantum state as uncharacterised. This is the *fully-device-independent* scenario, and if the joint conditional probability distributions arising from the uncharacterised measurements suffice for entanglement certification, the system is said to be *nonlocal* [49]. Nonlocality is therefore defined in terms of a stronger condition than steering, giving rise to the quantum correlation hierarchy illustrated in Figure 1.

In Chapter 5 of this thesis we investigate the quantum correlation structure of the totally antisymmetric tripartite state as a function of external noise. We find the maximum noise threshold within which the entanglement may be certified for all combinations of trusted and untrusted parties. Our work provides benchmarks for the noise robustness of relevance for experimental applications of entanglement certification schemes, as well as providing a characterization of the quantum correlation structure for an interesting class of exchange-symmetric states.

Outline

This thesis reports the characterization and quantification of quantum correlations in physical systems with exchange symmetry. The content is arranged according to the following structure:

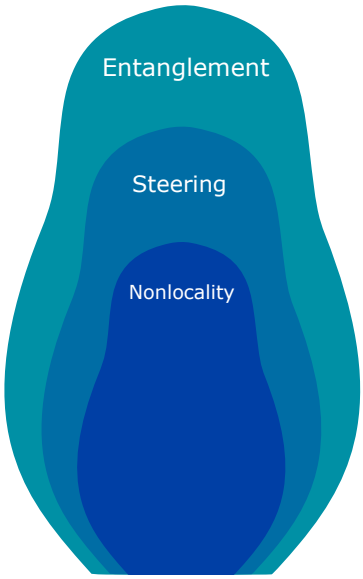

FIGURE 1: Matryoshka (russian doll) hierarchy of quantum correlations.

- In Chapter 1 we introduce the basic elements of quantum theory which will be applied in the rest of this work. We introduce the mathematical formalism of entanglement and the algebraic techniques which allow its quantification.

- In Chapter 2 we define a novel measure for identical-particle entanglement based on semidefinite programming. We begin by introducing the conceptual issues in defining entanglement for identical-particle systems which make the subject a very interesting one. A brief review of the existing approaches to the topic is outlined, with focus on a well-established identical-particle entanglement criteria which will be the basis of our entanglement measure. Finally, we introduce the notions of *symmetric* and *antisymmetric entanglement negativity*, our novel method for entanglement quantification of systems of identical bosons and fermions.

- In Chapter 3 we demonstrate an application of our novel entanglement measure, antisymmetric negativity, to the task of entanglement estimation based on experimental data resulting from measurements of correlation functions in systems of few ultracold identical fermionic atoms in an optical trap. Our measure provides the advantage of detecting the correlation structure in such systems, distinguishing the correlations arising from entanglement-generating processes from those due to the exchange symmetry. Furthermore, when incomplete information about the measured quantum state is available, antisymmetric negativity may be applied for providing a lower bound to the entanglement in the system.

- In Chapter 4 we present a novel class of bound-entangled states based on the properties of the antisymmetric subspace. We propose a method for the deterministic generation of states in said class based on semidefinite programming. In addition to this, the method may be adapted for the randomized generation of bound-entangled states. We further highlight an additional class of states which may be fully characterized analytically and is amenable to an intuitive geometrical representation. The class comprises Werner, Isotropic and bound-entangled states with a simple parametrization [50].

- In Chapter 5 we study the quantum correlation hierarchy for the totally antisymmetric tripartite state in presence of noise. We operate in the device-independent approach to quantum information and assess the noise threshold within which entanglement certification is possible for different combinations of trusted and untrusted parties. Our results benchmark the robustness to noise of multipartite entanglement, steering and nonlocality characterization of a state of great interest to quantum information theory and applications.

Contributions

Publications

- E. Sindici and M. Piani, *Simple class of bound entangled states based on the properties of the antisymmetric subspace*, Phys. Rev. A **97**, 032319, 2018.

  The author of this thesis performed analytical and numerical calculations, contributed to the writing of the article, and produced the related plots.

- E. Sindici and M. Piani, *Quantifying Identical-Particle Entanglement with Semidefinite Programming*, in preparation.

  The author of this thesis performed analytical and numerical calculations, contributed to the writing of the article, and produced the related plots.

- E. Sindici, P. Preiss, J. H. Becher, R. Klemt, A. Bergschneider, M. Piani, A. Daley and S. Jochim, *Recovering the identical-particle entanglement structure from momentum correlation measurements in a double-well system*, in preparation.

  The author of this thesis performed calculations to compare with experimental measurements and wrote the code for extracting estimates for the physical properties of the system.

Presentations

- E. Sindici, R. FLoreanini, S. Olivares and F. Benatti, *Degradation of entanglement in measurements of Planck-scale effects*, 605 Wilhelm und Else Heraeus - Seminar on Macroscopic Entanglement, (Bad Honnef, Germany), 2016.

- E. Sindici and M. Piani, *Quantifying Entanglement of Identical Particles*, Strathclyde Symposium on Quantum Information, Simulation and Metrology, (Glasgow, UK), 2016.

- E. Sindici and M. Piani, *Quantifying Identical-Particle Entanglement*, IQIS, (Rome, Italy), 2016.

- E. Sindici and M. Piani, *Identical-Particle Entanglement and Semidefinite Programming*, Invited talk at Universidad Autonoma de Barcelona, (Barcelona, Spain), 2016.

- E. Sindici and M. Piani, *Quantifying Identical-Particle Entanglement*, YQIS, (Barcelona, Spain), 2016.

- E. Sindici and M. Piani, *Quantifying Identical-Particle Entanglement*, Perth conference on Non-Equilibrium Collective Dynamics, (Perth, UK), 2017.
- E. Sindici and M. Piani, *Quantifying Identical-Particle Entanglement*, Granada Seminar on Quantum Systems In and Out of Equilibrium, (Granada, Spain) 2017.
- E. Sindici and M. Piani, *A simple class of bound entangled states based on the properties of the antisymmetric subspace*, 657. WE-Heraeus-Seminar on Quantum Correlations in Space and Time, (Bad Honnef, Germany) 2017.
- E. Sindici and M. Piani, *Quantifying Identical-Particle Entanglement*, Q2C Workshop Strathclyde, (Glasgow, UK), 2018.
- E. Sindici and M. Piani, *Quantifying Identical-Particle Entanglement*, YAO2018, (Glasgow, UK), 2018.
- E. Sindici and M. Piani, *Quantifying Identical-Particle Entanglement with Semidefinite Programming*, AQIS, (Nagoya, Japan), 2018.

Contents

Chapter 1

Elements of Quantum Theory

In this chapter we revise the background elements of quantum theory that are particularly important in this thesis, in order to establish properly the corresponding notation and definitions. Such revision of known concepts is not only incorporated for the sake of self-consistency, however, since even in the basic notions of quantum theory lie subtleties and assumptions which are often overlooked and may cause confusion and misunderstandings in the assessment of quantum correlations. In what follows we outline the key concepts underpinning our work and introduce the notation we rely on in the remainder of this thesis. For further reading we recommend a selection of quantum mechanics textbooks in references [51–54].

The state of a quantum system $\mathcal{S}$ is described in terms of a vector $|\psi\rangle$ of a Hilbert space $\mathcal{H}$ over the complex numbers. Unless otherwise stated, states will be assumed to be normalised ($|\langle\psi|\psi\rangle| = 1$) and Hilbert spaces to have a finite dimension d, therefore they will be equivalently indicated by $\mathcal{H} \equiv \mathcal{H}_d \equiv \mathcal{H}(d) \simeq \mathbb{C}^d$. The expectation values $\langle\psi|O|\psi\rangle$ of observables of the system are given by the action of hermitian operators $O = O^\dagger$ on the states $O|\psi\rangle$.

A general mixed state, a statistical mixture of pure quantum states, is described by the density operator ρ of the system $\mathcal{S}$. The density operator is a positive, hermitian, unit-trace operator on $\mathcal{H}$, and it can be expressed as a convex combination of projectors onto pure states $|\psi\rangle\langle\psi|$:

$$\rho = \sum_i p_i |\psi_i\rangle\langle\psi_i| , \tag{1.1}$$

where $\{p_i\}_i$ form a normalised probability distribution. The set of density operators on $\mathcal{H}$ will be indicated by $\mathcal{D}(\mathcal{H})$. Generalised measurements on mixed states are described in terms of *Positive Operator-Values Measures* (POVM), given by a set of hermitian positive-semidefinite operators $\{M_i = E_i^\dagger E_i\}_i$, such that $\sum_i M_i = 1$. The post-selected

states conditional to a measurement outcome i are given by

$$\rho_i = \frac{E_i \rho E_i^\dagger}{\mathrm{Tr}(E_i \rho E_i^\dagger)}, \tag{1.2}$$

where Tr is the trace operation and $\mathrm{Tr}(E_i \rho E_i^\dagger) = \mathrm{Tr}(M_i \rho)$ the probability of obtaining the post-selected state ρ_i.

The description of a composite quantum system $\mathcal{S}_{12}$ consisting of the subsystems $\mathcal{S}_1$ with Hilbert space $\mathcal{H}_1(d_1)$ and $\mathcal{S}_2$ with Hilbert space $\mathcal{H}_2(d_2)$ is given in terms of a vector $|\Psi\rangle_{12}$ belonging to the tensor product of the subsystems' spaces $\mathcal{H}_{12}(d_1 d_2) = \mathcal{H}_1(d_1) \otimes \mathcal{H}_2(d_2)$. Notice that in general, given a composite system, the partitioning in subsystems is not unique.

1.1 Quantum Entanglement

The paradigmatic scenario for the study of quantum correlations requires the identification of two (or more) *parties*, which are commonly given the names of *Alice* (A) and *Bob* (B). The two parties have access to a quantum system with which they may interact by means of physical quantum operations, for example *projective measurements*. A composite quantum system can be partitioned in subsystems, the mathematical representation of which may be given in terms of a tensor product structure of single-subsystem Hilbert spaces underlying the composite one. Let us focus on the case where the composite system is partitioned into subsystems with a tensor-product structure in such a way that each party has access to one of the subsystems only, unambiguously. This will allow us to establish a connection between the outcomes of operations performed by the distinct parties to the properties of the subsystem pertaining to each party. We may interpret this scenario formally by calling $\mathcal{S}_{AB} = \mathcal{S}_A + \mathcal{S}_B$ the composite quantum system whose states are vectors in the Hilbert space $\mathcal{H}_{AB} = \mathcal{H}_A \otimes \mathcal{H}_B$. We may appreciate how having required each subsystem to be unambiguously accessible by one party only allows to label the individual Hilbert spaces according to the party acting on them. We will call subsystems with this property *individually addressable* subsystems.

A vector state in the composite tensor product space is called unentangled if it can be written in the factorised form $|\alpha\rangle_A \otimes |\beta\rangle_B$. Any state $|\psi\rangle_{AB} \in \mathcal{H}_{AB}$ that is not unentangled, i.e. it may not be written in factorised form, is entangled. Composite states of the joint system always admit a decomposition in the form

$$|\psi\rangle = \sum_i \sqrt{p_i}\, |a_i\rangle\, |b_i\rangle\,, \tag{1.3}$$

called *Schmidt decomposition* [19], where $\{|a_i\rangle\}_{i=1}^{d_A}$ for A and $\{|b_i\rangle\}_{i=1}^{d_B}$ for B are an appropriate choice of orthonormal bases. The non-negative coefficients of the decomposition $\{p_i\}$ form a probability distribution and are called Schmidt coefficients. The number r of non-zero terms in such a probability distribution, which is equivalent to the number of non-trivial factorized terms entering in the Schmidt decomposition, is called the Schmidt rank of $|\psi\rangle$.

A generalisation of the Schmidt rank may be defined for mixed states. A density operator ρ has Schmidt number m if it can be written as convex combination of pure states $|\psi_i\rangle$, each having at most Schmidt rank m, and if for any convex combination corresponding to ρ there is at least one state $|\psi_i\rangle$ with Schmidt rank greater or equal to m (with non-zero probability) [55].

A mixed state is separable or unentangled if it has Schmidt number one, that is, if it can be expressed as

$$\rho = \sum_i p_i \, |\alpha_i\rangle\langle\alpha_i| \otimes |\beta_i\rangle\langle\beta_i| \, . \tag{1.4}$$

Notice that in such an expression, the states $|\alpha_i\rangle$ ($|\beta_i\rangle$) do not necessarily correspond to an orthonormal basis for A (for B). A mixed state is entangled if it has Schmidt number strictly larger than one, equivalently, if it is not of the form (1.4).

Peres PPT criterion

In general, the determination of separability of a mixed state is a hard task [34, 56]. For this reason a number of alternative strategies have been developed in order to test the entanglement of a state. One such criteria is given by partial transposition [57, 58]. The partial transposition of a separable state $\rho^{\Gamma_A} = (T_A \otimes \mathbb{1}_B)[\rho]$, where T indicates the transposition operation, is still a positive-semidefinite operator. Therefore, if ρ^{Γ_A} is not positive-semidefinite, then ρ must be entangled. The criterion is independent of the subsystem on which the partial transposition is performed, since the positivity of the partially transposed state only depends on its spectrum. It is easy to see that the latter does not depend on the subsystem on which the partial transposition is carried out. This enables us to indicate the partially transposed state simply by ρ^{Γ}, unless further specification is required.

Robustness

Separability may be analytically addressed for certain classes of states. A helpful tool for such purpose is given by the notion of *entanglement robustness*. Consider a bipartite system with local dimensions d_1 and d_2 respectively, a density operator ρ and a separable

state ρ_S acting on the Hilbert space $\mathcal{H} = \mathbb{C}^{d_1} \otimes \mathbb{C}^{d_2}$. We call *robustness* of ρ relative to ρ_S the quantity $R(\rho\|\rho_S)$ given by the minimal $s \geq 0$ such that

$$\rho(s) = \frac{1}{1+s}\left(\rho + s\rho_S\right) \tag{1.5}$$

is a separable state. In particular, the robustness of ρ relative to the maximally mixed state $\mathbb{1}/(d_1 d_2)$ is called *random robustness* of ρ.

The random robustness is known for pure bipartite states [59]. Given a pure state $|\psi\rangle$ on $\mathcal{H} = \mathbb{C}^{d_1} \otimes \mathbb{C}^{d_2}$ in its Schmidt decomposition

$$|\psi\rangle = \sum_{i=1}^{r} \sqrt{\lambda_i}\, |a_i\rangle\, |b_i\rangle\,, \tag{1.6}$$

where $r = \min\{d_1, d_2\}$ and $\lambda_1 > \lambda_2 > ... > \lambda_r$, the random robustness of $|\psi\rangle$ amounts to [59]

$$R(\psi\|\mathbb{1}/(d_1 d_2)) = d_1 d_2 \sqrt{\lambda_1 \lambda_2}. \tag{1.7}$$

The class of states of the form

$$\rho_\psi(s) = \frac{1}{1+s}\left(|\psi\rangle\langle\psi| + s\frac{\mathbb{1}}{d_1 d_2}\right) \tag{1.8}$$

is separable for $s \geq d_1 d_2 \sqrt{\lambda_1 \lambda_2}$.

1.1.1 Entanglement measures

Entanglement has become a major topic of research in light of theoretical developments showing its usefulness for a great number of applications [60, 61] and experimental advances allowing for unprecedented control of quantum systems [62–65]. The identification of entanglement as a resource naturally led to efforts concerning its quantification. A plethora of figures of merit, assigning some positive-valued number to a quantum state and a bipartition, have been put forward to quantify the presence of entanglement or its usefulness for a particular task, composing what is informally called the *zoo of entanglement measures* [66]. Many advances have been established in quantum information theory in laying out the properties of a well-defined entanglement measure and in proving connections and relationships between the known measures [66]. The quantification of entanglement is based on the concept of *local operations and classical communication* (LOCC), defined as the set of operations that local parties may perform restricted to either one of the individual subsystems associated with the ability to communicate, via a classical channel, information about the outcome of each party's

operation in order to coordinate the manipulation of the quantum system. The correlations that may be generated in a system by use of LOCC are called classical correlations. Correlations that may not be described as arising from LOCC operations are labelled *quantum correlations* [66].

Quantum operations are described in terms of *generalised measurements*, which describe manipulations beyond the wavefunction collapse following projective measurements and allow for cases where joint measurements are performed on the composite system+environment state and some of the environment's subsystems may be discarded. If the system and environment are initially uncorrelated then the evolution of the system may be described in terms of trace non-increasing, completely positive linear maps Φ mapping density operators to density operators with the property $\mathrm{Tr}(\Phi(\rho)) \leq 1$. The action of such maps, also called *quantum channels*, is given in terms of a set of operators $\{K_i\}_i$, called Kraus operators, such that

$$\Phi(\rho) = \sum_i K_i \rho K_i^\dagger, \tag{1.9}$$

with the property $\sum_i K_i^\dagger K_i \leq \mathbb{1}$ [19]. An important set of operations is given by the *separable operations*, where the Kraus operators admit a product decomposition $K_i = A_i \otimes B_i$, $\forall i$. Any LOCC operation can be written as a separable operation, but the converse is not always true [67].

Different axiomatic approaches exist for defining entanglement measures, but key requirements are that they map density matrices to real positive numbers, return 0 for separable states and do not increase under LOCC. Additional constraints, such as convexity and additivity [66] are often additionally imposed for mathematical convenience. An entanglement measure E is called convex if, for every convex combination $\sum_i p_i \rho_i$, the following relationship holds:

$$E(\sum_i p_i \rho_i) \leq \sum_i p_i E(\rho_i). \tag{1.10}$$

If an entanglement measure E satisfies the property $E(\sigma^{\otimes n}) = nE(\sigma)$, for any density matrix σ, then it is called *additive*.

The most notable pure-state entanglement measure is the *entropy of entanglement* $E_e(|\psi\rangle)$ [68], defined as the von Neumann entropy [69] of the partially transposed density matrix $\rho_1 = \mathrm{Tr}_1(|\psi\rangle\langle\psi|) = \sum_i \langle i|(|\psi\rangle\langle\psi|)|i\rangle$, where $\{|i\rangle\}$ is an *ortho-normal basis* ONB of subsystem 1:

$$E_e(|\psi\rangle) = -\mathrm{Tr}(\rho_1 \log \rho_1). \tag{1.11}$$

The relevance to many quantum information theory tasks of the many properties of entropy of entanglement, such as its connection with classical Shannon entropy [70], is such that it is often required for mixed state entanglement measures to boil down to E_e when applied to pure states.

The entropy of entanglement is not effective at quantifying entanglement of mixed states and a number of mixed-state entanglement measures have been studied [66]. Among these, *entanglement negativity* (or simply *negativity*) stands out for its intuitive definition and relative ease of evaluation. The entanglement negativity of a bipartite density matrix ρ is given by the expression

$$\mathcal{N}(\rho) = \frac{\|\rho^\Gamma\|_1 - 1}{2}, \tag{1.12}$$

where $\|x\|_1 = \mathrm{Tr}\sqrt{xx^\dagger}$ indicates the *1-norm*, or *trace norm*. It is equivalent to the absolute sum of the negative eigenvalues of the partial transposition of ρ. We will discuss how negativity may be evaluated in section 1.2 and recall a generalisation of the notion to the multipartite case in the following section.

1.1.2 Multipartite entanglement

The multipartite case, described by the Hilbert space $\mathcal{H} = \bigotimes_{i=1}^{N} \mathcal{H}_i$, presents a richer entanglement structure than the bipartite case. For pure states, the most straightforward extension of separability is called *full-separability* and is a property of products of N single-particle states

$$|\psi_{\mathrm{FS}}\rangle = \bigotimes_{i=1}^{N} |\phi_i\rangle \,. \tag{1.13}$$

Furthermore, pure N-partite states may be *k-separable* [71], and we call their set $\Sigma_{k-\mathrm{sep}}$ when they can be written as the tensor product of $k \leq N$ states. Given a partition labelled by the multi index $S_j^{d_j} = \{i_1, .., i_{d_j}\}$ such that $\{1, ..., N\} = \bigcup_{j=1}^{k} S_j^{d_j}$ and $S_j^{d_j} \cap S_l^{d_l} = \emptyset$, k-separable states are of the form

$$|\psi_{k-\mathrm{sep}}\rangle = \bigotimes_{j=1}^{k} |\phi_j\rangle_{S_j^d} \,, \tag{1.14}$$

where $|\phi_j\rangle \in \bigotimes_{i \in S_j^d} \mathcal{H}_i$. The notion of k-separability leads to a natural hierarchy of multipartite entanglement, since a k-separable state is also $(k-1)$-separable. States

which do not admit a k-separable representation for any $k > 1$ are called *genuinely multipartite entangled*.

A mixed state ρ is called k-separable when it admits a decomposition in terms of a convex combination of k-separable pure states,

$$\rho = \sum_j p_j \left|\psi^{(j)}_{k-\text{sep}}\right\rangle\!\left\langle\psi^{(j)}_{k-\text{sep}}\right|, \tag{1.15}$$

where $\{p_j\}_j$ form a probability distribution and $|\psi_{k-\text{sep}}\rangle \in \Sigma_{k-\text{sep}}$. Mixed k-separable states may well exhibit entanglement in all possible partitions in subsystems, therefore the attribution of genuine multipartite entanglement to a mixed state requires the testing of separability of all possible bipartitions and all convex combinations thereof. This may be a cumbersome task and the problem is often simplified by assessing whether a state is a *PPT-mixture* [42], that is whether it may be written as a convex combination of states satisfying the PPT condition in all partitions.

Genuine multipartite negativity

Entanglement negativity may be generalised to detect genuine multipartite entanglement [72, 73]. The intuitive idea is that the bipartite negativity needs to be minimised over all bipartitions of the quantum system, as well as for all possible convex combinations of density matrices. Let the index m label a bipartition $M|\bar{M}$, where M is a subsystem and $\bar{M}$ its complementary subsystem. The *genuine multipartite negativity* (GMN) of a state ρ is given by

$$\mathcal{N}_g(\rho) = \min_{\rho=\sum_k p_k\rho_k} \sum p_k \mu(\rho_k), \tag{1.16}$$

where $\mu(\rho) = \min_m(\|\rho^{\Gamma_m}\|_1 - 1)/2$ is the minimum negativity over all bipartitions. The definition in (1.16) may be expressed in the alternative form [74]

$$\mathcal{N}_g(\rho) = \min_{\rho=\sum_m p_m\rho_m} \sum p_m \mathcal{N}_m(\rho_m), \tag{1.17}$$

where the summation index runs over all possible bipartitions $M|\bar{M}$ and $\mathcal{N}_m(\rho) = (\|\rho^{\Gamma_m}\|_1 - 1)/2$.

1.2 Semidefinite Programming and Quantum Theory

The ubiquity of the concept of convexity in quantum statistical mechanics naturally feeds the temptation to formulate quantum problems as convex optimization programs.

Convex optimization programs are a special class of mathematical optimization problems, including, among others, least-squares, linear programming and semidefinite programs [33]. Many of these mathematical tools have important applications in physics and we will focus on semidefinite programming, which in recent years has become of growing interest for the quantum information theory [32]. In particular, the importance of positivity for density operators and the dynamical maps governing their evolution suggests that semidefinite programming [33] is a useful resource in giving operational formulations to quantum information tasks [75].

A *SemiDefinite Program* (SDP) is a convex optimization algorithm where the figure of merit is a linear function being minimized with hermiticity-preserving constraints on hermitian matrices. In mathematical terms, given a hermiticity-preserving map Φ and two hermitian operators A and B, a semidefinite program is given by a triple (Φ, A, B) associated with the following pair of optimization instances:

$$\begin{array}{lll} \underline{\text{Primal problem}} & & \\ \text{maximise} & \langle A, X\rangle & \\ \text{subject to:} & \Phi(X) = B, & \\ & X \geq 0 & \end{array} \qquad \begin{array}{lll} \underline{\text{Dual problem}} & & \\ \text{minimise} & \langle B, Y\rangle & \\ \text{subject to:} & \Phi^*(X) \geq A, & \\ & Y = Y^\dagger & \end{array} \tag{1.18}$$

where $\langle \cdot, \cdot \rangle$ is an inner product (given by the trace inner product $\mathrm{Tr}(AX)$ for density operators A, X), representing the objective function, and $\Phi^*(\cdot)$ is the adjoint of the map Φ [32]. It is also possible to consider semidefinite programs having both equality and inequality constraints in the primal problem. The primal and dual problem may be understood as computational tasks aimed at optimizing (i.e. maximizing or minizing) the figures of merit $\langle A, X\rangle$ ($\langle B, Y\rangle$) subject to some mathematical constraints. The duality of semidefinite programs is a useful resource for the reason that, for a given problem, a solution may be obtained by solving either its primal or dual formulation and the computational complexities in the two cases may vary significantly.

Semidefinite programs can be solved efficiently with numerical computer algorithms, allowing for the obtaining of a solution in polynomial time in the number of optimization variables [33]. There are several computational tools available implementing semidefinite optimization on common platforms, one of which is the CVX package for Matlab [76].

1.2.1 Entanglement negativity as a semidefinite program

Consider the partially transposed density operator $x = \rho^{\Gamma}$, which in general has a number r_+ and r_- of positive and negative eigenvalues respectively. Let us write x in the decomposition where its first r_+ eigenvalues are positive:

$$x = \sum_i x_i \left|x_i\right\rangle\!\left\langle x_i\right| = \sum_{i=1}^{r_+} x_i \left|x_i\right\rangle\!\left\langle x_i\right| + \sum_{i=r_++1}^{r_++r_-} x_i \left|x_i\right\rangle\!\left\langle x_i\right| = \sum_{i=1}^{r_+} x_i \left|x_i\right\rangle\!\left\langle x_i\right| - \sum_{i=r_++1}^{r_++r_-} \left|x_i\right| \left|x_i\right\rangle\!\left\langle x_i\right|$$
$$= x_+ - x_-, \tag{1.19}$$

where $x_+ = \sum_{i=1}^{r_+} x_i \left|x_i\right\rangle\!\left\langle x_i\right|$ and $x_- = \sum_{i=r_++1}^{r_++r_-} \left|x_i\right| \left|x_i\right\rangle\!\left\langle x_i\right|$ are positive-semidefinite operators. The trace norm of x may be seen to yield the sum of the absolute values of the eigenvalues of x, $\|x\|_1 = \sum_i |x_i|$, therefore the negativity (as defined in section 1.1) of a normalised density operator may be seen as the sum of the negative eigenvalues of its partial transposition

$$\mathcal{N}(\rho) = \sum_{i=r_++1}^{r_++r_-} |x_i|. \tag{1.20}$$

Furthermore, we have the matrix inequality $-x_- \leq x \leq x_+$ and one may always express x_+ and x_- to have orthogonal support, such that $x = x_+ - x_- = \tilde{x}_+ \oplus -\tilde{x}_-$. Consider now the matrix X given by

$$X = \left(\begin{array}{c|c} +x_+ & 0 \\ \hline 0 & -x_- \end{array}\right). \tag{1.21}$$

and a positive hermitian matrix $M \geq 0$ of the form

$$M = \left(\begin{array}{c|c} M_0 & * \\ \hline *' & M_1 \end{array}\right), \tag{1.22}$$

with the constraint $-M \leq X \leq M$, where $*$ indicates generic matrix blocks. Because of the block structure, we have that $\mathrm{Tr}M_0 \geq \mathrm{Tr}(x_+)$ and $\mathrm{Tr}M_1 \geq \mathrm{Tr}(x_-)$, so $\mathrm{Tr}M \geq \mathrm{Tr}(x_+) + \mathrm{Tr}(x_-)$, meaning that the trace of M is lower-bounded by the trace-norm of x. The lower bound for $\mathrm{Tr}M$ may indeed always be achieved when M is given by

$$M = \left(\begin{array}{c|c} x_+ & 0 \\ \hline 0 & x_- \end{array}\right). \tag{1.23}$$

Thus, this suggests the possibility of rewriting the trace-norm of an operator x as

$$\begin{aligned} \|x\|_1 = & \min \mathrm{Tr}(M) \\ & \text{such that} \quad M \geq 0 \\ & \qquad -M \leq x \leq M. \end{aligned} \tag{1.24}$$

The expression in (1.24) may be cast in the form (1.18) [32] and we may therefore put forward the following formulation of the entanglement negativity as an SDP:

Proposition 1. Given a normalised bipartite density matrix ρ, its entanglement negativity is given by the SDP

$$\begin{aligned} N(\rho) = & \min(\mathrm{Tr}(M) - 1)/2 \\ & \text{such that} \quad M \geq 0 \\ & \qquad -M \leq \rho^{\Gamma} \leq M. \end{aligned} \tag{1.25}$$

The formulation of entanglement measures in terms of semidefinite programs can be extended to the the multipartite regime [72]. We will show in Chapters 2 and 5 that genuine entanglement negativity, as expressed in equation (1.17), may also be thought of as an SDP. The formulation involves additional constraints, a higher level of complexity and is more demanding in terms of computational resources, however it is a direct generalization of the expression in 1.25.

Chapter 2

Quantifying Identical-Particle Entanglement

2.1 A Preamble of Intentions

It is well known that quantum mechanics has brought about a deep overturning of our understanding of nature. Our classical environment, based on the deterministic clockwork of trajectories of material points in phase space, bears little resemblance to the stochastic and immaterial behaviour of fields within the quantum realm. And yet quantum mechanics may be considered to be the most successful theory to date, based on the accuracy and the depth to which its predictions have been tested. It should be no surprise that a theory so mind-boggling yet undisputed has given rise since its first formulations to much heated debate and controversy, which persist to this day concerning certain of its facets. Interestingly, many of the greatest advances in our understanding of the theory and its technological breakthroughs have been the brainchildren of the most harsh and overarching of debates, which have been so profound as to involve mathematicians and philosophers in its resolution. It is safe to say that quantum theory has pushed the boundaries of what *doing physics* means.

Despite my awareness of the immense difficulty in making sense of many quantum features, it was not without surprise that I learnt about an ongoing debate involving two of the most "ancient" features of quantum mechanics: the identity of particles and entanglement, formulated respectively in the mid 1920's and 1930's. How is it possible that after over 80 years of investigation there are still papers being published on such a fundamental subject? A hint towards the answer to this question may come by looking at the breadth of the publications which have addressed the issue in recent years, spanning from mathematical physics to experimental quantum optics and even to philosophy [20–29, 77–81]. The picture emanating from this literature may lead one to appreciate the subtleties of the interplay of identity of particles and entanglement

and how recent experimental and theoretical advances have sparked new interest in a subject which had been perhaps prematurely set aside as an oddity. Entanglement of identical particles lies at the heart of most current research topics in quantum physics and of the technological advances it promises to achieve, yet there is still no universal consensus on a mathematical definition covering all aspects of this phenomenon, let alone the interpretation of predictions concerning it. It is no ambition of this work to resolve the dispute, but to lay it out, highlight certain critical points at the heart of it and put forward a new perspective on the subject; one that may be of theoretical and experimental interest in the hope that it may be of help in getting closer to understanding the true nature of entangled identical particles and unlocking their full potential applications.

2.2 Entanglement and Subsystems

Entanglement is not a property of quantum states. Given a set of vectors $|\psi_i\rangle$ in the Hilbert space $\mathcal{H}$ and the associated probabilities p_i there is no answer to the question "how entangled is the state $\rho = \sum_i p_i \, |\psi_i\rangle\langle\psi_i|$?", the information provided being insufficient for any assessment of entanglement. Entanglement is a property of subsystems and is therefore a notion that only applies to composite quantum systems allowing a partitioning into subsystems. This imposes a constraint on the types of physical systems for which entanglement is a meaningful concept, requiring them to be either *bipartite* or *multipartite*. A bipartite quantum system $\mathcal{S}_{AB} = \mathcal{S}_A + \mathcal{S}_B$ is described by states which are vectors of a Hilbert space with a structure $\mathcal{H}_{AB} = \mathcal{H}_A \otimes \mathcal{H}_B$ such that $\dim(\mathcal{H}_A) \times \dim(\mathcal{H}_B) = \dim(\mathcal{H}_{AB})$. The states of a K-partite system $\mathcal{S}_K = \sum_{i=1}^{K} \mathcal{S}_i$ are vectors of a Hilbert space with structure $\mathcal{H}_K = \bigotimes_{i=1}^{K} \mathcal{H}_i$ and $\prod_{i=1}^{k} \dim(\mathcal{H}_i) = \dim(\mathcal{H}_K)$.

It is important to notice that in general the partitioning into subsystems is not unique and there may be several alternative choices of single-subsystem Hilbert space. In addressing the entanglement in a composite physical system $\mathcal{S}_{AB}$ described by the global state ρ in $\mathcal{H}_{AB}$ it is therefore formally appropriate to use the phrasing *the entanglement of the state ρ with partitioning $A|B$*, where $A|B$ indicates the Hilbert space structure $\mathcal{H}_{AB} = \mathcal{H}_A \otimes \mathcal{H}_B$.

Entanglement is not an observable of the total system. It is a statement about the indivisibility of a composite quantum system, stemming from the interplay of the composite Hilbert space tensor-product structure and the superposition principle. It is the formalisation of the idea that for certain quantum systems the whole is more than the sum of its constituents. Nonetheless, entanglement is a fundamental feature

of composite systems and has been proven to be useful for a vast number of quantum information tasks, as discussed in the Introduction of this thesis.

The fact that for a given quantum system there are in general multiple partitions in terms of which the state may be described implies that an independent notion of entanglement may be associated with each partition. We will see that this is the case for systems of identical particles, for which the plurality of entanglement notions has caused confusion and debate.

Furthermore, no assumption is required about the subsystems in order to meaningfully define a notion of entanglement. As long as a tensor product structure is identified, given a quantum state and its partition it is possible to introduce some notion of entanglement, or *inseparability*.

2.3 Identical Particles

The identity of particles is a concept that goes back to the early days of quantum mechanics. Its roots lie in wave-particle duality: if particles may be described as energy levels of a field then the quantum numbers describing the state characterise it completely. This approach was first put forward as early as Debye's 1910 paper on the theory of radiation [82], but it wasn't until the connection between identity of particles and statistics became manifest that the identity of particles attracted much attention. The main breakthrough was the acknowledgement that in a statistical approach to quantum mechanics the counting of microstates of light quanta with same frequency required to consider states of particles which only differed by the exchange of two or more particles as the same state. In the span of the years 1924-1926 a series of physical and philosophical debates lead to a number of seminal results, including the definition of Bose-Einstein statistics [83] and the Pauli exclusion principle [84]. The latter, in particular, was a corollary of the discovery by Pauli of spin, or 'two-valued quantum degree of freedom', as he put it. In his seminal paper Pauli states:

> *There can never be two or more equivalent electrons in an atom for which in strong fields the values of all quantum numbers n, k1, k2, m1 (or, equivalently, n, k1, m1, m1) are the same. If an electron is present in the atom for which these quantum numbers (in an external field) have definite values, this state is "occupied" [84]*

The last sentence of the above quote foreshadows the introduction of the occupation number representation, which will be an important tool in the mathematical description of systems of identical particles.

The connection between spin and statistics was first established by Pauli in 1940 [85]. He argued that particles with half-integer spin should obey Fermi-Dirac statistics and particles with integral spin should obey Bose-Einstein statistics. However, it wasn't until 1964 that a rigorous proof was provided by Streater and Wightman [18]. Even so, the connection is established by a negative proof, showing that half-integer bosons are inconsistent (they lead to negative probabilities) and that the field of fermions with integer spins is always zero. It does not, in fact, prove that spin 1/2 particles must have Pauli exclusion, or that integer spin particles must have Bose-Einstein statistics. In other words, the spin-statistics connection is not shown to be *inevitable* [86].

The spin-statistics connection applied to Schrödinger's wave mechanics leads to the introduction of the symmetrization postulate. Identical-particle states need to be permutation invariant, thus they must be eigenstates with eigenvalue either $+1$ or -1 of the operator which permutes two particles. The postulate states that the particles with positive eigenvalue, which are thus symmetric under exchange of two particles, have integer spin and are called *bosons*. The particles with negative eigenvalue are antisymmetric under exchange of two particles, have half-integer spin and are called *fermions*. The association is consistent with the Pauli exclusion principle, since an antisymmetric state of two particles with the same quantum numbers is necessarily zero.

The spin-statistics connection and its relationship with the symmetrization postulate is still a somewhat mysterious one, since quantum formalism is compatible with parastatistics and there is ongoing research seeking violations of the spin-statistics connection [86]. Nonetheless, in this thesis we work within the standard formalism wherein spin-statistics and the symmetrization postulate are related according to the principles established above.

In the following sections we recall the two main formalisms developed for representing systems of identical particles, the so-called *first-quantised* and *second-quantised* representations.

2.3.1 First-quantised representation of identical particles

Let us consider a system of N identical particles $\mathcal{S}_N$ each having d internal degrees of freedom. In the usual Schrödinger representation of quantum states, also known as *first-quantised representation*, the system will be described by a vector in the total Hilbert space $\mathcal{H}_{d^N} \simeq \mathbb{C}^{d^N} \equiv (\mathbb{C}^d)^{\otimes N}$. The symmetrization postulate implies that two families of identical particles are possible. Consider the family of swap operators $\{V_{jk}\}_{jk}$ described

by their action on the factorised basis states for the global Hilbert space

$$V_{jk}\left|\psi_1\right\rangle_1\cdots\left|\psi_j\right\rangle_j\cdots\left|\psi_k\right\rangle_k\cdots\left|\psi_N\right\rangle_N=\left|\psi_1\right\rangle_1\cdots\left|\psi_k\right\rangle_j\cdots\left|\psi_j\right\rangle_k\cdots\left|\psi_N\right\rangle_N. \quad \forall j,k \tag{2.1}$$

Such permutation is hermitian and corresponds to its own inverse $V_{jk}=V_{jk}^{\dagger}=V_{jk}^{-1}\,\forall j,k$. The identical-particle states which are invariant under V_{jk}, $\forall j,k$ are called *symmetric* and correspond to states describing bosons. Those which have a π phase change under the swap operator are called *antisymmetric* and correspond to states describing fermions.

Bosonic states lie within the symmetric subspace of the total Hilbert space

$$\mathcal{H}_{\mathcal{S}}(d,N)=\mathcal{H}^{\vee N}=\{\left|\psi\right\rangle:V_{jk}\left|\psi\right\rangle=\left|\psi\right\rangle \quad \forall j,k=1,...,N,\,\left|\psi\right\rangle\in\mathcal{H}_{dN}\}, \tag{2.2}$$

where $\vee$ is the symmetric tensor product. The projector on the symmetric subspace is given by

$$P_{\mathcal{S}}^{(d,N)}=\frac{1}{N!}\sum_{\pi\in\mathfrak{S}_N}P_d(\pi), \tag{2.3}$$

where

$$P_d(\pi)=\sum_{i_1,...,i_N\in[d]}\left|i_{\pi^{-1}(1)},...,i_{\pi^{-1}(N)}\right\rangle\!\left\langle i_1,...,i_N\right| \tag{2.4}$$

is the permutation operator, $[d]=\{1,..,d\}$ is the set of integer values that may be taken by each index and $\pi\in\mathfrak{S}_N$ a permutation in the symmetric group $\mathfrak{S}_N$.

Fermionic states, on the other hand belong to the antisymmetric subspace

$$\mathcal{H}_{\mathcal{A}}(d,N)=\mathcal{H}^{\wedge N}=\mathrm{span}\,\{\left|\psi\right\rangle:V_{jk}\left|\psi\right\rangle=-\left|\psi\right\rangle \quad \forall j,k=1,...,N,\,\left|\psi\right\rangle\in\mathcal{H}_{dN}\}, \tag{2.5}$$

where $\wedge$ is the antisymmetric tensor product. The projector on the antisymmetric subspace is given by

$$P_{\mathcal{A}}^{(d,N)}=\frac{1}{N!}\sum_{\pi\in\mathfrak{S}_N}(-1)^{\mathrm{sgn}(\pi)}P_d(\pi). \tag{2.6}$$

The symmetric and antisymmetric subspaces are orthogonal, i.e.

$$P_{\mathcal{S}}^{(d,N)}P_{\mathcal{A}}^{(d,N)}=P_{\mathcal{A}}^{(d,N)}P_{\mathcal{S}}^{(d,N)}=0. \tag{2.7}$$

The indistinguishability of particles implies that all physical observables O need to be permutation invariant:

$$V_{jk}OV_{jk}=O \quad \forall j,k=1,...,N. \tag{2.8}$$

If this were not case the expectation values of observables would allow to physically distinguish between particles, which would be a contradiction.

The identity of particles in combination with the spin-statistics connection poses strong symmetry constraints on the first-quantised representation of states and operators. The possible states the systems may be found in and the operations that may be carried out on them are greatly restricted by the symmetry conditions. In particular, no statement can be made about a set of labelled particles, since that property could be attributed to any other set of the same number of particles. The lack of *individuality* of identical particles, however, does not imply that the concept of *particle* is a flawed one in identical-particle systems. Sets of identical particles are *enumerable*, that is to say they possess *cardinality*, but not *ordinality* [81]. In other words, it is not possible to make statements about a *specific* set of K particles within the system, but about an unspecified set of K particles. We will see a specific way to assert such statements in section 2.6.

2.3.2 Second quantisation and occupation number representation

The first-quantised representation of quantum mechanics does not incorporate special relativity and leads to inconsistencies when relativistic effects are incorporated naively into the theory [54]. The efforts to reconcile the two theories led to the development of *quantum field theory*, which is a more general framework encompassing both special relativity and quantum mechanics. As the name suggests, the fundamental constituents of quantum field theory are not particles but *quantum fields*. In this context particles may be identified as quantised excitations of the underlying fields. Quantum field theory retains many of the features of quantum mechanics, including the superposition principle and the Born rule for measurements, however it may account for phenomena which are not covered by non-relativistic QM, in particular particle number fluctuations. Systems described by quantum fields may be described by states with non-integer and fluctuating number of particles, the number of particles merely becoming an observable of the system with given expectation value and variance.

In the context of quantum field theory, the formalism which describes systems of many bosons and fermions is called *second-quantised representation*. In simple terms, whereas a first-quantised representation describes a quantum system in terms of statements of the kind "*Which particle is found in the state* $|\psi\rangle$*?*", the second-quantised language approaches the description in terms of "*How many particles occupy the state* $|\psi\rangle$*?*". It is evident that the latter approach is automatically consistent with the cardinality and lack of ordinality proper to systems of identical particles. Let us briefly outline the main features of the formalism.

Fock representation

Consider a single particle Hilbert space $\mathcal{H}$ spanned by the ONB of single-particle states $\{|\phi_i\rangle\}_{i=1}^{d}$. The i^{th} state is usually referred to as the i^{th} *mode*. The term *mode* comes from the analogy between the modes of a system of independent quantised harmonic oscillators and the single-particle states which may be occupied in the second-quantised formalism. Consistently with such analogy, the modes may be described in terms of creation and annihilation operators, represented respectively by $a_i^\dagger$ and a_i, acting on a zero-point energy state $|0\rangle$, called the *vacuum state*. The i^{th} mode is thus given by $|\phi_i\rangle = a_i^\dagger |0\rangle$, whereas the a_i operator *annihilates* the vacuum, $a_i |0\rangle = 0$. Fermionic and bosonic states can be represented in terms of these ingredients, in the so-called *occupation-number representation*, or *Fock representation*. The state of modes $|\phi_j\rangle$ each occupied by n_j bosons or fermions are called *Fock states* and may be written as

$$|n_1, ..., n_d\rangle_F = \frac{(a_1^\dagger)^{n_1}}{\sqrt{n_1!}} \cdots \frac{(a_d^\dagger)^{n_d}}{\sqrt{n_d!}} |0\rangle , \tag{2.9}$$

where $\sum_{j=1}^{d} n_j = N$ is the total number of particles.

The Bose and Fermi statistics are recovered by enforcing constraints on the creation and annihilation operators, known as *canonical commutation relations* (CCR).

The bosonic commutation relations are

$$\left[a_j, a_k^\dagger\right] \equiv a_j a_k^\dagger - a_k^\dagger a_j = \delta_{jk}, \quad [a_j, a_k] = [a_j^\dagger, a_k^\dagger] = 0, \tag{2.10}$$

whereas the fermionic anticommutation relations are

$$\left\{a_j, a_k^\dagger\right\} \equiv a_j a_k^\dagger + a_k^\dagger a_j = \delta_{jk}, \quad \{a_j, a_k\} = \{a_j^\dagger, a_k^\dagger\} = 0. \tag{2.11}$$

As a consequence of the CCR, bosonic and fermionic Fock states are amenable to a Hilbert space representation. For a fixed total number of particles $N = \sum_j n_j$, a given bosonic Fock state may be identified in its first-quantised representation as

$$|n_1, ..., n_d\rangle \equiv \mathcal{N}_{\mathcal{S}} P_{\mathcal{S}}^{(d,N)} \left[\bigotimes_{j=1}^{d} \left(\bigotimes_{k=1}^{n_j} |\phi_j\rangle\right)\right], \tag{2.12}$$

where $\mathcal{N}_{\mathcal{S}}$ is a bosonic-state-specific normalisation constant and $P_{\mathcal{S}}^{(d,N)}$ the projector on the symmetric subspace. For fermionic Fock states we have

$$|n_1, ..., n_d\rangle \equiv \mathcal{N}_{\mathcal{A}} P_{\mathcal{A}}^{(d,N)} \left[\bigotimes_{j=1}^{d} \left(\bigotimes_{k=1}^{n_j} |\phi_j\rangle \right) \right], \tag{2.13}$$

where $\mathcal{N}_{\mathcal{A}}$ is a fermionic-state-specific normalisation constant and $P_{\mathcal{A}}^{(d,N)}$ the projector on the antisymmetric subspace. We call the first-quantised representations of bosonic and fermionic Fock states *Slater permanents* and *Slater determinants* respectively. There is a one-to-one correspondence between the Fock and first-quantised representations. In fact, Fock states constitute a complete ONB of the second-quantised state space, whereas Slater permanents and determinants form complete ONBs for the bosonic and fermionic first-quantised sectors respectively.

When no constraint is enforced on the number of particles, we may represent the bosonic and fermionic Fock spaces respectively as

$$\begin{aligned} \mathcal{H}_F^{(S)} &= \bigoplus_{n=1}^{\infty} \mathcal{H}_{\mathcal{S}}(d, n) \\ \mathcal{H}_F^{(A)} &= \bigoplus_{n=1}^{\infty} \mathcal{H}_{\mathcal{A}}(d, n). \end{aligned} \tag{2.14}$$

Mode representation

While the Fock representation solves the labelling problem for identical particles by construction, it does not automatically provide a notion of subsystems. The states of the kind (2.9) do not have an explicit tensor product substructure of Hilbert spaces. The identification of subsystems requires an additional step, which is naturally achieved with the association

$$|n_1, ..., n_d\rangle_m \equiv |n_1\rangle \otimes \cdots \otimes |n_d\rangle = \otimes_{j=1}^{d} |n_j\rangle \,. \tag{2.15}$$

This is the *mode representation*, or occupation-number representation, and as we will discuss in section 2.5 it is amenable to the definition of a notion of entanglement. With no constraint on the total particle number and a finite number of modes d, the bosonic space is infinite-dimensional, whereas the fermionic case is 2^d-dimensional due to Pauli exclusion. Physical constraints on the total number of particles in a system may be enforced to further restrict the set of allowed states to a subspace of the $\mathcal{H}_B$ and $\mathcal{H}_F$ Hilbert spaces.

2.4 Particle Number Super-Selection Rules

The previous section highlights how the second-quantised approach is more general than the first-quantised one, covering systems with variable numbers of particles and relativistic energy regimes. There are physical systems, however, where the two representations are equivalent and may be mapped one into the other. Systems of massive particles in non-relativistic regimes, where the number of particles are fixed and free of fluctuations, are one of such instances. These systems may be formally characterised by introducing a conservation law, called *particle-number super-selection rule* (SSR) [87], constraining the set of physical states describing the system. Low-energy electrons, cold atoms and molecules are examples of such systems which are of great interest of current research seeking applications of quantum theory. An ultracold atom system, for instance, typically is unaffected by relativistic effects and the particle-number oscillations due to the field-excitation nature of the particles are suppressed enough to be negligible for the study and characterisation of their properties. In such systems, the notion of particle is a well-defined one, its first-quantised representation being a meaningful one and viable of bringing insights in the understanding of the physical properties which the mode representation does not capture in its entirety.

In the Fock representation, fixing a number of particles amounts to restricting the set of possible states to the fixed-number N-particle sectors $\mathcal{H}_{\mathcal{S}}(d,N)$ and $\mathcal{H}_{\mathcal{A}}(d,N)$ for bosons and fermions respectively. A similar correspondence may be established under particle number SSR between mode-represented states and first-quantised ones.

The particle number SSR constraining the system to having fixed number N of particles restricts the possible set of states to those which may be written in the mode representation in the form

$$|\psi\rangle = \sum_{j=0}^{N} \psi_j \bigotimes_{i=1}^{d} \left|n_i^j\right\rangle, \quad \sum_{i=1}^{d} n_i^j = N, \, \forall j. \tag{2.16}$$

Bosonic states of the form (2.16) may be represented in a $\binom{d+N-1}{d-1}$-dimensional Hilbert space. Fermionic systems, on the other hand, need to account for Pauli exclusion, therefore the mode-occupation quantum numbers n_i^j are constrained to the dichotomic values 0 or 1. This further constrains systems of fermions to have local dimension d larger or equal than the number of particles N:

$$N = \sum_{\substack{i=1,\ldots,N \\ n_i=0,1}} n_i \leq d. \tag{2.17}$$

Fermionic states of N particles may therefore be written in the mode representation as vectors in a $\binom{d}{N}$-dimensional Hilbert space.

It is clear that the Hilbert space representations in the first and second quantised pictures have different dimensions, however the particle number superselection rule ensures that there is an isomorphism connecting the two state spaces [88]. The first and second quantised approach are therefore equivalent in presence of a particle number SSR, leading to the same predictions for expectation values of observables. The entanglement properties associated with the two representations, however, are inequivalent. As previously discussed statements about entanglement depend not only on the state of the system but also on the partitioning into subsystems. Clearly, the subsystem structures in the first and second-quantised representations in general do not coincide.

2.5 Entanglement of Identical Particles

Before carrying out a formal analysis of identical-particle entanglement, let us draw upon a simple example that illustrates the issues involved in describing entanglement of fermions with the standard approach. Consider two very well separated laboratories, for instance in different galaxies, where scientists are able to prepare pure (to a good enough degree of approximation for practical purposes) single-fermion states. Suppose *one* of the fermions is prepared in a spin up eigenstate with spatial amplitude given by $\psi_L(x) = \langle x|L\rangle$ and the other is prepared in a spin down state with spatial amplitude $\psi_L(x) = \langle x|L\rangle$. The two fermion state would therefore still necessarily be described by wavefunction

$$|\psi\rangle_{12} = \frac{1}{\sqrt{2}}\left(|L\rangle_{1,x}|\uparrow\rangle_{1,\sigma}|R\rangle_{2,x}|\downarrow\rangle_{2,\sigma} - |R\rangle_{1,x}|\downarrow\rangle_{1,\sigma}|L\rangle_{2,x}|\uparrow\rangle_{2,\sigma}\right), \tag{2.18}$$

since the symmetrization requirement holds regardless of the particles' states. In the above equation the labels $1, 2$ refer to the two distinct single-particle Hilbert spaces, x and σ refer to the position and spin degrees of freedom respectively of each single-particle Hilbert space. In the following equations we will omit this explicit notation for the sake of clarity where this will be unambiguous as a result of the ordering of the *kets*. The state (2.18) would be labelled as entangled according to the standard entanglement definition (section 1.1), however it may not be used to perform entanglement-enabled quantum information tasks, such as violating a Bell inequality [21]. To show this, let us consider an example in a typical Bell experiment. Here, the two parties, typically referred to as Alice and Bob, and the particles are considered to be well-separated, in order to assess the nonlocality of the correlations between the outcomes of measurements. We

therefore consider a state of the kind

$$|\psi_-\rangle = \frac{1}{\sqrt{2}}(|L\rangle\,|\uparrow\rangle\,|R\rangle\,|\downarrow\rangle - |R\rangle\,|\downarrow\rangle\,|L\rangle\,|\uparrow\rangle), \tag{2.19}$$

where $\langle L|R\rangle = 0$. In the Bell scenario the parties each measure the internal (spin) degree of freedom in its own localised spatial region, L for Alice and R for Bob. The measurement operators need to be exchange symmetric, because of the identical nature of the particles, therefore Alice's measurement operator is of the kind

$$M_A = (|L\rangle\langle L| \otimes \sigma_A) \otimes (\mathbb{1} \otimes \mathbb{1}) + (\mathbb{1} \otimes \mathbb{1}) \otimes (|L\rangle\langle L| \otimes \sigma_A), \tag{2.20}$$

and Bob's takes on the form

$$M_B = (|R\rangle\langle R| \otimes \sigma_B) \otimes (\mathbb{1} \otimes \mathbb{1}) + (\mathbb{1} \otimes \mathbb{1}) \otimes (|R\rangle\langle R| \otimes \sigma_A), \tag{2.21}$$

where σ_A and σ_B are projective measurement operators for the single-particle spin degree of freedom. The expectation value of the joint measurement is given by

$$\langle\psi_-|M_A M_B|\psi_-\rangle = \langle\uparrow|\sigma_A|\uparrow\rangle\ \langle\downarrow|\sigma_B|\downarrow\rangle\,. \tag{2.22}$$

Equation (2.22) shows that the expectation value for the joint measurements factorises in the spin degree of freedom, which is therefore uncorrelated. The probability distributions generated by such a setup are uncorrelated and may not violate a Bell inequality [89].

In this perspective, it would appear that despite the fact that the wavefunction looks like that of an entangled state, the entanglement arising does not exhibit correlations in the same way that the entanglement of a distinguishable-particle state would. On the contrary, let us consider the state

$$|\phi\rangle_{12} = \frac{1}{2}\left(|L\rangle\,|R\rangle + |R\rangle\,|L\rangle\right)\left(|\uparrow\rangle\,|\downarrow\rangle - |\downarrow\rangle\,|\uparrow\rangle\right), \tag{2.23}$$

where $\langle L|R\rangle = 0$. The state (2.18) may result from the appropriate tuning of interactions between two particles, for example two photons with a common optical path in a beam-splitter or two ultracold atoms trapped in a double-well shaped magneto-optical trap. It is also clearly an entangled state, but it is the state of a spin singlet and it can be used to violate Bell inequalities and for quantum state teleportation [21]. If one evaluates the expectation value in the left-hand side of equation (2.22) over the state $|\phi\rangle_{12}$, one does not obtain a factorised expression as in the right-hand side of (2.22). Indeed, it is shown explicitly in references [21, 90, 91] that the joint measurement yields

correlations of EPR (Einstein, Podolski and Rosen, discussed in section 5.1.3) kind, which are known to violate a Bell inequality [62, 89].

States which violate Bell inequalities are said to exhibit *nonlocality*, a notable physical property of quantum states with many applications of great practical and theoretical interest, a number of which will be reviewed in Chapter 5. It is therefore of great interest to identify the source of such nonlocality and gain a better understanding of the structure of states which bring it about. In such context, what is it that makes the state $|\phi\rangle_{12}$ different from the previous state $|\psi\rangle_{12}$? It is easy to see that the former state arises from the antisymmetrization, i.e. the projection onto the antisymmetric subspace, of a state of the kind

$$|\sigma\rangle_{12} = \frac{1}{\sqrt{2}} \left(|L\rangle |\uparrow\rangle |R\rangle |\downarrow\rangle + |R\rangle |\downarrow\rangle |L\rangle |\uparrow\rangle \right), \tag{2.24}$$

which is entangled, whereas the state in equation (2.23) is the antisymmetrization of $|A\rangle |B\rangle$, which is separable. This seems to suggest that the entanglement properties should be addressed somewhat *prior* to antisymmetrization, the latter being a mathematical requirement due to the field nature of identical particles. Antisymmetrization, however, should not be considered on the same grounds as entanglement. With this intuition in mind, we will review in section 2.6 a proposal for an entanglement criteria for identical particles which takes into account the aforementioned problems. Before we proceed, however we will recall an important class of permutation-invariant entangled states, which we will investigate from an identical-particle entanglement perspective in section 2.7. Its properties will be of use in highlighting the structure of the symmetric and antisymmetric subspaces. Furthermore, we will summarize a selection of recent literature tackling the problem of characterizing and quantifying identical-particle entanglement.

2.5.1 Maximally entangled symmetric and antisymmetric distinguishable-particle states

One of the reasons of interest in entanglement is its usefulness as a resource in quantum information and metrological tasks. The class of states with the most entanglement, as quantified in terms of the LOCC paradigm, in a physical system is thus a specially interesting one and is called that of *maximally entangled states* (MES) [92]. We will briefly review some well-known features of MES in the distinguishable-particle bipartite case and investigate the structure of the class when restricted to the symmetric and antisymmetric subspace, suitable for the description of bosons and fermions.

Let us consider a state of 2 particles each described by a Hilbert space $\mathcal{H} \simeq \mathbb{C}^d$ spanned by basis vectors $\{|i\rangle\,,\, i = 1, ..., d\}$. One definition for a maximally entangled state is requiring that its partial trace in one of the subsystems yields the maximally mixed state in the other subsystem [56]. The canonical maximally entangled state of two qudits is given by

$$\left|\psi^+\right\rangle = \frac{1}{\sqrt{d}} \sum_{i=1}^{d} |i\rangle\, |i\rangle\,, \tag{2.25}$$

hence

$$\mathrm{Tr}_B(\psi^+) = \mathrm{Tr}_B\Big(\frac{1}{d} \sum_{i,j} |i\rangle\langle j| \otimes |i\rangle\langle j|\Big) = \frac{1}{d} \sum_{i} |i\rangle\langle i| = \frac{1}{d}\mathbb{1}_A. \tag{2.26}$$

The definition we adopted for a maximally entangled state entails the fact that also all states of the kind

$$\mathbb{1} \otimes U \left|\psi^+\right\rangle \tag{2.27}$$

are maximally entangled. In fact, we have the relation

$$\mathrm{Tr}_B(\mathbb{1} \otimes U\psi^+\mathbb{1} \otimes U^\dagger) = \mathrm{Tr}_B(\psi^+\mathbb{1} \otimes UU^\dagger) = \mathrm{Tr}_B(\psi^+) = \frac{1}{d}\mathbb{1}_A, \tag{2.28}$$

owing to the cyclicity of the trace and the unitarity of $U^\dagger U = \mathbb{1}$. On the other hand, it can also be shown that every maximally entangled state can be written in the same form (2.27) [19]. Furthermore, the useful property

$$\mathbb{1} \otimes B \left|\psi^+\right\rangle = B^T \otimes \mathbb{1} \left|\psi^+\right\rangle, \tag{2.29}$$

for any $d \times d$ matrix $B = \sum_{ij} b_{ij} |i\rangle\langle j|$ and its transpose $B^T = \sum_{ij} b_{ji} |i\rangle\langle j|$, helps us understand how a maximally entangled state behaves under the swap operation. In fact, we have that

$$V(\mathbb{1} \otimes U) \left|\psi^+\right\rangle = U \otimes \mathbb{1} \left|\psi^+\right\rangle. \tag{2.30}$$

and for identical particles the following requirement holds:

$$V(\mathbb{1} \otimes U \left|\psi^+\right\rangle) = \pm\mathbb{1} \otimes U \left|\psi^+\right\rangle = \pm U^T \otimes \mathbb{1} \left|\psi^+\right\rangle, \tag{2.31}$$

with a plus sign for bosons and minus for fermions. The right-hand sides of equations (2.30) and (2.31) imply that the symmetry properties of identical-particle maximally entangled states boil down to the symmetry properties of the unitary matrix U characterizing the states. Specifically, for bosons we require a unitary symmetric matrix and for fermions a unitary antisymmetric matrix. Let us consider the cases separately.

Bosons

The canonical distinguishable-particle maximally entangled state $|\psi^+\rangle$ is a symmetric state itself so it is a maximally entangled state also in the bosonic subspace. The class of MES derived from $|\psi^+\rangle$, though, is restricted to those of the form

$$\mathbb{1} \otimes U_+ \left|\psi^+\right\rangle, \tag{2.32}$$

where U_+ is a unitary symmetric matrix. In general, any unitary symmetric matrix may be obtained as the exponential of a symmetric matrix $X = X^{\mathrm{T}}$. The class of maximally entangled bosonic states is thus generated by the symmetric matrices X which define symmetric unitaries via

$$U_+ = e^{iX}. \tag{2.33}$$

It is possible to define maximally entangled states for bosons in any dimension for the bipartite case, a property which we will see does not apply in general for fermions.

Fermions

The fermion case requires more care since $|\psi^+\rangle$ is a symmetric state and does not lie in the fermionic subspace. Antisymmetric maximally entangled states need therefore be in the form

$$\mathbb{1} \otimes U_- \left|\psi^+\right\rangle, \tag{2.34}$$

where U_- is an antisymmetric unitary matrix. A striking consequence of this result is that it is not possible to define a class of maximally entangled antisymmetric states for fermions in odd dimensions, for it is impossible to construct a $d \times d$ antisymmetric unitary matrix. Let us prove this result by pointing out a constraint on antisymmetric matrices with odd dimensions. In fact,

$$\det(A) = \det\left(A^T\right) = \det(-A) = (-1)^d \det(A), \tag{2.35}$$

so if d is odd A is singular, i.e. $\det(A) = 0$. There is no such thing, however, as a singular unitary matrix, so the antisymmetric unitary matrix may exist only in even dimensions. The analysis must therefore be restricted to the antisymmetric matrices $U_- \in M_{2k}(\mathbb{C})$. We begin by introducing the canonical antisymmetric unitary matrix

$$U_0 = \mathbb{1}_k \otimes J \in M_{2k}(\mathbb{C}), \tag{2.36}$$

where $\mathbb{1}_k$ is the identity in $M_k(\mathbb{C})$ and

$$J = \begin{pmatrix} 0 & 1 \\ -1 & 0 \end{pmatrix} \tag{2.37}$$

is the symplectic matrix in $M_2(\mathbb{C})$. A generic antisymmetric unitary matrix may thus be obtained from

$$U_- = OU_0O^T \tag{2.38}$$

where O is an orthogonal matrix, i.e. $OO^T = \mathbb{1}_{2k}$ [93]. The maximally entangled antisymmetric subspace is thus generated by that of the orthogonal matrices O.

2.5.2 Review of recent literature on identical-particle entanglement

In this section we give a brief summary of the recent developments in the study of entanglement of identical particles. It does not intend to be an exhaustive literature review, but rather an introduction to the criticalities of the subject and the diverse approaches at their solution. Our aim is to lay out the context of our work, the stage of development of the field and most importantly the existing acknowledged notions which we base our results upon.

Before the last 20 years the entanglement of identical particles was treated effectively in the same way as entanglement of distinguishable particles. This entails regarding the particles as subsystems in the first-quantised representation and applying standard entanglement measures to the states and partitioning provided. The symmetry or antisymmetry of the states under particle exchange means that in this perspective all pure states, with the exception of factorised copies of the same single-particle state for bosons, are to be regarded as entangled [94]. As we have argued in a previous section, such an approach does not address the conceptual problem of considering as subsystems the individual labelled particles, which are not physically accessible. Furthermore, it may not distinguish between correlations due solely to statistics and those arising from known entanglement-generating processes, such as interaction.

Mode Entanglement

A number of different approaches have been put forward to deal with the interplay of symmetrization and entanglement. One such approach relies on the second-quantised mode representation, which is outlined in section 2.3.2. This approach relies on the

introduction of an alternate partitioning into subsystems, in such a way that the subsystems are distinguishable and the symmetry constraints become implicit in the definition of the modes that the particles in the system may occupy. Because it maps a system of indistinguishable subsystems to an equivalent system of distinguishable ones, where well-established theoretical machinery exists for entanglement classification and quantification, *mode-entanglement* is a very powerful resource. The subsystems identified by the modes are physically and operationally accessible and provide an intuitive understanding of the correlations arising between them. Standard mode entanglement is in fact quantified by applying a distinguishable particle entanglement measure, such as entanglement entropy (1.11), to a second quantised state partitioned between the modes according to the occupation number representation (2.15).

For such reasons mode entanglement has become the standard approach at the evaluation of entanglement in identical-particle systems, both in quantum optics, quantum information theory and quantum many-body physics [95, 96].

Recent developments, however, have put such approach under closer inspection and identified substructures in the mode-entanglement paradigm depending on the constraints that the systems of identical particles underlying the mode representation structure possess [95]. The presence of particle number super-selection rules (SSR) has led to the alternate definitions of mode entanglement discussed in references [25, 87, 97]. Such efforts established a connection between a notion of entanglement of particles and mode entanglement projected onto a fixed particle-number subspace. In [25], in particular, the relationship between such SSR and the notion of entanglement between particles was explored. Applying standard entanglement measures to systems of massive non-relativistic particles in the mode representation does not account for the fact that the operations that the parties acting on the system may perform are restricted due to the particle number SSR. This fact leads to an overestimation of the entanglement which is operationally accessible to the parties, if the standard mode entanglement notion is considered. To account for this, Wiseman and Vaccaro [25] introduce the notion of *entropy of particle entanglement* $E_p(|\psi_{AB}\rangle)$ of a pure state $|\psi_{AB}\rangle$ of N identical particles shared between two parties, Alice and Bob. Such entanglement measure is related to the standard mode entanglement $E_M(|\psi\rangle)$ via the definition

$$E_p(|\psi_{AB}\rangle) = \sum_n P_n E_M(\left|\psi_{AB}^{(n)}\right\rangle), \tag{2.39}$$

where $\left|\psi_{AB}^{(n)}\right\rangle = \Pi_n |\psi_{AB}\rangle$ is the projection of the state on the fixed particle-number subset (n for Alice, $N-n$ for Bob) and P_n is the associated projection probability.

Such considerations were further developed in [97] to address the entanglement of

mixed states in presence of SSRs. Here, the preferred entanglement measure is taken to be Entanglement of Formation [56] $E_f(\rho)$, which in its SSR constrained version is expressed as

$$E_f^{\mathrm{SSR}}(\rho) = \min_{\{p_i,\psi_i\}} \sum_i p_i E_M(|\psi_i\rangle), \tag{2.40}$$

where the minimum is taken over all decompositions of ρ such that $|\psi_i\rangle$ obey the SSR, i.e. they have constant particle number.

A novel and powerful tool for entanglement characterization in the second-quantised representation emerged in the early 2010's, shifting the focus from the properties of states to those of algebras of commuting observables, identified as subsystems [27, 98–104]. The approach is based on identifying an algebra $\mathcal{A}$, generated by polynomials in the bosonic or fermionic creation and annihilation operators and containing all physically relevant observables. States are given by positive normalized linear functionals $\omega : \mathcal{A} \to \mathbb{C}$ with the properties

$$\begin{aligned} &\omega(A) \geq 0 \text{ if } A \geq 0, \\ &\omega(\mathbb{1}) = 1. \end{aligned} \tag{2.41}$$

Within such an algebraic approach entanglement is defined in terms of *commuting subalgebras* $(\mathcal{A}_1, \mathcal{A}_2)$ of $\mathcal{A}$, such that $\mathcal{A}_1 \cup \mathcal{A}_2 = \mathcal{A}$ and every element of $\mathcal{A}_1$ commutes with $\mathcal{A}_2$ and vice-versa, for short $[\mathcal{A}_1, \mathcal{A}_2] = 0$. This structure generalizes the partitioning of subsystems in terms of Hilbert spaces, and allows for the definition of *local observables* $\mathcal{O} = A_1 A_2$, where $A_1 \in \mathcal{A}_1$ and $A_2 \in \mathcal{A}_2$. A state ω is defined as separable if the expectation values for all local observables can be decomposed in convex combinations of factorised expectations:

$$\omega(A_1 A_2) = \sum_k \lambda_k \omega_k^{(1)}(A_1)\omega_k^{(2)}(A_2), \tag{2.42}$$

where $\omega^{(1,2)}$ are other states and $\lambda_k \geq 0 \, \forall k$, $\sum_k \lambda_k = 1$.

Research in the second-quantised picture investigated the entanglement and nonlocality properties of a system in relation to the choice of mode description [29, 105, 106]. In fact, systems of identical particles possessing both spin and spatial degrees of freedom are amenable to different partitioning into modes. Mode entanglement in many-body systems is addressed in such cases as either *spin entanglement* or *spatial entanglement*, depending on the fundamental subsystems chosen [107, 108].

In the early 2000's, instead, a series of publications was released looking at the first-quantised representation of systems of identical particles and the introduction of a notion

of entanglement which would account for the symmetry properties of the states [24,109]. Separability criteria are introduced for systems of two or more identical particles based on whether or not a symmetrized state was obtainable or not by projection on the relevant symmetry sector of a factorised state. We dedicate special focus to such results, for our work will be based in the first-quantised representation and briefly summarise the concept in the following section.

Slater Rank

An entanglement criterion for distinguishable-particle pure states is given by the assessment of the number of nonzero coefficients of a unique canonical representation, the Schmidt decomposition. An analogous canonical form can be obtained for symmetric and antisymmetric states. The derivation of the decomposition is based on the second-quantised representation but its form is also reflected in the first-quantised representation as well, in view of the duality between the two for fixed particle numbers. Let us consider the bipartite case first.

A generic state of two fermions can be expressed as

$$|\psi_{\mathcal{A}}\rangle = \sum_{j,k} w_{jk} c_j^\dagger c_k^\dagger |0\rangle \,, \tag{2.43}$$

where $w_{jk} = -w_{kj}$ are the coefficients of an antisymmetric matrix and $c_i^\dagger |0\rangle = |\phi_i\rangle$ are the fermionic creation operators whose action on the vacuum gives a single particle state. Any state of the form (2.43) is unitarily equivalent to a decomposition in a canonical form [24], analogous to the Schmidt decomposition, such that

$$|\psi_{\mathcal{A}}\rangle = \sum_{i=1}^{r_{\mathcal{A}}} \sqrt{\lambda_i} a_i^\dagger b_i^\dagger |0\rangle = \sum_{i=1}^{r_{\mathcal{A}}} \sqrt{\frac{\lambda_i}{2}} (|a_i\rangle |b_i\rangle - |b_i\rangle |a_i\rangle), \tag{2.44}$$

where $\{a_i, b_i\}_i$ are a set of orthonormal modes, $\lambda_i \geq 0$ are called *Slater coefficients* and $r_{\mathcal{A}}$ is called the *fermionic Slater rank* of the state. In order to distinguish standard entanglement arising from antisymmetrization from that independent of it, the authors in [24] call states with a Slater rank larger than one *correlated*.

Similarly, the generic bosonic state

$$|\psi_{\mathcal{S}}\rangle = \sum_{j,k} v_{jk} d_j^\dagger d_k^\dagger |0\rangle \,, \tag{2.45}$$

where $v_{jk} = v_{kj}$ are symmetric and $\{d_i^\dagger\}_i$ are the bosonic creation operators, admits a decomposition of doubly occupied orthonormal states [109]

$$|\psi_{\mathcal{S}}\rangle = \sum_{i=1}^{r_{\mathcal{S}}} \sqrt{\lambda_i} \left(b_i^\dagger\right)^2 |0\rangle = \sum_{i=1}^{r_{\mathcal{S}}} \sqrt{\lambda_i}\, |i\rangle\, |i\rangle\,, \tag{2.46}$$

where $r_{\mathcal{S}}$ is called *bosonic Slater rank*. A pure bosonic state is considered non-correlated [109] if it has bosonic Slater rank $r_{\mathcal{S}} = 1$.

The notion of Slater Rank may be generalised to systems of many identical particles, where it counts the minimum number of orthogonal Slater determinants or permanents in a superposition describing the quantum state [109]. Furthermore, a notion of *Slater number* may be defined for mixed states of identical bosons and fermions in analogy with the Schmidt number.

An identical-particle entanglement measure was put forward in [24] for pure fermionic states in connection with the notion of Slater rank. Given a fermionic state of the form (2.43), consider the quantity

$$\eta(|\psi_{\mathcal{A}}\rangle) = |\left\langle \tilde{\psi}_{\mathcal{A}} \middle| \psi_{\mathcal{A}} \right\rangle| = \left| \sum_{ijkl} \epsilon^{ijkl} w_{ij} w_{kl} \right|, \tag{2.47}$$

where the dual state $\left|\tilde{\psi}_{\mathcal{A}}\right\rangle = \sum_{kl} \tilde{w}_{kl} c_k^\dagger c_l^\dagger |0\rangle$ is defined in terms of the dual coefficient matrix $\tilde{w}_{kl} = \sum ij\epsilon^{ijkl} w_{kl}^*$, ϵ^{ijkl} being the totally antisymmetric tensor. It was proven in [110], and further discussed in [24, 109], that if $\eta(|\psi_{\mathcal{A}}\rangle) = 0$, then the Slater rank of $|\psi_{\mathcal{A}}\rangle$ is equal to 1. Therefore, it was argued in [109], that the quantity $\eta(|\psi_{\mathcal{A}}\rangle)$, referred to as *Slater correlation measure*, could be regarded as an identical-particle concurrence of entanglement measure, quantifying the correlations of states which are not given by a single Slater determinant. The measure was extended to cover mixed states by minimizing $\eta(|\psi_{\mathcal{A}}\rangle)$ over all pure state convex combinations:

$$\mathcal{C}_{sl}(\rho) = \inf \sum_i p_i \eta(|\psi_i\rangle). \tag{2.48}$$

Furthermore, a generalisation of the Slater correlation measure for multipartite states was put forward in [109].

The idea of Slater rank has inspired a number of publications over the course of the last two decades which have focused on the first-quantised representation of identical-particle systems and investigated the entanglement properties trying to set aside the

correlations arising from statistics. A variety of criteria and measures for identical-particle entanglement have been proposed in such works [28, 30, 31, 111], in some cases attributing different entanglement properties to the same states. For instance, in [28] a pure bosonic state is considered separable if and only if all particles are in the same single-particle state, that is to say if the state is a bosonic product state. In [111], on the other hand, the only bosonic pure separable states are identified as the Slater permanents (the symmetric counterpart of the determinant), that is to say when it is given by the symmetrization of orthogonal single-particle product states.

Role of detection process

The topic of entanglement of identical particles is yet to be settled, with debate and controversy still arising for certain aspects. For instance, in a 2014 paper by Killoran et al. [77], the authors claim to have established an extraction protocol obtaining a quantum enhancement by manipulation of a state whose correlations were due only to symmetrization. The procedure applied a beam splitter operation on an identical-particle Slater determinant state, obtaining a final state which was mode-entangled and with the same form as the original first-quantised state. The claim was backed by a series of papers by Lo Franco et al., who developed an independent identical-particle entanglement criteria [112] such that symmetrization was to be considered as entanglement as it could be used as a resource. In other publications however, [95, 113], it was argued that the entanglement in the output of the setup may be understood to be generated by the extraction process, which is nonlocal in the partitioning in which the final state entanglement is considered. This would contradict the statement that the entanglement from the symmetrization was transferred into the mode picture.

These considerations show that a relevant role in the characterization and detection of entanglement is played by the measurement process. In particular, for identical-particle systems the detection process may generate entanglement [114]. An elegant solution to account for measurement-induced entanglement and provide a characterization of entanglement with a subsystem structure reflecting the experimental setting was put forward in [115, 116]. Observables associated with experimental measurements of systems with an internal and an external (position) degree of freedom are of the form

$$O_D = (O_L \otimes \alpha) \otimes (O_R \otimes \beta) + (O_R \otimes \beta) \otimes (O_L \otimes \alpha), \tag{2.49}$$

where O_L and O_R are mutually orthogonal projectors describing spatial detectors, whereas α and β are observables for the internal degree of freedom. If measurements on a state ρ are performed spanning all elements of a complete set of observables $\{\chi_i\}_i$ for

the internal degree of freedom, the *detector-level* density matrix may be tomographically reconstructed by means of

$$\rho_D = \mathcal{N} \sum_{ij} \chi_i \otimes \chi_j \mathrm{Tr}\left(O_D \rho\right), \tag{2.50}$$

where $\mathcal{N}$ is a normalization constant. Thereby, by applying an entanglement measure to the detector-level state ρ_D, which is a composite state partitioned according to the measurement settings, one measures the *detector-level entanglement* between the two detectors.

To sum up, entanglement of identical particles is a rich and diverse field with unresolved questions still on the table. For instance, there are still opposing views concerning whether (anti)symmetrization should be considered on the same footing as entanglement generated by other processes, such as interaction or measurement [81, 90, 95, 112, 113]. In the following section we will introduce an entanglement criteria which takes an original approach at the identification of subsystems upon which we base the entanglement measure in our work.

2.6 Criteria for Entanglement of Identical Particles

An extensive treatment of the problem of classification of entanglement in identical-particle systems was put forward in the early 2000's in a series of papers by Ghirardi, Marinatto and Weber (GMW) [20, 21, 90, 91] providing entanglement criteria for identical-particle entanglement. The criterion does not rely only on the mathematical structure of the wavefunction, as in the standard definition of entanglement. Instead, it is based on the possibility of making objective statements about the properties of the individual subsystems, thus enabling to assign an *element of reality*, in Einstein's terms, to each particle. The GMW criteria is cast in terms of distinguishable-particle states where each particle may be labeled and addressed separately, however it is straightforwardly applicable to fermionic and bosonic states. The concept of objective properties may be described in mathematical terms and is introduced in this section.

Definition 2.1. Consider a composite quantum system $\mathcal{S} = \mathcal{S}_1 + \mathcal{S}_2$ of two distinguishable particles described by the pure density operator $\rho = |\psi\rangle\langle\psi|$ on the composite Hilbert space $\mathcal{H}^{(12)} = \mathcal{H}^{(1)} \otimes \mathcal{H}^{(2)}$. We will say that the subsystem $\mathcal{S}_1$ has a *complete set of properties* if and only if there exists a one dimensional projection operator P, defined on the Hilbert space $H^{(1)}$ of $\mathcal{S}_1$, such that:

$$\mathrm{Tr}(\mathcal{E}(P)\rho) = 1 \tag{2.51}$$

where

$$\mathcal{E}(P) = P \otimes \mathbb{1}. \tag{2.52}$$

This condition may be seen [21] to be equivalent to the standard notion of separability for distinguishable particles in pure states. In fact, given a pure separable state $|\psi\rangle = |\alpha\rangle\,|\beta\rangle$, we may choose $P = |\alpha\rangle\langle\alpha|$ and trivially satisfy condition (2.51). On the other hand, if we have a projector $P = |\alpha\rangle\langle\alpha|$, for a generic state $|\psi\rangle = \sum_i \sqrt{\lambda_i}\,|a_i\rangle\,|b_i\rangle$ in its Schmidt decomposition, the left-hand side of (2.51) reads

$$\mathrm{Tr}(\mathcal{E}(P)\rho) = \sum_{ij} \sqrt{\lambda_i\lambda_j}\,\langle a_i|\alpha\rangle\,\langle\alpha|a_i\rangle\,\langle b_i|b_j\rangle = \sum_i \lambda_i |\,\langle a_i|\alpha\rangle\,|^2, \tag{2.53}$$

which is equal to one only if there is only one term in the Schmidt decomposition of $|\psi\rangle$, e.g. $|a_1\rangle = |\alpha\rangle$. The state $|\psi\rangle$ is therefore a separable state. Furthermore, the above considerations grant that if one of the subsystems has a complete set of properties, necessarily so does the other [91].

The following definition was therefore put forward in [91] for the entanglement of pure states of distinguishable particles:

Definition 2.2. Consider the composite two-distinguishable-particle system $\mathcal{S} = \mathcal{S}_1 + \mathcal{S}_2$ described by the pure density operator $\rho = |\psi\rangle\langle\psi|$ on $\mathcal{H}^{(12)} = \mathcal{H}^{(1)} \otimes \mathcal{H}^{(2)}$. The subsystem $\mathcal{S}_1$ is non-entangled with $\mathcal{S}_2$ if it possesses a complete set of properties.

In dealing with identical particles, instead, one needs to account for the indistinguishability and thus the impossibility of applying labels to the particles. The following notion of complete set of properties for a subsystem is given for a two-identical-particle system (Definition 7.2 in [91]).

Definition 2.3. Given a composite quantum system $\mathcal{S} = \mathcal{S}_1 + \mathcal{S}_2$ of two identical particles described by the pure density operator $\rho = |\psi\rangle\langle\psi|$ on $\mathcal{H}^{(12)} = \mathcal{H} \otimes \mathcal{H}$, we will say that one of the constituents has a complete set of properties if and only if there exists a one dimensional projection operator P, defined on the Hilbert space $\mathcal{H}$ of each of the subsystems, such that:

$$\mathrm{Tr}(\mathcal{E}^{(2)}(P)\rho) = 1, \tag{2.54}$$

where

$$\mathcal{E}^{(2)}(P) = P \otimes (\mathbb{1} - P) + (\mathbb{1} - P) \otimes P + P \otimes P. \tag{2.55}$$

The above definition differs from 2.1 in that the operator $\mathcal{E}(P)$ in equation (2.52) is replaced by its exchange symmetric counterpart $\mathcal{E}^{(2)}(P)$ in (2.55). The quantity $\mathrm{Tr}(\mathcal{E}^{(2)}(P)\rho)$ now gives the probability of finding *at least* one particle, without specifying

which one, into the state onto which the one-dimensional operator P projects onto. In fact, the term $\mathrm{Tr}(P \otimes (\mathbb{1} - P)\rho)$ in (2.54) gives the probability that particle 1 has the property associated with P while the second one does not have said property, the term $\mathrm{Tr}((\mathbb{1} - P) \otimes P\rho)$ gives the same probability with particles interchanged and the term $\mathrm{Tr}(P \otimes P)\rho)$ gives the probability that both particles have the property P. The three aforementioned cases are mutually exclusive and therefore the sum of the three terms yields the probability that at least one particle possesses the property specified by P.

In the case of two identical fermions, Pauli exclusion prevents double occupation, so the third term always yields zero probability and the projection operator (2.55) can be replaced by

$$\mathcal{E}_F^{(2)}(P) = P \otimes \mathbb{1} + \mathbb{1} \otimes P. \tag{2.56}$$

In the fermionic case, in analogy with the distinguishable particle case, if one of the subsystems has a complete set of properties, so does the other. This is not true in general for bosons, though, since both particles may have the same property. Based on the above considerations, the authors of [91] introduce the following definition of identical-particle separability:

Definition 2.4. GMW criterion The identical constituents $\mathcal{S}_1$ and $\mathcal{S}_2$ of a composite quantum system $\mathcal{S} = \mathcal{S}_1 + \mathcal{S}_2$ are defined as non-entangled when both constituents possess a complete set of properties.

With the insight from such definition, Ghirardi, Marinatto and Weber were able to derive a Theorem for the pure state case, connecting complete sets of properties to the entanglement present *prior* to symmetrization or antisymmetrization. We outline a brief sketch of the proof to gain insight on the structure of the states classified as separable according to definition 2.4.

Theorem 2.5. *(Th. 7.1 in [91])* One of the identical constituents of a composite quantum system $\mathcal{S} = \mathcal{S}_1 + \mathcal{S}_2$, described by the pure normalized state $|\psi\rangle$ has a complete set of properties iff $|\psi\rangle$ is obtained by symmetrizing or antisymmetrizing a factorized state.

Proof. Suppose ψ is obtained by symmetrization of a factorized state, then we have

$$|\psi\rangle = N(|\chi\rangle\,|\phi\rangle \pm |\phi\rangle\,|\chi\rangle). \tag{2.57}$$

As the single particle Hilbert spaces are identical we may always write

$$|\chi\rangle = \alpha\,|\phi\rangle + \beta\,|\phi_\perp\rangle\,, \qquad \langle\phi|\phi_\perp\rangle = 0 \tag{2.58}$$

and by choosing $P = |\phi\rangle\langle\phi|$ we get

$$\mathrm{Tr}(\mathcal{E}^{(2)}(P)\rho) = \frac{2(1 \pm |\alpha|^2)}{2(1 \pm |\alpha|^2)} = 1 \tag{2.59}$$

On the other hand, if $\mathrm{Tr}(\mathcal{E}^{(2)}(P)\rho) = 1$, since $\mathcal{E}^{(2)}(P)$ is a projector

$$\mathcal{E}^{(2)}(P)\,|\psi\rangle = |\psi\rangle\,. \tag{2.60}$$

However, if we choose an orthonormal set of single-particle states $\{|\varphi_i\rangle\}$ such that $P\,|\varphi_0\rangle = |\varphi_0\rangle$ and decompose the state as

$$|\psi\rangle = \sum_{ij} c_{ij}\,|\varphi_i\rangle\,|\varphi_j\rangle\,, \qquad \sum_{ij} |c_{ij}|^2 = 1 \tag{2.61}$$

one gets

$$\mathcal{E}^{(2)}(P)\,|\psi\rangle = c_{00}\,|\varphi_o\rangle\,|\varphi_o\rangle + |\varphi_0\rangle \left(\sum_{j\neq 0} c_{0j}\,|\varphi_j\rangle\right) + \left(\sum_{j\neq 0} c_{j0}\,|\varphi_j\rangle\right)|\varphi_0\rangle = |\psi\rangle\,. \tag{2.62}$$

Now consider the fermionic case, where $c_{00} = 0$. If we introduce the normalized state $|\Xi\rangle = \sqrt{2}\sum_{j\neq 0} c_{0j}\,|\varphi_j\rangle$, then

$$|\psi\rangle = \frac{1}{\sqrt{2}}\left(|\varphi_0\rangle\,|\Xi\rangle - |\Xi\rangle\,|\varphi_0\rangle\right). \tag{2.63}$$

In the bosonic case, instead, we introduce the state

$$|\Theta\rangle = \sqrt{\frac{4}{2 - |c_{00}|^2}}\left(\frac{c_{00}}{2}\,|\varphi_0\rangle + \sum_{j\neq 0} c_{0j}\,|\varphi_j\rangle\right) \tag{2.64}$$

and obtain the two particle state

$$|\psi\rangle = \sqrt{\frac{2 - |c_{00}|^2}{4}}(|\varphi_0\rangle\,|\Theta\rangle + |\Theta\rangle\,|\varphi_0\rangle). \tag{2.65}$$

We point out for further reference that $|\varphi_0\rangle$ and $|\Theta\rangle$ are orthogonal only if $c_{00} = 0$, in which case $|\psi\rangle$ is obtained by symmetrizing a state of factorised orthogonal single-particle states, with projection probability $1/2$. □

It is therefore possible to state the following Theorems for the bosonic and fermionic case:

Theorem 2.6. *(Th. 7.2 in [91]) The identical fermions $\mathcal{S}_1$ and $\mathcal{S}_2$ of a composite quantum system $\mathcal{S} = \mathcal{S}_1 + \mathcal{S}_2$ described by the pure normalized state $|\psi\rangle$ are non-entangled iff $|\psi\rangle$ is obtained by antisymmetrizing a factorized state.*

Theorem 2.7. *(Th. 7.3 in [91]) The identical bosons of a composite quantum system $\mathcal{S} = \mathcal{S}_1 + \mathcal{S}_2$ described by the pure normalized state $|\psi\rangle$ are non-entangled iff either the state is obtained by symmetrizing a factorized product of two orthogonal states or if it is the product of the same state for the two particles.*

Having reviewed a number of seminal papers tackling the topic of identical-particle entanglement and analysed the critical aspects which make the quantification of said entanglement a difficult task, we may proceed to lay out the original work in the field carried out within this thesis. Our work relies on the framework and the definitions for separability and entanglement reviewed in section 2.6. In our proposal we will take further the implications of Theorems 2.6, 2.7 and put forward a quantitative entanglement measure for identical particles.

2.7 Quantifying Identical-Particle Entanglement

The Theorems 2.6 and 2.7 arising from the GMW identical-particle entanglement criteria state that the separability of a fermionic or bosonic pure state may be inferred by its separability properties *prior* to the (anti)symmetrization due to spin-statistics. It is desirable to extend this principle to allow for the quantification of entanglement in identical-particle systems.

For fermionic systems, the notion of quantification of entanglement prior to symmetrization is captured by the Slater rank. To show this, let us consider the simplest nontrivial scenario of two spin 1/2 fermions with spatial degree of freedom of dimension 2. The total first-quantised Hilbert space will thus be given by $\mathcal{H}_{\mathcal{A}} = (\mathcal{H}_x \otimes \mathcal{H}_\sigma) \wedge (\mathcal{H}_x \otimes \mathcal{H}_\sigma)$, where $\mathcal{H}_x \simeq \mathbb{C}^2$ is the Hilbert space for the space d.o.f. spanned by the ONB $\{|L\rangle, |R\rangle\}$ and $\mathcal{H}_\sigma \simeq \mathbb{C}^2$ is relative to the spin d.o.f spanned by the ONB $\{|\uparrow\rangle, |\downarrow\rangle\}$.

Consider the two fermion state given by

$$|\psi_s\rangle = \frac{1}{\sqrt{2}}(|L\uparrow\rangle |R\downarrow\rangle - |R\downarrow\rangle |L\uparrow\rangle), \tag{2.66}$$

which has Schmidt rank equal to two, Slater rank equal to one and is thus unentangled according to the GMW criteria. In fact, a state with Slater rank 1 is the antisymmetrization of a product state, and is therefore unentangled according to definition 2.4.

It is straightforward to see that the state may be obtained as the antisymmetrization of the factorised state

$$|\sigma_s\rangle = |L\uparrow\rangle\,|R\downarrow\rangle\,. \tag{2.67}$$

Indeed, $|\sigma_s\rangle$ is the state with the minimum entanglement (it is separable) projecting on (2.66) and it has Schmidt rank equal to 1. Now consider the state

$$|\psi_e\rangle = \frac{1}{2}(|L\uparrow\rangle\,|R\downarrow\rangle + |L\downarrow\rangle\,|R\uparrow\rangle - |R\downarrow\rangle\,|L\uparrow\rangle - |R\uparrow\rangle\,|L\downarrow\rangle), \tag{2.68}$$

it has Schmidt rank 4 and Slater rank 2. Furthermore, it may be obtained by antisymmetrizing the entangled state

$$|\sigma_e\rangle = \frac{1}{\sqrt{2}}((|L\uparrow\rangle\,|R\downarrow\rangle + |L\downarrow\rangle\,|R\uparrow\rangle), \tag{2.69}$$

which has Schmidt rank 2. Indeed, no pure state with Schmidt rank smaller than 2, i.e. a product state, exists whose antisymmetric image is (2.68) [24]. The Schmidt rank is a coarse-grained entanglement measure, such that states with higher Schmidt rank can be considered as more entangled. Therefore, the previous examples suggest that the Slater rank is a coarse-grained identical-particle entanglement measure and it can be interpreted as the Schmidt rank of a given fermionic state prior to the antisymmetrization. The concept is illustrated in Figure 2.1.

The picture emerging from these considerations suggests to define an entanglement measure for a target identical-particle state based on a distinguishable-particle measure, many of which are known and well-characterised, and applying it to an unsymmetrized state which projects onto the target symmetric or antisymmetric state. For any state ρ with a given symmetry, however, there are infinite states whose projection on the corresponding symmetry sector is equal to ρ.

It appears clear that for all fermionic and almost all bosonic states the symmetrization procedure increases the entanglement, so this suggests to measure the entanglement of ρ as the minimum entanglement of a state σ whose antisymmetric image is proportional to ρ. We may put forward a definition for such a measure.

Given a target identical-particle state ρ_μ, where $\mu = \mathcal{S}$ indicates the symmetric subspace and $\mu = \mathcal{A}$ indicates the antisymmetric subspace, its identical-particle entanglement may quantified by a measure $\tilde{E}_\mu$ such that

$$\tilde{E}_\mu(\rho_\mu) = \min_\sigma\{E(\sigma) :\ P_\mu\sigma P_\mu = \mathrm{Tr}(P_\mu\sigma)\rho_\mu\}, \tag{2.70}$$

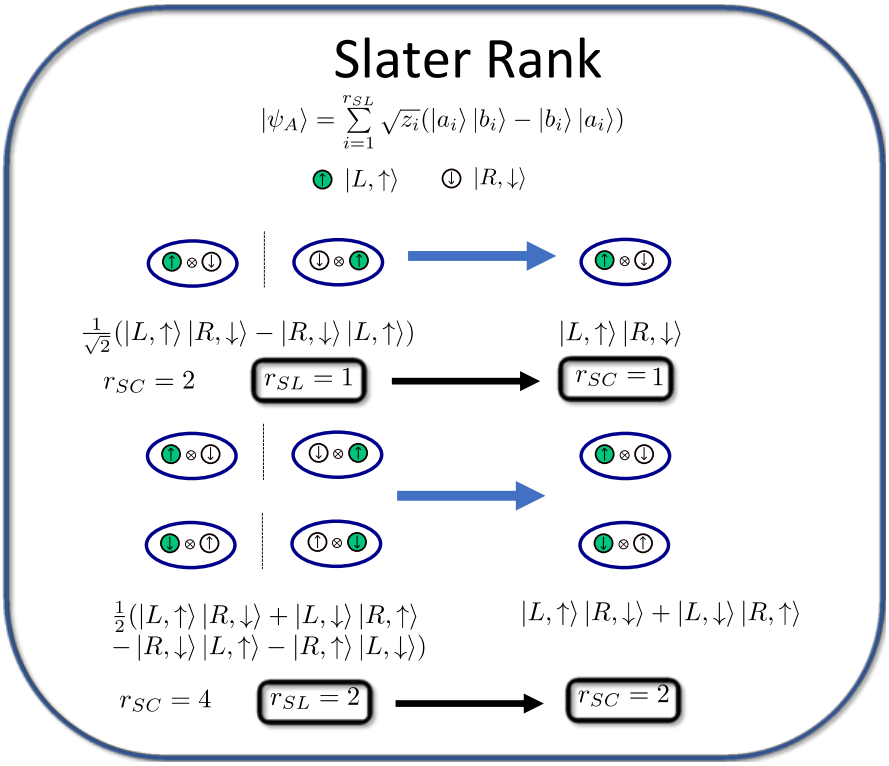

FIGURE 2.1: Illustration of interpretation of the Slater rank as a coarse grained measure identical-particle entanglement. We consider two example states of a system of two spin-1/2 fermions in a double well. The single particle states are colour labelled according to the left (L) or right (R) well and up ($\uparrow$) and down ($\downarrow$) spin. The schematic vertical line on the left-hand side represents the exchange symmetry directive, whereas r_{SC} and r_{SL} indicate the Schmidt and Slater rank of the state respectively. The states indicated on the right-hand side of the illustration belong to the class of states with minimum Schmidt rank projecting on their exchange symmetric counterparts on the left-hand side. The minimum Schmidt rank of the states prior to antisymmetrization matches the Slater rank of the antisymmetrized states.

where σ is a state with no symmetry constraint and E is a standard distinguishable-particle entanglement measure.

There is a problem with definition (2.70) in the fermionic case, however, since it does not account for the probability of the mapping on ρ_μ. This opens the possibility of having trivial minima for the optimization instance. In fact, for a given antisymmetric target state $\rho_{\mathcal{A}}$, any symmetric state automatically satisfies the constraint in the minimization on the right-hand side of (2.70), including all those which are separable. Such a measure would therefore classify all fermionic states as separable, trivializing the entanglement measure. An additional constraint is required in the minimization

instance in (2.70), which we may derive by looking into the properties of the symmetric and antisymmetric images of separable states. In particular, in order to overcome the problem of classifying all fermionic states as separable it is sufficient to lower bound the projection probability on the antisymmetric subspace. We will therefore look at a class of entanglement measures given by

$$E_\mu(\rho_\mu, p_\mu) = \min_\sigma\{E(\sigma) : \ P_\mu \sigma P_\mu = \mathrm{Tr}(P_\mu\sigma)\rho_\mu, \ \mathrm{Tr}(P_\mu\sigma) \geq p_\mu\}, \tag{2.71}$$

where $p_\mu > 0$ is the projection probability lower bound for a given symmetry class μ.

We will see how an appropriate choice for such constraint leads to a well-defined entanglement measure which we will prove to be consistent with the GMW criteria.

2.7.1 Properties of the bipartite (anti)symmetric subspace

We will look into the properties of the symmetry sectors in the fermionic and bosonic cases separately.

Fermions

To begin with, we investigate the structure of separable pure states in the bipartite case. Such states are of the kind $|\psi_{\mathrm{sep}}\rangle = |\alpha\rangle\,|\beta\rangle$, with normalized single particle states α and β which need not necessarily be orthogonal. The normalized antisymmetrization of such states, which describes fermionic non-entangled states (adopting the Ghirardi et al. [21] criterion), reads

$$\frac{P_{\mathcal{A}}\,|\psi_{\mathrm{sep}}\rangle}{\|P_{\mathcal{A}}\,|\psi_{\mathrm{sep}}\rangle\,\|} = \frac{|\alpha\rangle\,|\beta\rangle - |\beta\rangle\,|\alpha\rangle}{\sqrt{2(1 - |\,\langle\alpha|\beta\rangle\,|^2)}}. \tag{2.72}$$

Given a vector $|v\rangle$ in a state vector space $\mathcal{H} \simeq \mathbb{C}^d$, it can be expressed as a linear combination of $|\alpha\rangle$ and a vector $|\bar{\alpha}\rangle$ which is orthogonal to $|\alpha\rangle$ and dependent on the vector $|v\rangle$. Therefore, any state belonging to the vector space may be written as

$$|\beta\rangle = \langle\alpha|\beta\rangle\,|\alpha\rangle + \sqrt{1 - |\,\langle\alpha|\beta\rangle\,|^2}\,|\bar{\alpha}\rangle \tag{2.73}$$

and it is straightforward to see that any separable antisymmetric state is equivalent to one obtained antisymmetrizing orthogonal states:

$$\frac{P_{\mathcal{A}}\,|\psi_{\mathrm{sep}}\rangle}{\|P_{\mathcal{A}}\,|\psi_{\mathrm{sep}}\rangle\,\|} = \frac{|\alpha\rangle\,|\bar{\alpha}\rangle - |\bar{\alpha}\rangle\,|\alpha\rangle}{\sqrt{2}}. \tag{2.74}$$

We may show that the projection probability is related to the overlap of the two single particle states for a given state $\psi_{\text{sep}} = |\alpha\rangle\langle\alpha| \otimes |\beta\rangle\langle\beta|$,

$$\text{Tr}(P_{\mathcal{A}}\psi_{\text{sep}}) = \text{Tr}\left(\frac{1}{2}(\mathbb{1} - V)\psi_{\text{sep}}\right) = \frac{1}{2}(1 - |\langle\alpha|\beta\rangle|^2) \tag{2.75}$$

where V is the swap operator. Thus if an antisymmetric state can be obtained by antisymmetrizing a separable pure state, it can always be obtained by antisymmetrizing a separable pure state with extremal projection probability $\text{Tr}(P_{\mathcal{A}}\psi'_{\text{sep}}) = \max\{\text{Tr}(P_{\mathcal{A}}\psi) : \psi = \psi_{\text{sep}}\} = 1/2$. The result may be extended to the mixed case by considering separable density matrices of the form

$$\sigma_{\text{sep}} = \sum_i p_i \sigma_i \otimes \rho_i \tag{2.76}$$

with $\sigma_i = |\psi_i\rangle\langle\psi_i|$ and $\rho_i = |\phi_i\rangle\langle\phi_i|$ and noting that the projected state has the same form if we replace each $|\phi_i\rangle$ with the orthogonal complement $|\bar{\psi}_i\rangle$ of $|\psi_i\rangle$. If we call the mixed state obtained with the latter modification σ'_{sep}, we also have $\text{Tr}(P_{\mathcal{A}}\sigma'_{\text{sep}}) = 1/2$.

A useful outer approximation, for the purpose of entanglement quantification, of the set of separable states is given by the set $\{\rho^{\Gamma}_{\text{PPT}} \geq 0\}$ of PPT states, so it will prove interesting to investigate the antisymmetric image of this class of states. Let us therefore evaluate $\max\{\text{Tr}(P_{\mathcal{A}}\rho) : \rho = \rho_{\text{PPT}}\}$ for mixed states. We will show that it is equivalent to maximizing over a set of special states, called *Werner states*, which have the important feature of being separable if and only if they are PPT [117].

Consider the following functional $\tau[\cdot]$, called *twirling operator*:

$$\tau(\sigma) = \int \mathrm{d}U (U \otimes U)\sigma(U^{\dagger} \otimes U^{\dagger}), \tag{2.77}$$

where the integration is performed over the *Haar measure* $\mathrm{d}U$ for unitary operators [118]. Functional τ projects a generic density matrix σ onto the subset of the Werner states parametrized by a single parameter p_σ,

$$\tau(\sigma) = (1 - p_\sigma)\frac{2}{d(d+1)}P_{\mathcal{S}} + p_\sigma \frac{2}{d(d-1)}P_{\mathcal{A}}. \tag{2.78}$$

It is trivial to see that $\tau(P_{\mathcal{A}}) = P_{\mathcal{A}}$ and thus it is possible to write

$$\text{Tr}\big(P_{\mathcal{A}}\sigma\big) = \text{Tr}\big(\tau(P_{\mathcal{A}})\sigma\big) \tag{2.79}$$

and by cyclicity of the trace operator

$$\mathrm{Tr}\big(\tau(P_{\mathcal{A}})\sigma\big) = \mathrm{Tr}\big(P_{\mathcal{A}} \int \mathrm{d}U (U^\dagger \otimes U^\dagger)\sigma(U \otimes U)\big). \tag{2.80}$$

Being the integration over all unitaries it is true that

$$\tau(\sigma) = \int \mathrm{d}U (U^\dagger \otimes U^\dagger)\sigma(U \otimes U), \tag{2.81}$$

thus giving us the result

$$\mathrm{Tr}\big(P_{\mathcal{A}}\sigma\big) = \mathrm{Tr}\big(P_{\mathcal{A}}\tau(\sigma)\big) = p_\sigma \frac{2}{d(d-1)} \mathrm{Tr}\big(P_{\mathcal{A}}^2\big) = p_\sigma \tag{2.82}$$

We have just shown that the maximization of $\mathrm{Tr}(P_{\mathcal{A}}\sigma)$ over all possible PPT states is equivalent to maximizing over the set of PPT Werner states, wherein the extremal value for separability in the bipartite case is $p_\sigma = 1/2$ and is identical to that for PPT-ness.

In general, therefore, we may state the following proposition:

Proposition 2. If $\exists\ \sigma_{\mathrm{sep}}$:

$$\frac{P_{\mathcal{A}}\sigma_{\mathrm{sep}}P_{\mathcal{A}}}{\mathrm{Tr}(P_{\mathcal{A}}\sigma_{\mathrm{sep}})} = \rho_{\mathcal{A}}$$

then $\exists\ \sigma'_{\mathrm{sep}}$ with the same projection on the antisymmetric subspace but projection probability

$$\mathrm{Tr}(P_{\mathcal{A}}\sigma'_{\mathrm{sep}}) = \max\{\mathrm{Tr}(P_{\mathcal{A}}\sigma) :\ \sigma = \sigma_{\mathrm{sep}}\} = \max\{\mathrm{Tr}(P_{\mathcal{A}}\sigma) :\ \sigma^\Gamma = \sigma\} = \frac{1}{2}. \tag{2.83}$$

Bosons

The bosonic case presents some differences from the fermionic one, for instance there may be symmetric pure separable states. Again, let us begin with a pure separable state $|\psi_{\mathrm{sep}}\rangle = |\alpha\rangle \otimes |\beta\rangle$ and let's take its symmetrization

$$\frac{P_{\mathcal{S}}\,|\psi_{\mathrm{sep}}\rangle}{\|P_{\mathcal{S}}\,|\psi_{\mathrm{sep}}\rangle\,\|} = \frac{|\alpha\rangle\,|\beta\rangle + |\beta\rangle\,|\alpha\rangle}{\sqrt{2(1 + |\,\langle\alpha|\beta\rangle\,|^2)}}. \tag{2.84}$$

Decomposing $|\beta\rangle$ in its component along $|\alpha\rangle$ and its orthogonal component we may find that

$$\frac{P_{\mathcal{S}}\,|\psi_{\mathrm{sep}}\rangle}{\|P_{\mathcal{S}}\,|\psi_{\mathrm{sep}}\rangle\,\|} = \frac{2\,\langle\alpha|\beta\rangle\,|\alpha\rangle\,|\alpha\rangle + \sqrt{2(1 - |\,\langle\alpha|\beta\rangle\,|^2)}(|\alpha\rangle\,|\bar{\alpha}\rangle + |\bar{\alpha}\rangle\,|\alpha\rangle)}{\sqrt{2(1 + |\,\langle\alpha|\beta\rangle\,|^2)}}. \tag{2.85}$$

It is evident that, unlike the fermionic case, choosing $|\beta\rangle = |\bar{\alpha}\rangle$ does not yield the same state, due to the non-cancellation of the $|\alpha\rangle\,|\alpha\rangle$ term. In general, thus, a statement similar to Proposition 2, which we proved in the fermionic case, does not hold in the bosonic case. Let us investigate the pure state case in order to show why.

Consider the parametrization $|\beta\rangle = \cos\theta\,|\alpha\rangle + e^{i\varphi}\sin\theta\,|\bar{\alpha}\rangle$, leading to the expression

$$|\psi_{\text{sep}}\rangle = |\alpha\rangle\,|\beta\rangle = |\alpha\rangle\left(\cos\theta\,|\alpha\rangle + e^{i\varphi}\sin\theta\,|\bar{\alpha}\rangle\right) \tag{2.86}$$

with overlap $\langle\alpha|\beta\rangle = \cos\theta$. The symmetrization of $|\psi_{\text{sep}}\rangle$ reads

$$\frac{P_{\mathcal{S}}\,|\psi_{\text{sep}}\rangle}{\|P_{\mathcal{S}}\,|\psi_{\text{sep}}\rangle\,\|} = \frac{2\cos\theta\,|\alpha\rangle\,|\alpha\rangle + e^{i\varphi}\sin\theta(|\alpha\rangle\,|\bar{\alpha}\rangle + |\bar{\alpha}\rangle\,|\alpha\rangle)}{\sqrt{2(1+\cos^2\theta)}}. \tag{2.87}$$

Suppose now we want to obtain the same vector by symmetrizing a separable state given by the tensor product of two non-overlapping single-particle states:

$$\frac{P_{\mathcal{S}}\,|\psi_{\text{sep}}\rangle}{\|P_{\mathcal{S}}\,|\psi_{\text{sep}}\rangle\,\|} = \frac{P_{\mathcal{S}}\,|\alpha'\rangle\,|\beta'\rangle}{\|P_{\mathcal{S}}\,|\alpha'\rangle\,|\beta'\rangle\,\|} \tag{2.88}$$

with $\langle\alpha'|\beta'\rangle = 0$. In general we may parametrize the new states as $|\alpha'\rangle = \cos\varepsilon\,|\alpha\rangle + e^{i\phi}\sin\varepsilon\,|\bar{\alpha}\rangle$ and $|\beta'\rangle = -\sin\varepsilon\,|\alpha\rangle + e^{i\phi}\cos\varepsilon\,|\bar{\alpha}\rangle$ and obtain the symmetric state

$$\begin{aligned}\frac{P_{\mathcal{S}}\,|\alpha'\rangle\,|\beta'\rangle}{\|P_{\mathcal{S}}\,|\alpha'\rangle\,|\beta'\rangle\,\|} =& \frac{1}{\sqrt{2}}\big(-2\cos\varepsilon\sin\varepsilon\,|\alpha\rangle\,|\alpha\rangle + 2e^{2i\phi}\cos\varepsilon\sin\varepsilon\,|\bar{\alpha}\rangle\,|\bar{\alpha}\rangle + \\ & e^{i\phi}(\cos^2\varepsilon - \sin^2\varepsilon)(|\alpha\rangle\,|\bar{\alpha}\rangle + |\bar{\alpha}\rangle\,|\alpha\rangle)\big).\end{aligned} \tag{2.89}$$

It is easy to see that in order for equations (2.87) and (2.89) to be equal the two conditions

$$\begin{cases}\cos\epsilon\sin\epsilon = \frac{\cos\theta}{\sqrt{1+\cos^2\theta}}, & \forall\theta,\varepsilon \\ \cos\epsilon\sin\epsilon = 0 & \forall\varepsilon,\end{cases} \tag{2.90}$$

must be met, which is impossible. The symmetrization of two factorised non-orthogonal states may not be obtained by symmetrizing two orthogonal ones, which would have projection probability on the symmetric subspace equal to $1/2$.

We have thus shown that in general it is not possible, au contraire to the fermionic case, to reproduce a state given by the symmetrization of the tensor product of two non-orthogonal states by symmetrizing another product state with orthogonal single-particle wavefunctions.

Furthermore, we may look into the symmetric image of PPT states by applying the twirling operator (2.77) in analogy with Equation (2.83). We thus obtain

$$\min\{\mathrm{Tr}(P_{\mathcal{S}}\sigma) : \sigma^{\Gamma} = \sigma\} = \frac{1}{2}. \tag{2.91}$$

2.7.2 Identical-particle entanglement and projection probability on the (anti)symmetric subspace.

In the previous section we investigated the relationship between the (anti)symmetric image of separable states and the projection probability on the respective symmetry subspace. We may draw conclusions from such relations to fix the projection probability in definition (2.71) of identical-particle entanglement.

First, it is evident that the projection probability on the antisymmetric subspace for a separable state $\mathrm{Tr}(P_{\mathcal{A}}\sigma_{\mathrm{sep}})$ needs to lie in the $]0, 1/2]$ interval. For the purpose of quantifying identical-particle entanglement of an antisymmetric state using the measure (2.70), in order to establish whether or not there exists a separable state projecting onto the target state $\rho_{\mathcal{A}}$, based on Proposition 2 it is sufficient to constrain the minimisation in (2.70) to the states with projection probability $\mathrm{Tr}(P_{\mathcal{A}}\sigma) \geq p$, with $p \equiv p_{\mathrm{sep}} = 1/2$. In fact, with such lower bound our entanglement measure will correctly return zero if there exist a separable state projecting on the target antisymmetric state. We may indeed argue that p_{sep} is the best choice of projection probability in our optimization instance. States with projection probability larger that p_{sep} lie outside of the antisymmetric image of separable and PPT states and would fail to detect if a state may be obtained by antisymmetrizing a PPT state. On the other hand, for small enough values of p we will prove in section 4.3 that the optimal state for the optimization instance may return PPT-entangled states, thus failing to the detect entanglement. Setting $p = p_{\mathrm{sep}} = 1/2$ fixes the bound to the maximum projection probability (on the antisymmetric subspace) of a separable state, avoiding both the lack of sensitivity to PPT-entanglement for $p \in [0, 1/2[$, and the lack of unentangled identical-particle states for $p \in]1/2, 1]$. Furthermore, we will see in section 2.11 that such choice is consistent with the GMW criteria and its corollaries.

The bosonic case has a richer structure, and we will see that special care is required in treating the projection probability in relation to identical-particle entanglement. Let us begin by observing that

$$\mathrm{Tr}(P_{\mathcal{S}}\psi_{\mathrm{sep}}) = \frac{1}{2}(1 + |\langle\alpha|\beta\rangle|^2), \quad \in \left[\frac{1}{2}, 1\right]. \tag{2.92}$$

Using the same reasoning as for the fermionic case the codomain of the probability projection for separable and PPT states can be shown to be the same also for mixed states. We thus know that if there exists a separable state that projects onto the target symmetric state, its projection probability must lie in the $[1/2, 1]$ interval. This would seem to suggest, similarly to the fermionic case, that the lower bound for the probability of projecting on the symmetric subspace should be given by $1/2$.

An additional consideration is required in the bosonic case, however. In order for separable identical-boson pure states to be correctly identified as those obtained by symmetrizing *orthogonal* factorised states (Theorem 2.7), the projection probability needs to be fixed to $1/2$. Consider the expression in equation (2.65), defining the structure of separable bosonic states according to the GMW criteria (2.4). The coefficient c_{00} is equivalent to the overlap $\langle\alpha|\beta\rangle$ in (2.87), and therefore related to the projection probability $\mathrm{Tr}(P_{\mathcal{S}} |\psi_{\mathrm{sep}}\rangle\langle\psi_{\mathrm{sep}}|) = 1/2(1 + |\langle\alpha|\beta\rangle|^2)$. Allowing a projection probability larger than $1/2$ in the IPE definition (2.71) would imply defining states which are the symmetrization of non-orthogonal factorised states as separable, which is in contradiction with the GMW criteria (2.7). Let us discuss a simple example of this fact.

Consider a non-orthogonal two-identical-qubit product state $|\psi\rangle = |0\rangle |+\rangle$, where $|+\rangle = (|0\rangle + |1\rangle)/\sqrt{2}$, and its symmetrization

$$|\psi_{\mathcal{S}}\rangle = \frac{P_{\mathcal{S}} |\psi\rangle}{\| P_{\mathcal{S}} |\psi\rangle \|} = \frac{1}{\sqrt{3}}\Big[\sqrt{2} |0\rangle |0\rangle + \frac{1}{\sqrt{2}}(|0\rangle |1\rangle + |1\rangle |0\rangle)\Big]. \tag{2.93}$$

We may immediately verify that $|\psi\rangle$ is an optimal state for $E_{\mathcal{S}}(|\psi_{\mathcal{S}}\rangle\langle\psi_{\mathcal{S}}|, 1/2)$ in equation (2.71), since $\mathrm{Tr}(P_{\mathcal{S}} |\psi\rangle\langle\psi|) \geq 1/2$ and $P_{\mathcal{S}} |\psi\rangle\langle\psi| P_{\mathcal{S}} = \mathrm{Tr}(P_{\mathcal{S}} |\psi\rangle\langle\psi|) |\psi_{\mathcal{S}}\rangle\langle\psi_{\mathcal{S}}|$.

Therefore $E_{\mathcal{S}}(|\psi_{\mathcal{S}}\rangle\langle\psi_{\mathcal{S}}|, 1/2) = E(|\psi\rangle\langle\psi|) = 0$, because $|\psi\rangle$ is a separable state. With the projection probability lower bounded by $1/2$ our identical-particle entanglement measure (2.71) classifies as unentangled a state which is obtained by symmetrizing a non-orthogonal product state, which is incompatible with the GMW criteria (2.4) and the associated Theorem (2.7).

Consistency with the criteria for the case of symmetrized orthogonal product states may be recovered by replacing the inequality for the projection probability in (2.71) with an equality to $1/2$. We will refer to the bosonic identical-particle entanglement measure for a state $\rho_{\mathcal{S}}$ with fixed projection probability on the symmetric subspace as

$$E_{\mathcal{S}}(\rho_{\mathcal{S}}) = \min_{\sigma}\{E(\sigma) : P_{\mathcal{S}}\sigma P_{\mathcal{S}} = \frac{1}{2}\rho_{\mathcal{S}}\}. \tag{2.94}$$

Because $\mathrm{Tr}(P_{\mathcal{S}} |\psi\rangle\langle\psi|) = 3/4$, $|\psi\rangle$ is not an optimal state for the instance $E_{\mathcal{S}}(|\psi_{\mathcal{S}}\rangle\langle\psi_{\mathcal{S}}|)$ with the projection probability fixed. Furthermore, we proved in section 2.7.1 that no

product state exists projecting on $\psi_{\mathcal{S}}$ with probability 1/2.

On the other hand, the state

$$|\psi_+\rangle = \frac{1}{\sqrt{2}}(|0\rangle\,|1\rangle + |1\rangle\,|0\rangle) \tag{2.95}$$

is classified as separable by $E_{\mathcal{S}}$, since $E_{\mathcal{S}}(|\psi_+\rangle\langle\psi_+|) = 0$ with optimal state $|\phi\rangle = |0\rangle\,|1\rangle$ and $\mathrm{Tr}(P_{\mathcal{S}}\,|\phi\rangle\langle\phi|) = 1/2$. This is consistent with the GMW criteria, since $|\psi_+\rangle$ is the symmetrization of the orthogonal product state $|\phi\rangle$. The examples we provided consist of an argument in favour of having a fixed projection probability as a constraint in (2.71), rather than a lower bound. The bosonic case has a special set of states, however, where this argument does not apply. In fact, symmetric product states are clearly separable, yet they cannot be obtained by symmetrizing a product of orthogonal states with projection probability on the symmetric subspace equal to $1/2$, as shown in section 2.7.1.

The above considerations suggest that, in analogy with the formulation of Theorem 2.7, the quantification of entanglement prior to symmetrization should treat the case of symmetric product states and symmetrized orthogonal product states separately. The IPE quantification of bosonic states may then be carried out in the following way. Given a bosonic state $\rho_{\mathcal{S}}$, if the standard entanglement of the bosonic state is zero, that is to say if the state is separable even *post* symmetrization, then its identical-particle entanglement is zero. If the standard entanglement of $\rho_{\mathcal{S}}$ is nonzero, then its entanglement measure is given by $E_{\mathcal{S}}(\rho_{\mathcal{S}})$. An intuitive argument which justifies this approach is that the key problem with the quantification of identical-particle entanglement is associated with the fact that, in most cases, the symmetrization of states increases entanglement. In the case of symmetric product states this is not an issue and there is no need to assess the entanglement prior to symmetrization.

Fixing the projection probability is not necessary for fermions, due to the property of antisymmetric states of cancelling the c_{00} terms in eq. (2.65) by construction. We may however prove that replacing the lower bound in (2.71) on the projection probability with an equality yields the same optimal value for the entanglement measure, provided the measure of choice is convex.

To prove this let us begin with considering the state σ_f, taken as the optimal state of our minimization instance in (2.71). By definition, σ_f needs to satisfy the following properties:

- $P_{\mathcal{A}}\sigma_f P_{\mathcal{A}} = \mathrm{Tr}(P_{\mathcal{A}}\sigma_f)\rho_{\mathcal{A}}$
- $\mathrm{Tr}(P_{\mathcal{A}}\sigma_f) \geq p$

- $E(\sigma_f) \leq E(\sigma)\, \forall \sigma$ satisfying the previous two conditions.

Now let us suppose that $\exists \sigma_f : \mathrm{Tr}(P_{\mathcal{A}}\sigma_f) > p$. We may parametrize it as

$$\mathrm{Tr}(P_{\mathcal{A}}\sigma_f) = \frac{p}{t} \quad t \in]0,1[. \tag{2.96}$$

Also, it is always possible to construct a second state

$$\sigma' = t\sigma_f + (1-t)\frac{P_{\mathcal{S}}}{d_{\mathcal{S}}}, \tag{2.97}$$

where $P_{\mathcal{S}}/d_{\mathcal{S}}$ is the normalized projector on the symmetric subspace. It is straightforward to see that σ' satisfies the first two conditions for being an optimal state but we may see, by bearing in mind that $E(P_{\mathcal{S}}/d_{\mathcal{S}}) = 0$, that

$$E(\sigma') \leq tE(\sigma_f) + (1-t)E(P_{\mathcal{S}}/d_{\mathcal{S}}) = tE(\sigma_f) < E(\sigma_f) \tag{2.98}$$

where we applied the convexity of the entanglement measure E. The last equation contradicts the third condition for optimality for σ_f, thus leading to the conclusion that the hypothesis $\mathrm{Tr}(P_{\mathcal{A}}\sigma_f) > p$ is absurd if σ_f is an optimal state.

Based the above considerations we may replace the lower bound on the projection probability in the definition (2.71) of identical-particle entanglement with an equality both in the bosonic and fermionic case. In the bipartite case, therefore, we may put forward the following mathematically rigorous definition:

Definition 2.8. Given a bipartite identical-particle state ρ_μ, where $\mu = \mathcal{A}$ indicates a fermionic state and $\mu = \mathcal{S}$ a bosonic one, its identical-particle entanglement (IPE) is given by

$$E_\mu(\rho_\mu) = \min_\sigma \left\{ E(\sigma) :\ P_\mu \sigma P_\mu = \mathrm{Tr}(P_\mu \sigma)\rho_\mu,\ \mathrm{Tr}(P_\mu \sigma) = \frac{1}{2} \right\}. \tag{2.99}$$

The quantity in (2.99) may not be calculated analytically or in an efficient numerical way for all entanglement measures E. If the measure of choice is the entanglement negativity $\mathcal{N}$, however, the optimization problem may be formulated as a semidefinite program (SDP). SDPs allow to find an exact solution, up to arbitrary precision, in such a way that the time required for obtaining a solution is polynomial in the number of optimization variables [33]. In the following section we will therefore show how identical-particle entanglement measures may be calculated by means of semi-definite programming.

2.8 Identical-Particle Entanglement as a Semidefinite Program

Entanglement quantification may be a complicated task and only in few cases is an analytical evaluation possible. For this purpose a number of numerical techniques exist that enable the evaluation of entanglement measures to an arbitrary degree of accuracy, depending only on the computational resources available. One such technique is given by semidefinite programming, which may be used to calculate entanglement measures when they may be expressed as the convex optimization of a linear functional of matrices with positive-semidefiniteness constraints. One such measure is entanglement negativity, which we expressed as an SDP in section 1.2.1.

The fact that entanglement negativity may be evaluated as a minimisation instance suggests that it may be a good measure for the purpose of evaluating identical-particle entanglement according to the formulation in (2.99), where we minimize the entanglement measure with additional linear constraints. Bearing this in mind, we may cast the identical-particle entanglement of a bipartite state ρ_μ evaluated by the entanglement measure N as the semidefinite program

$$\begin{aligned} N_\mu(\rho_\mu) = & \min_{M,X} (\mathrm{Tr}(M) - 1)/2 \\ & \text{such that} \\ & \qquad -M \leq X^\Gamma \leq M \\ & \qquad M \geq 0 \\ & \qquad X \geq 0 \\ & \qquad \mathrm{Tr}(X) = 1 \\ & \qquad P_\mu X P_\mu = \mathrm{Tr}(P_\mu X)\rho_\mu \\ & \qquad \mathrm{Tr}(P_\mu X) = \frac{1}{2}. \end{aligned} \tag{2.100}$$

The above expression may be related to that for standard entanglement negativity, which we recalled in (1.25). In (2.100), however, we minimize over two sets of positive semidefinite matrices M and X. The optimization over M returns the values of the negativity of the positive and normalised density matrix X, which in turn is optimized to minimize negativity, compatibly with the constraints that X projects onto the target state ρ_μ with projection probability given by $\mathrm{Tr}(P_\mu X) = \frac{1}{2}$.

In other words, the identical-particle negativity of the target state ρ_μ is given by the minimum negativity of the normalised state X, provided that the symmetric or

antisymmetric image of X is ρ_μ itself and that the projection probability is $1/2$. We have argued in the previous section as to why $1/2$ is a suitable option for projection probability. We call this identical-particle entanglement measure *symmetric negativity* and *antisymmetric negativity* for the bosonic and fermionic case respectively. The measure may be evaluated numerically by means of the SDP in (2.100) and applies to both pure and mixed states in any dimension. In the following section we define explicitly the entanglement measure in the bosonic and fermionic cases and illustrate their main properties.

2.9 Quantification of Identical-Particle Entanglement by Means of Symmetric and Antisymmetric Entanglement Negativity

In sections 2.7 and 2.8 we introduced respectively a novel notion of inter-particle entanglement quantification for states of identical particles and a strategy to compute it explicitly as a semidefinite program. We will call such entanglement measure *identical-particle entanglement negativity* (IPN) when not specific to either fermions or bosons. In the following we will define IPN in the fermionic and bosonic cases explicitly and outline some of the key properties of the resulting entanglement measures.

Definition 2.9. Given a target symmetric state $\rho_{\mathcal{S}}$, its *symmetric negativity* (SN) is given by

$$N_{\mathcal{S}}(\rho_{\mathcal{S}}) = \min\big\{N(\sigma) :\ P_{\mathcal{S}}\sigma P_{\mathcal{S}} = \mathrm{Tr}(P_{\mathcal{S}}\sigma)\rho_{\mathcal{S}},\ \mathrm{Tr}(P_{\mathcal{S}}\sigma) = p_{\mathcal{S}}\big\}. \tag{2.101}$$

with $p_{\mathcal{S}} = \min\limits_{\sigma^\Gamma\geq 0}\{\mathrm{Tr}(P_{\mathcal{S}}\sigma)\} = 1/2$.

Definition 2.10. Given a target antisymmetric state $\rho_{\mathcal{A}}$, its *antisymmetric negativity* (AN) is given by

$$N_{\mathcal{A}}(\rho_{\mathcal{A}}) = \min\big\{N(\sigma) :\ P_{\mathcal{A}}\sigma P_{\mathcal{A}} = \mathrm{Tr}(P_{\mathcal{A}}\sigma)\rho_{\mathcal{A}},\ \mathrm{Tr}(P_{\mathcal{A}}\sigma) = p_{\mathcal{A}}\big\}. \tag{2.102}$$

with $p_{\mathcal{A}} = \max\limits_{\sigma^\Gamma\geq 0}\{\mathrm{Tr}(P_{\mathcal{A}}\sigma)\} = 1/2$.

In the bipartite case, we have argued in Equations (2.83) and (2.91) that the projection probabilities $p_{\mathcal{S}} = \min\limits_{\sigma^\Gamma\geq 0}\{\mathrm{Tr}(P_{\mathcal{S}}\sigma)\}$ and $p_{\mathcal{A}} = \max\limits_{\sigma^\Gamma\geq 0}\{\mathrm{Tr}(P_{\mathcal{A}}\sigma)\}$ are both equal to $p_{\mathcal{S}} = p_{\mathcal{A}} = 1/2$. We point out that the expressions for $p_{\mathcal{S}}$ and $p_{\mathcal{A}}$ can be cast as semidefinite programs. This will be of use in introducing an identical-particle entanglement

measure in the multipartite case, where such quantities are not known from analytical considerations (section 2.12.1). Let us look into the properties of the symmetric and antisymmetric negativity.

2.9.1 Properties of Identical-Particle Entanglement Negativity

Convexity

The objective functions of the SDPs defining antisymmetric and symmetric negativity are convex by definition. In this section we show explicitly that the measure of entanglement for identical particles given by the SDP (2.100) is convex for convex combinations of density matrices. The argument is similar to the proof of convexity for a measure of distillable entanglement formulated as a semidefinite program in [119]. In general, this result holds even if a different entanglement measure is chosen as objective function for the class of identical-particle entanglement measures we discuss in Equation (2.99), provided the chosen measure E is convex.

In what follows we are consistent with definitions 2.10 and 2.9 in fixing the projection probability to $1/2$, however our argument holds regardless the value of the projection probability.

To begin with, a function f acting on a convex set X such that $f : X \to \mathbf{R}$ is said to be convex if

$$\forall x_1, x_2 \in X,\, \forall t \in [0,1] : \quad f\big(tx_1 + (1-t)x_2\big) \leq tf(x_1) + (1-t)f(x_2). \tag{2.103}$$

What we want to prove is

$$N_\mu(\tilde{\rho}) = N_\mu\big(t\rho + (1-t)\rho'\big) \leq tN_\mu(\rho) + (1-t)N_\mu(\rho'), \tag{2.104}$$

with $t \in [0,1]$ and the identical-particle negativity N_μ is defined as

$$N_\mu(\rho) = \min\Big\{N(\sigma) \,:\, P_\mu \sigma P_\mu = \mathrm{Tr}(P_\mu\sigma)\rho,\, \mathrm{Tr}(P_\mu\sigma) = 1/2\Big\}. \tag{2.105}$$

We may start by noting that, by applying the definition of IPN, the optimal value for the SDP in (2.100) may be expressed as $N_\mu(\tilde{\rho}) = N(\tilde{\sigma}_f)$ where N is the standard entanglement negativity and $\tilde{\sigma}_f$ satisfies a number of conditions. First, it must satisfy the conditions

$$P_\mu \tilde{\sigma}_f P_\mu = \mathrm{Tr}(P_\mu \tilde{\sigma}_f)\tilde{\rho}, \tag{2.106}$$

and

$$\mathrm{Tr}(P_\mu \tilde{\sigma}_f) = 1/2 \tag{2.107}$$

which is are the constraints in (2.105). Second, it must be an optimal state for (**??**) and must therefore have the minimum negativity N among all states σ satisfying the previous two conditions:

$$N(\tilde{\sigma}_f) \leq N(\sigma). \tag{2.108}$$

We will refer to $\tilde{sigma}_f$ as the optimal state for the instance $N_\mu(\tilde{\rho})$. Consider now two density matrices ρ and ρ',for which we may define σ_f and σ'_f optimal states respectively for $N_\mu(\rho)$ and $N_\mu(\rho')$. Consider the definition of $\tilde{\sigma}_f$, alongside the following observation:

$$P_\mu(t\sigma_f + (1-t)\sigma'_f)P_\mu = \mathrm{Tr}(P_\mu(t\sigma_f + (1-t)\sigma'_f))(t\rho + (1-t)\rho'). \tag{2.109}$$

We then have the relationship given by

$$N(\tilde{\sigma}_f) \leq N(t\sigma_f + (1-t)\sigma'_f). \tag{2.110}$$

Standard negativity, however, is a convex function itself, so we obtain the desired inequality:

$$N_\mu(\tilde{\rho}) = N(\tilde{\sigma}_f) \leq N(t\sigma_f + (1-t)\sigma'_f) \leq tN(\sigma_f) + (1-t)N(\sigma'_f) = tN_\mu(\rho) + (1-t)N_\mu(\rho'). \tag{2.111}$$

Non-increasing under LOCC

Similarly to the argument for convexity, we know that any well-defined entanglement measure E to be used as an objective function in (2.99) is non-increasing under local operations and classical communication (LOCC) [56]. Here, we show explicitly that our identical-particle entanglement measure E_μ of Definition 2.8 is LOCC non-increasing. Our proof does not depend on the fixing of the projection probability in (2.99), so we will derive it for a generic projection probability constraint $\mathrm{Tr}(P_\mu\sigma) = p \in]0, 1]$.

To begin with, we need to take into account the identity of particles and therefore restrict the physical set of LOCC non-increasing maps to those which are symmetry preserving. We refer to such maps as $\Lambda^{\mathrm{SP}}_{\mathrm{LOCC}}$ and they have the following structure:

$$\Lambda^{\mathrm{SP}}_{\mathrm{LOCC}}(\cdot) = P_\mathcal{S}\Lambda^{\mathrm{SP}}_{\mathrm{LOCC}}(P_\mathcal{S} \cdot P_\mathcal{S})P_\mathcal{S} + P_\mathcal{A}\Lambda^{\mathrm{SP}}_{\mathrm{LOCC}}(P_\mathcal{A} \cdot P_\mathcal{A})P_\mathcal{A}. \tag{2.112}$$

Therefore, given a state ρ_μ with symmetry $\mu \in \{\mathcal{A}, \mathcal{S}\}$ we have

$$\Lambda^{\mathrm{SP}}_{\mathrm{LOCC}}(\rho_\mu) = P_\mu\Lambda^{\mathrm{SP}}_{\mathrm{LOCC}}(P_\mu\rho_\mu P_\mu)P_\mu = P_\mu\Lambda^{\mathrm{SP}}_{\mathrm{LOCC}}(\rho_\mu)P_\mu. \tag{2.113}$$

Proposition 3. Given a symmetry-preserving LOCC map $\Lambda^{\mathrm{SP}}_{\mathrm{LOCC}}$ and an identical-particle state ρ_μ with symmetry $\mu \in \{\mathcal{A}, \mathcal{S}\}$, the following inequality holds:

$$E_\mu\big(\Lambda^{\mathrm{SP}}_{\mathrm{LOCC}}(\rho_\mu)\big) \leq E_\mu(\rho_\mu). \tag{2.114}$$

Proof. Let us call Σ the optimal state for the minimization instance defining $E_\mu(\rho_\mu)$, which therefore has the property $P_\mu \Sigma P_\mu = p\rho_\mu$, with $\mathrm{Tr}(P_\mu \Sigma) = p$. By looking at the action of $\Lambda^{\mathrm{SP}}_{\mathrm{LOCC}}$ on Σ, we obtain the expression

$$P_\mu \Lambda^{\mathrm{SP}}_{\mathrm{LOCC}}(\Sigma) P_\mu = P_\mu \Lambda^{\mathrm{SP}}_{\mathrm{LOCC}}(P_\mu \Sigma P_\mu) P_\mu = p P_\mu \Lambda^{\mathrm{SP}}_{\mathrm{LOCC}}(\rho_\mu) P_\mu = p \Lambda^{\mathrm{SP}}_{\mathrm{LOCC}}(\rho_\mu), \tag{2.115}$$

which is the condition constraining the minimization for $E_\mu\big(\Lambda^{\mathrm{SP}}_{\mathrm{LOCC}}(\rho_\mu)\big)$. The density operator $\Lambda^{\mathrm{SP}}_{\mathrm{LOCC}}(\Sigma)$ therefore satisfies the constraints for $E_\mu\big(\Lambda^{\mathrm{SP}}_{\mathrm{LOCC}}(\rho_\mu)\big)$, and because $E\big(\Lambda^{\mathrm{SP}}_{\mathrm{LOCC}}(\Sigma)\big) \leq E\big(\Sigma\big)$, we necessarily have that $E_\mu\big(\Lambda^{\mathrm{SP}}_{\mathrm{LOCC}}(\rho_\mu)\big) \leq E_\mu(\rho_\mu)$. □

Structure of the optimal states

Consider a target identical-particle state ρ_μ and its identical-particle negativity

$$N_\mu(\rho_\mu) = \min\big\{N(\sigma) :\ P_\mu \sigma P_\mu = \frac{1}{2}\rho_\mu\big\}. \tag{2.116}$$

Let $\tilde{\sigma}$ be an optimal state for the minimization (2.116). Then the permutation invariant state

$$\tilde{\sigma}_V = \frac{\tilde{\sigma} + V\tilde{\sigma}V}{2} \tag{2.117}$$

is also an optimal state for (2.116). In fact, we have

$$P_\mu \tilde{\sigma}_V P_\mu = P_\mu \tilde{\sigma} P_\mu = \frac{1}{2}\rho_\mu \tag{2.118}$$

by construction and

$$\|\tilde{\sigma}_V^\Gamma\|_1 = \frac{1}{2}\|\tilde{\sigma}^\Gamma + V\tilde{\sigma}^\Gamma V\|_1 \leq \frac{1}{2}(\|\tilde{\sigma}^\Gamma\|_1 + \|V\tilde{\sigma}^\Gamma V\|_1) = \|\tilde{\sigma}^\Gamma\|_1. \tag{2.119}$$

Therefore if $\tilde{\sigma}$ is an optimal state for (2.116) then so is $\tilde{\sigma_V}$.

By construction, the state $\tilde{\sigma}_V$ is a direct sum of symmetric and antisymmetric density operators

$$\tilde{\sigma}_V = P_\mu \tilde{\sigma}_V P_\mu \oplus P_{\bar{\mu}} \tilde{\sigma} P_{\bar{\mu}}. \tag{2.120}$$

where $\bar{\mu}$ indicates the complementary symmetry subspace to μ (i.e. if $\mu = \mathcal{A}$ then $\bar{\mu} = \mathcal{S}$ and vice-versa). The set of optimal states for the identical-particle negativity of a given

state ρ_μ therefore always includes states of the kind

$$\sigma = \frac{1}{2}(\rho_\mu + \sigma_{\bar{\mu}}). \tag{2.121}$$

2.9.2 Pure-state antisymmetric entanglement negativity

We have seen in the previous sections that antisymmetric negativity is a well-defined and general entanglement measure, applying both to pure and mixed states. Its evaluation, however, relies on the solution of the associated SDP and may not be carried out analytically except for special cases. It is useful to define a restricted version of the measure applying only to pure states, which may however be evaluated analytically. We will discuss an application of this notion in Chapter 4.

Consider a pure antisymmetric state $|\psi_{\mathcal{A}}\rangle$, it may always be represented in its Slater Decomposition

$$|\psi_{\mathcal{A}}\rangle = \sum_{i=1}^{\lfloor \frac{d}{2} \rfloor} \sqrt{\frac{\lambda_i}{2}} \left(|a_i\rangle |b_i\rangle - |b_i\rangle |a_i\rangle \right), \tag{2.122}$$

where $\{|a_i\rangle\}_{i=1}^{\lfloor \frac{d}{2} \rfloor}$, $\{|b_i\rangle\}_{i=\lfloor \frac{d}{2} \rfloor + 1}^{2\lfloor \frac{d}{2} \rfloor}$ and $\langle a_i | b_j \rangle = \delta_{ab}\delta_{ij}$. We may define an unsymmetrized state

$$|\sigma\rangle = \sum_{i=1}^{\lfloor \frac{d}{2} \rfloor} \sqrt{\lambda_i} |a_i\rangle |b_i\rangle \tag{2.123}$$

such that $|\psi_{\mathcal{A}}\rangle = \frac{1}{\sqrt{2}}(|\sigma\rangle - V|\sigma\rangle)$, V being the swap operator.

Consider now a generic bipartite state in its Schmidt decomposition

$$|\psi\rangle = \sum_{i=1}^{r} \sqrt{\psi_i} |\alpha_i\rangle |\beta_i\rangle, \tag{2.124}$$

its entanglement negativity will be

$$N(\psi) = \frac{(\sum_i \sqrt{\psi_i})^2 - 1}{2}. \tag{2.125}$$

We may define the function $f(\psi) = \sum_i \sqrt{\psi_i}$ such that $N(\psi) = \frac{f(\psi)^2 - 1}{2}$ and $f(\psi) = \sqrt{2N(\psi) + 1}$. It follows directly from equation (2.123) that $f(\sigma) = \sum_i \sqrt{\lambda_i}$ and thus $f(\psi_{\mathcal{A}}) = f\big(\frac{1}{\sqrt{2}}(|\sigma\rangle - V|\sigma\rangle)\big) = \sqrt{2} f(\sigma)$. The relationship between the negativity of the state $\psi_{\mathcal{A}}$ and σ is therefore given by:

$$N(\psi_{\mathcal{A}}) = \frac{f^2(\psi_{\mathcal{A}}) - 1}{2} = \frac{2f^2(\sigma) - 1}{2} = 2N(\sigma) + \frac{1}{2}. \tag{2.126}$$

Based on the above considerations, we may put forward the following definition of *pure-state antisymmetric negativity* (PS-AN):

$$N_{\mathcal{A}}^{\text{pure}}(\psi_{\mathcal{A}}) = \frac{N(\psi_{\mathcal{A}}) - \frac{1}{2}}{2}. \tag{2.127}$$

The above quantity is a restriction of the antisymmetric negativity of Definition 2.10 when the minimization is restricted to pure states only. The purity of a state σ, which may be expressed as $\text{Tr}(\sigma^2)$, is a nonlinear constraint for the elements of σ, so it may not be enforced in an SDP. By relying on the Slater decomposition, however, we may assign a quantitative value to the entanglement of an antisymmetric state prior to the antisymmetrization. In this sense, the pure-state antisymmetric negativity is a generalisation of the concept of Slater rank.

2.9.3 Antisymmetric negativity and violation of the GMW criteria

Our approach to quantifying identical-particle entanglement relies on the separability criteria proposed by Ghirardi, Marinatto and Weber which is based on the possibility to attribute a complete set of properties to separable pure states.

The connection between identical-particle negativity and the GMW criteria is given by the generalisation of the Theorems 2.6 and 2.7 and we are able to prove, in the fermionic case, that nonzero values of antisymmetric negativity imply a violation of the GMW criteria. In the following section we establish this connection and put forward an upper bound to the violation, in terms of the pure-state antisymmetric negativity.

Le us recall the formulation of the GMW criteria in order to investigate the possible ways in which it may be violated. In particular, we focus on the mathematical definition of a *complete set of properties*, which may be formulated for distinguishable and indistinguishable-particle systems alike.

Given a composite quantum system $\mathcal{S} = \mathcal{S}_1 + \mathcal{S}_2$ described by the pure density operator $\chi_{\mathcal{A}}$, one of the subsystems has a complete set of properties iff there exists a one dimensional projection operator $P = |\phi\rangle\langle\phi|$, defined on the Hilbert space $H^{(1)}$ of $\mathcal{S}_1$, such that:

$$\text{Tr}[(P \otimes \mathbb{1} + \mathbb{1} \otimes P)\chi_{\mathcal{A}}] = 2\text{Tr}(P \otimes \mathbb{1}\chi_{\mathcal{A}}) = 1.$$

We prove that nonzero values of antisymmetric negativity imply a violation of such condition.

Theorem 2.11. *Given the pure antisymmetric density operator $\chi_{\mathcal{A}} = |\chi_{\mathcal{A}}\rangle\langle\chi_{\mathcal{A}}|$, if $N_{\mathcal{A}}^{\text{pure}}(\chi_{\mathcal{A}}) > 0$, then the subsystems of $\chi_{\mathcal{A}}$ do not have a complete set of properties.*

Proof. To begin with, we may use the symmetry properties of the state $|\chi_{\mathcal{A}}\rangle$ and the cyclicity of the trace operator to rewrite the projection probability as

$$\mathrm{Tr}(\mathcal{E}(\phi)\chi_{\mathcal{A}}) = 2\mathrm{Tr}(P_{\mathcal{A}} |\phi\rangle\langle\phi| \otimes \mathbb{1} P_{\mathcal{A}} |\chi_{\mathcal{A}}\rangle\langle\chi_{\mathcal{A}}|). \tag{2.128}$$

If we now choose an orthonormal basis $\{|\phi_i\rangle\}_{i=0}^{d-1}$ of the single particle Hilbert space such that $|\phi_0\rangle = |\phi\rangle$ we may use the spectral decomposition of the identity operator $\mathbb{1} = \sum_{i=0}^{d-1} |\phi_i\rangle\langle\phi_i|$ to obtain

$$P_{\mathcal{A}} |\phi\rangle\langle\phi| \otimes \mathbb{1} P_{\mathcal{A}} = \sum_{i=0}^{d-1} P_{\mathcal{A}} |\phi_0\rangle |\phi_i\rangle \langle\phi_0| \langle\phi_i| P_{\mathcal{A}} = \sum_{i=0}^{d-1} \frac{1}{2} |\psi_{0i}^-\rangle\langle\psi_{0i}^-| =: \frac{Q}{2}, \tag{2.129}$$

where $|\psi_{0i}^-\rangle = (|\phi_0\rangle |\phi_i\rangle - |\phi_i\rangle |\phi_0\rangle)/\sqrt{2}$. The projection probability thus reduces to the expectation value over $|\chi_{\mathcal{A}}\rangle$ of the operator Q we defined above. The action of Q on the antisymmetric state is given by

$$\begin{aligned} Q |\chi_{\mathcal{A}}\rangle &= \frac{1}{\sqrt{2}} \sum_{i=0}^{d-1} \langle\psi_{0i}^-|\chi_{\mathcal{A}}\rangle (|\phi_0\rangle |\phi_i\rangle - |\phi_i\rangle |\phi_0\rangle) \\ &= \frac{1}{\sqrt{2}} \big(|\phi_0\rangle \big(\sum_{i=0}^{d-1} \langle\psi_{0i}^-|\chi_{\mathcal{A}}\rangle |\phi_i\rangle\big) - \big(\sum_{i=0}^{d-1} \langle\psi_{0i}^-|\chi_{\mathcal{A}}\rangle |\phi_i\rangle\big) |\phi_0\rangle\big) = \\ &= \| Q |\chi_{\mathcal{A}}\rangle \| \frac{1}{\sqrt{2}} (|\phi\rangle |\bar{\phi}\rangle - |\bar{\phi}\rangle |\phi\rangle), \end{aligned} \tag{2.130}$$

where $|\bar{\phi}\rangle = \| Q |\chi_{\mathcal{A}}\rangle \|^{-1/2} \sum_{i=0}^{d-1} \langle\psi_{0i}^-|\chi_{\mathcal{A}}\rangle |\phi_i\rangle$ is orthogonal to $|\phi\rangle$, therefore $\| Q |\chi_{\mathcal{A}}\rangle \|^2 = \| Q |\chi_{\mathcal{A}}\rangle \| \sqrt{2} |\langle\phi| \langle\bar{\phi}| P_{\mathcal{A}} |\chi_{\mathcal{A}}\rangle|$ and we obtain

$$\| Q |\chi_{\mathcal{A}}\rangle \| = \sqrt{2} |\langle\phi| \langle\bar{\phi}| P_{\mathcal{A}} |\chi_{\mathcal{A}}\rangle|. \tag{2.131}$$

An upper bound on the projection probability is therefore given by

$$\max_{\phi} \mathrm{Tr}(\mathcal{E}(\phi)\chi_{\mathcal{A}}) = \max_{\phi} 2 |\langle\phi| \langle\bar{\phi}|\chi_{\mathcal{A}}\rangle|^2. \tag{2.132}$$

We want to find an upper bound for the right-hand side of (2.132) in terms of an unsymmetrized pure state which projects onto our target antisymmetric state $|\chi_{\mathcal{A}}\rangle$. This would allow us to relate the negativity of the optimal state for $N_{\mathcal{A}}(\chi_{\mathcal{A}})$ to the

left-hand side of (2.132). Consider the quantity

$$\max_{\alpha,\beta,\chi_S} |\langle \alpha,\beta|\chi\rangle|, \tag{2.133}$$

where $\langle \alpha,\beta| \equiv \langle\alpha|\langle\beta|$, $|\chi\rangle = \sqrt{p}\,|\chi_{\mathcal{A}}\rangle + \sqrt{1-p}\,|\chi_S\rangle$ and we maximise over $|\chi_{\mathcal{S}}\rangle$, which is a pure state with support on the symmetric subspace. We will see how this expression is connected with the entanglement properties of the state $|\chi\rangle$, so we will relate it to the upper bound we are seeking. In fact, if we expand the absolute value in equation (2.133) as

$$|\sqrt{p}\,\langle \alpha,\beta|\chi_{\mathcal{A}}\rangle + \sqrt{1-p}\,\langle \alpha,\beta|\chi_{\mathcal{S}}\rangle|, \tag{2.134}$$

the maximization of the absolute value of two terms in expression (2.134) is necessarily larger than the sum of the moduli of the individual terms. Performing the maximization over the symmetric component yields

$$\max_{\chi_S} |\langle \phi,\bar{\phi}|\chi_S\rangle| = \max_{\chi_S} |\langle \phi,\bar{\phi}|\, P_{\mathcal{S}}\,|\chi_S\rangle| = \frac{1}{\sqrt{2}}\max_{\chi_S}|\frac{1}{\sqrt{2}}(\langle \phi,\bar{\phi}| + \langle \bar{\phi},\phi|)\,|\chi_S\rangle| = \frac{1}{\sqrt{2}}. \tag{2.135}$$

The quantity (2.133) is therefore lower bounded according to the inequality

$$\max_{\alpha,\beta,\chi_S} |\langle \alpha,\beta|\chi\rangle| \geq \max_{\phi,\chi_S} \sqrt{p}|\langle \phi,\bar{\phi}|\chi_{\mathcal{A}}\rangle| + \sqrt{\frac{1-p}{2}}. \tag{2.136}$$

We may now formulate our desired upper bound on the projection probability as

$$\max_{\phi} 2|\langle \phi,\bar{\phi}|\chi_{\mathcal{A}}\rangle|^2 \leq \frac{2}{p}\left|\max_{\alpha,\beta,\chi_S} |\langle \alpha,\beta|\chi\rangle| - \sqrt{\frac{1-p}{2}}\right|^2, \tag{2.137}$$

which may be further simplified if we adopt a probability projection onto the antisymmetric space $p = 1/2$ consistent with the entanglement measure 2.8, introduced in this thesis, and note that

$$\max_{\alpha,\beta,\chi_S} |\langle \alpha,\beta|\chi\rangle| = \sqrt{q_0}, \tag{2.138}$$

where $\sqrt{q_0}$ is the largest Schmidt coefficient in the decomposition

$$|\chi\rangle = \sqrt{q_0}\,|a_0\rangle\,|b_0\rangle + \sum_{i=1}^{d-1}\sqrt{q_i}\,|a_i\rangle\,|b_i\rangle\,, \tag{2.139}$$

and the maximum is indeed reached for $|\alpha\rangle = |a_0\rangle$ and $|\beta\rangle = |b_0\rangle$. Note that for $|\tilde{\chi}\rangle$ which reaches the maximum over $|\chi_{\mathcal{S}}\rangle$ we have that the maximum for the largest Schmidt coefficient corresponds to the minimum of the negativity, so that we have

$N(\tilde{\chi}) = N_{\mathcal{A}}^{\text{pure}}(\chi_{\mathcal{A}})$. We may thus formulate the desired upper bound as

$$\max_{\phi} \text{Tr}(\mathcal{E}(\phi)\chi_{\mathcal{A}}) \leq 4(\sqrt{q_0} - 1/2)^2. \tag{2.140}$$

We are still not done yet, as we would like to relate the right-hand side of inequality (2.140) to the negativity of the non-symmetrized state $|\chi\rangle$. To do so we may begin by taking into account the relationship between negativity of a state and its Schmidt coefficients:

$$N(\chi) = \frac{(\sum_{i=0}^{d-1} \sqrt{q_i})^2 - 1}{2}. \tag{2.141}$$

The maximum negativity will be thus achieved via the maximization

$$\max_{q_i \neq q_0} \sum_{i=0}^{d-1} \sqrt{q_i} \tag{2.142}$$

with the constraint that $\sum_{i=0}^{d-1} q_i = 1$, and we may prove that it is reached when the Schmidt coefficients $q_{i\neq 0}$ are all equal, thus leading to the inequality

$$(\sum_{i=0}^{d-1} \sqrt{q_i})^2 \leq \left(\sqrt{q_0} + (d-1)\sqrt{\frac{1-q_0}{d-1}}\right)^2. \tag{2.143}$$

To prove it, we may resort to the theory of majorization. Consider two decreasingly ordered probability distributions $\bar{p}$, $\bar{q} \in \mathbb{R}_+^d$ such that $\sum_{i=0}^{d-1} p_i = \sum_{i=0}^{d-1} q_i = 1$ and $p_0 \leq p_1 \leq ... \leq p_{d-1}$, $q_0 \leq q_1 \leq ... \leq q_{d-1}$. We may associate with each distribution a quantum state whose Schmidt coefficients are the square roots of the elements of the probability distribution :

$$\begin{aligned} |\psi(\bar{p})\rangle &= \sum_{i=0}^{d-1} \sqrt{p_i}\, |i\rangle\, |i\rangle \\ |\psi(\bar{q})\rangle &= \sum_{i=0}^{d-1} \sqrt{q_i}\, |i\rangle\, |i\rangle\,. \end{aligned} \tag{2.144}$$

There is a known Theorem [19] which connects the entanglement properties of the quantum states to the majorization properties of the associated probability distributions. Namely, there exists an LOCC map Λ_{LOCC} : $\quad \Lambda_{\text{LOCC}}[\psi(\bar{p})] = \psi(\bar{q})$ iff $p \preceq q$, i.e. $\sum_{i=0}^{k} p_i \leq \sum_{i=0}^{k} q_i \, \forall k \in [0, d-1]$. In general, given a probability distribution $\bar{p}$ with a fixed

element p_0, it majorizes a distribution $\bar{q}$ given by [120]

$$q_0 = p_0, \quad q_i = \frac{1-p_0}{d-1} \forall i \neq 0. \tag{2.145}$$

By taking this into account alongside the fact that the action of the map $\Lambda_{\text{LOCC}}[\psi(\bar{p})] = \psi(\bar{q})$ and that entanglement negativity is LOCC non-increasing, we have:

$$N\big(\psi(\bar{p})\big) = \mathcal{N}\big(\Lambda_{\text{LOCC}}[\psi(\bar{p})]\big) \leq N\big(\psi(\bar{q})\big). \tag{2.146}$$

The above equation amounts to the inequality

$$(\sum_{i=0}^{d-1} \sqrt{p_i})^2 \leq (\sqrt{q_0} + (d-1)\sqrt{\frac{1-q_0}{d-1}})^2. \tag{2.147}$$

We may thus obtain the dependence of q_0 on the negativity by finding the solutions for q_0 to equation

$$\big(\sqrt{q_0} + (d-1)\sqrt{\frac{1-q_0}{d-1}}\big)^2 = 2N(\tilde{\chi}) + 1, \tag{2.148}$$

where $\tilde{\chi}$ is defined below equation (2.139). The resulting solution has two branches for $d \geq 2$ and $N(\tilde{\chi}) \geq 0$, namely

$$q_0^{\pm} = \frac{1}{d^2}\left(d(d-1) - (d-2)(2N(\tilde{\chi})+1) \pm \sqrt{(d-1)(2N(\tilde{\chi})+1)(d-2N(\tilde{\chi})-1)}\right). \tag{2.149}$$

Since q_0 gives the upper bound to $\max_{\phi} \text{Tr}(\mathcal{E}(\phi)\chi_{\mathcal{A}})$ in (2.140), which we want to prove is < 1 for $N(\tilde{\chi}) > 0$, we only need to focus on the upper branch q_0^+. Indeed, the quantity

$$\varepsilon\big(q_0^+(N)\big) = 1 - 4\left(\sqrt{q_0^+(N)} - 1/2\right)^2 \tag{2.150}$$

lower bounds the violation of the GMW condition (2.9.3) and is strictly larger that zero for any $d \geq 2$ and $N(\tilde{\chi}) = N_{\mathcal{A}}^{\text{pure}}(\chi_{\mathcal{A}}) > 0$. □

The proof of Theorem 2.11 shows that the relationship between the violation of the GMW criteria and the pure state antisymmetric negativity depends on the local dimension d. We report in Figure 2.2 the quantity $\varepsilon\big(q_0^+(N_A)\big)$ as a function of the pure state antisymmetric negativity $N_A = N_{\mathcal{A}}^{\text{pure}}(\chi_{\mathcal{A}})$ of a generic antisymmetric pure state $\chi_{\mathcal{A}}$, for $d = 4$.

Figure 2.2 illustrates a typical relationship between antisymmetric negativity values and a quantification of the violation of the GMW separability criterion. The caveat is

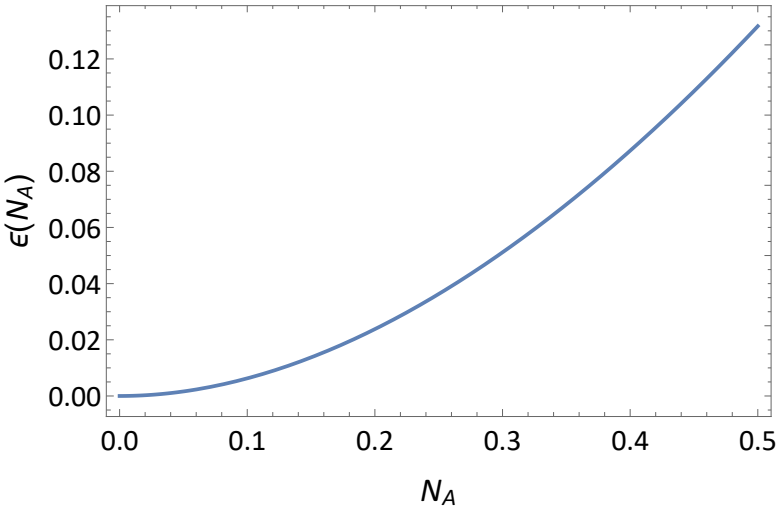

FIGURE 2.2: Lower bound to the violation $\varepsilon(N_A)$ of the GMW condition (2.9.3) as a function of the pure state antisymmetric negativity N_A for local dimension $d = 4$.

that, given a two-fermion pure quantum state described by the density matrix $\rho_{\mathcal{A}}$, if its antisymmetric negativity $N_{\mathcal{A}}(\rho_{\mathcal{A}})$ is nonzero then its pure-state antisymmetric negativity is necessarily nonzero and Theorem 2.11 implies $\rho_{\mathcal{A}}$ violates the GMW separability criterion.

Theorem 2.11 therefore establishes an explicit connection between our novel identical-particle entanglement measure (Definition 2.10) and the well-established identical-particle entanglement criteria introduced in references [21, 90, 91]. In the following section we focus on the application of symmetric and antisymmetric negativity to a number of notable states, in order to outline the measure's principal features.

2.10 Examples of the Application of AN and SN

Having laid out a mathematically precise definition of identical-particle entanglement and characterised its main features, we showcase its usefulness by applying our novel entanglement measures, introduced at the beginning of section 2.9, to simple states of particular interest. Let us begin with antisymmetric negativity. For all local dimensions d, states of the form

$$\left|\psi^0_{\mathcal{A}}\right\rangle = \frac{|A\rangle\,|B\rangle - |B\rangle\,|A\rangle}{\sqrt{2(1 - |\,\langle A|B\rangle\,|^2)}}, \tag{2.151}$$

where $|A\rangle$ and $|B\rangle$ are arbitrary single-particle states, one may directly verify the statement $N_{\mathcal{A}}(\left|\psi^0_{\mathcal{A}}\right\rangle\!\left\langle\psi^0_{\mathcal{A}}\right|) = 0$, given that $|AB\rangle$ is an optimal state for $N_{\mathcal{A}}(\left|\psi^0_{\mathcal{A}}\right\rangle\!\left\langle\psi^0_{\mathcal{A}}\right|)$ and

is also separable. The separability according to AN of state (2.151) is consistent with the GMW criteria, since it is given by the antisymmetrization of orthogonal factorised states. This means that there is no two-qubit fermionic entangled state, since for $d = 2$ the antisymmetric subspace is one-dimensional and given by the state (2.151). This should not be alarming, since real fermions always possess both a spatial and a spin degree of freedom, so that entangled fermionic states may exist even in the simplest cases. In fact, if we consider fermionic singlet states of the form (2.23), they may be represented as

$$\left|\psi^1_{\mathcal{A}}\right\rangle = \frac{1}{2}\left(|L\uparrow\rangle|R\downarrow\rangle + |R\uparrow\rangle|L\downarrow\rangle - |R\downarrow\rangle|L\uparrow\rangle - |L\downarrow\rangle|R\uparrow\rangle\right). \tag{2.152}$$

By applying the SDP associated with the definition 2.10 of antisymmetric negativity, we obtain $N_{\mathcal{A}}(\left|\psi^1_{\mathcal{A}}\right\rangle\!\left\langle\psi^1_{\mathcal{A}}\right|) = 1/2$, which corresponds to the standard negativity of the state

$$\left|\sigma^1\right\rangle = \frac{1}{\sqrt{2}}\left(|L\uparrow\rangle|R\downarrow\rangle + |R\uparrow\rangle|L\downarrow\rangle\right). \tag{2.153}$$

The state $\left|\psi^1_{\mathcal{A}}\right\rangle$ can be easily seen to be the antisymmetric projection of $\left|\sigma^1\right\rangle$ with projection probability $1/2$. Furthermore, if $\langle L|R\rangle = 0$, the second-quantised spin-mode representation of eq. (2.152) reads

$$|\sigma_2\rangle = \frac{1}{\sqrt{2}}\left(|L\rangle_\uparrow|R\rangle_\downarrow + |R\rangle_\uparrow|L\rangle_\downarrow\right), \tag{2.154}$$

where we have used spin as a subsystem subscript. For the above states we obtain the relationship $N_{\mathcal{A}}(\left|\psi^1_{\mathcal{A}}\right\rangle\!\left\langle\psi^1_{\mathcal{A}}\right|) = N(\left|\sigma^1\right\rangle\!\left\langle\sigma^1\right|) = N(|\sigma_2\rangle\langle\sigma_2|) = 1/2$, highlighting in this simple case the connection between the notion of antisymmetric negativity and mode entanglement. Such connection will be discussed in additional detail in Chapter 3 of this thesis, where we investigate the different notions of entanglement for spin-1/2 fermionic systems.

Let us now look into the bosonic case, focusing on a fixed local dimension $d = 4$ and basis $\{|i\rangle\}_{i=0}^3$. As mentioned in section 2.7.1, factorized bosonic states of the form $|A\rangle|A\rangle$, for arbitrary $|A\rangle$, are unentangled and do not require the application of symmetric negativity. On the other hand, a state of the form

$$\left|\psi^0_{\mathcal{S}}\right\rangle = \frac{1}{\sqrt{2}}(|0\rangle|1\rangle + |1\rangle|0\rangle) \tag{2.155}$$

is entangled in the standard sense and its IPE is given by applying symmetric negativity. The state $\left|\sigma^0\right\rangle = |0\rangle|1\rangle$ with $\mathrm{Tr}(P_{\mathcal{S}}\left|\sigma^0\right\rangle\!\left\langle\sigma^0\right|)$ is clearly optimal for $N_{\mathcal{S}}(\psi^0_{\mathcal{S}})$, which is therefore equal to zero, consistently with the GMW criteria defining as separable a state

given by the symmetrization of a product state of orthogonal single-particle states. A more interesting example is provided by considering the symmetrization of a product state of *non-orthogonal* single-particle states,

$$\left|\psi^1_{\mathcal{S}}\right\rangle = \frac{|A\rangle\,|B\rangle + |B\rangle\,|A\rangle}{\sqrt{2(1+|\,\langle A|B\rangle\,|^2)}}, \tag{2.156}$$

with $\langle A|B\rangle \neq 0$ and where we may choose for example $|A\rangle = |0\rangle$ and $|B\rangle = (|0\rangle + |1\rangle)/\sqrt{2}$. The state $\left|\psi^1_{\mathcal{S}}\right\rangle$ may not be obtained by symmetrizing a product state of orthogonal single-particle states and in fact we find that

$$N_{\mathcal{S}}(\left|\psi^1_{\mathcal{S}}\right\rangle\!\left\langle\psi^1_{\mathcal{S}}\right|) \simeq 0.0352, \tag{2.157}$$

where the numerical value on the right-hand side of (2.157) is obtained by numerically solving the SDP associated with $N_{\mathcal{S}}(\left|\psi^1_{\mathcal{S}}\right\rangle\!\left\langle\psi^1_{\mathcal{S}}\right|)$. A nonzero value for the symmetric negativity is in agreement with the GMW criteria, which label the state (2.156) as entangled. This difference between the fermionic and bosonic case may seem surprising, but is consistent with the requirement that both subsystems possess a complete set of properties, and that each CSP be unequivocally associated with one and only one subsystem. The overlap between the two identical-boson single-particle states, which we have shown not to be an issue for fermions, prevents this from being so and requires to describe the state (2.156) as entangled in the identical-particle sense. Finally, we may consider the bosonic analogue of the the state (2.152) which, in the basis defined above equation (2.155), reads

$$\left|\psi^2_{\mathcal{S}}\right\rangle = \frac{1}{2}(|0\rangle\,|1\rangle + |1\rangle\,|0\rangle + |2\rangle\,|3\rangle + |3\rangle\,|2\rangle\,, \tag{2.158}$$

which is clearly the symmetrization of $\left|\sigma^2\right\rangle = \frac{1}{\sqrt{2}}(|0\rangle\,|1\rangle + |2\rangle\,|3\rangle$ with $\mathrm{Tr}(P_{\mathcal{S}}\left|\sigma^2\right\rangle\!\left\langle\sigma^2\right|) = 1/2$. In analogy with the fermionic case, we have $N_{\mathcal{S}}(\left|\psi^2_{\mathcal{S}}\right\rangle\!\left\langle\psi^2_{\mathcal{S}}\right|) = N(\left|\sigma^2\right\rangle\!\left\langle\sigma^2\right|) = 1/2$, in accordance with the idea of evaluating identical-particle entanglement prior to symmetrization.

It is worth stressing once again out that the above results are consistent with the GMW criteria provided the projection probability for the optimal state is fixed to $1/2$, thus highlighting such choice as crucial in the definition of our identical-particle entanglement measure. In fact, such choice is particularly crucial in the bosonic case, where the GMW criteria identify as separable the states which are obtained by symmetrizing orthogonal product states, but not non-orthogonal ones.

2.11 Maximally Entangled Fermionic States

Entanglement being a resource that one typically desires to maximise, we will look into the maximally entangled states of identical fermions. The structure of maximally entangled antisymmetric states was outlined in section 2.5.1, however the entanglement was there assessed with standard entanglement measures, thus treating the particles identifying the subsystems as distinguishable. In this section we argue that the same states are maximally entangled also in terms of identical-particle negativity and we provide the relationship between the maximum antisymmetric negativity and the dimension of the local subsystems.

The Slater decomposition of a maximally entangled antisymmetric state, the latter being well-defined only in even dimension, is given by the form (2.122) where all the Slater coefficients λ_i are equal to $1/d$. The pure-state antisymmetric entanglement negativity of a maximally entangled antisymmetric state is straightforward to compute analytically by means of equation (2.127) and is equal to

$$N_{\mathcal{A}}^{\text{pure}}(\psi_{\mathcal{A}}^{+}) = \frac{d-2}{4}, \tag{2.159}$$

where $\psi_{\mathcal{A}}^{+}$ is the density operator of a maximally entangled pure antisymmetric state. Because $N_{\mathcal{A}}^{\text{pure}}$ is a linear monotonical function of the standard negativity, we know that this is the maximum pure-state antisymmetric negativity for a given dimension d. We also know that $N_{\mathcal{A}}(\psi_{\mathcal{A}}^{+}) \leq N_{\mathcal{A}}^{\text{pure}}(\psi_{\mathcal{A}}^{+})$, because the latter is a minimization problem equivalent to $N_{\mathcal{A}}(\psi_{\mathcal{A}}^{+})$ with an additional constraint of purity on the density matrices in the optimization set. Therefore if the optimal state for $N_{\mathcal{A}}^{\text{pure}}(\psi_{\mathcal{A}}^{+})$ is also an optimal state for $N_{\mathcal{A}}(\psi_{\mathcal{A}}^{+})$, as calculated by means of the SDP (2.100), the associated optimal value is the maximum antisymmetric negativity achievable. As reported in table 2.1, we may show that this is the case for local dimensions up to $d = 8$ and conjecture that the relationship holds for any dimension. We therefore identify the conjectured maximally identical-particle-entangled fermionic states as those identified in section 2.5.1.

Furthermore, the relationship between the PS-AN and the standard negativity allows us to establish the maximum identical-particle negativity even for odd dimensions. The maximum standard negativity for odd dimensions is in fact given by $(d-1)/2$, compared to $d/2$ for even dimension. The conjectured maximum value for the antisymmetric negativity in any dimension may thus be expressed as

$$N_{\mathcal{A}}^{\max}(d) = \frac{1}{2}\lfloor\frac{d-2}{2}\rfloor. \tag{2.160}$$

Before continuing it is worth pointing out that the relationships established in this

d	$N_{\mathcal{A}}(\psi_{\mathcal{A}}^{+})$	$N_{\mathcal{A}}^{\text{pure}}(\psi_{\mathcal{A}}^{+})$
2	0	0
4	0.5	0.5
6	1	1
8	1.5	1.5

TABLE 2.1: Tabulated values of maximum identical-particle entanglement, as quantified by AN $N_{\mathcal{A}}(\psi_{\mathcal{A}}^{+})$ (calculated by means of the SDP 2.100) and the PS-AN $N_{\mathcal{A}}^{\text{pure}}(\psi_{\mathcal{A}}^{+})$ (given by (2.159)) applied the maximally entangled antisymmetric state $\psi_{\mathcal{A}}^{+}$ with local dimension d.

section between antisymmetric negativity and standard negativity only hold for the classes of states we have investigated. In general, an analytical formulation for the IPN of any mixed identical-particle state is not known, however it can be obtained as the solution of the corresponding SDP.

2.12 Multipartite Entanglement of Identical Particles

The study of entanglement of identical particles may be extended beyond the bipartite case. In particular, the definition of IPE in terms of entanglement negativity allows a direct generalisation of the bipartite notion. Entanglement negativity, in fact, may be modified to detect genuine multipartite entanglement [73]. The intuitive idea is that the negativity needs to be evaluated in all bipartitions of the quantum system. Let the index m label a bipartition $M|\bar{M}$, where M is a subsystem and $\bar{M}$ its complementary subsystem. The *genuine multipartite negativity* (GMN) of a state ρ is given by

$$\mathcal{N}_g(\rho) = \min_{\rho=\sum_k p_k\rho_k} \sum p_k \mu(\rho_k), \tag{2.161}$$

where $\mu(\rho) = \min_m(\|\rho^{\Gamma_m}\|_1 - 1)/2$ is the minimum negativity over all bipartitions. The definition in (2.161) may be expressed in the alternative form [72]

$$\mathcal{N}_g(\rho) = \min_{\rho=\sum_m p_m\rho_m} \sum p_m \mathcal{N}_m(\rho_m), \tag{2.162}$$

where the summation index runs over all possible bipartitions $M|\bar{M}$ and $\mathcal{N}_m(\rho) = (\|\rho^{\Gamma_m}\|_1 - 1)/2$. In this last formulation, we may appreciate how GMN can be cast as an SDP stemming from a generalisation of (1.25) to the multipartite case. Let us look into the tripartite case for the sake of clarity, bearing in mind that the results extend to the N-partite case without loss of generality.

Consider a tripartite state ρ_{ABC}, it is called PPT-mixture (PPTm) if

$$\rho_{ABC} = p_A \rho^{\text{PPT}}_{A|BC} + p_B \rho^{\text{PPT}}_{B|AC} + p_C \rho^{\text{PPT}}_{C|AB}, \tag{2.163}$$

where $\rho^{\text{PPT}}_{X|YZ}$ is PPT in the bipartition $X|YZ$. The genuine negativity of ρ_{ABC} is given by the minimum of the sum of negativities in any bipartition for all decompositions of ρ_{ABC}, as per equation (2.162). In terms of semidefinite programming, equation (2.162) may be expressed as

$$\begin{aligned}
\mathcal{N}_g(\rho_{ABC}) = \min(&\text{Tr}(M_{A|BC} + M_{B|AC} + M_{C|AB}) - 1)/2 \\
\text{subject to}: \quad & M_{A|BC}, M_{B|AC}, M_{C|AB} \geq 0, \\
& \tilde{\rho}_{A|BC}, \tilde{\rho}_{B|AC}, \tilde{\rho}_{C|AB} \geq 0, \\
& -M_{A|BC} \leq \tilde{\rho}^{\Gamma}_{A|BC} \leq M_{A|BC} \\
& -M_{B|AC} \leq \tilde{\rho}^{\Gamma}_{B|AC} \leq M_{B|AC} \\
& -M_{C|AB} \leq \tilde{\rho}^{\Gamma}_{C|AB} \leq M_{C|AB} \\
& \tilde{\rho}_{A|BC} + \tilde{\rho}_{B|AC} + \tilde{\rho}_{C|AB} = \rho_{ABC}
\end{aligned} \tag{2.164}$$

where the optimization is performed over decompositions of ρ_{ABC} into un-normalised positive hermitian operators, one for every bipartition.

2.12.1 Genuine multipartite (anti)symmetric negativity

The notion of identical-particle negativity can be extended to the multipartite case in analogy with genuine multipartite negativity. The idea is to quantify the entanglement of a state ρ_μ with given symmetry as the minimum entanglement of an unsymmetrized state projecting on ρ_μ with projection probability fixed by $p = \max\{\text{Tr}(P_{\mathcal{A}}\sigma) : \sigma = \sigma_{\text{PPTm}}\}$, in analogy with the bipartite case. In the tripartite case, it was shown in [121] that $p = 1/3$. An entanglement measure may be associated with this idea, *genuine multipartite identical-particle entanglement*, and it may be evaluated as a semi-definite program when the genuine multipartite negativity is the figure of merit and the corresponding SDP is analogous to (5.19) with additional constraints.

Definition 2.12. Given an (anti)symmetric state ρ_μ, we call *genuine tripartite (anti)symmetric negativity* the optimal value for the SDP

$$\begin{aligned}
\mathcal{N}_g(\rho_\mu) = \min(&\mathrm{Tr}(M_{A|BC} + M_{B|AC} + M_{C|AB}) - 1)/2 \\
\text{subject to}: \quad & M_{A|BC}, M_{B|AC}, M_{C|AB} \geq 0, \\
& \tilde{\rho}_{A|BC}, \tilde{\rho}_{B|AC}, \tilde{\rho}_{C|AB} \geq 0, \\
& -M_{A|BC} \leq \tilde{\rho}^{\Gamma}_{A|BC} \leq M_{A|BC} \\
& -M_{B|AC} \leq \tilde{\rho}^{\Gamma}_{B|AC} \leq M_{B|AC} \\
& -M_{C|AB} \leq \tilde{\rho}^{\Gamma}_{C|AB} \leq M_{C|AB} \\
& \tilde{\rho} = \tilde{\rho}_{A|BC} + \tilde{\rho}_{B|AC} + \tilde{\rho}_{C|AB} \\
& P_\mu \tilde{\rho} P_\mu = \mathrm{Tr}(P_\mu \tilde{\rho}) \rho_\mu \\
& \mathrm{Tr}(P_\mu \tilde{\rho}) = p,
\end{aligned} \tag{2.165}$$

where $p = \max\{\mathrm{Tr}(P_{\mathcal{A}}\sigma) : \sigma = \sigma_{\mathrm{PPTm}}\} = 1/3$ in the tripartite case. The generalisation to the N-partite case is straightforward, introducing the index m labelling bipartitions, we may define *genuine multipartite (anti)symmetric negativity* as

$$\begin{aligned}
\mathcal{N}_g(\rho_\mu) = \min(&\mathrm{Tr}(\sum_m M_m) - 1)/2 \\
\text{subject to}: \quad & M_m \geq 0 \\
& \tilde{\rho}_m \geq 0 \\
& -M_m \leq \tilde{\rho}_m \leq M_m \quad \text{for all bipartitions m} \\
& \tilde{\rho} = \sum_m \tilde{\rho}_m \\
& \mathrm{Tr}(\tilde{\rho}) = 1 \\
& P_\mu \tilde{\rho} P_\mu = \mathrm{Tr}(P_\mu \tilde{\rho}) \rho_\mu \\
& \mathrm{Tr}(P_\mu \tilde{\rho}) = p,
\end{aligned} \tag{2.166}$$

where the parameter $p = \max\{\mathrm{Tr}(P_{\mathcal{A}}\sigma) : \sigma = \sigma_{\mathrm{PPTm}}\}$ may be itself independently evaluated numerically as an SDP, when it is not known from analytical considerations. As a concluding remark we may point out that while the quantity (2.166) is well-defined, it is affected by a problem common to most multipartite entanglement measures. The size of the operators involved in the optimisation scales exponentially in the number of parties, so it becomes intractable even for small numbers. The problem of efficiently quantifying multipartite entanglement in many-body systems is still an open one.

In conclusion, in this chapter we have introduced a new entanglement measure, *(anti)symmetric negativity*, for systems of identical (fermions)bosons with a solid mathematical formalism, an intuitive interpretation and the possibility of being computed efficiently by means of semidefinite programming. We arrived at the formulation of the measure based on the GMW [21] entanglement criteria and showed that when the antisymmetric negativity of a fermionic pure state is not null, then the state violates the GMW separability conditions (2.54). We reported the results of the application of (anti)symmetric negativity to a number of example bipartite states and outlined a possible extension of the measure to the multipartite case.

The entanglement measure we introduce brings new insight into the study of correlations in identical particle systems, characterised by exchange symmetry. Its application to fermionic and bosonic states can be understood as the quantification of the entanglement prior to the symmetrization prescription, required by the spin-statistics connection, and is the direct extension of a series of entanglement criteria that have become well established in this field of research. Our efforts, however, are not only of fundamental but also of practical interest, since antisymmetric negativity can be directly applied at entanglement estimation in ultracold atom experiments. We will discuss an example of the application of antisymmetric negativity in a specific experimental setting.

Chapter 3

Identical Particle Entanglement in Physical Systems of Two Ultracold Fermionic Atoms

The problem of fully understanding many-body systems of strongly correlated fermions has long resisted a general solution [122]. The exponential increase in complexity as a function of number of particles required in accurately reproducing density matrices goes beyond the capabilities of classical computers, whereas the strongly interacting regime prevents the application of most standard approximate methods [123, 124]. A notable solution to this problem was first put forward in 1982 by Richard Feynman [125], suggesting that quantum mechanical systems could be used to *simulate* a controllable version of the condensed matter system under investigation. This idea of *quantum simulation* has recently become a flourishing field of research [15] and one of the four pillars of the recent Quantum Flagship European funding programme [2].

One of the main branches of current research in quantum simulation is the study of ultracold atoms in optical lattices. Techniques such as laser cooling [126] and evaporative cooling [127] bring atoms to temperatures as low as $\sim 0.5\,nK$, and have been a powerful tool for the study of materials, such as the experimental realization of the Bose-Einstein Condensate (BEC) [128,129], classified as an independent state of matter, in dilute atomic gases [130, 131]. The degree of control achieved over cold atomic gases sparked interest in attempting to further manipulate such systems with coherent radiation by confining them in optical lattices, in order to reach strongly interacting regimes whose understanding is still a challenge. One of the main goals of current research in cold atom physics is the simulation of condensed matter systems whose theoretical description remains an open problem, including exotic phases, frustrated spin systems and high-critical-temperature superconductors [132].

An important tool for the analysis of many-body systems is the study of correlation functions, in particular related to the detection of entanglement [133–135]. As was first observed in the notable Hanbury-Brown-Twiss (HBT) experiment [136], however, exchange symmetry strongly affects the correlation functions of identical particle systems. In fact, one of the key features of fermionic systems is the inevitable presence of correlations due to the exchange symmetry of identical particle systems and the wavefunction antisymmetrization in the first-quantised representation. Such correlations are a *kinematic* effect, in the sense that they are related to the system geometry and intrinsic properties, rather than originating due to interactions. They are connected with the quantum field nature of fermions and are intrinsic to all many-fermion states. In the original HBT experiment, an intensity interferometer, originally aimed at the astronomical observation of the star Sirius [136], an interference effect was detected in the signal from the two photomultiplier tubes at the interferometer output, despite the fact that no phase information was being collected. The quantum interpretation of such interference attributed the effect to the bunching of photons, which results from the fact that they are identical particles with integer spin and therefore their wavefunction is symmetric under particle exchange.

There are strategies to generate entanglement without direct interactions (e.g. via measurement) [137–139] and not all dynamical processes involving interactions lead to entanglement. In fact, the entanglement in the final state for any such strategy will depend on the initial state of the system. Entanglement may also arise from dynamical physical processes, in particular those involving interactions between particles. Most experimental efforts aimed at entanglement generation, in fact, rely on interactions [140]. Furthermore, entanglement growth is connected with phase transitions in interacting quantum matter [141], for example in the quench dynamics in the one-dimensional Bose Hubbard model [142–145].

Based on the above considerations, the ability to distinguish correlations arising from interactions and those due to wavefunction antisymmetrization is of fundamental and practical interest. Our efforts in defining an entanglement measure for identical systems which removes the wavefunction antisymmetrization, suggest that the antisymmetric negativity is well-suited for such a task.

In this chapter we apply the identical-particle measure antisymmetric negativity (AN) to systems of few identical ultracold fermionic atoms with the aim of quantifying correlations due to interactions and distinguishing them from those due to antisymmetrization. We focus on low-dimensional systems, where there is a good degree of experimental and theoretical control of the system and its representation, in order to obtain a full understanding of the interplay of exchange symmetry and entanglement

and provide a building-block that can be useful in the study of genuinely many-body systems.

In section 3.1 we introduce the Fermi-Hubbard dimer, the main focus of our analysis, and its theoretical description in terms of the Hubbard model and a discretized space representation. Section 3.2 reviews current experimental techniques for the measurement of momentum correlations of a fermionic dimer. The connection between entanglement, antisymmetrization and correlations in fermionic systems is introduced in section 3.3. Such connection is investigated in section 3.4 by applying antisymmetric negativity for entanglement estimation based on measured momentum correlations in a Fermi-Hubbard dimer. Finally, the methods and results of the investigation are outlined in section 3.5.

3.1 Fermionic Dimer: a Building Block for Strongly Interacting Fermionic Systems

Gases of ultracold atoms are a suitable physical system for simulating strongly-correlated quantum many-body systems. In fact, by loading an ultracold atomic gas into an array of retroreflected far-detuned laser beams with a fixed wavelength λ, one may create a conservative sinusoidal potential with periodicity $\lambda/2$, which traps the atoms around fixed points, simulating a crystal lattice. When the atomic gas is sufficiently dilute, the scattering between the atoms is accurately described solely in terms of two-body processes [146]. The features of the interaction are dependent on the atomic species and on the lattice potential.

Interactions may be tuned between the trapped atoms by magnetic Feshbach resonance [124, 147]. A magnetic Feshbach resonance occurs when the energy associated with the formation of a bound molecular state approaches the kinetic energy of the scattering process between two atoms [146]. The energy difference can be controlled by means of an external magnetic offset Δ_M, thus tuning the interaction between the atoms without manipulating the optical lattice potential.

The properties of the system may be measured with high precision and up to a controllable degree of noise [15, 148]. One of the main tools of investigation for such systems is given by site-resolved imaging, which allows measurement of correlations in position space between the individual particles [149]. Several important properties, such as transport, phase fluctuations and long-range coherence [147] are, however, only accessible by addressing correlations in momentum space. In the following sections we review the mathematical models in terms of which ultracold fermionic lattices may be

understood and momentum correlations may be experimentally accessed. We focus on the simplest instance of such physical systems: the fermionic dimer.

Many-body systems have traditionally been treated in statistical terms, due to the impossibility of controlling the individual degrees of freedom. The degree of control over the fundamental constituents of many-body systems achieved in current experiments [147, 150, 151] are paving the way for a bottom-up approach aimed at the simulation of condensed matter systems. For such efforts to be successful, a complete understanding of the properties of the building blocks of such quantum simulators is crucial. Entanglement has also been connected with many macroscopic properties of condensed matter systems [145, 152, 153]. We investigate the entanglement properties of the Fermi-Hubbard dimer and propose a novel scheme for the characterization and quantification of inter-particle entanglement based on current experimental measurement techniques.

3.1.1 Hubbard model

A very successful model for the description of condensed matter systems, which ultracold atoms in optical lattices may be a simulation of, is the Hubbard model [154]. Developed in 1963 to describe electrons in periodic potentials, the Hubbard model describes the dynamics of two fermionic species, labelled by the (pseudo)spin variable σ, in terms of the tunneling amplitude between neighbouring lattice sites J and an onsite interaction term U. The model also applies to systems of cold atoms in optical lattices, if appropriate conditions are met [155]. In order to provide the description of such complex systems in simple terms, the model relies on a number of approximations.

- The tight-binding approximation, associated with deep lattice sites, allows for a description in terms of non-orthogonal Wannier functions localised on the lattice sites. Appropriate lattice depth also ensures that tunneling amplitudes between non-neighbouring sites are negligible.

- The periodicity of the potential leads to an energy band structure, but for a Fermi energy low enough a description in terms of a single band may give accurate predictions. Furthermore, the low energy regime allows for treatment of the interaction potential in the Born approximation.

- Low density allows restriction of interactions to two-body interaction terms only.

Provided the above prescriptions are satisfied, the physical system of two fermionic atoms in a double-well potential, also referred to as a Fermi-Hubbard or fermionic dimer,

may be described in terms of the Fermi-Hubbard Hamiltonian (FHH) [147]

$$H = -J \sum_{\sigma=\uparrow,\downarrow} (a^\dagger_{L\sigma} a_{R\sigma} + a^\dagger_{R\sigma} a_{L\sigma}) + U \sum_{X=L,R} n_{X\uparrow} n_{X\downarrow}, \tag{3.1}$$

where J is the tunnelling term, U the on-site interaction and $a^\dagger_{X\sigma}$, $a_{X\sigma}$ and $n_{X\sigma} = a^\dagger_{X\sigma} a_{X\sigma}$ are the canonical creation, annihilation and number operators of a second-quantised representation. The labels L and R represent the single-site wavefunctions which are well approximated by Gaussians centred in the corresponding site for periodic potentials. The model describes a system of $1-D$ potential wells displaced by a distance a.

We may look into the symmetries of the FHH. Consider the site-specific spin operators

$$\begin{aligned} S_{ix} &= \frac{1}{2}(a^\dagger_{i\uparrow} a_{i\downarrow} + a^\dagger_{i\downarrow} a_{i\uparrow}) \\ S_{iy} &= \frac{i}{2}(-a^\dagger_{i\uparrow} a_{i\downarrow} + a^\dagger_{i\downarrow} a_{i\uparrow}) \\ S_{iz} &= \frac{1}{2}(a^\dagger_{i\uparrow} a_{i\uparrow} + a^\dagger_{i\downarrow} a_{i\downarrow}), \qquad \forall i = L, R, \end{aligned} \tag{3.2}$$

and the total spin operator

$$S^2 = \sum_{ij=L,R} (S_{ix} S_{jx} + S_{iy} S_{jy} + S_{iz} S_{jz}). \tag{3.3}$$

The total spin operator commutes with the FHH and it may be diagonalised simultaneously alongside one of its components, i.e. $S_z = \frac{1}{2}(a^\dagger_{L\uparrow} a_{L\uparrow} + a^\dagger_{L\downarrow} a_{L\downarrow} + a^\dagger_{R\uparrow} a_{R\uparrow} + a^\dagger_{R\downarrow} a_{R\downarrow})$, and they may thus be used as quantum numbers S and m_S respectively.

By introducing two-fermion wavefunctions in terms of creation operators $|X_\sigma Y_\tau\rangle \equiv a^\dagger_{X\sigma} a^\dagger_{Y\tau} |0\rangle$, the FHH may be described in terms of the Fermi-Hubbard basis $\{|\phi_i\rangle\}_i = \{|L_\uparrow L_\downarrow\rangle, |R_\uparrow L_\downarrow\rangle, |L_\uparrow R_\downarrow\rangle, |R_\uparrow R_\downarrow\rangle\}$ and is given by

$$H_{\text{FH}} = \begin{pmatrix} U & -J & -J & 0 \\ -J & 0 & 0 & -J \\ -J & 0 & 0 & -J \\ 0 & -J & -J & U \end{pmatrix}. \tag{3.4}$$

For any $U, J > 0$, the ground state of Hamiltonian (3.4) is nondegenerate and given by the eigenvector

$$|\psi_{\rm gs}\rangle \equiv |\psi_0\rangle = \frac{\left[|L_\uparrow L_\downarrow\rangle + |R_\uparrow R_\downarrow\rangle + \left(\frac{U}{4J} + \sqrt{1+\left(\frac{U}{4J}\right)^2}\right)(|L_\uparrow R_\downarrow\rangle + |R_\uparrow L_\downarrow\rangle)\right]}{\sqrt{\left(2 + \frac{U}{4J} + \sqrt{1+\left(\frac{U}{4J}\right)^2}\right)}} \tag{3.5}$$

and ground state energy $E_{\rm gs} \equiv E_0 = U/2 - \sqrt{4J^2 + U^2/4}$. The remaining eigenstates are given by

$$\begin{aligned}
|\psi_1\rangle &= \frac{1}{\sqrt{2}}(|R_\uparrow L_\downarrow\rangle - |L_\uparrow R_\downarrow\rangle) \\
|\psi_2\rangle &= \frac{1}{\sqrt{2}}(|R_\uparrow R_\downarrow\rangle - |L_\uparrow L_\downarrow\rangle) \\
|\psi_3\rangle &= \frac{\left[|L_\uparrow L_\downarrow\rangle + |R_\uparrow R_\downarrow\rangle + \left(\frac{U}{4J} - \sqrt{1+\left(\frac{U}{4J}\right)^2}\right)(|L_\uparrow R_\downarrow\rangle + |R_\uparrow L_\downarrow\rangle)\right]}{\sqrt{\left(2 + \frac{U}{4J} - \sqrt{1+\left(\frac{U}{4J}\right)^2}\right)}},
\end{aligned} \tag{3.6}$$

with respective eigenenergies given by $E_1 = 0$, $E_2 = U$ and $E_3 = U/2 + \sqrt{4J^2 + U^2/4}$. A generic mixed state is instead given by the density operator

$$\rho_{\rm FH} = \begin{pmatrix} P_{\rm LL} & \rho_{12} & \rho_{13} & \rho_{14} \\ & P_{\rm LR} & \rho_{23} & \rho_{24} \\ & & P_{\rm RL} & \rho_{34} \\ \text{h.c.} & & & P_{\rm RR} \end{pmatrix}, \tag{3.7}$$

where $P_{\rm XY}$ are the populations of the wells and ρ_{ij} the coherences.

Momentum correlations

In momentum space the basis wavefunctions are well approximated by Gaussian functions of position $\phi_X(x)$ for $X = L, R$, which depend on the details of the potential wells. The momentum wavefunction representation can be obtained by Fourier-transforming the position wavefunction, and the Fourier transform of a Gaussian is also a Gaussian

with an added phase shift proportional to the lattice spacing a:

$$\begin{aligned}\phi_L(x) &= g\left(x - \frac{a}{2}\right) \to \tilde{g}(k)e^{-ik\frac{a}{2}} \\ \phi_R(x) &= g\left(x + \frac{a}{2}\right) \to \tilde{g}(k)e^{+ik\frac{a}{2}}.\end{aligned} \tag{3.8}$$

The two-body momentum correlations $\langle n_\uparrow(k_1)n_\downarrow(k_2)\rangle$ in the fermionic dimer can therefore be described as the expectation value $G(k_1,k_2) = \langle n_\uparrow(k_1)n_\downarrow(k_2)\rangle = \mathrm{Tr}(\rho_{\mathrm{FH}}Z(k_1,k_2))$ of the momentum correlator

$$Z(k_1,k_2) = \begin{pmatrix} 1 & e^{-iak_2} & e^{-iak_1} & e^{-ia(k_1+k_2)} \\ & 1 & e^{-ia(k_1-k_2)} & e^{-iak_1} \\ & & 1 & e^{-iak_2} \\ \text{h.c.} & & & 1 \end{pmatrix}. \tag{3.9}$$

If we insert equation (3.7) in the expression for the momentum correlations, in the quadrature representation we have [147]

$$\begin{aligned}\langle n_\uparrow(k_1)n_\downarrow(k_2)\rangle \;=\; & 1 \\ & +2\ \mathrm{Re}(\rho_{13}+\rho_{24})\cos ak_1 - 2\ \mathrm{Im}(\rho_{13}+\rho_{24})\sin ak_1 \\ & +2\ \mathrm{Re}(\rho_{12}+\rho_{34})\cos ak_2 - 2\ \mathrm{Im}(\rho_{12}+\rho_{34})\sin ak_2 \\ & +2\ \mathrm{Re}\,\rho_{23}\cos a(k_1-k_2) - 2\ \mathrm{Im}\,\rho_{23}\sin a(k_1-k_2) \\ & +2\ \mathrm{Re}\,\rho_{14}\cos a(k_1+k_2) - 2\ \mathrm{Im}\,\rho_{14}\sin a(k_1+k_2).\end{aligned} \tag{3.10}$$

The above expression shows that the measurement of momentum correlations only provides partial information about an unknown mixed state. This makes entanglement estimation from such measurements a problematic task, since full state reconstruction is not an option. In fact, the coherences ρ_{12}, ρ_{24}, ρ_{13} and ρ_{34} only appear pairwise summed in eq. (3.10). Even if the momentum correlations are associated with in-situ measurements of the populations P_{XY}, these may only constrain the coherences owing to density matrix positivity constraints, but does not allow for a full reconstruction of ρ_{FH}. For the purpose of entanglement estimation, we will need to account for the partial information available and therefore only provide bounds for the value of appropriate entanglement measures.

3.1.2 Discretized space model

One of the strengths of the Fermi-Hubbard model is that it provides a simple representation suitable for the treatment of genuinely many-body systems. It may also be applied

to describe systems of few components, where it can be compared to first-quantized representations of the physical system. For a fermionic dimer, consisting of only two particles, it is possible to adopt numerical techniques for the solution of the associated Schrödinger equation. One of such techniques involves the discretization of the space and momentum degrees of freedom, deriving in the first instance a single-particle finite dimensional Hamiltonian H_N providing an approximate description of the dynamics of a single, free particle. The spectrum of this single-particle Hamiltonian is useful in connecting the discretized space representation to the Fermi-Hubbard model. In fact, a discretized version of the Wannier functions in equation (3.8) can be obtained in terms of the two lowest eigenvectors of H_N, $\bar{\varepsilon}_0$ and $\bar{\varepsilon}_1$. Within this section we provide a detailed description at the discretized-space approach for the description of the dynamics of a fermionic dimer.

This approach relies on a microscopic description of the interaction between the fermions, wherein the system kinematics and dynamics are determined by a Hamiltonian of the form

$$H^{(12)} = H \otimes \mathbb{1} + \mathbb{1} \otimes H + I(x, y), \tag{3.11}$$

where H is the single-particle Hamiltonian

$$H = \frac{\hbar}{2m}\nabla_x^2 + V(x). \tag{3.12}$$

The operator $V(x)$ models the double-well potential the particles are trapped in and $I(x, y)$ describes the interaction between the particles. A suitable parametrization of a double-well potential is given by the quartic function

$$V(x) = \frac{V_{\max}}{a^4}\left(x^2 - a^2\right)^2, \tag{3.13}$$

where a and $V_{\max}$ are the inter-well distance and potential barrier respectively. The interaction between the fermions is taken to be point-like, and thus described by a Dirac-delta function $I(x, y) = g\delta(x - y)$, with the coupling constant g tuning the strength of the interaction.

It is important to take into account which subsystems are being identified in the tensor product structure of equation (3.11). If the fermions may be distinguished by having opposite spin, the value of each spin may be used as a subsystem label and no additional exchange symmetry constraint is required. If, however, the fermions are spin polarised they need to be treated as identical subsystems and the set of available states is restricted to the antisymmetric subspace. In this case, the Pauli exclusion principle is enforced and the point-like interaction term bears no effect. We will therefore study

the spin-polarized case in the non-interacting regime only.

An analytical solution for the Schrödinger equation associated with Hamiltonian (3.12) is not known, however approximate numerical methods may be applied to reproduce the system dynamics to a satisfactory degree of accuracy. One such approach may be obtained by assuming a discretization of the position variables to a finite number N of available position *bins* of width Δ, thus transforming the continuous variable differential equation into a matrix equation [156]. The key point in this manipulation is the matrix representation of the Laplacian operator. Consider the action of the Laplacian on a wavefunction

$$\nabla^2\psi(x) = \lim_{\Delta\to 0} \frac{[\psi(x+\Delta)-\psi(x)]+[\psi(x-\Delta)-\psi(x)]}{\Delta^2}. \tag{3.14}$$

If the position space is discretized to the values $\{x_i\}_{i=1}^N$ such that $x_i - x_{i-1} = \Delta$, $\forall i$, then an approximate expression for the action of the Laplacian reads

$$\nabla^2\psi(x_i) \simeq \frac{[\psi(x_{i+1})-\psi(x_i)]+[\psi(x_{i-1})-\psi(x_i)]}{\Delta^2}. \tag{3.15}$$

With such discretization, the single particle Hamiltonian is represented by an $N \times N$ matrix in the discretized position basis $\{|x_i\rangle\}_{i=1}^N$

$$H_N = -\frac{\hbar}{2m\Delta^2}\begin{pmatrix} 2 & -1 & & & & \\ -1 & 2 & -1 & & & \\ & -1 & \ddots & \ddots & & \\ & & \ddots & \ddots & -1 & \\ & & & -1 & 2 & -1 \\ & & & & -1 & 2 \end{pmatrix} + \begin{pmatrix} V_1 & & & & & \\ & V_2 & & & & \\ & & \ddots & & & \\ & & & \ddots & & \\ & & & & V_{N-1} & \\ & & & & & V_N \end{pmatrix}, \tag{3.16}$$

where $V_i = V(x_i)$ is the potential evaluated at the centre of the i-th position bin. For deep potentials, the values of the vector $\bar{\xi}_L = \bar{\varepsilon}_0 - \bar{\varepsilon}_1$, where $\bar{\varepsilon}_0$ and $\bar{\varepsilon}_1$ are respectively the lowest and second-lowest energy eigenvalues of H_N, are distributed according to a Gaussian function centred in the left well. Analogously, a discretized Gaussian centred in the right well is given by $\bar{\xi}_R = \bar{\varepsilon}_0 + \bar{\varepsilon}_1$ [157]. When the potential barrier is relaxed tunneling between the sites is possible and the Wannier functions are non-orthogonal. Furthermore, the quartic potential we used to represent the discretized Hamiltonian is not periodic and therefore when tunneling is enabled the single-site wavefunctions cease to be symmetric Gaussians.

When represented in the orthonormal basis $\{|x_i\rangle\,|y_j\rangle\}_{i,j=1}^{N}$, the delta function is represented by an $N^2 \times N^2$ diagonal matrix given by $[\delta_N]_{ik,jl} = \langle x_i|x_k\rangle\,\langle y_j|y_l\rangle = \delta_{ik}\delta_{jl}$. Approximate discretized eigenvalues and eigenvectors for the problem may be thus derived by diagonalising the Hamiltonian matrix

$$H_N^{(12)} = H_N \otimes \mathbb{1} + \mathbb{1} \otimes H_N + g\delta_N, \tag{3.17}$$

which is the discretized version of equation (3.11).

A generic mixed state ρ_N of the system may be represented in a spectral decomposition of the Hamiltonian eigenvectors. We may obtain a discretized momentum correlation function G_N by writing ρ_N in its discretized momentum representation $\tilde{\rho}_N$ and considering its expectation values in the discrete momentum basis $\{|\varphi_i\rangle\}_{i=1}^{N}$ (whose derivation is discussed in Appendix A):

$$G_N(p,q) = \mathrm{Tr}\Big[\big(|\varphi_p\rangle\langle\varphi_p| \otimes |\varphi_q\rangle\langle\varphi_q|\big)\tilde{\rho}_N\Big], \quad \forall p,q = 1,..,N. \tag{3.18}$$

3.2 Momentum Correlations Measurement of a Fermionic Dimer

In this section we report the main features of interest for our work of the experimental setup from ref. [147] aimed at the detection of momentum correlations for a system of two fermions in a double-well potential. The physical system consists of two ^{6}**Li** atoms confined in a quasi-1D double-well potential realized with two far-red-detuned optical tweezers. The system is a realization of a fermionic dimer, where the tunneling parameter J is controlled by varying the depth of the well potentials and the on-site interaction U is tuned with a Feshbach resonance.

Measurements of the state of the system are carried out by a spin-resolved imaging technique [158]. The atoms are resonantly driven to emit fluorescence photons which are detected by a single-photon sensitive camera. Spin resolution is obtained by applying a magnetic offset [151]. The resolution of the atom position measurements is of the order of $4\,\mu m$, which is larger than the well separation $a \simeq 1.5\,\mu m$. In order to assess the in-situ position distribution, therefore, an imaging scheme is employed separating the individual atoms up to $180\,\mu m$ and by means of fluorescence imaging achieving a high fidelity of identifying each atom in the correct well [147].

In similar fashion the momentum space distribution may be measured by appropriate manipulation of the system prior to imaging. After the system is prepared in the desired

state, the atoms are allowed to expand in a weak optical potential along the double-well axis. Because of the quasi-ballistic expansion, the imaging of the atoms after a quarter of the trap period T returns the Fourier transform of the original position space distribution:

$$\langle n(p)\rangle_{t=0} \propto \langle n(x)\rangle_{t=T/4}\,, \tag{3.19}$$

where $\langle n(p)\rangle_{t=0}$ is the momentum distribution before the expansion and $\langle n(x)\rangle_{t=T/4}$ is the position distribution after a time-of-flight $t = T/4$. By rescaling the resulting distribution to a numerical factor due to the time-of-flight it is possible to average the spin-resolved momentum measurements in order to construct the momentum correlation function $G(k_1, k_2)$ discussed in section 3.1.1 [147].

3.3 Entanglement Estimation Based on Joint Measurements

Following up on the previous section, where we briefly reviewed a measurement strategy to obtain correlation functions based on joint measurements of a composite system of two ultracold fermionic atoms, we now argue that such correlations are *per se* ineffective at demonstrating particle-entanglement unless the identity of the particles is assessed. Specifically, we consider an instance where the correlations arising from measurements on an entangled distinguishable-fermion state display the same structure as those obtained from the same measurements on an identical-particle separable state.

In this section, moreover, we discuss some simple examples highlighting the effects of exchange symmetry on the statistics and correlation functions resulting from joint measurement outcomes on systems with exchange symmetry. In particular, we focus on correlations between subsystems in a first-quantised representation, where the relevant physical entities are considered to be the particles composing the system. These are of the kind first measured in Hanbury-Brown-Twiss (HBT) [136] experiments.

Consider the composite bipartite quantum state $|\Psi\rangle \in \mathcal{H} \otimes \mathcal{H}$ and two observables $A = \sum_i a_i\, |i\rangle\langle i|$ and $B = \sum_i b_i\, |i\rangle\langle i|$ represented in their spectral decomposition over the ONB $\{|i\rangle\}$ of $\mathcal{H} \equiv \mathbb{C}^d$. The collection of outcomes $\bar{a} = (a_1, ..., a_d)$ and $\bar{b} = (b_1, ..., b_d)$ are random variables with a state-dependent probability distribution. One may define a bivariate correlation function $C(\bar{a}, \bar{b}) = \langle\Psi|A \otimes B|\Psi\rangle$ such that if $C(\bar{a}, \bar{b}) = f(\bar{a})g(\bar{b})$ for some functions $f, g : \mathbb{C}^d \to \mathbb{R}$, then the random variables $\bar{a}$ and $\bar{b}$ are uncorrelated. Such is the case for a pure state of two distinguishable and separable particles $|\Psi_s\rangle = |\psi\rangle\,|\phi\rangle$. In fact, the correlation function may be expressed as

$$C(\bar{a}, \bar{b}) = \sum_{ij} a_i|\psi_i|^2 b_j|\phi_j|^2 = \sum_i a_i|\psi_i|^2 \sum_j b_j|\phi_j|^2 \equiv f_\psi(\bar{a})g_\phi(\bar{b}). \tag{3.20}$$

A different structure emerges when a bipartite state which is antisymmetric under exchange symmetry is considered. At this stage we still consider the subsystems as distinguishable, meaning that no symmetry constraint is necessary on the observables. Given the state

$$|\Psi\rangle_A = \frac{1}{\sqrt{2\mathcal{N}}}(|\psi\rangle\,|\phi\rangle - |\phi\rangle\,|\psi\rangle), \tag{3.21}$$

where $\mathcal{N} = 1 - |\,\langle\psi|\phi\rangle\,|^2$, the correlation function reads

$$C(\bar{a},\bar{b}) = \frac{1}{2\mathcal{N}}\left(f_\psi(\bar{a})g_\phi(\bar{b}) + f_\psi(\bar{a})g_\phi(\bar{b}) - 2\,\mathrm{Re}\,\langle\psi|A|\phi\rangle\,\langle\phi|B|\psi\rangle\right), \tag{3.22}$$

which in general is not factorizable. The entangled state $|\Psi\rangle_A$ therefore leads to correlations which may be extracted and quantified from $C(\bar{a},\bar{b})$.

Consider now the case when the state in equation (3.21) describes two identical fermions. As we have argued in Chapter 2, there is good reason to regard such state as separable. The observable describing the joint measurement needs to be permutation invariant and unless $A = B$, it is therefore given by $A \otimes B + B \otimes A$. The correlation function in this case reads

$$C_{\mathcal{A}}(\bar{a},\bar{b}) = \frac{1}{\mathcal{N}}\left(f_\psi(\bar{a})g_\phi(\bar{b}) + f_\psi(\bar{a})g_\phi(\bar{b}) - 2\,\mathrm{Re}\,\langle\psi|A|\phi\rangle\,\langle\phi|B|\psi\rangle\right), \tag{3.23}$$

which, apart from a normalization factor, has the same structure as the expression (3.22). This simple example shows how in general, by looking at the structure of correlation functions alone without taking into account the nature of the subsystems which yield the random variables $\bar{a}$ and $\bar{b}$, it is not possible to distinguish between the case of entangled distinguishable systems and that of separable identical-particle systems. The problem lies in the antisymmetrization requirement for fermionic first-quantised states, which leads to analogous correlation patterns as those obtained with entangled systems. This makes it a difficult task to estimate the entanglement in identical-fermion systems based on measurements of correlations, one that antisymmetric negativity is useful for. In fact, correlation measurement outcomes may be incorporated as constraints in the optimization instance (2.10) which defines antisymmetric negativity, making it possible to estimate the minimum entanglement between the subsystems which is not due to antisymmetrization and is compatible with the information available within the measurement dataset.

3.4 Antisymmetric Negativity for Experimental Entanglement Estimation

The theoretical description of the experimental measurements acquisition discussed in section 3.2 enables a great degree of control over the state preparation for two trapped ultracold fermions and the possibility of precise measurement of the system's properties including position and momentum space probability distributions, but not entanglement. Entanglement, in fact, is not an observable of the system, but an algebraic property of a given quantum state and its partitioning in subsystems. In order to extract an exact characterization of the entanglement in the physical system it is necessary to reconstruct completely the density operator describing the state in a process called *full quantum tomography* [159, 160]. Full tomographic reconstruction of a state is in general a challenging task so alternative methods of entanglement certification and quantification in presence of unknown states have been developed, such as device-independent entanglement certification and entanglement witnesses (which we review in Chapter 5). In this section we discuss the usefulness of antisymmetric negativity for identical-particle entanglement estimation when incomplete information about the state is available, that is, when full a tomographic reconstruction is not available.

Let us consider a two-identical-fermion system characterized by an unknown density matrix ρ. As discussed extensively in Chapter 2, alternative representations may be employed for the state of identical fermions, both in terms of distinguishable modes and identical particles. We are interested in the assessment of identical-particle entanglement properties so we focus on the first-quantised representation in terms of identical particles, which in presence of a particle number SSR may always be obtained from a mode representation. The state in the particle representation is therefore described by the antisymmetric density matrix $\rho_{\mathcal{A}}$. If $\rho_{\mathcal{A}}$ can be perfectly reconstructed from measurements the antisymmetric negativity may be directly applied to the reconstructed density matrix and an exact measured value of identical-particle entanglement provided. Suppose, instead, that the state is unknown but there is partial information available from a set of measurements $\{M_\mu\}_{\mu=1}^n$ with measurement outcomes given by

$$\mathrm{Tr}(M_\mu \rho_{\mathcal{A}}) = m_\mu \quad \forall \mu = 1, ..., n. \tag{3.24}$$

Assuming the measurements are characterised, equation (3.24) is a linear constraint on the density matrix $\rho_{\mathcal{A}}$ and may thus be enforced as a constraint in a semidefinite program. Our aim is to incorporate such constraint in the SDP 2.10 defining antisymmetric negativity. The unknown state $\rho_{\mathcal{A}}$ may be related to the optimization variable

σ in Definition 2.10 via the constraint

$$P_{\mathcal{A}}\sigma P_{\mathcal{A}} = \frac{1}{2}\rho_{\mathcal{A}}, \tag{3.25}$$

where we recall $P_{\mathcal{A}}$ is the projection on the antisymmetric subspace. By inserting equation (3.25) in (3.24) we obtain the constraint

$$2\mathrm{Tr}(M_\mu P_{\mathcal{A}}\sigma P_{\mathcal{A}}) = m_\mu, \quad \forall \mu = 1, ..., n, \tag{3.26}$$

where we also need to require the antisymmetric image of σ to be a positive operator:

$$P_{\mathcal{A}}\sigma P_{\mathcal{A}} \geq 0. \tag{3.27}$$

Normalization is ensured by the $\mathrm{Tr}(P_{\mathcal{A}}\sigma) = 1/2$ condition in the SDP 2.10. If we run the SDP 2.10 replacing constraint (3.25) with (3.26) and (3.27), the optimal value returned is the minimum antisymmetric negativity consistent with the partial information available of the state $\rho_{\mathcal{A}}$. The numerical value obtained by applying this SDP is therefore a lower bound for the identical-particle entanglement present between the identical fermions.

In real experimental scenarios the outcomes of measurements are not known exactly, but are given by a random variable with a probability distribution and associated confidence intervals. The real value of the outcome of measurement M_μ lies in the interval $[m_\mu^{\min}, m_\mu^{\max}]$. Semidefinite programs, however, allow for the enforcing of matrix inequality constraints. As a consequence, given a measurement outcome and its confidence interval we may replace the constraint (3.26) with

$$\begin{aligned} &2\mathrm{Tr}(M_\mu P_{\mathcal{A}}\sigma P_{\mathcal{A}}) \geq m_\mu^{\min} \\ &2\mathrm{Tr}(M_\mu P_{\mathcal{A}}\sigma P_{\mathcal{A}}) \leq m_\mu^{\max}, \quad \forall \mu = 1, ..., n, \end{aligned} \tag{3.28}$$

in such a way that the optimal value of the antisymmetric negativity SDP provides a lower bound on the antisymmetric negativity compatible with the confidence interval associated with the measurement outcome.

3.5 Identical-Particle Entanglement of a Fermionic Dimer

Having discussed the experimental techniques associated with measurements of the properties of two fermionic atoms in a double-well potential and a strategy to find a lower-bound for identical-particle entanglement in such systems, let us present specific results of the application of such method to cases of particular interest. The bounds

on the quantitative estimate are based on two key ingredients: the measured outcomes of experiments and the well justified assumptions about the physical model. In this section we discuss how the ability to enforce stronger assumptions about the system can provide stricter bounds on the estimated entanglement measures and we quantify the associated improvement.

A preliminary discussion of the different possible notions of entanglement for a double-well system of two fermions is required at this stage. As we discussed in Chapters 1 and 2, entanglement is a notion relative to the representation of quantum states and their partitioning into subsystems. In the case of two identical fermions, states may be given in the first or second quantised representation. Each representation is in turn subject to different possible partitionings.

For spin-1/2 fermions the single-particle Hilbert space is spanned by the four vectors

$$\{|\varphi_i\rangle\}_{i=1}^{4} = \{|L\uparrow\rangle, |L\downarrow\rangle, |R\uparrow\rangle, |R\downarrow\rangle\}, \tag{3.29}$$

where the position space amplitude is given by $\langle x|X\rangle = \phi_X(x)$, for $X = L, R$. One may therefore write a state of the system as the first-quantised wavefunction

$$|\psi\rangle = \sum_{i>j} \frac{\psi_{ij}}{\sqrt{2}}(|\varphi_i\rangle|\varphi_j\rangle - |\varphi_j\rangle|\varphi_i\rangle), \tag{3.30}$$

where the partition is carried out between *particles*. We have argued in Chapter 2 that the appropriate identical-particle entanglement notion for the state (3.30) is given by the GMW criteria and it may be quantified by antisymmetric negativity. We will compare AN with the standard negativity applied to (3.30), in order to quantify how much a standard distinguishable-particle entanglement measure applied to an identical-particle state overestimates the IPE.

Furthermore, one may consider the state in its occupation number representation of the four modes in (3.29). This representation allows to further partition the total Hilbert space, for instance between the two modes with spin up and those with spin down,

$$|\psi_\sigma\rangle = \sum_{\substack{klmn=0,1 \\ k+l+m+n=2}} \psi_{klmn} |k\rangle_{L\uparrow} |l\rangle_{R\uparrow} \Big| |m\rangle_{L\downarrow} |n\rangle_{R\downarrow}, \tag{3.31}$$

where the vertical bar represents the partition along which the entanglement may be evaluated. Such partition, using spin as a subsystem label, is equivalent to that of the Fermi-Hubbard basis $\{|\phi_i\rangle\}_i$ and the entanglement properties will coincide.

Analogously, one may consider the partition between the left and right well:

$$|\psi_x\rangle = \sum_{\substack{klmn=0,1 \\ k+l+m+n=2}} \psi_{klmn} |k\rangle_{L\uparrow} |l\rangle_{L\downarrow} \Big| |m\rangle_{R\uparrow} |n\rangle_{R\downarrow} . \tag{3.32}$$

This notion identifies the sites of the Hubbard model as the subsystems and is typically adopted when there are more than two particles, thus making a labelling of the particles in terms of only two spin variables inconvenient.

We will compare the above described notions of entanglement for a series of states of interest and investigate the connections and differences emerging therein. This kind of analysis aims at showing that under certain regimes mode entanglement may capture the entanglement properties of the particles in the system, whereas in others this is not the case and an analysis in terms of a first-quantised representation is preferred.

3.5.1 Fermi-Hubbard regime

We begin by operating in the regime of validity of the Fermi-Hubbard model, with no further assumption. The states of the system are therefore described by a density matrix ρ_{FH} of the form (3.7). As argued in section 3.2, the populations of ρ_{FH} may be estimated by in-situ position measurements. The coherences, on the other hand, are constrained by the momentum correlation measurements via the relation (3.10), but they are not completely determined. It is possible to provide bounds for the off-diagonal elements of ρ_{FH}, however, by generating a reconstruction of the correlations and, by comparison with the measured data, obtaining an estimate of the systematic and statistical errors of the matrix elements. We briefly review the procedure established in ref. [147] and apply it to obtain confidence intervals for the entries of ρ_{FH}.

Let us call $\bar{R}$ the discretized reconstruction of the binned momentum correlations $\bar{D}$. The reconstruction is given by a weighted sum over the discretized Fermi-Hubbard basis functions $\bar{B}$

$$\bar{R} = \sum_i w_i \bar{B}_i, \tag{3.33}$$

where the weights w_i are chosen as those minimising the difference between data and reconstruction. A suitable figure of merit is given by the total square error $[(\bar{R} - \bar{D}).(\bar{R} - \bar{D})]$, where the dot $(\cdot.\cdot)$ multiplication is the element-wise multiplication of the discretized vectors and the square brackets $[\cdot]$ indicate summation over all discretized momentum variables.

The systematic errors may be evaluated by repeating the reconstruction multiple times with a random sampling of the parameters describing the basis $\bar{B}$ according to a

normal distribution. The statistical errors are obtained by resampling the momentum correlations with fixed basis parameters but adding simulated shot noise and evaluating the resulting reconstructions. The final errors on the matrix entries are given by the standard deviation of the distribution resulting from all the instances of the resampling, adding up the systematic and statistical contributions.

The result of this procedure is an optimal density matrix $\tilde{\rho}_{\mathrm{FH}}$ and an error matrix ρ_ε, such that the real values for the system's density matrix entries $[\rho_{\mathrm{FH}}]_{ij}$ are subject to the relation

$$[\tilde{\rho}_{\mathrm{FH}}]_{ij} - [\rho_\varepsilon]_{ij} \leq [\rho_{\mathrm{FH}}]_{ij} \leq [\tilde{\rho}_{\mathrm{FH}}]_{ij} + [\rho_\varepsilon]_{ij}, \quad \forall i,j. \tag{3.34}$$

In order to assess the spin-mode entanglement compatible with the errors on the entries of ρ_{FH}, we may apply the SDP (1.25), defining the entanglement negativity of a distinguishable-subsystem state, with incorporated the constraints (3.34). If we call $N^L(\rho^\varepsilon_{\mathrm{FH}})$ the negativity lower bound associated with the measurement of ρ_{FH} with uncertainty given by ρ_ε, its explicit formulation is given by

$$\begin{aligned} N^L(\rho^\varepsilon_{\mathrm{FH}}) = & \min_{M,X} (\mathrm{Tr}(M) - 1)/2 \\ \text{such that} \quad & M \geq 0 \\ & -M \leq X^\Gamma \leq M \\ & X \geq 0 \\ & \mathrm{Tr}(X) = 1 \\ & [\tilde{\rho}_{\mathrm{FH}}]_{ij} - [\rho_\varepsilon]_{ij} \leq [X]_{ij} \leq [\tilde{\rho}_{\mathrm{FH}}]_{ij} + [\rho_\varepsilon]_{ij} \quad \forall i,j. \end{aligned} \tag{3.35}$$

It is worth pointing out that not all the matrices satisfying the constraint (3.34) are density matrices, because the nature of the reconstruction procedure does not enforce such constraint automatically. This is not a problem in the extraction of a lower bound for the negativity in terms of an SDP, since the positivity and normalization of the optimal state can be expressed as a constraint in the optimization instance.

In order to address the identical-particle entanglement we need to write the first-quantised representation of ρ_{FH}, by mapping it onto the 16-dimensional basis $\{|X\sigma\rangle\,|Y\tau\rangle\}$, for $X,Y = L,R$ and $\sigma,\tau = \uparrow,\downarrow$. Recalling the discussion about the relation between representations in Chapter 1, the substitution rule is given by $|X\rangle_\uparrow |Y\rangle_\downarrow \to \frac{1}{\sqrt{2}}(|X\uparrow\rangle\,|Y\downarrow\rangle - |Y\downarrow\rangle\,|X\uparrow\rangle)$. With such substitution we may map the optimal reconstructed matrix elements and the corresponding confidence intervals onto a first

quantised representation and run the constrained SDP described in section 3.4 in order to obtain a lower bound $N^L_{\mathcal{A}}(\rho^{\varepsilon}_{\mathcal{A}})$ for the antisymmetric negativity. We will compare such value with that of the standard negativity applied to the antisymmetric optimal state constrained by the confidence intervals, which we will call $N^L(\rho^{\varepsilon}_{\mathcal{A}})$.

We apply the above described entanglement measures to reconstructions based on experimentally measured well populations and momentum correlations for different estimated values of the magnetic offset Δ_M, measured in Gauss, which brings about the on-site interaction via Feshbach resonance. We show the resulting momentum correlations in the noninteracting ($\delta_M = 568\,G$) and strongly interacting ($\delta_M = 625\,G$) cases in Figures 3.1a and 3.1b respectively. A collection of values for the different entanglement notions associated with magnetic offset are reported in Table 3.1.

Δ_M(G)	568	580	590	600	610	625
$N^L(\rho^{\varepsilon}_{\mathrm{FH}})$	0	0.1165	0.2019	0.2991	0.3228	0.3190
$N^L_{\mathcal{A}}(\rho^{\varepsilon}_{\mathcal{A}})$	0	0.1165	0.2018	0.2991	0.3228	0.3189
$N^L(\rho^{\varepsilon}_{\mathcal{A}})$	0.4480	0.7331	0.9037	1.0982	1.1455	1.1379

TABLE 3.1: Table of values of the spin-mode negativity $N^L(\rho^{\varepsilon}_{\mathrm{FH}})$, antisymmetric negativity $N^L_{\mathcal{A}}(\rho^{\varepsilon}_{\mathcal{A}})$ and standard negativity $N^L(\rho^{\varepsilon}_{\mathcal{A}})$ as a function of magnetic offset Δ_M measured in Gauss. The system is prepared close to the ground state of the Fermi-Hubbard model with fixed double-well potential and the on-site interaction determined by the magnetic offset. The spin-mode and antisymmetric negativity coincide up to three decimal places, indicating that for such state preparations mode entanglement reflects that of particles. The small differences in the values for the $625\,G$ case may be attributed to the algorithmic evaluation of the entanglement measures.

The first striking feature of Table 3.1 is the coincidence of the values of spin-mode negativity and antisymmetric negativity, up to three decimal places. We conjecture the small discrepancy is due to the algorithmic nature of the evaluation of antisymmetric negativity, which minimizes over a very broad set of both pure and mixed states. When the two fermions in the double well potential are described by a spin singlet, using the spin z-component to label the modes captures the same entanglement properties as thinking about the system in terms of identical particles. In other words, partitioning the system in terms of spin-modes and identical-fermions yields the same value for entanglement negativity, up to three decimal places. In particular, we can see how both measures capture the onset of entanglement due to interactions. On the other hand, the standard negativity applied to the antisymmetric first-quantised state overestimates the entanglement due to interaction, because it does not take into account wavefunction antisymmetrization.

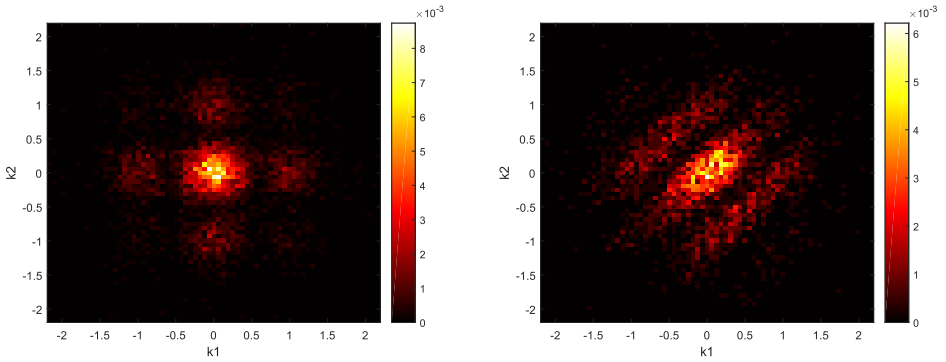

(A) $\langle n(k_1)n(k_2)\rangle$
$\Delta_M = 568\,G$

(B) $\langle n(k_1)n(k_2)\rangle$
$\Delta_M = 625\,G$

FIGURE 3.1: Experimentally measured momentum correlations $\langle n(k_1)n(k_2)\rangle$ for two fermions with opposite spin in a double-well potential in the non interacting (3.1a) and strongly interacting (3.1b) cases. The data was provided by the Ultracold Quantum Gases Group at the Physikalisches Institut of Heidelberg University [147].

Physical assumptions and entanglement estimates

The tightness of the lower bounds provided in the previous section depends on the unavailable information about the system. Here we show that if additional data is available about the system, or if more stringent assumptions can be made about it, the lower bounds can be improved. We rely on the discretized space model described in section 3.1.2, so that we may implement assumptions in terms of a microscopic description of the system.

The discretized Hamiltonian (3.17) is parametrized by parameters $V_{\max}$, a and g. The interplay of such parameters will determine the basis eigenfunctions in terms of which the state prepared in the experiment may be described. By making assumptions about the state preparation, we may derive a parametric model that can be fitted to the measured position coordinates and momentum correlations. The value of entanglement measure associated with the optimal states of the fit procedure may be used as an estimate of the entanglement in the system. In particular, we want to show the connection between the assumptions about the system and the entanglement lower bounds.

We first consider the case when the only assumption is that we are operating in the Hubbard regime. This means that there should exist a mapping between the states in the Fermi-Hubbard basis (3.7) and the state represented in the discretized model, which we will call ρ_D. We may establish this connection by recalling the modelling of Wannier functions in section 3.1.2, meaning we can use the replacement rule $|X_\uparrow Y_\downarrow\rangle \to \xi_X \otimes \xi_Y$. We recall that in the Fermi-Hubbard regime the distinct spin values allow us

to label and distinguish the subsystems, so we do not require the antisymmetrization of wavefunctions and we can address the spin-mode entanglement properties. The model parameters are therefore the matrix elements of ρ_{FH} alongside those describing the potential and interaction.

Information about the experiment can be used to reduce the degrees of freedom. Typically, the inter-well distance is related to the wavelength of the trapping laser, which is a known parameter in experiments. Furthermore, the relationship $J = (E_1 - E_0)/2$ between the tunneling parameter, which may also be measured, and the lowest energy eigenvalues of the double-well potential allows to fix the inter-well barrier $V_{\max}$. The in-situ measurements can also fix the populations of ρ_{FH}. We may therefore estimate the quantum state by fitting the discretized state representation, parametrized by the coherences and the coupling constant g, to the measured momentum correlations.

A further reduction of the free parameters may be enforced if the system energy is much lower than the first-excited state of Hamiltonian (3.11). Then one may adopt a pseudo-2D description where the only the ground and first excited states are populated. The density matrix may in this case be modelled by

$$\rho_D^{(2)} = \begin{pmatrix} p & \mathrm{Re}\, z + i\, \mathrm{Im}\, z \\ \mathrm{Re}\, z - i\, \mathrm{Im}\, z & 1-p \end{pmatrix}, \tag{3.36}$$

where p is the population of the ground state, z is the coherence and the state is represented in the $\{|\epsilon_0\rangle, |\epsilon_1\rangle\}$ basis given by

$$\begin{aligned} H_N^{(12)} |\epsilon_0\rangle &= \epsilon_0 |\epsilon_0\rangle, \\ H_N^{(12)} |\epsilon_1\rangle &= \epsilon_1 |\epsilon_1\rangle, \end{aligned} \tag{3.37}$$

having written ϵ_0 and ϵ_1 for the lowest and second-lowest energies respectively. Assuming the double-well potential can be experimentally characterised, the free parameters for $\rho_D^{(2)}$ are the coupling constant g, the ground-state population p, the coherence real ($\mathrm{Re}\, z$) and imaginary ($\mathrm{Im}\, z$) parts, which are linked to p due to positivity constraints.

Finally, if the state can be prepared very close to the ground state energy, it is possible to model it in terms of the pure ground state $\rho_D^{\mathrm{gs}} = |\epsilon_0\rangle\langle\epsilon_0|$, which amounts to the previous case with fixed $p = 1$. The only free parameter in this case is the interaction coupling constant.

The simulated momentum correlations may be calculated for states ρ_D, $\rho_D^{(2)}$ and ρ_D^{gs} by means of equation (3.18) and the resulting distribution can be fitted to the experimentally measured momentum correlations. We report examples of the simulated plots in Figure 3.2.

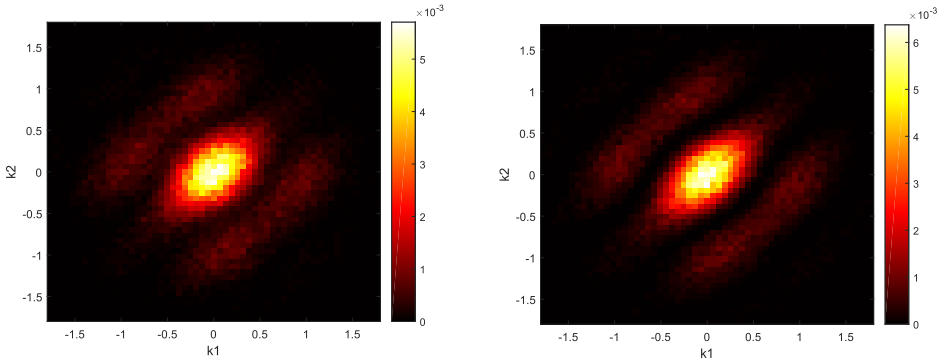

(A) $\rho_D^{(2)}$ (B) ρ_D^{gs}

FIGURE 3.2: Optimal fitted momentum correlations obtained with the discretized model and simulated shot noise. Figure 3.2a applies the pseudo-2D description (3.36) and Figure 3.2b is obtained from the simulated pure ground state. The purity of the state increases the visibility of the fringes in the correlation plots.

To demonstrate how additional physical assumptions affect the ability to estimate entanglement in the double-well system, we apply the three models discussed above to fit the momentum correlations in the strongly interacting case with magnetic offset $\Delta_M = 625\,G$. We calculate the spin-mode, antisymmetric and standard negativity for the optimal states resulting and compare the estimated value for the entanglement measures in Table 3.2. The fitting method is discussed in detail in Appendix A.

Negativities			
Case	$N^L(\rho_{\mathrm{FH}})$	$N^L_{\mathcal{A}}(\rho_{\mathcal{A}})$	$N^L(\rho_{\mathcal{A}})$
ρ_D	0.29	0.29	1.09
$\rho_D^{(2)}$	0.37	0.37	1.24
ρ_D^{gs}	0.46	0.46	1.42

TABLE 3.2: Table of Negativities from left to right: negativity for spins (mode entanglement) $N^L(\rho_{\mathrm{FH}})$, antisymmetric negativity for particles $N^L_{\mathcal{A}}(\rho_{\mathcal{A}})$ and standard negativity for particles $N^L(\rho_{\mathcal{A}})$ estimated from the momentum correlations measured in the strongly interacting case $\Delta_M = 625\,G$. We compare the entanglement measures for three density matrices with different assumptions fitted to the measured momentum correlations: ρ_D is in the generic Fermi-Hubbard regime, $\rho_D^{(2)}$ assumes occupation of the ground and first-excited state only and ρ_D^{gs} is the pure ground state.

Analogously to the results reported in Table 3.1 for entanglement estimation, we see coincidence between the spin-mode and antisymmetric negativity. We see as expected that stricter assumptions lead to higher estimated values for the entanglement measure.

In particular, the pure state model exhibits entanglement close to that of a maximally entangled two-qubit state, as is expected for a double-well system of two strongly-interacting fermions with fixed opposite spin, where the only available states are the two single-well occupation states. Standard negativity, on the other hand, overestimates the entanglement of the particles and the spins.

3.5.2 Spin-polarised dimer

Aside from the Fermi-Hubbard model, it is interesting to look into the case of the fermionic dimer with fixed identical spin. Here, it is not possible to use the spin to label the subsystems, since it is the same for both particles, unlike in the Hubbard model. This fact makes it a meaningless task to address spin-mode entanglement, whereas a description in terms of particles is required. The fermions here may not be labelled and are described in the first-quantised representation by an antisymmetric wavefunction.

Let us review the experimental preparation of such states as presented in [158]. First, a single well is switched on and loaded with two atoms occupying the lowest and first-excited levels respectively. Subsequently, a second well is adiabatically introduced so that one of the atoms shifts to the lowest excited state of the second well. When the two wells are equalised, both particles occupy the ground state of the respective well. Because it is possible to image the particles spin-selectively, the cases with identical polarised spin are post-selected from the overall measurement outcomes. The measurement of momentum correlations is carried out with the same technique as discussed in section 3.2, via ballistic expansion and imaging after a quarter trap period, obtaining

$$\langle n(x)n(x')\rangle_{t=T/4} \propto \langle n(p)n(p')\rangle_{t=0}\,. \tag{3.38}$$

An example of a measured momentum correlation is given in Figure 3.3. The momentum correlations exhibit interference fringes due to the spin-statistics leading to Pauli exclusion. This apparent correlation is present even when interactions between the atoms are tuned off.

Let us investigate what possible states generate such a momentum distribution. If we assume we are in the regime of validity of the Fermi-Hubbard model, we only allow the occupation of one level of each well. We may focus, without loss of generality, on the case when the spin degree of freedom is given by the wavefunction $|\psi_\sigma\rangle = |\uparrow\rangle\,|\uparrow\rangle$. The Pauli exclusion implies that the only state available for the position degree of freedom is therefore given by

$$|\psi_x\rangle = \frac{|L\rangle\,|R\rangle - |R\rangle\,|L\rangle}{\sqrt{2(1-|\,\langle L|R\rangle\,|^2)}}. \tag{3.39}$$

The momentum space representation of eq. (3.39) may be obtained by Fourier transforming the single-particle states. We may appreciate that the spin-polarised case strictly constrains the possible states of the system, in the Fermi-Hubbard regime, to only one allowed antisymmetric pure state

$$|\Psi_{\mathcal{A}}\rangle = |\psi_x\rangle\,|\psi_\sigma\rangle = \frac{|L\uparrow\rangle\,|R\uparrow\rangle - |R\uparrow\rangle\,|L\uparrow\rangle}{\sqrt{2(1-|\,\langle L|R\rangle\,|^2)}}. \tag{3.40}$$

The state (3.40) is clearly obtained by antisymmetrizing the factorised state $|L\uparrow\rangle\,|R\uparrow\rangle$, therefore in accordance with the GMW criteria (reviewed in section 2.6) it is to be considered a separable state of two identical fermions. Furthermore, its antisymmetric negativity may be analytically verified to be zero, being $|L\uparrow\rangle\,|R\uparrow\rangle$ an optimal state for the SDP defining AN.

We may reproduce the measured momentum correlations by applying the discretized space model of section 3.1.2. The subsystems associated with the Hilbert space tensor product structure are the identical fermionic atoms, therefore the solutions of the diagonalization of Hamiltonian (3.11) need to be projected on the antisymmetric subspace. Because of this, the Pauli exclusion prevents the point-like interaction $g\delta(x_1 - x_2)$ from having any effect, so the fermions are effectively treated as noninteracting. If we operate in the Fermi-Hubbard regime, the only allowed state is the antisymmetric ground state given by a discretization of (3.39). With these assumptions the only free parameters of the model are given by $V_{\max}$ and a, which may be either measured experimentally or fitted to the measured momentum correlations. In Figure 3.3 we show the results of a fit of the potential barrier parameter and the antisymmetric negativity of the resulting optimal state. As expected, the identical particle entanglement is zero, whereas the standard negativity is that of a maximally entangled qubit state. As we discussed earlier in this section, there is no meaningful notion of spin-entanglement in a spin-polarised case.

This case shows the usefulness of antisymmetric negativity for correctly quantifying the entanglement due to interactions even based on measurements exhibiting strong correlations. When the correlations are due to antisymmetrization, rather than some entanglement-generating process, the antisymmetric negativity verifies whether they can be obtained by a separable state projected on the antisymmetric subspace.

3.5.3 RF coupling

In the previous sections we examined separately the case of the two fermions having opposite and polarised spins. We now look into the cases when they are in a superposition

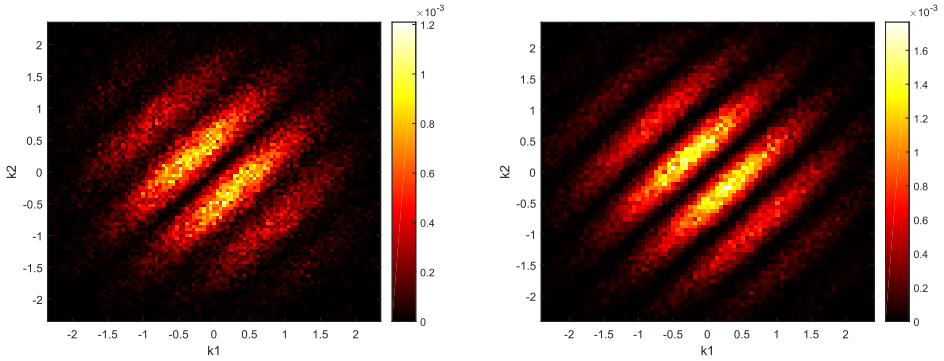

(A) Experimentally measured $\langle n(k_1)n(k_2)\rangle$ (B) Simulated $\langle n(k_1)n(k_2)\rangle$

FIGURE 3.3: Experimentally measured (3.3a) and optimal simulated (3.3b) momentum correlations obtained with the discretized model in the spin-polarised case. The antisymmetric negativity of the simulated state is 0, whereas its standard negativity is 1/2. The data was provided by the Ultracold Quantum Gases Group at the Physikalisches Institut of Heidelberg University [147].

of both. Such condition is met when the state is in a spin triplet, given by quantum numbers $S = 1$ and $m_S = 0$. The ground state of the FHH Hamiltonian is always given by a spin singlet, so additional terms are required in order for the preparation of a spin triplet may be obtained by ground state preparation of a Hamiltonian matrix. This may be done experimentally by inducing a spin imbalance via a radio-frequency (RF) magnetic coupling in orthogonal directions. The resulting interaction term in the system Hamiltonian is linear in the magnetic field intensity and the interaction strength can be parametrised in terms of RF coupling constants. The effect of such coupling is represented in the second-quantised picture as an additional interaction term in the FHH:

$$H = -J \sum_{\sigma=\uparrow,\downarrow} (a^\dagger_{L\sigma} a_{R\sigma} + a^\dagger_{R\sigma} a_{L\sigma}) + U \sum_{X=L,R} n_{X\uparrow} n_{X\downarrow} + g_x S_x + g_z S_z, \tag{3.41}$$

where $S_x = S_{Lx} + S_{Rx}$ and $S_z = S_{Lz} + S_{Rz}$ are the global spin terms introduced in eq. (3.2), g_x and g_z are the coupling constants tuning the RF coupling. The Hamiltonian (3.41) can not be represented in the four-dimensional Fermi-Hubbard basis, since the S_x and S_z terms introduce the following additional spin-polarised states in the representation: $\{|L\uparrow R\uparrow\rangle, |R\uparrow L\uparrow\rangle, |L\downarrow R\downarrow\rangle, |R\downarrow L\downarrow\rangle\}$. The Hamiltonian may be therefore represented and diagonalised in the 16-dimensional Hilbert spaces given by the mode representation (3.31) and the particle representation (3.30).

Different combinations of the parameters U/J, g_x and g_z will lead to different spin sectors in the ground state. When the RF coupling is switched off, the system is a

Fermi-Hubbard dimer and it's ground state is a spin singlet, as discussed in section 3.1. When the RF coupling is the dominant contribution, on the other hand, the magnetic field rotates the spins of the ground state out of the z axis and the lowest energy state is given by a spin triplet. We will look into the intermediate regime to highlight how different RF coupling strengths can bring about qualitative variations in the interplay of mode and particle entanglement.

As a benchmark example, we consider the ground state $|\Psi\rangle$ of a Fermi-Hubbard Hamiltonian with $U/J = 10$ and vary the coupling constants g_x and g_z in the $[0, J]$ range. First, let us consider the case of strong S_z coupling, with $g_z/J = 1$. The ground state in this regime is given by a spin triplet with a spin imbalance for the $\uparrow\uparrow$ terms given by S_z favouring such alignment. We may compare the spin-mode and antisymmetric negativity as a function of g_x, as shown in Figure 3.4. This example highlights a

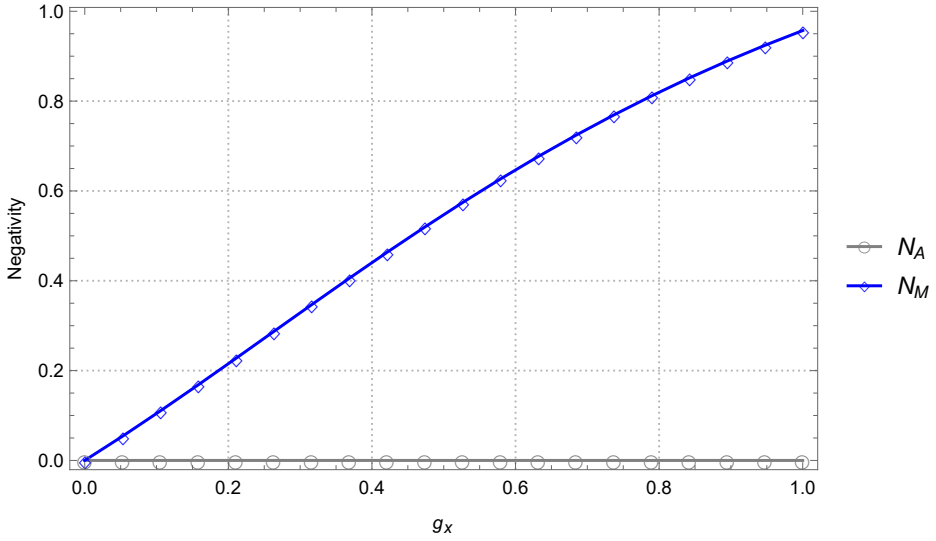

FIGURE 3.4: Antisymmetric negativity N_A (circle markers) and spin-mode entanglement negativity N_M (diamond markers) as a function of g_x(in units of J) and $g_z = J$ applied to the ground state of eq. (3.41) with $U/J = 10$. The discrete numerically calculated values are linearly interpolated in the graphic. The identical particles are unentangled, but the mode entanglement increases with the g_x coupling.

regime where the description in terms of spin-modes does not capture the entanglement between the identical-particles. With no S_x coupling the ground state triplet is separable according to both entanglement notions, but the onset of coupling in the x axis yields an increase in spin-mode entanglement, but not in particle entanglement.

An even richer structure is available when we consider a weaker S_z coupling with $g_z/J = 1/3$. The entanglement structure in this case is reported in Figure 3.5. We

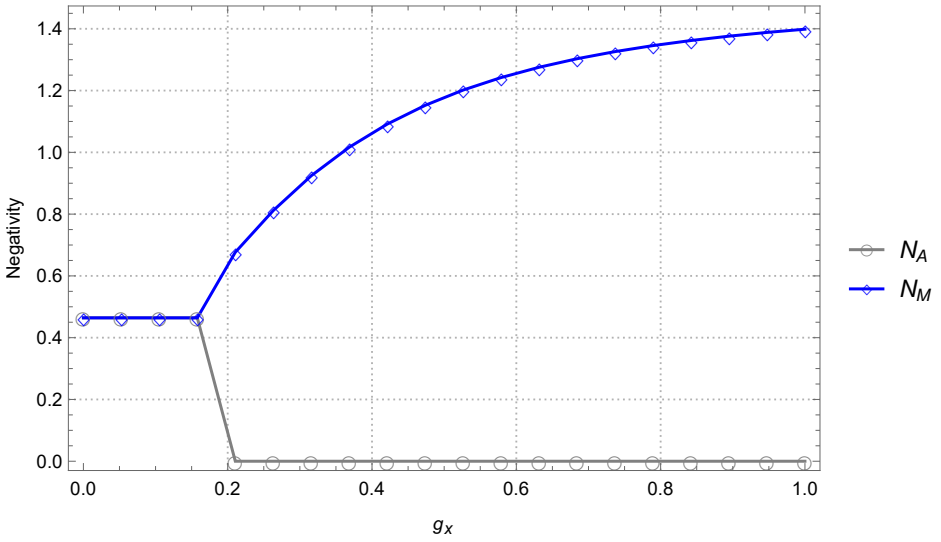

FIGURE 3.5: Antisymmetric negativity N_A (circle markers) and spin-mode entanglement negativity N_M (diamond markers) as a function of g_x (in units of J) and $g_z = J/3$ applied to the ground state of eq. (3.41) with $U/J = 10$. The discrete numerically calculated values are linearly interpolated in the graphic. We notice a transition from a singlet regime $g_x < 0.2J$ to a triplet regime $g_x > 0.2J$. Correspondingly, the entanglement notions go from being coincident to having different behaviour.

may notice that by tuning one experimentally controllable parameter, we transition from a singlet regime $g_x < 0.2J$ where the notions of antisymmetric and spin-mode negativity coincide, to a triplet regime $g_x > 0.2J$ where the two entanglement notions differ. The antisymmetric negativity drops to zero, since the triplet ground state may be obtained by antisymmetrizing a factorised state, whereas the spin-mode negativity increases monotonically with g_x.

This scenario quantifies the difference between the measures of entanglement given by the antisymmetric negativity and spin-mode negativity. When the system is prepared in a spin-singlet state, there is no difference between the entanglement of the spin modes and the entanglement due to interactions between the particles. On the other hand, when the state is given by a spin triplet, this is not the case and our measure quantifies how much the spin-mode entanglement overestimates the identical-particle entanglement, as measured when antisymmetrization is removed.

In order to provide an estimate of the identical-particle entanglement in the system we need to be able to measure the momentum correlations spin-selectively. In fact, the state will populate the eigenstates of the 16-dimensional Hilbert space of the kind in (3.31) and the ability to assess the momentum for different combinations of spin is required to witness the differences between the particle-particle entanglement and the

mode entanglement. Therefore one needs to measure the joint momentum distribution in the four spin sectors $\{\uparrow\uparrow, \uparrow\downarrow, \downarrow\uparrow, \downarrow\downarrow\}$. In the first quantised picture, the measurement operators are given by

$$P_{1\uparrow} \otimes P_{2\uparrow} + P_{2\uparrow} \otimes P_{1\uparrow} \tag{3.42}$$

$$P_{1\uparrow} \otimes P_{2\downarrow} + P_{2\downarrow} \otimes P_{1\uparrow} \tag{3.43}$$

$$P_{1\downarrow} \otimes P_{2\uparrow} + P_{2\uparrow} \otimes P_{1\downarrow} \tag{3.44}$$

$$P_{1\downarrow} \otimes P_{2\downarrow} + P_{2\downarrow} \otimes P_{1\downarrow}. \tag{3.45}$$

We may further exploit the state's symmetries to simplify the entanglement estimation procedure. When the ground state is a $S = 1$ state, the total wavefunction antisymmetry constrains the state to be of the form

$$|\psi_A(a,b)\rangle = \frac{1}{\mathcal{N}}(|LR\rangle - |RL\rangle)\left[a\,|\uparrow\uparrow\rangle + b\,|\downarrow\downarrow\rangle + c(|\uparrow\downarrow\rangle + |\downarrow\uparrow\rangle)\right], \tag{3.46}$$

where a and b are the only free parameters (taking c fixed by normalization). The negativity of the state will therefore only be a function of a and b, so it suffices to estimate these two parameters from the data. To do so, one may prepare the system in the identical spin ground state and measure the resulting momentum correlations, to be used as a reference. Subsequently one prepares the target state $|\Psi(g_x, g_z)\rangle$ in a regime where it is a spin triplet and thus of the form (3.46). By measuring the $P_{1\uparrow} \otimes P_{2\uparrow} + P_{2\uparrow} \otimes P_{1\uparrow}$ and $P_{1\uparrow} \otimes P_{2\downarrow} + P_{2\downarrow} \otimes P_{1\uparrow}$ operators one obtains momentum distributions analogous to the ones from the reference measurement up to detection noise and a proportionality factor of a and b respectively. From the reconstructed optimal states one may estimate spin-mode and entanglement negativity, thereby obtaining a version of Figures 3.4 and 3.5 with entanglement estimates based on momentum correlation measurements.

In this Chapter we applied antisymmetric negativity to the problem of estimating identical-particle entanglement in a Fermi-Hubbard dimer. Based on experimentally measured momentum correlations and physical assumptions about a theoretical model for their simulation, we provided entanglement lower bounds in different regimes of the fermionic dimer. We studied the connection between the application of stricter physical assumptions and tighter lower bounds for the estimated entanglement. Furthermore, we probed the relationship between identical-particle and mode entanglement, identifying regimes where the notions coincide and differ. These results show the usefulness of antisymmetric negativity, and in general the SDP approach at entanglement quantification, for understanding identical-fermion systems beyond a description in terms of modes. In

particular, we overcome some of the difficulties in entanglement quantification which arise from the exchange symmetry of identical-particle systems by quantifying the entanglement due only to interactions.

Our approach is effective at dealing with an issue of many strategies for experimental entanglement quantification, that of the availability of partial information about the state. Due to its formulation as a constrained optimization algorithm, antisymmetric negativity provides lower bounds consistent with the information that can be extracted from the measurements. In addition to this, our approach in terms of entanglement quantification with semidefinite programming can be applied more broadly for entanglement estimation in bipartite physical systems, regardless of distinguishability. The intuitive interpretation of the outcomes of such entanglement estimation strategy and the robustness of the mathematical definitions underlying it have the potential to make it an attractive experimental method for a broad scope of physical systems [158].

A drawback of our approach is given by scalability, since the numerical evaluation requires to optimize over all the unconstrained degrees of freedom, i.e. the elements of the variable density matrix. The number of such elements has a poor scalability with dimension and number of subsystems, an issue which is inherited by our entanglement estimation strategy based on semidefinite programming.

Chapter 4

Simple Class of Bound Entangled States Based on the Properties of the Antisymmetric Subspace

In the previous Chapters we dealt with the interplay of exchange symmetry and entanglement in systems of identical-particles, focusing on a strategy to account for the spin-statistics connection and quantifying the entanglement therein. In order to introduce the novel identical particle measure 2.8 put forward in Chapter 2, we investigated a number of properties of the symmetric and antisymmetric subspaces. Such algebraic subspaces are independent of the nature of the physical systems they describe, therefore we may apply some of the findings from the study of identical particles to systems of distiguishable particles. In this Chapter we introduce a novel class of states, characterised by having properties of experimental and theoretical interest, based on considerations emerging from the study of the exchange symmetric subspaces for 2 distinguishable subsystems.

Unravelling the entanglement properties of quantum states is often not an easy task [66]. Similarly to many other fields of physics, symmetry provides an useful tool in the evaluation of entanglement properties, by requiring additional constraints and relationships in the properties of quantum states and the operations which may be carried out upon them.

By studying the properties of the symmetric and antisymmetric subspace we will address the presence of bound entanglement in bipartite qudit systems and put forward a prescription for generation of *bound entangled* states using semi-definite programming as well as a novel family of states which exhibits bound entanglement in a well-defined parameter regime. Let us begin by introducing bound entanglement and its main features.

4.1 Distillable Entanglement

Entanglement has been shown to be a key feature for the realisation of many quantum information tasks, such as cryptography, dense coding and teleportation [19, 92]. Interaction with a noisy environment typically (albeit not always) reduces the entanglement between subsystems and affects the performance of the tasks, up to an extent where the enhancements brought about by the use of a quantum resource are vanquished. Perfectly isolating a quantum system from its environment is however a technological challenge and a major drawback in the onset of quantum-based technologies so several strategies have been devised to mitigate the detrimental effect of noise on quantum systems, the most notable being quantum error correction. An alternative approach was put forward in 1996 by Bennett et al. [161] showing the possibility, by means of local operations, to take many copies of a noisy weakly-entangled state and obtain a smaller number of states with higher entanglement. The procedure was given the name of *entanglement distillation*, in analogy with the homonymous liquid purification process.

The ability to distill highly entangled states is a good measure for the usefulness of a noisy quantum state in performing quantum information tasks. Therefore, the entanglement measure of *distillable entanglement* was put forward based upon these ideas. Distillable entanglement may be defined as

$$E_D(\rho) = \sup\Big\{ r : \lim_{n\to\infty} \Big[\inf_{\Lambda} \mathrm{Tr}|\Lambda(\rho^{\otimes n}) - \Psi^+_{2^{rn}}| \Big] = 0 \Big\}, \tag{4.1}$$

where $\Lambda(\cdot)$ is a trace-preserving LOCC operation and Ψ^+_k is the maximally entangled density matrix in k dimensions. When the state ρ is pure the quantity in (4.1) is called *entanglement concentration*. On the other hand, states for which the rate $E_D(\rho)$ is zero are called *undistillable*. States which are entangled, yet undistillable are called *bound entangled*. Distillable entanglement can be interpreted as the rate of production of maximally entangled pure states from a large number of copies of a given state by means of a *distillation* process employing LOCC operations.

4.1.1 Bound entanglement

Bound entangled states are interesting for a number of reasons. They provide a natural benchmark for testing entanglement detection schemes, as well as probing the relationships and differences between quantum correlations such as entanglement, steering and nonlocality [34, 44, 45]. Furthermore, they are a useful tool in the mathematical study of positive but not completely positive maps [58]. The PPT criterion is of relevance

for the study of bound entanglement since it is a known result that all PPT-entangled states are bound entangled [43].

In the bipartite case bound entangled states cannot be used for certain tasks such as teleportation and dense coding, however they have been shown to be useful in other contexts, such as in *superactivation* effects in quantum information [162]. Several examples of bound entangled states have been proposed in the literature [163–167], however they often rely on a complex structure not amenable to a simple parametrization in terms of a noise parameter or the system dimensionality. Being able to provide such a class of states may enhance the understanding of the features of bound entanglement, its relationship with other notions of quantum correlations and provide guidance in realising bound entanglement experimentally, thus enabling the study of potentially technologically relevant features such as superactivation.

4.2 Permutation Symmetry and Separability

Consider two subsystems A and B having identical local dimension d and described by the total Hilbert space $\mathcal{H}_{AB} \simeq \mathbb{C}^d \otimes \mathbb{C}^d$. When the local dimension of a bipartite system is the same for both subsystems, a composite Hilbert space can be written as the direct sum of the symmetric and antisymmetric subspaces: $\mathcal{H}_{AB} = \mathcal{H}_{\mathcal{S}} \oplus \mathcal{H}_{\mathcal{A}}$, with the symmetric subspace $\mathcal{H}_{\mathcal{S}} = \mathbb{C}^d \vee \mathbb{C}^d$ and the antisymmetric subspace $\mathcal{H}_{\mathcal{A}} = \mathbb{C}^d \wedge \mathbb{C}^d$. We adopt the notation where the symbol $\oplus$ denotes direct sum, while $\vee$ and $\wedge$ denote the symmetric and antisymmetric tensor product, respectively [93]. The symmetric and antisymmetric subspaces respectively have dimensions $d_{\mathcal{S}} := d(d+1)/2$ and $d_{\mathcal{A}} := d(d-1)/2$.

The projector onto the symmetric space is given by

$$P_{\mathcal{S}} = \frac{\mathbb{1} + V}{2}, \tag{4.2}$$

whereas the projector onto the antisymmetric space is given by

$$P_{\mathcal{A}} = \frac{\mathbb{1} - V}{2}. \tag{4.3}$$

The projector in (4.2) and (4.3) are orthogonal and their sum is the identity operator $P_{\mathcal{S}} + P_{\mathcal{A}} = \mathbb{1}$. Let us investigate the action of the projectors on the factorised vectors

$|\alpha\rangle$ and $|\beta\rangle$:

$$P_{\mathcal{S}} |\alpha\rangle |\beta\rangle = \frac{1}{2} (|\alpha\rangle |\beta\rangle + |\beta\rangle |\alpha\rangle) \tag{4.4}$$

$$P_{\mathcal{A}} |\alpha\rangle |\beta\rangle = \frac{1}{2} (|\alpha\rangle |\beta\rangle - |\beta\rangle |\alpha\rangle) \tag{4.5}$$

$$\langle\alpha| \langle\beta| P_{\mathcal{S}} |\alpha\rangle |\beta\rangle = \frac{1 + |\langle\alpha|\beta\rangle|^2}{2} \tag{4.6}$$

$$\langle\alpha| \langle\beta| P_{\mathcal{A}} |\alpha\rangle |\beta\rangle = \frac{1 - |\langle\alpha|\beta\rangle|^2}{2}. \tag{4.7}$$

The above considerations are of relevance to the individuation of the properties of the images of separable states on the symmetric and antisymmetric subspaces.

4.2.1 Antisymmetric image of separable states

We may put forward a few simple properties pertaining to projections of factorised states onto the antisymmetric subspace. We recall some of the results outlined in Chapter 2 completing them with proofs in a compact form. Let $|\psi_{\text{sep}}\rangle = |\alpha\rangle |\beta\rangle$ be the separable state given by the tensor product of the normalised states $|\alpha\rangle$ and $|\beta\rangle$. The following proposition holds:

Proposition 4. Given the separable bipartite pure state $|\psi_{\text{sep}}\rangle$, then either $\|P_{\mathcal{A}} |\psi_{\text{sep}}\rangle\| = 0$, or

$$|\psi_{\mathcal{A}}\rangle = P_{\mathcal{A}} |\alpha\rangle |\beta\rangle / \|P_{\mathcal{A}} |\alpha\rangle |\beta\rangle\| \tag{4.8}$$

is a normalized state with Schmidt rank equal to two.

Proof. If we recall the expression for $|\beta\rangle$ in (2.73) we may rewrite the unnormalised antisymmetric projection of $|\psi_{\text{sep}}\rangle$ as

$$P_{\mathcal{A}} |\alpha\rangle |\beta\rangle = \frac{1}{2} \left(\sqrt{1 - |\langle\alpha|\beta\rangle|^2} (|\alpha\rangle |\bar{\alpha}\rangle - |\bar{\alpha}\rangle |\alpha\rangle) \right). \tag{4.9}$$

It is evident that the only two options are $P_{\mathcal{A}} |\alpha\rangle |\beta\rangle = 0$ when $|\langle\alpha|\beta\rangle| = 1$ or the normalised state reads

$$\frac{P_{\mathcal{A}} |\alpha\rangle |\beta\rangle}{\|P_{\mathcal{A}} |\alpha\rangle |\beta\rangle\|} = \frac{1}{\sqrt{2}} (|\alpha\rangle |\bar{\alpha}\rangle - |\bar{\alpha}\rangle |\alpha\rangle), \tag{4.10}$$

which is written in its Schmidt decomposition with both Schmidt coefficients equal to $1/\sqrt{2}$ and Schmidt basis given by $\{|\alpha\rangle |\bar{\alpha}\rangle\}$ and $\{|\bar{\alpha}\rangle |\alpha\rangle\}$ for the two subsystems respectively. □

It is worth noting that the Schmidt coefficients of the image of separable states are equal (in the nontrivial case), which implies a degeneracy in the Schmidt coefficients and a non-uniqueness of basis choice in the Schmidt decomposition. We may generalise this result to the case of mixed states.

Proposition 5. Given the mixed separable state $\rho = \sum_i p_i \left|\alpha_i\right\rangle\!\left\langle\alpha_i\right| \otimes \left|\beta_i\right\rangle\!\left\langle\beta_i\right|$, then its projection on the antisymmetric subspace $\rho_{\mathcal{A}} = P_{\mathcal{A}}\rho P_{\mathcal{A}}/\mathrm{Tr}(P_{\mathcal{A}}\rho)$ will either be null or have Schmidt number equal to 2.

Proof. By virtue of Proposition 4, the antisymmetric projection of each of the pure states in the decomposition of ρ may either be null or be written in the form (4.10). The resulting antisymmetric state $\rho_{\mathcal{A}}$ has therefore Schmidt number at most equal to 2. Furthermore, all antisymmetric mixed states have at least Schmidt number two, because the antisymmetric subspace does not contain product states, as can be verified by using (4.7). □

Proposition 6. Let us consider the state

$$\left|\psi\right\rangle_{AB} = \frac{P_{\mathcal{A}}\left|\alpha\right\rangle\left|\beta\right\rangle}{\left\|P_{\mathcal{A}}\left|\alpha\right\rangle\left|\beta\right\rangle\right\|}, \tag{4.11}$$

where $\left|\alpha\right\rangle\left|\beta\right\rangle$ is a normalized product state with $\left|\left\langle\alpha|\beta\right\rangle\right| < 1$. Then there is another normalized state $\left|\alpha'\right\rangle\left|\beta'\right\rangle$ such that $\left|\psi\right\rangle_{AB} = \sqrt{2}P_{\mathcal{A}}\left|\alpha'\right\rangle\left|\beta'\right\rangle$, with projection probability on the antisymmetric subspace given by $\left\|P_{\mathcal{A}}\left|\alpha'\right\rangle\left|\beta'\right\rangle\right\|^2 = 1/2$.

Proof. It suffices to make the choice $\left|\alpha'\right\rangle = \left|\alpha\right\rangle$ and

$$\left|\beta'\right\rangle = \left|\bar{\alpha}\right\rangle = \frac{\left|\beta\right\rangle - \left\langle\alpha|\beta\right\rangle\left|\alpha\right\rangle}{\left\|\left|\beta\right\rangle - \left\langle\alpha|\beta\right\rangle\left|\alpha\right\rangle\right\|}. \tag{4.12}$$

□

The above propositions lead to the following Lemma, which is a generalisation of proposition 6 to the case of mixed states.

Lemma 1. Let ρ_{sep} be a separable state such that $\mathrm{Tr}(P_{\mathcal{A}}\rho_{\mathrm{sep}}) > 0$. Then there is a separable state ρ'_{sep} such that $\mathrm{Tr}\big(P_{\mathcal{A}}\rho'_{\mathrm{sep}}\big) = 1/2$ and

$$\frac{P_{\mathcal{A}}\rho_{\mathrm{sep}}P_{\mathcal{A}}}{\mathrm{Tr}(P_{\mathcal{A}}\rho_{\mathrm{sep}})} = \frac{P_{\mathcal{A}}\rho'_{\mathrm{sep}}P_{\mathcal{A}}}{\mathrm{Tr}\big(P_{\mathcal{A}}\rho'_{\mathrm{sep}}\big)}. \tag{4.13}$$

Proof. Let $\rho_{\mathrm{sep}} = \sum_i p_i \left|\alpha_i\right\rangle\!\left\langle\alpha_i\right| \otimes \left|\beta_i\right\rangle\!\left\langle\beta_i\right|$. To any term in the sum such that $p_i > 0$ and $\left|\left\langle\alpha_i|\beta_i\right\rangle\right| < 1$, associate a probability

$$p'_i = p_i \frac{\langle\alpha_i| \langle\beta_i| P_{\mathcal{A}} |\alpha_i\rangle |\beta_i\rangle}{\mathrm{Tr}(\rho_{\mathrm{sep}} P_{\mathcal{A}})} \tag{4.14}$$

and local states

$$\begin{aligned} \left|\alpha'_i\right\rangle &= |\alpha_i\rangle \\ \left|\beta'_i\right\rangle &= (|\beta\rangle - \langle\alpha|\beta\rangle |\alpha\rangle)/\| |\beta\rangle - \langle\alpha|\beta\rangle |\alpha\rangle \|. \end{aligned} \tag{4.15}$$

Then the separable state $\rho'_{\mathrm{sep}} = \sum_i p'_i |\alpha'_i\rangle\langle\alpha'_i| \otimes |\beta'_i\rangle\langle\beta'_i|$ verifies the stated conditions, as it can be checked by the application of Proposition 6. □

4.3 PPT-Entangled States and Semidefinite Programs

The result of Lemma 1 essentially poses a constraint on the projection probability onto the antisymmetric subspace of a separable bipartite state. It is therefore possible to obtain a state which is bound entangled by simply identifying a state which is PPT and has a probability of projection on the antisymmetric subspace incompatible with the constraint of Lemma 1. We will see that there are several possibilities to do so, both based on numerical algorithms and analytical considerations.

The first method we may put forward relies on defining a class of semidefinite programs whose output is a bound entangled state, because the condition of positivity under partial transposition is a linear one and is amenable to be enforced as a constraint in an SDP.

Let $\rho_{\mathcal{A}}$ be a bipartite antisymmetric state, so that it is fully supported in the antisymmetric subspace: $\rho_{\mathcal{A}} = P_{\mathcal{A}} \rho_{\mathcal{A}} P_{\mathcal{A}}$. We are interested in finding the largest probability of obtaining such a state from a PPT state by projecting onto the antisymmetric subspace, that is the following quantity, defined as the solution to an SDP:

$$\begin{aligned} p^{\mathrm{PPT}}(\rho_{\mathcal{A}}) := \quad & \max_{\sigma} \quad \mathrm{Tr}(P_{\mathcal{A}}\sigma) \\ & \text{s.t.} \quad P_{\mathcal{A}}\sigma P_{\mathcal{A}} = \mathrm{Tr}(P_{\mathcal{A}}\sigma)\rho_{\mathcal{A}} \\ & \quad\quad \sigma \geq 0 \\ & \quad\quad \mathrm{Tr}(\sigma) = 1 \\ & \quad\quad \sigma^{\Gamma} \geq 0. \end{aligned} \tag{4.16}$$

The following relation may be proved.

Theorem 4.1. *For all antisymmetric states $\rho_{\mathcal{A}}$ the quantity $p^{PPT}(\rho_{\mathcal{A}})$ satisfies the inequality $2/(d(d+1)+2) \leq p^{PPT}(\rho_{\mathcal{A}}) \leq 1/2$.*

Proof. Let us start from the lower bound. For the given $\rho_{\mathcal{A}}$, let us consider the family of states $\sigma(p) = p\rho_{\mathcal{A}} + (1-p)P_{\mathcal{S}}/d_{\mathcal{S}}$. By construction, $\sigma(p)$ is a valid quantum state, and it holds that $P_{\mathcal{A}}\sigma(p)P_{\mathcal{A}} = p\rho_{\mathcal{A}}$, with $\mathrm{Tr}(P_{\mathcal{A}}\sigma(p)) = p$. We now want to find a $\bar{p}$ such that $\sigma(p)^{\Gamma} \geq 0$ for all $p \leq \bar{p}$. One has

$$\sigma(p)^{\Gamma} = p\rho_{\mathcal{A}}^{\Gamma} + (1-p)\frac{\mathbb{1} + d\,|\psi^+\rangle\langle\psi^+|}{2d_{\mathcal{S}}}. \tag{4.17}$$

Requiring positivity of an operator is analogous to imposing the constraint that its smallest eigenvalue is positive. This amounts to requiring that the inequality

$$\begin{aligned}
&\min_{|\phi\rangle} \langle\phi|\sigma(p)^{\Gamma}|\phi\rangle \\
&= \min_{|\phi\rangle}\{p\,\langle\phi|\rho_{\mathcal{A}}^{\Gamma}|\phi\rangle + \frac{1-p}{2d_{\mathcal{S}}}(1 + d|\,\langle\phi|\psi^+\rangle\,|^2)\} \\
&\geq \min_{|\phi\rangle}\left\{p\,\langle\phi|\rho_{\mathcal{A}}^{\Gamma}|\phi\rangle\right\} + \frac{1-p}{2d_{\mathcal{S}}} \geq 0
\end{aligned} \tag{4.18}$$

be satisfied. We may now focus on minimising the first term of the right-hand side of the inequality (4.18). Consider the decomposition of the density matrix in terms of pure state projectors

$$\rho_{\mathcal{A}} = \sum_i p_i\,|\psi_i\rangle\langle\psi_i| \equiv \sum_i p_i\psi_i, \tag{4.19}$$

we then have the inequality

$$\min_{|\phi\rangle} \sum_i p_i\,\langle\phi|\,\psi_i^{\Gamma}\,|\phi\rangle \geq \min_{\{p_i,\psi_i\}} \sum_i p_i \min_{|\phi\rangle} \langle\phi|\,\psi_i^{\Gamma}\,|\phi\rangle \geq \min_{\psi,\phi} \langle\psi|\,\phi^{\Gamma}\,|\psi\rangle\,. \tag{4.20}$$

If we now take the Schmidt decomposition $|\phi\rangle = \sum_i \sqrt{p_i}\,|i\rangle\,|i\rangle$, having the Schmidt coefficients p_i arranged in decreasing order $p_1 \geq p_2 ...$ we may study

$$|\phi\rangle\,\langle\phi|^{\Gamma} = \sum_i p_i\,|i\rangle\,\langle i| \otimes |i\rangle\,\langle i| + \sum_{i>j} \sqrt{p_i p_j}(\psi_{ij}^{+} - \psi_{ij}^{-}), \tag{4.21}$$

where $\left|\psi_{ij}^{\pm}\right\rangle = \frac{1}{\sqrt{2}}(|ij\rangle \pm |ji\rangle$. This allows us to reformulate the minimization on the right-hand side of equation (4.20) as

$$\min_{\phi,\psi} \langle\psi|\,\phi^{\Gamma}\,|\psi\rangle = \min_{p_1\geq p_2\geq ...} -\sqrt{p_1 p_2} = \min_{p} -\sqrt{p(1-p)} = -\frac{1}{2}, \tag{4.22}$$

where we have shown that the smallest eigenvalue of the partial transposition of a pure state is at most $-1/2$, and its corresponding eigenstate is antisymmetric.

Imposing

$$\frac{1}{2}(-p + (1-p)/d_{\mathcal{S}}) \geq 0 \tag{4.23}$$

one finds

$$p \leq \frac{1}{d_{\mathcal{S}}+1} = \frac{2}{d(d+1)+2} =: \bar{p}. \tag{4.24}$$

The upper bound can be found by considering that, for an arbitrary PPT state σ, that is, such that $\sigma^{\Gamma} \geq 0$, one has

$$\mathrm{Tr}(P_{\mathcal{A}}\sigma) = \frac{1}{2}(1 - \mathrm{Tr}(V\sigma)) = \frac{1}{2}(1 - \mathrm{Tr}\big(V^{\Gamma}\sigma^{\Gamma}\big)) = \frac{1}{2}(1 - d\,\langle\psi^{+}|\sigma^{\Gamma}|\psi^{+}\rangle) \leq \frac{1}{2}. \tag{4.25}$$

□

We may put together the observations from the previous sections and notice that, for a given antisymmetric state $\rho_{\mathcal{A}}$, it is possible to obtain $p^{\mathrm{PPT}}(\rho_{\mathcal{A}}) < 1/2$. The optimal PPT state achieving the value, σ^{*} can now be shown to be a PPT entangled state. Indeed, if σ^{*} were separable, then by virtue of Lemma 1 there should exist another separable state, which is necessarily PPT, that would also project onto $\rho_{\mathcal{A}}$ with probability $1/2$. We would therefore incur in a contradiction, since we have assumed that $p^{\mathrm{PPT}}(\rho_{\mathcal{A}}) < 1/2$ is the maximum value of projection probability for a PPT state projecting on $\rho_{\mathcal{A}}$.

Thus, one can generate PPT entangled states through the following prescription:

1. Generate an arbitrary antisymmetric state $\rho_{\mathcal{A}}$;
2. Compute $p^{\mathrm{PPT}}(\rho_{\mathcal{A}})$ via the SDP in (4.16);
3. If $p^{\mathrm{PPT}}(\rho_{\mathcal{A}}) < 1/2$, then the optimal state satisfying the constraints of the SDP is a PPT entangled state.

Notice that antisymmetric states $\rho_{\mathcal{A}}$ can be generated at random, for example by generating a random bipartite state ρ, and considering $\rho_{\mathcal{A}} = P_{\mathcal{A}}\rho P_{\mathcal{A}}/\,\mathrm{Tr}(P_{\mathcal{A}}\rho)$.

4.4 A New Class of Bound-Entangled States

The structure of the optimal PPT-entangled states of the SDP (4.16) may give precious insight in the definition of an analytical class of states exhibiting bound entanglement.

4.4.1 Structure of PPT states that generate an antisymmetric state

In the derivation of the lower bound for the maximum projection probability of a PPT state onto a given antisymmetric state $p^{\mathrm{PPT}}(\rho_{\mathcal{A}})$ we relied on the class of states

$$\sigma(p) = p\rho_{\mathcal{A}} + (1-p)\frac{P_{\mathcal{S}}}{d_{\mathcal{S}}}, \tag{4.26}$$

showing that they belong to the class of feasible solutions to the SDP (4.16). It is worthwhile remembering that in the bipartite case the direct sum of antisymmetric subspace and of the symmetric subspace is equal to the total Hilbert space. Moreover, a convex combination of a symmetric and antisymmetric density operator is equivalent to the direct sum of the two:

$$\sigma(p) = p\rho_{\mathcal{A}} + (1-p)\frac{P_{\mathcal{S}}}{d_{\mathcal{S}}} = p\tilde{\rho}_{\mathcal{A}} \oplus (1-p)\frac{\tilde{P}_{\mathcal{S}}}{d_{\mathcal{S}}}. \tag{4.27}$$

Furthermore, the optimal solution to the SDP (4.16) is not unique, but spans a class of states σ^*. We argue here that, among the PPT states σ^* that are optimal for the sake of the probability $p^{\mathrm{PPT}}(\rho_{\mathcal{A}})$ defined in (4.16), there are always states with the structure

$$\sigma^* = p^{\mathrm{PPT}}(\rho_{\mathcal{A}})\rho_{\mathcal{A}} \oplus \left[1 - p^{\mathrm{PPT}}(\rho_{\mathcal{A}})\right]\rho_{\mathcal{S}}, \tag{4.28}$$

where $\rho_{\mathcal{S}}$ is a state with support on the symmetric subspace $\mathcal{H}_{\mathcal{S}}$.

This may be seen by noting that if σ^* is the optimal solution to the SDP (4.16), then we may always construct an associated permutation invariant state

$$\sigma_V^* = \frac{(\sigma^* + V\sigma^* V)}{2}, \tag{4.29}$$

which also belongs to the class of optimal states. By construction we have that σ_V^* is a direct sum of symmetric and antisymmetric density operators $\sigma_V^* = P_{\mathcal{A}}\sigma_V^* P_A \oplus P_{\mathcal{S}}\sigma_V^* P_{\mathcal{S}}$. In order to check the optimality of σ_V^* we need to meet the constraints in (4.16). First, we begin by noting that $(V\tau V)^{\Gamma_A} = V\tau^{\Gamma_B}V$, so that $V\tau V$ is PPT if and only if τ is PPT. Therefore, σ_V^* is PPT because it is the convex combination of two PPT states. Finally, in order to satisfy the constraint

$$P_{\mathcal{A}}\sigma_V^* P_A = P_{\mathcal{A}}\sigma^* P_A = p^{\mathrm{PPT}}(\rho_{\mathcal{A}})\rho_{\mathcal{A}}, \tag{4.30}$$

we find the desired structure

$$\sigma_V^* = p^{\mathrm{PPT}}(\rho_{\mathcal{A}})\rho_{\mathcal{A}} \oplus P_{\mathcal{S}}\sigma_V^* P_{\mathcal{S}} = p^{\mathrm{PPT}}(\rho_{\mathcal{A}})\rho_{\mathcal{A}} \oplus (1 - p^{\mathrm{PPT}}(\rho_{\mathcal{A}}))\rho_{\mathcal{S}}. \tag{4.31}$$

4.4.2 Analytic example of PPT-entangled states

We have shown in the previous sections that states with the structure

$$\sigma = p\rho_{\mathcal{A}} \oplus (1-p)\rho_{\mathcal{S}} \tag{4.32}$$

are PPT-entangled for appropriate choices of p, $\rho_{\mathcal{A}}$ and $\rho_{\mathcal{S}}$. So far we have shown how to generate such states by means of SDPs and random generation of antisymmetric matrices, however it is possible to put forward simple choices for the free parameters of σ in order for it to be a PPT-entangled state.

From the proof of Theorem 4.1 we already know that choosing $\rho_{\mathcal{S}} = P_{\mathcal{S}}/d_{\mathcal{S}}$ with a small enough projection probability $p \leq \bar{p}$, then σ is going to be PPT. What remains to do is to find a simple condition on $\rho_{\mathcal{A}}$ ensuring for σ to be entangled. To this purpose we may make use of Proposition 5, ensuring that any separable state will be mapped onto antisymmetric mixed states of Schmidt number at most equal to two. We conclude that as long as $\rho_{\mathcal{A}}$ has Schmidt number strictly larger than 2 then the state $\sigma = p\rho_{\mathcal{A}} \oplus (1-p)\rho_{\mathcal{S}}$ is entangled.

The simplest way to make sure that $\rho_{\mathcal{A}}$ has Schmidt number strictly larger than two is to choose $\rho_{\mathcal{A}} = |\psi_{\mathcal{A}}\rangle\langle\psi_{\mathcal{A}}|$, for $|\psi_{\mathcal{A}}\rangle$ an antisymmetric vector state with Schmidt rank strictly larger than two.

We remark that generic random antisymmetric vector states in dimension $d = 2m$ have Schmidt rank $2m$, and can in principle be generated (up to normalization) starting from a generic vector state without a definite symmetry, and projecting onto the antisymmetric space.

Let us put forward an analytical non-random example for this class of PPT-entangled states. Let us consider the case of even dimension $d = 2m$. Consider the antisymmetric vector states

$$|\psi_{\mathcal{A}}\rangle = \sum_{i=1}^{m} c_i \left|\psi^-_{2i-1,2i}\right\rangle, \quad \sum_{i=1}^{m} |c_i|^2 = 1, \tag{4.33}$$

where

$$\left|\psi^-_{k,l}\right\rangle = \frac{1}{\sqrt{2}}(|k\rangle\,|l\rangle - |l\rangle\,|k\rangle),$$

for $k, l = 1, 2, \ldots, d$ and $k < l$. The vector state $|\psi_{\mathcal{A}}\rangle$ in eq. (4.33) has Schmidt rank equal to twice the number of non-zero amplitudes c_i, so it is sufficient for two of the coefficients to be nonzero in order to have Schmidt rank larger than 2. Then the state

$$\sigma = p\,|\psi_{\mathcal{A}}\rangle\langle\psi_{\mathcal{A}}| + (1-p)\frac{P_{\mathcal{S}}}{d_{\mathcal{S}}}, \quad p \leq \bar{p} \tag{4.34}$$

is PPT-entangled.

4.4.3 New class of states comprising Werner, Isotropic and PPT-entangled states

The class of states derived in eq. (4.34) provides a satisfactory characterisation of the entanglement properties as a function of the parametrisation, but there is a more interesting class of states amenable to the same type of considerations, which comprises Werner states and states which are local-unitary equivalent to isotropic states. Let us briefly recall the structure of such classes of states.

Werner states

Bipartite Werner states [117] are the set of mixed states in $d \times d$ dimensions which are invariant under local unitaries of the form $U \otimes U$. Any Werner state may be expressed in terms of the parametrization

$$\rho_W(p_{\mathcal{A}}) = p_{\mathcal{A}}\frac{P_{\mathcal{A}}}{d_{\mathcal{A}}} + (1-p_{\mathcal{A}})\frac{P_{\mathcal{S}}}{d_{\mathcal{S}}}, \tag{4.35}$$

where $P_{\mathcal{A}}, P_{\mathcal{S}}$ are the projectors on the antisymmetric and symmetric subspaces and $d_{\mathcal{A}}, d_{\mathcal{S}}$ the dimensions of the respective subsystems. Werner states are separable for $p_A \leq 1/2$, which is the same interval within which they are PPT. There are therefore no PPT-entangled Werner states.

Isotropic states

Isotropic states are instead $d \times d$ dimensional density operators characterised by invariance under a different kind of local unitary transformations, of the form $U \otimes U^*$, where $\cdot^*$ indicates element-wise complex conjugation. Isotropic states may be parametrised as

$$\rho_I(\alpha) = \alpha\,|\psi_+\rangle\langle\psi_+| + (1-\alpha)\frac{\mathbb{1}}{d^2}, \quad -\frac{1}{d^2-1} \leq \alpha \leq 1, \tag{4.36}$$

where $|\psi^+\rangle$ is the maximally entangled state. Isotropic states are separable for $\alpha \leq 1/(d+1)$ and they are always distillable, thus cannot be bound entangled.

Mixture of Werner, Isotropic and maximally entangled antisymmetric states

As we have shown in the introduction section, states which are equivalent up to a one-subsystem local unitary to the maximally entangled state are likewise maximally entangled. Let us consider states of the kind

$$|\phi_+\rangle = U_{\mathcal{A}} \otimes \mathbb{1} \, |\psi_+\rangle \,, \tag{4.37}$$

where $U_{\mathcal{A}}$ is an antisymmetric unitary matrix ($U_{\mathcal{A}}^T = -U_{\mathcal{A}}$). The class of states given by

$$\sigma(p) = p \, |\phi_+\rangle\langle\phi_+| + (1-p)\frac{1}{d^2} \tag{4.38}$$

is local unitary equivalent to the class of Isotropic states. It is important to notice that antisymmetric unitary matrices only exist in even dimensions, so as discussed in chapter 2, maximally entangled antisymmetric states only exist in even dimension. Furthermore, the case of $d = 2$ is the case of two qubits for which there is known not to be any bound entanglement. The following considerations will therefore apply to even local dimension greater or equal to four. Having introduced and characterised a novel class of bound entangled states and reviewed the entanglement and PPT-ness properties of Werner and Isotropic states, we may put forward a family of mixed states comprising such well-known states, but also bound entanglement. We define a 2-parameter class of states, given by

$$\rho(p_{\mathcal{A}}, p_{\mathcal{S}}) = (1 - p_{\mathcal{A}} - p_{\mathcal{S}}) \, |\phi_+\rangle\langle\phi_+| + p_{\mathcal{A}}\frac{P_{\mathcal{A}}}{d_{\mathcal{A}}} + p_{\mathcal{S}}\frac{P_{\mathcal{S}}}{d_{\mathcal{S}}}, \tag{4.39}$$

with $0 \leq p_{\mathcal{A}}, p_{\mathcal{S}} \leq 1$. It is straightforward to see that when $p_{\mathcal{A}} + p_{\mathcal{S}} = 1$ the class is restricted to Werner states:

$$\rho(p_{\mathcal{A}}, 1 - p_{\mathcal{A}}) = p_{\mathcal{A}}\frac{P_{\mathcal{A}}}{d_{\mathcal{A}}} + (1 - p_{\mathcal{A}})\frac{P_{\mathcal{S}}}{d_{\mathcal{S}}} = \rho_W(p_{\mathcal{A}}). \tag{4.40}$$

Furthermore if $p_{\mathcal{S}} = (d+1)/(d-1)p_{\mathcal{A}}$ the class comprises (up to a local unitary transformation) the Isotropic states

$$\rho\left(p_{\mathcal{A}}, \frac{d+1}{d-1}p_{\mathcal{A}}\right) = \left(1 - \frac{2d}{d-1}p_{\mathcal{A}}\right) |\psi_+\rangle\langle\psi_+| + \frac{2d}{d-1}p_{\mathcal{A}}\frac{\mathbb{1}}{d^2} = \rho_I\left(1 - \frac{2d}{d-1}p_{\mathcal{A}}\right), \tag{4.41}$$

when $p_{\mathcal{A}} \leq (d^2-2)/[2d(d+1)]$.

It is likewise straightforward to find a parameter range where the states are bound entangled. We know that for $p_{\mathcal{A}} = 0$, we obtain the states in eq. (4.34),

$$\rho(0, p_{\mathcal{S}}) = (1 - p_{\mathcal{S}}) \, |\psi_{\mathcal{A}}\rangle\langle\psi_{\mathcal{A}}| + p_{\mathcal{S}} \frac{P_{\mathcal{S}}}{d_{\mathcal{S}}} \tag{4.42}$$

which were shown in the above section to be PPT-entangled when $p_{\mathcal{S}} \geq 1 - \bar{p}$.

We may investigate the parameter space further and find the full entanglement, PPT-ness and separability properties for this class of states. It is helpful to rely on a representation of the parameter space in order to make considerations about the entanglement properties and visualise the different regions of interest. A simple and intuitive graphical representation may be provided of the entanglement properties of the class of states in the Cartesian plane $(p_{\mathcal{A}}, p_{\mathcal{S}})$. The representation is reported in Figure 4.1.

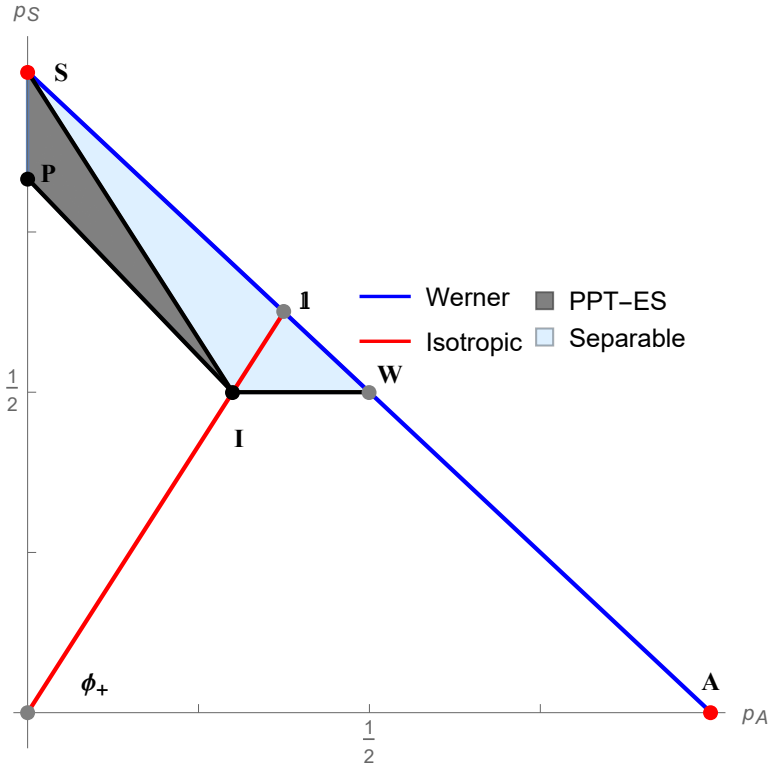

FIGURE 4.1: Entanglement properties of the class of states in (4.39) represented in the Cartesian plane $(p_{\mathcal{A}}, p_{\mathcal{S}})$. The local dimension is fixed at $d = 4$. The light blue area represents the separable states, the dark grey comprises the PPT-entangled states. The isotropic states are found along the $\phi_+ - \mathbb{1}$ red segment, whereas the Werner states along the blue $S - A$ segment.

We may represent a density matrix of the class of states (4.39) $\rho(p_{\mathcal{A}}, p_{\mathcal{S}})$ as a point with coordinates $(p_{\mathcal{A}}, p_{\mathcal{S}})$. The states belonging to the class are given by the convex hull of three extremal states:

- $\pi_{\mathcal{S}} = P_{\mathcal{S}}/d_{\mathcal{S}}$ represented by the point $S = (0, 1)$
- $\pi_{\mathcal{A}} = P_{\mathcal{A}}/d_{\mathcal{A}}$ represented by the point $A = (0, 1)$
- $|\phi_+\rangle\langle\phi_+|$ is represented by the origin of the axes, $\phi_+ = (0, 0)$

Let us begin by looking at separability. We know that the separable set is convex, so its full characterisation may be obtained by taking the convex hull of the extremal separable states in parameter space. Proposition 5 requires the condition $p_{\mathcal{S}} \geq 1/2$ for separable states. The extremal points may thus be obtained on the $p_{\mathcal{S}} = 1/2$ segment by the separability conditions for the Werner and Isotropic states. The extremal Werner state is independent of the system dimension and is represented by the point $W = (1/2, 1/2)$, its density operator being given by

$$\pi_W = \frac{1}{2}\left(\frac{P_{\mathcal{A}}}{d_{\mathcal{A}}} + \frac{P_{\mathcal{S}}}{d_{\mathcal{S}}}\right). \tag{4.43}$$

The separability properties for states which are local unitary equivalent are the same, so we may apply the separability condition for Isotropic states obtaining $I = (\frac{1}{2}(d-1)/(d+1), \frac{1}{2})$, representing the extremal state

$$\pi_I = \frac{1}{d+1}\phi_+ + \left(1 - \frac{1}{d+1}\right)\frac{\mathbb{1}}{d^2}. \tag{4.44}$$

Le us indeed prove that the convex hull of these three extremal points give the whole set of separable states Σ_{sep} for our family by first looking at the set Σ_{PPT} of PPT states. The task may be solved analytically for our class of states. Consider the partial transpose of the state in (4.39)

$$\rho^\Gamma(p_{\mathcal{A}}, p_{\mathcal{S}}) = \frac{1 - p_{\mathcal{A}} - p_{\mathcal{S}}}{d}(U_{\mathcal{A}} \otimes \mathbb{1})V(U_{\mathcal{A}}^\dagger \otimes \mathbb{1}) + \frac{p_{\mathcal{A}}}{2d_{\mathcal{A}}}(\mathbb{1} - d\psi_+) + \frac{p_{\mathcal{S}}}{2d_{\mathcal{S}}}(\mathbb{1} + d\psi_+), \tag{4.45}$$

where ψ_+ is the projector on the maximally entangled state. The positivity of $\rho^\Gamma(p_{\mathcal{A}}, p_{\mathcal{S}})$ only depends on its spectrum, so we may consider the unitarily equivalent matrix

$$\tilde{\rho}^\Gamma(p_{\mathcal{A}}, p_{\mathcal{S}}) = (U_{\mathcal{A}}^\dagger \otimes \mathbb{1})\rho^\Gamma(p_{\mathcal{A}}, p_{\mathcal{S}})(U_{\mathcal{A}} \otimes \mathbb{1}) = \frac{1 - p_{\mathcal{A}} - p_{\mathcal{S}}}{d}V + \frac{p_{\mathcal{A}}}{2d_{\mathcal{A}}}(\mathbb{1} - d\phi_+) + \frac{p_{\mathcal{S}}}{2d_{\mathcal{S}}}(\mathbb{1} + d\phi_+). \tag{4.46}$$

The operators V, $\mathbb{1}$ and ϕ_+ are mutually commuting, so they may be diagonalised simultaneously. In the basis where the operators are diagonal, the eigenvalues of the

sum operator $\tilde{\rho}^{\Gamma}(p_{\mathcal{A}}, p_{\mathcal{S}})$ will be given by the sum of the corresponding eigenvalues from each addendum matrix. We need to establish for which values of $p_{\mathcal{A}}$ and $p_{\mathcal{S}}$ are all eigenvalues positive. We know that operator V only has two eigenvalues, ± 1 and their multiplicities are respectively $d_{\mathcal{A}}$ for the negatives and $d_{\mathcal{S}}$ for the positives. The identity operator and the projector on the maximally entangled states are both positive by construction. Given that the eigenvalues of the sum matrix are obtained from the sum of the individual eigenvalues, the positivity of $\tilde{\rho}^{\Gamma}(p_{\mathcal{A}}, p_{\mathcal{S}})$ will be determined by the positivity of its minimum eigenvalue, which is given by the two cases

$$\begin{cases} -\frac{1-p_{\mathcal{S}}-p_{\mathcal{A}}}{d} + \frac{p_{\mathcal{A}}}{d(d-1)} + \frac{p_{\mathcal{S}}}{d(d+1)} + \frac{p_{\mathcal{S}}}{d+1} - \frac{p_{\mathcal{A}}}{d-1} \geq 0, & \text{if } p_{\mathcal{S}} \leq \frac{d+1}{d-1} p_{\mathcal{A}}, \\ -\frac{1-p_{\mathcal{S}}-p_{\mathcal{A}}}{d} + \frac{p_{\mathcal{A}}}{d(d-1)} + \frac{p_{\mathcal{S}}}{d(d+1)} \geq 0, & \text{if } p_{\mathcal{S}} \geq \frac{d+1}{d-1} p_{\mathcal{A}}. \end{cases} \tag{4.47}$$

The first case boils down to the condition $p_{\mathcal{S}} \geq 1/2$, whereas the second holds for

$$p_{\mathcal{S}} \geq -\frac{d(d+1)}{d(d+1)-2} p_{\mathcal{A}} + \frac{d+1}{d+2}. \tag{4.48}$$

The states from the class $\rho(0, p_{\mathcal{S}})$ are therefore PPT for $p_{\mathcal{S}} \geq (d+1)/(d+2)$. We may therefore indicate the extremal point with $P = (0, (d+1)/(d+2))$ and its corresponding state with

$$\pi_P = \rho(0, (d+1)/(d+2)) = \frac{1}{d+2}\phi_+ + \frac{d+1}{d+2}\frac{P_{\mathcal{S}}}{d_{\mathcal{S}}}. \tag{4.49}$$

The set Σ_{PPT} of PPT states is thus given by the convex hull of the states π_S, π_W, π_I and π_P and it holds $\Sigma_{\text{sep}} \subset \Sigma_{\text{PPT}}$, where the inclusion is strict. This means that the set $\Sigma_{\text{PPT}} \setminus \Sigma_{\text{sep}}$ is the set of PPT-entangled states.

Let us now return to considering separability. We have just shown that the state π_I is extremal for separability, because the states $\rho(p_{\mathcal{A}} < \frac{1}{2}\frac{d-1}{d+1}, 1/2)$ are not PPT, and therefore entangled. Moreover, $\pi_{\mathcal{S}}$ is extremal for the separable set because states $\rho(0, p_{\mathcal{S}} \geq 1-\bar{p})$ belong to the family (4.34), which is PPT-entangled. We may therefore parametrise the states in Σ_{sep} as

$$\sigma(p_W, p_I) = p_w \pi_W + p_I \pi_I + (1 - p_W - p_I)\frac{P_{\mathcal{S}}}{d_{\mathcal{S}}}, \tag{4.50}$$

with $0 \leq p_W, p_I \leq 1$.

It is worth noting that the area of the region of PPT-entangled states decreases for increasing dimension d. In fact, the length of the segment PS scales as $1/(d+2)$, whereas the height of the PSI triangle is given by $\frac{1}{2}(d-1)/(d+1)$. The area $\mathcal{A}_{\text{PPTe}}$ of

PPT entangled states therefore scales as

$$\mathcal{A}_{\mathrm{PPTe}} = \frac{(d-1)^2}{8(d+1)^2(d+2)^2}, \tag{4.51}$$

exhibiting a quadratic decrease in surface for increasing local dimension d. This result suggests that experimental preparation of PPT-entangled states from the class (4.39) would require a less stringent confidence interval concerning the parameters describing the state in lower dimensions than it would in higher. We recall that $d = 4$ is the lowest dimension exhibiting PPT-entanglement, thus appearing to be the most suitable case for experimental verification.

Chapter 5

Multipartite Entanglement, Steering and Nonlocality of the Totally Antisymmetric State

Quantum mechanics has provided a description of Nature which has been revolutionary in many of the basic notions upon which we understood physical phenomena. Wave-particle duality and the intrinsic randomness of measurement outcomes have demolished the positivist interpretation of our world, wherein a sufficiently accurate knowledge of the phase-space coordinates and the laws governing the evolution of states of its constituents would enable a perfect predictability of all future and past states of any system. This revolution, which in itself was ground-breaking, has had enormous influence over the subsequent development of science and technology, as well as a deep cultural impact, forever changing our world-view and shaping the collective perspective in the 20^{th} century.

It wasn't until 1935 and a series of famed discussions involving Einstein and the other leading physicists in the field, however, than another *quantum weirdness* became manifest and lay the foundation for the challenge to a fundamental principle governing the laws of physics and our understanding of the universe up to that point: the principle of *local realism* [89, 168].

In their seminal 1935 article [89], also known as EPR paper, Einstein, Podolsky and Rosen, showed that certain predictions of quantum mechanics were incompatible with those of theories where systems could possess locally an *element of reality* [21, 89] and are therefore completely independent on any physical process in separate regions of space-time.

We will not use the EPR thought experiment as a benchmark example to introduce the notions of steering and nonlocality and their relationship to entanglement. Instead,

we will consider a variation of the EPR scenario which covers the fundamental aspects of our interest.

Consider the two-qubit state

$$|\phi_-\rangle = \frac{1}{\sqrt{2}}(|0\rangle \otimes |1\rangle - |1\rangle \otimes |0\rangle) = \frac{1}{\sqrt{2}}(|+\rangle \otimes |-\rangle - |-\rangle \otimes |+\rangle), \tag{5.1}$$

where $|\pm\rangle = (|0\rangle \pm |1\rangle)/\sqrt{2}$. The state $|\phi_-\rangle$ may be seen as a spin-singlet state for the two subsystems. It is manifest that the pure state in (5.1) is a non-factorizable one, i.e. it may not be written in the form $|\sigma\rangle \otimes |\varphi\rangle$ and is thus an entangled state of the two subsystems. The entanglement of the state may be seen to bring about some degree of correlation between the outcomes of measurements performed on the two subsystems. Suppose Alice can measure the observable σ_z: this amounts to projecting in the $\{|0\rangle, |1\rangle\}$ basis. If the outcome of Alice's measurement is $+1$, Bob's reduced state immediately after Alice's measurement becomes, according to the Born rule,

$$|\varphi\rangle\langle\varphi|_B = \mathrm{Tr}_A\left[(|0\rangle\langle 0| \otimes \mathbb{1})\, |\phi_-\rangle\langle\phi_-|\right] = \frac{1}{2}\, |1\rangle\langle 1|_B \tag{5.2}$$

so Bob's measurement of σ_z would deterministically give outcome -1. The opposite scenario occurs for the other outcome, meaning that the outcomes are perfectly anti-correlated. On the other hand, if Alice measures in the σ_x basis, Bob's system is in one or the other $|\pm\rangle$ basis states, again deterministically, and the outcomes of Bob's measurements will be perfectly anti-correlated with Alice's outcomes, even if the two parties are in causally disconnected regions. Such anti-correlation is enabled by the entanglement in the shared state and is removed when the shared state is a separable one. This phenomenon was called *steering* by Schrödinger and reflects the non-local nature of quantum mechanics. It is important to point out that such non-locality may not be used for faster than light signaling, which may be proven as a corollary to the no-cloning theorem [169]. The nonlocality of quantum correlations does not affect causality. However, with the aid of classical communication between parties, important technological applications are enabled by quantum nonlocality, such as self-testing [170], randomness certification [171] and device-independent quantum key distribution [172].

A common goal of many quantum information tasks is that of certification of entanglement, which is one of the main resources bringing about quantum advantages. This may be carried out by tomography, i.e. the reconstruction procedure of the density matrix of a quantum state by means of the outcomes of measurements, or by means of entanglement witnesses. Unfortunately, both are highly sensitive to systematic errors, which may be extremely difficult if not impossible to remove to a satisfactory degree

from actual experiments [173]. Furthermore, it is of crucial interest in quantum key distribution and other cryptography protocols to assess the entanglement in a system of communicating parties when a number of the parties, or the corresponding measurements devices, are untrusted. This has sparked interest in a new approach at studying quantum correlations, that of device-independent quantum information [35, 48]. The main idea is somewhat of a reversal of the original EPR argument: assuming quantum mechanics is correct, if one may not find any local theory describing the correlations arising from measurements one needs to conclude that the state is entangled to a certain degree [174].

In the Section 5.1 we review a formal introduction to the device-independent outlook on entanglement certification and relate it to the concepts of steering and nonlocality. Section 5.2 extends the concepts to the multipartite scenario. We introduce the noisy totally antisymmetric tripartite state, which we want to investigate the quantum correlation structure of, in Section 5.3. The quantum correlations of the state are compared to the better known generalised GHZ and W states, and we compare the multipartite entanglement, steering and nonlocality of the three in Sections 5.4, 5.5 and 5.6 respectively. Finally, the hierarchy of quantum correlations for the states under consideration is reported in Section 5.7.

5.1 Device-independent Bipartite Entanglement Certification

We want to study the hierarchy of quantum correlations in the device-independent outlook [35, 48, 174, 175] based on the ability to certify the entanglement of an unknown state for given number of untrusted parties or, in other words, of uncharacterized measurement devices [48]. In the bipartite case this amounts to investigating the following three cases:

- *Measurements of both parties are characterized.* The task we investigate is that of entanglement certification of an unknown state and it may be achieved, for instance, by means of *entanglement witnesses* [34].

- *Measurements of one party are uncharacterized.* This is the *steering* scenario [176], where one (trusted) party performs entanglement certification based on the conditional states arising from the untrusted party and its own (trusted) measurements.

- *Both parties' measurements are uncharacterized.* Those states for which entanglement may be certified solely based on the conditional probability distributions of outcomes of measurements, without any previous knowledge of the state or assumptions about the measurement devices, are said to possess *nonlocality* [49, 176–178].

In the following sections we will summarize a few of the principal mathematical concepts underlying the above three cases.

5.1.1 Entanglement witnesses

Entanglement is not an observable, so its experimental detection needs to rely on some indirect measurement. In the case where both parties sharing a composite unknown state have full control over their measurement devices the entanglement certification is possible via measurement of physical observables [34]. There exist, in fact, necessary and sufficient entanglement criteria in terms of directly measurable observables, called *entaglement witnesses* [58, 179–181]. An observable $\mathcal{W}$ is called an entanglement witness if $\mathrm{Tr}(\mathcal{W}\rho_{\mathrm{sep}}) \geq 0$ for all separable ρ_{sep} and $\mathrm{Tr}(\mathcal{W}\rho_{\mathrm{e}}) < 0$ for at least one entangled ρ_{e}. Entanglement witnesses are a very powerful tool for the study of entanglement in experiments and it is proven that for every entangled state there exists a witness which *detects* it [58].

A simple example of entanglement witness is given by the swap operator V, introduced in Chapter 2, detecting the entanglement of Werner states (sec. 4.4.3). A Werner state may be written as

$$W = \frac{1}{d(d^2)-1}\left[(d-\Phi)\mathbb{1} + (d\Phi - 1)V\right] \quad \forall \Phi \in [-1, 1]. \tag{5.3}$$

If a Werner state is a product state $W = W_1 \otimes W_2$ the expectation value of the swap operator is positive,

$$\Phi = \mathrm{Tr}(WV) = \mathrm{Tr}(W_1 \otimes W_2 V) = \mathrm{Tr}(W_1 W_2) \geq 0, \tag{5.4}$$

and the same holds for convex combinations of product states. The extremal value $\mathrm{Tr}(WV) = 0$ is reached for pure orthogonal states W_1 and W_2 and a Werner state is separable iff $\mathrm{Tr}(WV) \geq 0$. The swap operator may therefore detect an entangled Werner state when its expectation value is negative [182].

5.1.2 Steering

Our summary of the basic concepts of steering will loosely follow the review in [35]. Let us consider the case of two subsystems individually addressable by two parties, Alice and Bob. The parties share an unknown bipartite quantum state ρ_{AB} on which Alice may perform m_A measurements labelled $x = 1, ..., m_A$ each having o_A outcomes $a = 1, .., o_A$. This labelling will be implied throughout the sections covering steering. The action of the measurements on the quantum state may be described in terms of POVM elements $\{M_{a|x}\}_{a,x}$ acting on the Hilbert space $\mathcal{H}_A$, such that $\sum_a M_{a|x} = \mathbb{1}$ and $M_{a|x} \geq 0$, $\forall a, x$. According to the Born rule, the conditional states available to Bob after Alice's measurements are given by the unnormalized operator

$$\sigma_{a|x} = \mathrm{Tr}_A[(M_{a|x} \otimes \mathbb{1})\rho_{AB}] \tag{5.5}$$

with probability

$$p(a|x) = \mathrm{Tr}[(M_{a|x} \otimes \mathbb{1})\rho_{AB}]. \tag{5.6}$$

The set of unnormalized quantum states $\Sigma_B = \{\sigma_{a|x}\}_{a,x}$ is called an *assemblage*. In the typical steering scenario the quantum state ρ_{AB} and Alice's measurements $\{M_{a|x}\}_{a,x}$ are completely uncharacterized, whereas Bob has full control of the measurements on his subsystem and may fully reconstruct the elements of the assemblage Σ_B. This scenario is also called *one-sided device-independent scenario*.

Local Hidden State models

In order for Bob to certify entanglement between his subsystem and Alice's, he needs to rule out the possibility that the conditional states he observes can be described by a *local hidden state model*, that is obtained with a strategy involving no quantum entanglement. Consider the situation where an external source provides Alice with a classical message λ with probability distribution $\mu(\lambda)$ and Bob with a corresponding quantum state ρ_λ, unbeknownst by Bob. The source may instruct Alice, or her measurement apparatus, to output the outcome a associated with Alice's choice of measurement x, with probability $p(a|x, \lambda)$. Because the local variable λ is not known by Bob, the assemblage he has access to is given by the elements

$$\sigma_{a|x} = \int \mathrm{d}\lambda \mu(\lambda) p(a|x, \lambda) \rho_\lambda. \tag{5.7}$$

The assemblages with elements of the form (5.7) are said to have a *local hidden state model* (LHS) and do not enable Bob to certify the steering of his own subsystem on

behalf of Alice. On the other hand, an assemblage is said to demonstrate *steering* if it does not admit a decomposition in the form (5.7). We may therefore put forward the following definition of steering for a quantum state ρ_{AB}

Definition 5.1. The bipartite quantum state ρ_{AB} acting on the composite Hilbert space $\mathcal{H}_A \otimes \mathcal{H}_B$ is called *steerable from A to B* if there exists measurements on $\mathcal{H}_A$ that produce an assemblage which does not admit a decomposition of the form (5.7).

On the contrary, states which produce assemblages admitting a decomposition (5.7) for all local measurements by Alice are called *unsteerable* by Alice. It is worth noting the asymmetry in the notion of steering. A state which is steerable from A to B is not necessarily steerable from B to A and vice-versa. The case of states that are steerable by one party but not the other is called *one-way steering*, whereas when they are steerable by both parties we call the scenario *two-way steering*.

Steering and entanglement certification

We may now ask what is the relationship between the definition of steering 5.1 and entanglement. An answer may be obtained by looking at the assemblages generated by separable quantum states

$$\rho_{AB}^{\text{sep}} = \int \mathrm{d}\lambda \mu(\lambda) \rho_A^\lambda \otimes \rho_B^\lambda. \tag{5.8}$$

The assemblages generated by Alice's measurements on ρ_{AB}^{sep} are of the kind

$$\sigma_{a|x} = \mathrm{Tr}_A[(M_{a|x} \otimes \mathbb{1})\rho_{AB}^{\text{sep}}] = \int \mathrm{d}\lambda \mu(\lambda) \mathrm{Tr}(M_{a|x}\rho_A^\lambda)\rho_B^\lambda = \int \mathrm{d}\lambda \mu(\lambda) p(a|x,\lambda)\rho_B^\lambda, \tag{5.9}$$

which is of the same form as (5.7). It is manifest that separable states may only give rise to LHS assemblages. Therefore, if Bob is able to prove steering from his assemblage, the assemblage may have not originated from Alice's measurement on a separable global state ρ_{AB}^{sep}. Steering is a sufficient condition for entanglement in this instance. It is not however necessary, since there are entangled states that produce always unsteerable assemblages, independently of the choice of measurements of Alice [183]. We may thus understand steering as a *one-sided device-independent entanglement certification*, where one party (Bob) controls one subsystem of a global quantum state and the other party (Alice) is *untrusted*, that is to say her measurements are uncharacterized.

5.1.3 Bell Nonlocality

As we have mentioned in the introductory paragraphs of this Chapter, the EPR scenario opens to the possibility of studying Bell nonlocality of quantum systems. Typically, the

understanding of nonlocality is carried out in terms of the correlations extracted from measurements performed by parties which are space-like separated on a shared quantum system. The main idea is that if there is no local theory describing the probabilities associated with different measurement outcomes for the two parties, then one has to conclude that nonlocality is present in the system. Furthermore, one may adopt a similar approach to the steering scenario and interpret the correlations that exhibit nonlocality to be the witness of entanglement between the subsystems. This is a powerful tool for entanglement certification since it does not require any assumption or information about the measurement devices for both parties, so it is called *fully-device-independent* [35,49].

For a comprehensive review of the concepts we will introduce now, the reader may refer to [49]. We will base our study of nonlocality on the analysis of joint conditional probability distributions $p(ab|xy)$, where x, y label the measurement choice and a, b the outcomes of the measurements by the distant parties Alice and Bob respectively, which we may refer to as *behaviours*. The first requirement we need to impose on the behaviours in order to make statements about the locality of the system is that of *no-signaling*. A behaviour is said to be *no-signaling* if

$$\begin{aligned} \sum_b p(ab|xy) &= \sum_b p(ab|xy') \quad \forall a, x, y, y', \\ \sum_a p(ab|xy) &= \sum_a p(ab|x'y) \quad \forall a, x, x', y. \end{aligned} \tag{5.10}$$

The physical interpretation of no-signaling correlations is that the marginal probabilities $p_A(a|xy) = \sum_b p(ab|xy)$ of Alice are independent of Bob's choice of measurement and vice-versa. Bob may not signal to Alice his choice of measurement in any way, and the other way round. If Bob and Alice's measurements are space-like separated this is equivalent to requiring no faster-than-light signaling between the two parties.

The locality of the behaviours is given by a stricter condition, however. The set of local correlations are those given by

$$p(ab|xy) = \int \mathrm{d}\lambda \mu(\lambda) p(a|x,\lambda) p(b|y,\lambda). \tag{5.11}$$

where λ are hidden variables distributed according to the probability density $\mu(\lambda)$ and where $p(a|x,\lambda)$ and $p(b|y,\lambda)$ are Alice and Bob's local probability distributions, respectively. Correlations which may not be written in the form (5.11) are said to be *nonlocal* and to belong to the set of *quantum correlations*. Indeed, the no-signaling and locality conditions are inequivalent and it has been proved that there exist states exhibiting no-signaling correlations but violating the locality condition. An example of a behaviour

which is not local albeit being non-signaling is given by the Popescu-Rohrlich box [184]. A nonlocal box is an idealized device shared between Alice and Bob which, given the input x on Alice's and y on Bob's side, returns an output a and b respectively to each party according to some probability distribution $p(ab|xy)$. It describes a more general set of behaviours than can be generated by measurements of parties on a quantum state. The Popescu-Rohrlich box, also referred to as PR box, is given by

$$p(ab|xy) = \begin{cases} \frac{1}{2}, & \text{if } a \oplus b = xy \\ 0, & \text{otherwise,} \end{cases} \tag{5.12}$$

where $\oplus$ denotes addition modulo 2. The behaviour in equation (5.12) satisfies the no-signaling condition, but not the locality one [49].

The no-signaling and local correlations have a powerful geometrical representation. Represented in a vector space, the set of behaviours belonging to the no-signaling set ($\mathcal{NS}$) and local set ($\mathcal{L}$) may each be described as the convex-hull of a finite number of vertices, a *polytope* [185]. The vertices of the local polytope are given by the finite set of *deterministic behaviours*. Consider an assignment $\lambda : \{a_1, ..., a_m\} \to \{b_1, .., b_m\}$ between the outputs a_x and b_y associated with inputs $x, y = 1, ..., m$. Let $\mathbf{d}_\lambda = \{d_\lambda(ab|xy)\}$ indicate the set of all the probabilities, i.e. the behaviour, $\mathbf{d}_\lambda$ is a deterministic behaviour if it can be written as

$$d_\lambda(ab|xy) = \begin{cases} 1, & \text{if } a = a_x \text{ and } b = b_y \\ 0, & \text{otherwise.} \end{cases} \tag{5.13}$$

There are $(o_A)^{2m}$ such behaviours and a behaviour $\mathbf{p}_\mathcal{L}$ is local if and only if it can be expressed as a convex combination of these deterministic vertices

$$\mathbf{p}_\mathcal{L} = \sum_\lambda q_\lambda \mathbf{d}_\lambda, \tag{5.14}$$

with $q_\lambda \geq 0$ and $\sum_\lambda q_\lambda = 1$. The local deterministic behaviours thus correspond to the vertices, or extreme points, of the local polytope $\mathcal{L}$. The set of vertices of the non-signaling polytope $\mathcal{NS}$ is instead given by the union of the vertices of $\mathcal{L}$ and the set of nonlocal vertices, which are given by a generalization of PR boxes [49].

Any inequality which is satisfied by all elements of the local polytope, but not for those outside of it is called a *Bell inequality*, the facets of this polytope being called *tight Bell inequalities*.

CHSH inequality

A notable example of bipartite Bell inequality is given by the Clauser-Horne-Shimony-Holt (CHSH) inequality [63]. The inequality applies to the case of two measurement settings $x, y \in \{0, 1\}$ and two possible outcomes $a, b \in \{-1, 1\}$. Consider the expectation values

$$\langle a_x b_y \rangle = \sum_{a,b} abp(ab|xy) \tag{5.15}$$

for the product ab and the Bell parameter

$$S = \langle a_0 b_0 \rangle + \langle a_0 b_1 \rangle + \langle a_1 b_0 \rangle - \langle a_1 b_1 \rangle . \tag{5.16}$$

By inserting the locality condition (5.11) for the behaviours $p(ab|xy)$ in equation (5.16), one may derive [49] the following Bell inequality

$$S \leq 2, \tag{5.17}$$

called *CHSH inequality*. We may show a violation of the CHSH inequality for the singlet state $|\psi^-\rangle = \frac{1}{\sqrt{2}}(|0\rangle |1\rangle - |1\rangle |0\rangle)$. Consider the Pauli vector $\bar{\sigma} = (\sigma_x, \sigma_y, \sigma_z)$ and measurement x and y corresponding to $\bar{x} \cdot \bar{\sigma}$ and $\bar{y} \cdot \bar{\sigma}$ respectively, such that $\langle a_x b_y \rangle = -\bar{x} \cdot \bar{y}$. As measurement settings let x correspond to projecting in the orthogonal directions $\bar{v_1} = (1, 0, 0)$ and $\bar{v_2} = (0, 1, 0)$, whereas y projects in $\bar{w_1} = -\frac{1}{\sqrt{2}}(1, 1, 0)$ and $\bar{w_2} = \frac{1}{\sqrt{2}}(-1, 1, 0)$. The expectation values for the product of the outcomes now read

$$\begin{aligned} \langle a_0 b_0 \rangle = \langle a_1 b_0 \rangle = \langle a_0 b_1 \rangle &= \frac{1}{\sqrt{2}} \\ \langle a_1 b_1 \rangle &= -\frac{1}{\sqrt{2}}, \end{aligned} \tag{5.18}$$

so that $S = 2\sqrt{2} > 2$ and the CHSH inequality is violated. This example is paradigmatic in showing the power of Bell inequalities at detecting the nonlocal behaviour of quantum systems.

5.2 Device-Independent Multipartite Entanglement Certification

Entanglement certification in the multipartite case presents a much richer structure than the bipartite case. In the first instance, as discussed in section 1.1.2, there are several inequivalent notions of entanglement that one may wish to detect. Furthermore,

in the device independent outlook, one needs to account for the increasing number of different possible combinations of trusted and untrusted parties. We discuss some known approaches to the matter in the following sections.

5.2.1 Genuine multipartite entanglement witnesses

The detection of genuine multipartite entanglement can be thought of as the problem of disproving the existence of a biseparable decomposition for the composite state [34]. For arbitrary mixed states, however, there is still no general result that allows to prove or disprove the existence of a biseparable decomposition [186]. A typical approach to overcome this problem is that of testing for decompositions of PPT states, or in other words checking whether the state is described by a PPT-mixture (sec. 1.1.2) or not, the set of which may be fully characterised by means of semidefinite programming [72, 73]. It was in fact proven that the non-existence of such a decomposition for a mixed state ρ is equivalent to the existence of a witness $\mathcal{W}$ *detecting the entanglement* by virtue of the property $\mathrm{Tr}(\mathcal{W}\rho) < 0$. Such witness is called *fully-decomposable* and its structure is such that for every bipartition $M|\bar{M}$ of a subsystem M and its complement $\bar{M}$, the operator may be written as $W = P_M + Q_M^{\Gamma_M}$, where P_M and Q_M are positive operators [72, 73].

The following SDP, introduced in reference [72], returns a decomposable witness for a PPT-mixture, if it exists, and is a quantifier of genuine multipartite entanglement:

$$\begin{aligned} N_{\mathrm{GM}}(\rho) = -\min \mathrm{Tr}(\rho\mathcal{W}) & \\ \text{subject to}: \quad & \mathcal{W} = P_M + Q_M^{\Gamma_M}, \\ & 0 \leq P_M \leq \mathbb{1} \\ & 0 \leq Q_M \leq \mathbb{1} \quad \text{for all bipartitions } M. \end{aligned} \tag{5.19}$$

This measure quantifies the entanglement of states which are not PPT-mixtures, however it is unable to detect the entanglement of states which are PPT-mixtures but not biseparable.

5.2.2 Multipartite steering

In the multipartite steering scenario it is a hard task to make general statements for any number of parties, so we will focus here in describing the tripartite case, for it showcases the main departures from the bipartite description and the main additional features arising by adding parties to the scenario. The three parties are called Alice, Bob and Charlie and we will assume they each have their own individually addressable

subsystem, so the total Hilbert space is given by $\mathcal{H}_A \otimes \mathcal{H}_B \otimes \mathcal{H}_C$. We assume again for simplicity that they each have the same local dimension d.

In analogy with the bipartite case, the steering of the global quantum state may be thought of as entanglement certification in presence of a number of untrusted parties. As discussed in Chapter 1, however, the multipartite case presents two different notions of separability or entanglement. Let us briefly recall such notions. A tripartite quantum state is *fully-separable* if it can be written in the form

$$\rho^{\mathrm{FS}}_{ABC} = \int \mathrm{d}\lambda \mu(\lambda) \rho^A_\lambda \otimes \rho^B_\lambda \otimes \rho^C_\lambda. \tag{5.20}$$

A multipartite state which is not fully separable is called *multipartite entangled*. There are states, however, in which two subsystems are entangled, the global state may be written as a convex combination of states which are separable in one bipartition. The states in this class are called *bi-separable* and may be written as

$$\begin{aligned} &\rho^{\mathrm{BS}}_{ABC} = p_A \rho^{\mathrm{sep}}_{A|BC} + p_B \rho^{\mathrm{sep}}_{B|AC} + p_C \rho^{\mathrm{sep}}_{C|AB} = \\ &\int \mathrm{d}\lambda \mu(\lambda) \rho^A_\lambda \otimes \rho^{BC}_\lambda + \int \mathrm{d}\nu \mu(\nu) \rho^B_\nu \otimes \rho^{AC}_\nu + \int \mathrm{d}\omega \mu(\omega) \rho^C_\omega \otimes \rho^{AB}_\omega \end{aligned} \tag{5.21}$$

where $\rho^{\mathrm{sep}}_{X|YZ}$ is a state which is separable in the partition $X|YZ$. States which are not biseparable are called *genuinely multipartite entangled*. It is clear that states which are genuinely multipartite entangled are also multipartite entangled, but the converse is not always true. From the steering perspective, an additional possibility compared to the entanglement scenario is that of having two parties collaborating in steering the assemblage of the third, as opposed to the case when one party steers the assemblage of the other two. We may label the two scenarios by the number of parties whose local measurements are uncharacterized, calling them respectively *one untrusted party scenario* and *two untrusted parties scenario*.

One untrusted party

Let us now look at the structure of assemblages generated by fully separable and biseparable states in the case of one untrusted party, which we may call *one-to-two steering scenario*. Assuming Alice is performing measurements $\{M_{a|x}\}_{a,x}$ on a fully separable state, we have the assemblage

$$\sigma^{BC}_{a|x} = \mathrm{Tr}\big[(M_{a|x} \otimes \mathbb{1} \otimes \mathbb{1})\rho^{\mathrm{FS}}\big] = \int \mathrm{d}\mu(\lambda) p(a|x,\lambda) \rho^B_\lambda \otimes \rho^C_\lambda, \tag{5.22}$$

for Bob and Charlie, where $p(a|x,\lambda) = \mathrm{Tr}(M_{a|x}\rho^A_\lambda)$. The above is the structure of a multipartite LHS assemblage between Alice and the composite system Bob-Charlie. We refer to this as the *fully-separable case* (FS) of entanglement certification with one untrusted party.

The assemblages arising from measurements on bi-separable states are instead given by [35]

$$\sigma^{BC}_{a|x} = \mathrm{Tr}\big[(M_{a|x}\otimes \mathbb{1}\otimes\mathbb{1})\rho^{BS}\big] = \int \mathrm{d}\nu\mu(\nu)p(a|x,\nu)\rho^{BC}_\nu + \int \mathrm{d}\lambda\mu(\lambda)\rho^B_\lambda\otimes\sigma^C_{a|x,\lambda} + \int \mathrm{d}\omega\mu(\omega)\sigma^B_{a|x,\omega}\otimes\rho^C_\omega, \tag{5.23}$$

where $\sigma_{a|x,\lambda} = \mathrm{Tr}[(M_{a|x}\otimes\mathbb{1})\rho^{AC}_\lambda]$. Assemblages which do not admit a decomposition of the kind (5.23) are said to possess *genuine multipartite steering*. We refer to this as the *biseparable case* (BS) of entanglement certification with one untrusted party.

Two untrusted parties

In the scenario of Alice and Bob steering Charlie's assemblage (*two-to-one steering*) via local measurements on a fully separable state we have

$$\sigma^C_{ab|xy} = \mathrm{Tr}\big[(M_{a|x}\otimes M_{b|y}\otimes\mathbb{1})\rho^{\mathrm{FS}}\big] = \int \mathrm{d}\mu(\lambda)p(a|x,\lambda)p(b|y,\lambda)\rho^C_\lambda, \tag{5.24}$$

where $p(b|y,\lambda) = \mathrm{Tr}(M_{b|y}\rho^B_\lambda)$. For the biseparable case, instead, the assemblage takes on the form

$$\sigma^C_{ab|xy} = \mathrm{Tr}\big[(M_{a|x}\otimes M_{b|y}\otimes\mathbb{1})\rho^{\mathrm{BS}}\big] = \int \mathrm{d}\nu\mu(\nu)p(a|x,\nu)\sigma^C_{b|y,\nu} + \int \mathrm{d}\lambda\mu(\lambda)p(b|y,\lambda)\sigma^C_{a|x,\lambda} + \int \mathrm{d}\omega\mu(\omega)p(ab|xy,\omega)\rho^C_\omega. \tag{5.25}$$

The following section gives a brief overview of the computational techniques which allow the evaluation of multipartite and genuine multipartite steering. An approximate, yet arbitrarily accurate, version of the task may be solved numerically via semidefinite programming [35].

5.2.3 Multipartite steering testing with Semidefinite Programs

The task of testing the membership of assemblages to the classes defined in section 5.2.2 is not a trivial one. Since being able to certify steering requires being able to exclude that all possible decompositions of an assemblage may not be of the LHS kind,

this is a task that may only be carried out analytically in few cases [187]. Fortunately, an approximate but converging version of this problem may be cast as a semidefinite program (section 1.2).

In this section we will follow along the lines of the review paper [35] in order to show how the device-independent entanglement certification may be formulated as an instance of a semidefinite program (SDP).

SDPs for entanglement certification with one-to-two steering

The separability of a state may not be expressed as a set of linear equations, so it may not be enforced as a constraint in an SDP. However, one may restrict the set of optimization variables to a class of states that provides a good approximation of the separable set and may be fully characterised in an SDP. This is the case for states possessing a *k-symmetric PPT extension* (KSE) introduced in reference [188], which are defined as those states ρ_{AB} such that exists $\sigma_{AB_1\ldots B_k}$, invariant under permutations of the B_i subsystems, with the properties $\mathrm{Tr}_{B_2\ldots B_k}(\sigma_{AB_1\ldots B_k}) = \rho_{AB}$ and $(\sigma_{AB_1\ldots B_k})^{\Gamma_{B_1\ldots B_l}}$ for $l = 1, .., k$. In [188] it was shown that a state is separable if and only if it possesses a KSE for all k. Therefore, membership to the class of states having a KSE for fixed k is a necessary condition for separability and membership to the class may be tested for with SDP [35]. The case $k = 1$ simply tests for PPT-ness in the case of fully-separable states and for PPT-mixtures in the case of biseparable states.

In the case of fully-separable states it was noted that $p(a|x, \lambda)$ in equation (5.22) can be expressed as

$$p(a|x, \lambda) = \sum_{\nu=1}^{N_{\mathrm{det}}} p(\nu|\lambda) D(a|x, \nu), \tag{5.26}$$

where $D(a|x, \nu)$ are the elements of the set of deterministic behaviours. There are $N_{\mathrm{det}} = o_A^{m_A}$ possible elements of the latter, and they may be given by $D(a|x, \lambda) = \delta_{a\lambda(x)}$, where $\lambda : \{0, ..., m_A\} \to \{0, .., o_A\}$. Therefore, the structure of the assemblages in equation (5.22) with a multipartite LHS model may be written in the simpler form

$$\sigma_{a|x} = \sum_{\lambda=1}^{N_{\mathrm{det}}} D(a|x, \lambda) \rho_\lambda^B \otimes \rho_\lambda^C, \tag{5.27}$$

which significantly simplifies the expression of LHS assemblages, passing from one expressed in terms of an integral over unknown probability distributions to a finite sum of fixed deterministic behaviours.

A multipartite steering test in the one-sided device-independent scenario may be thus expressed as the SDP:

$$\begin{aligned} \text{given} \quad & \{\sigma^{BC}_{a|x}\}_{ax},\, k \\ \text{find} \quad & \{\sigma^{BC}_{\lambda}\}_{\lambda} \\ \text{s.t.} \quad & \sum_{\lambda} D(a|x,\lambda)\sigma^{BC}_{\lambda} = \sigma^{BC}_{a|x} \quad \forall a,x, \\ & \{\sigma^{BC}_{\lambda}\} \in \Sigma^{BC}_{k-\text{sym}}, \end{aligned} \tag{5.28}$$

where each member of the LHS model is tested for membership to the set $\Sigma^{BC}_{k-\text{sym}}$ of states possessing a k-symmetric extension, rather than the set of separable states. The test is inconclusive if the SDP admits a feasible solution, but certifies multipartite steering if it fails for a given k.

With analogous considerations, in [35] it was shown that for genuine multipartite steering testing instead we have the following more complicated expression for the semidefinite program:

$$\begin{aligned} \text{given} \quad & \{\sigma^{BC}_{a|x}\}_{ax},\, k \\ \text{find} \quad & \{\sigma^{BC}_{\mu}\}_{\mu},\, \{\pi^{BC}_{a|x}\}_{ax},\, \{\pi^{C}_{\nu}\}_{\nu},\, \{\gamma^{BC}_{a|x}\}_{ax},\, \{\gamma^{B}_{\lambda}\}_{\lambda} \\ \text{s.t.} \quad & \sum_{\mu} D(a|x,\mu)\sigma^{BC}_{\mu} + \pi^{BC}_{a|x} + \gamma^{BC}_{a|x} = \sigma^{BC}_{a|x} \quad \forall a,x, \\ & \text{tr}_B[\pi^{BC}_{a|x}] = \sum_{\nu} D(a|x,\nu)\pi^{C}_{\nu} \quad \forall a,x, \\ & \text{tr}_C[\gamma^{BC}_{a|x}] = \sum_{\lambda} D(a|x,\lambda)\gamma^{B}_{\lambda} \quad \forall a,x, \\ & \{\pi^{BC}_{a|x}\} \in \Sigma^{BC}_{KSE}, \quad \{\gamma^{BC}_{a|x}\} \in \Sigma^{BC}_{KSE}, \\ & \sigma^{BC}_{\mu} \geq 0 \quad \forall \mu, \quad \pi^{C}_{\nu} \geq 0 \quad \forall \nu, \quad \gamma^{B}_{\lambda} \geq 0 \quad \forall \lambda. \end{aligned} \tag{5.29}$$

Let us break down the above complicated expression in terms of the three addends of the right hand side of equation (5.23), following the logic in reference [189]. The first term has the same structure as equation (5.22) and is therefore enforced with an analogous expression to the one in SDP (5.28).

The second term is characterised by two main features. First, it does not demonstrate steering from A to B, therefore the partial trace over subsystem C leaves B an assemblage which is LHS with respect to A. This is enforced in SDP (5.29) in terms of the decomposition in terms of local deterministic behaviours $\text{tr}_B[\pi^{BC}_{a|x}] = \sum_{\nu} D(a|x,\nu)\pi^{C}_{\nu} \quad \forall a,x$. Second, it is separable, the condition of which may be replaced

in the SDP with the possession of a KSE $\{\pi^{BC}_{a|x}\} \in \Sigma^{BC}_{KSE}$. The third term is identical to the second with the interchange of the B and C subsystem labels.

If the test fails for a given k, the assemblage is proven to demonstrate genuine multipartite steering. Again, no conclusion can be drawn about the genuine multipartite steering of the assemblage if the test is successful.

SDPs for entanglement certification with two-to-one steering

The case of fully-separable states is relatively easy to implement, similarly to the one-untrusted-party case:

$$\begin{aligned} \text{given} \quad & \{\sigma^C_{ab|xy}\}_{abxy} \\ \text{find} \quad & \{\sigma^C_{\mu\nu}\}_{\mu\nu} \\ \text{s.t.} \quad & \sum_{\mu\nu} D(a|x,\mu)D(b|y,\nu)\sigma^C_{\mu\nu} = \sigma^C_{ab|xy} \quad \forall a,b,x,y, \\ & \sigma^C_{\mu\nu} \geq 0 \quad \forall \mu,\nu. \end{aligned} \tag{5.30}$$

Here, the locality condition for the behaviour in equation (5.24) is expressed in terms of the deterministic behaviours $D(a|x,\mu)$ and $D(b|y,\nu)$ for A and B respectively [189].

The formulation of the membership problem as an SDP in the biseparable case of two untrusted parties has additional requirements to take into account. The behaviours $p(ab|xy,\omega)$ in equation (5.25) need to be tested to belong to the set of possible *quantum correlations* (discussed in section 5.1.3). This is hard problem in general, which may be simplified to approximate solutions [190] relying on the identification of all the vertices of the no-signaling polytope (sec. 5.1.3). The number of such vertices increases very rapidly with the size of the system, for instance, there are 53856 vertices in the no-signaling polytope for three qubits [191]. Such large numbers of constraints pose a computational challenge for the solution of SDPs and will not be discussed here.

5.2.4 Multipartite Bell nonlocality

The main ideas in defining multipartite Bell nonlocality consist of a natural generalization of the bipartite case [49]. A no-signaling polytope in the tripartite case has defining property

$$\sum_c p(abc|xyz) = \sum_c p(abc|xyz') \quad \forall a,b,x,y,z,z', \tag{5.31}$$

and permutation of the other parties. Similarly, local correlations must have a decomposition

$$p(abc|xyz) = \int \mathrm{d}\lambda \mu(\lambda) p(a|x,\lambda) p(b|y,\lambda) p(c|z,\lambda). \tag{5.32}$$

Nonetheless, in the same sense as entanglement and steering, the nonlocality may be present between a subset of the parties or among all of them. The first such notion of genuine multipartite nonlocality was introduced by Svetlichny [192], wherein behaviours that can not be written in the form

$$\begin{aligned} p(abc|xyz) = &\int \mathrm{d}\lambda q(\lambda) p_\lambda(ab|xy) p_\lambda(c|z) \\ &+ \int \mathrm{d}\mu q(\mu) p_\mu(bc|yz) p_\mu(a|x) \\ &+ \int \mathrm{d}\nu q(\nu) p_\nu(ac|xz) p_\mu(b|y), \end{aligned} \tag{5.33}$$

with $\int \mathrm{d}\lambda q(\lambda) + \int \mathrm{d}\mu q(\mu) + \int \mathrm{d}\nu q(\nu) = 1$, are said to be *3-way nonlocal* or *genuinely tripartite nonlocal*. The convex combinations in the form of equation (5.33) describe states where only two parties share a nonlocal resource (or signal for every measurement run) and are called *2-way nonlocal* or *bilocal*. Refinements of condition (5.33) have been put forward to define stronger forms of nonlocality, a discussion of which may be found in [49].

Different Bell inequalities may test for the different definitions of locality in the multipartite scenario. Let us consider the specific case of three subsystems, each of which is subject to one of two measurements: A and A' for subsystem 1, B and B' for subsystem 2, C and C' for subsystem 3. We indicate by $E(ABC)$ the correlation function representing the expectation value of the product of the measurement outcomes of observables A, B and C. An inequality which holds for local behaviours of the form (5.32) is given by the *Mermin inequality* [193]

$$|M| = |E(ABC) + E(AB'C) + E(A'BC) - E(A'B'C')| \leq 2. \tag{5.34}$$

On the other hand, Svetlichny [192] derived an inequality for bilocal behaviours (5.33), testing for genuinely tripartite nonlocality. The inequality is given by

$$\begin{aligned} |S_V| = &|E(ABC) + E(ABC') + E(AB'C) + E(A'BC) \\ &- E(A'B'C') - E(A'B'C) - E(A'BC') - E(AB'C')| \leq 4, \end{aligned} \tag{5.35}$$

which is referred to as *Svetlichny inequality*. An example of the difference between a local and a bilocal behaviour is given by performing local measurements on a three-qubit

GHZ state

$$|\text{GHZ}\rangle = \frac{1}{2}(|000\rangle + |111\rangle). \tag{5.36}$$

It was shown in [194, 195] that for certain local measurements the Mermin inequality is violated, but not the Svetlichny inequality, meaning that the associated behaviours are bilocal albeit exhibiting nonlocality. Different measurement settings applied to the GHZ state, however, generate behaviours that may violate both the Mermin and Svetlichny inequality, and therefore exhibit genuine tripartite nonlocality. This is a useful reminder that nonlocality is not a property of quantum states, but probability distributions, and thus depends on how the probabilities are generated.

From the device-independent perspective, the violation of a Bell inequality by a given behaviour, which does not require any characterization of the measurement devices that generate it, certifies the notion of entanglement which the Bell inequality is derived for. In other words, if a Bell inequality holds for local behaviours, its violation certifies entanglement, if it holds for bilocal behaviours, a violation implies genuine multipartite entanglement.

In the following, we recall a tripartite Bell inequality for systems of 3 qutrits aimed at detection of tripartite (not genuine tripartite) nonlocality. We refer to it according to its original authors' nomenclature: *coincidence Bell inequality* [175].

Coincidence Bell Inequality

We review here a Bell inequality for the three qutrit case introduced in [175]. The inequality applies to a specific Bell scenario. Three parties with individually addressable subsystems, Alice, Bob and Charlie; have access to two measurement settings each with three possible outcomes. The outcomes $\{a_i, b_j, c_k\}_{i,j,k=1,2}$ are labelled according to the measurement setting 1 or 2 chosen by the respective party. An inequality which is valid only for tripartite local behaviours is given by:

$$\begin{aligned} S =& p(a_1 + b_1 + c_1 = 0) + p(a_1 + b_2 + c_1 = 1) + p(a_2 + b_1 + c_2 = 1) \\ &+ p(a_2 + b_2 + c_1 = 1) + p(a_2 + b_2 + c_2 = 0) - p(a_2 + b_1 + c_1 = 2) \\ &- p(a_1 + b_2 + c_1 = 2) - p(a_1 + b_1 + c_2 = 2) \leq 3, \end{aligned} \tag{5.37}$$

where

$$p(a_i + b_j + c_k = r) = \sum_{a,b=0,1,2} p(a_i = a, b_j = b, c_k = r - a - b) \tag{5.38}$$

and all equalities within the behaviours are to be intended as modulo three. The inequality was derived to probe the nonlocality of the state

$$|\mathrm{GHZ}\rangle = \frac{1}{\sqrt{3}}(|000\rangle + |111\rangle + |222\rangle), \tag{5.39}$$

which can be thought of as the generalization to the tripartite case of the maximally entangled two qutrit state, as well as of the three-qubit Greenberger–Horne–Zeilinger (GHZ) state

$$\frac{1}{\sqrt{2}}(|000\rangle + |111\rangle). \tag{5.40}$$

Acín et al. [175] show a violation of inequality (5.37) for a specific class of measurements, representing unbiased symmetric three-port beam splitters [196,197], where each subsystem represents a port of the beam splitter. Each party has access to a local measurement setting given by the phase shift applied to the state an the input end of each port. These measurements can be labelled by the choice of two phases characterising a three-component phase vector $\bar{\varphi} = (0, \phi, \phi')$, where ϕ and ϕ' represent the two measurement settings available to the three parties. The measurements are given by the unitary transformation $M(\bar{\varphi})$, whose matrix elements are given by

$$[M(\bar{\varphi})]_{jk} = \frac{1}{\sqrt{3}} \exp\Big\{\frac{2\pi i}{3}(j-1)(k-1)\Big\} e^{i\varphi_{(j-1)}}. \tag{5.41}$$

for all $j, k = 0, 1, 2$.

We will apply measurements (5.41) and inequality (5.37) to probe the nonlocality of the noisy totally antisymmetric tripartite state, which we introduce in the following section.

5.3 Totally Antisymmetric State

The totally antisymmetric state is an interesting multipartite quantum state for quantum information processing. It has been shown to have possible applications in QKD, quantum state sharing and state discrimination [198], as well as being a useful theoretical tool, for instance as a counterexample for monogamy relation conjectures [199].

The dimension of the antisymmetric subspace $\mathcal{A}$ (Section 2.3) for a system of N qudits is $\binom{d}{N}$ [93], meaning it has nontrivial support only if $d \geq N$. In particular, when $N = d$, $\mathcal{A}$ is one-dimensional and is spanned by the *totally antisymmetric* state

$$\left|\psi_{\mathcal{A}}^{(N)}\right\rangle = \frac{1}{N!} \sum_{\pi \in S_n} (-1)^{\mathrm{sgn}(\pi)} \left|\pi(i_1)\right\rangle \ldots \left|\pi(i_N)\right\rangle, \tag{5.42}$$

where the sum runs over all the permutations of the indices associated with the orthonormal basis $\{|i\rangle\}_{i=0}^{d-1}$ of $\mathcal{H} = \mathbb{C}^d$. Being the antisymmetric subspace one-dimensional, we may express the projector on the antisymmetric subspace as the density operator associated with the pure state $\left|\psi_{\mathcal{A}}^{(N)}\right\rangle$,

$$P_{\mathcal{A}}^{(N)} = \left|\psi_{\mathcal{A}}^{(N)}\right\rangle\!\left\langle\psi_{\mathcal{A}}^{(N)}\right|. \tag{5.43}$$

We may list some of the properties of $\left|\psi_{\mathcal{A}}^{(N)}\right\rangle$ [198]. Given $\left|\psi_{\mathcal{A}}^{(N)}\right\rangle$, for all single-subsystem unitary operators $U \in \mathcal{H}$ we have $U^{\otimes N}\left|\psi_{\mathcal{A}}^{(N)}\right\rangle = \left|\psi_{\mathcal{A}}^{(N)}\right\rangle$. Furthermore, it is the only pure state with this property [200, 201]. In addition to this, it is completely determined by its two-party reductions. Every two-party reduced density matrix of the totally antisymmetric state is proportional to $P_{\mathcal{A}}(N)$, the projection on the two-quNit antisymmetric subspace [201].

In this chapter we wish to determine the hierarchy of the quantum correlations for the tripartite totally antisymmetric state and its relationship to external noise. We will address the entanglement, steering and nonlocality properties, both in the bipartite and genuinely multipartite case and study the robustness of the state's applications when subject to white noise.

Our aim is to explore the multipartite quantum correlations for the totally antisymmetric state from a device-independent perspective. In particular, we are interested in the aspect of entanglement certification when a given number of parties is untrusted, investigating how much white noise may be added to the state before no entanglement may be detected. If all three parties are *trusted*, they may each be assumed to have full control on the measurements performed on their respective subsystem of the total quantum state. Given enough measurements, the parties may perform a full quantum tomography and reconstruct the total quantum state. The certification of entanglement in this case may be carried out by means of standard entanglement criteria and measures. Because there are different notions of entanglement in the multipartite setting, in the three-partite case, specifically, we are interested in confronting the fully-separable and biseparable case, the partitioning being symmetric owing to the target state's symmetry.

When one of the parties is untrusted we are in the one-sided device-independent scenario. Due to the symmetry of the system the steering properties are independent on which of the parties performs the measurements. Without loss of generality, we will consider only the case when Alice steers the Bob-Charlie composite subsystem. Furthermore, we will see that the steering assemblages $\sigma_{a|x}^{BC}$ generated by Alice's measurements

are independent (up to local unitary transformations) of the choice of measurement settings, however the number of measurements does affect the ability of Bob-Charlie to detect entanglement. In this scenario we will assume that Bob and Charlie have full control of their measurements and are capable of reconstructing the elements of their assemblage. The membership of the $\sigma_{a|x}^{BC}$ assemblages may be then assessed by means of semidefinite programs (SDPs) (as illustrated in section 5.2.2). In particular, there are two distinct SDPs which may be employed to test respectively the bipartite and genuinely multipartite entanglement of the global quantum state.

When two parties are untrusted, again due to symmetry we may only focus on the case when Alice and Bob steer Charlie's subsystem. We are in the two-sided device-independent scenario. It is Charlie alone in this case which has full control of his measurements and may reconstruct the elements of the assemblage $\sigma_{ab|xy}^{C}$ he is provided with as a result of Alice and Bob's measurement outcomes. Again, the membership of $\sigma_{ab|xy}^{C}$ may be assessed via SDPs. As discussed in section 5.2, the SDP assessing biseparability in the two-sided device-independent scenario implies some difficulties in individuating the correlations between Alice and Bob, so in this work we will focus on full separability.

Finally, when none of the parties are trusted we are in the situation of a multipartite Bell test. This is usually referred to as the totally device-independent scenario. None of the parties' local measurements are characterized, but we are simply provided with the behaviours $p(abc|xyz)$ and need to assess whether they may be described by a *deterministic local hidden variable model* (LHV) [49]. This may be done by putting forward a multipartite Bell inequality which is satisfied by all behaviours in the set of LHV correlations, but not by those outside of it. If the violation of such a Bell inequality may be established, we may certify the presence of entanglement in the system. There may be different Bell inequalities for certifying multipartite and genuinely multipartite entanglement.

From the perspective of device-independent entanglement certification, it is worth pointing out the inequivalence of entanglement, steering and nonlocality [177]. In particular, there are states which are entangled but do not exhibit steering and states which are steerable but show no nonlocality. For the purpose of device-independent entanglement certification thus, showing that an assemblage or a behaviour lacks a LHS or LHV model does not certify the separability of the global quantum state. Only when one finds a steerable assemblage, or violates a Bell inequality may one make conclusive statements about the presence of entanglement.

Another point worth stressing is that the entanglement certification may be considered as device-independent even if specific measurements are used to generate the

assemblages and behaviours. In fact, each assemblage (or behaviour) is the result of applying some measurements, but the (semi)device-independent analysis of the resulting assemblage (or behaviour) does not depend on the knowledge of that measurement.

Antisymmetric, GHZ and W states

Our main goal for this chapter is to investigate the quantum correlation hierarchy for the totally antisymmetric tripartite state,

$$|\psi_{\mathcal{A}}\rangle = \frac{1}{\sqrt{6}}\left(|012\rangle + |120\rangle + |201\rangle - |102\rangle - |021\rangle - |210\rangle\right). \tag{5.44}$$

We will confront the quantum correlations of the state (5.44) with that of the generalised GHZ state

$$|\psi_{\text{GHZ}}\rangle = \frac{1}{\sqrt{3}}(|000\rangle + |111\rangle + |222\rangle) \tag{5.45}$$

and the totally symmetric generalised W state

$$|\psi_{W}\rangle = \frac{1}{\sqrt{6}}\left(|012\rangle + |120\rangle + |201\rangle + |102\rangle + |021\rangle + |210\rangle\right), \tag{5.46}$$

which have already been studied in the literature [35, 72]. Specifically, we will address the robustness to white noise of the quantum correlations by studying the state

$$\rho_{\mathcal{A}} = (1-p)\,|\psi_x\rangle\langle\psi_x| + p\mathbb{1}/27, \tag{5.47}$$

where $|\psi_x\rangle$ is either the totally antisymmetric, GHZ or W state. We will indicate with p^* the maximum noise threshold within which the entanglement certification is possible with a given measurement scheme and compare values obtained for the antisymmetric state to the GHZ and W cases. Such resistance to noise parameter, which specifies the amount of white noise to be added to a quantum state so that its nonclassical correlations are lost, is regarded as a measure of the strength of quantum correlations [175, 202]. In the following sections we will refer to p^* as *noise robustness*.

5.4 Multipartite Entanglement Certification and Noise Robustness

In evaluating the entanglement of the noisy totally antisymmetric state we need to take into account the different notions of entanglement applicable to multipartite systems. In the device-independent outlook on entanglement certification the task corresponds

to the scenario when all three parties have full control of the measurement devices and are capable of fully reconstructing the density operator of the global quantum state, performing full quantum tomography.

Bipartite entanglement

As far as bipartite entanglement is concerned, due to the symmetry of the state (5.47) it is sufficient to consider the entanglement in the partition of any one subsystem versus the remaining two. The quantification of bipartite entanglement maybe carried out via established entanglement measures. We will apply entanglement negativity, since it applies to both pure and mixed states and presents a straightforward generalization to the multipartite case. Such is genuine multipartite negativity (introduced in Section 1.1.2), which is likewise based on the PPT criterion and may be evaluated by means of semidefinite programming [72, 73].

It is worth noting that the notions of entanglement and genuine entanglement coincide for pure states with fixed permutation symmetry, meaning that exchange-symmetric states which are entangled are also genuinely multipartite entangled [73]. Our case provides an example that the converse is not true for mixed states.

We begin by noting that the state (5.47) is of the form presented in (1.8), whose separability may be characterised analytically. We recall that the random robustness of the pure state $|\psi_x\rangle$ is given by

$$R(\psi_x \| \mathbb{1}/(d_1 d_2)) = d_1 d_2 \sqrt{\lambda_1 \lambda_2}, \tag{5.48}$$

where d_1, d_2 are the local dimensions of the subsystems and $\sqrt{\lambda_1}, \sqrt{\lambda_2}$ are the largest and second largest coefficients respectively in the Schmidt decomposition of $|\psi_x\rangle$. If we consider the entanglement between one subsystem of our tripartite state and the composite subsystem given by the other two, we have $d_1 = 3$ and $d_2 = 3^2 = 9$. For the three states (5.44), (5.45) and (5.46) under investigation, the Schmidt coefficients are $\{1/\sqrt{3}, 1/\sqrt{3}, 1/\sqrt{3}\}$, therefore we have $R(\psi_x \| \mathbb{1}/27) = 9$. The comparison between (5.47) and (1.8) allows to characterise as separable the states of class (5.47) with $p = s/(s+1) \geq p_E \equiv 9/10$. The totally antisymmetric, GHZ and W states therefore display a noise robustness of 90%.

We may check that the separability region coincides with that which satisfies the PPT criterion by calculating the entanglement negativity for the three states. We apply the SDP (1.25) for bipartite negativity to do so. The optimal value of the SDP for entanglement negativity as a function of the noise parameter p is reported in Figure 5.1 and is the same for the three states. It is worth noting that the PPT criterion for

these states detects entanglement up to the maximum noise threshold obtainable by looking at separability. This means that the class of states we are considering does not contain any PPT-entangled states for any bipartition.

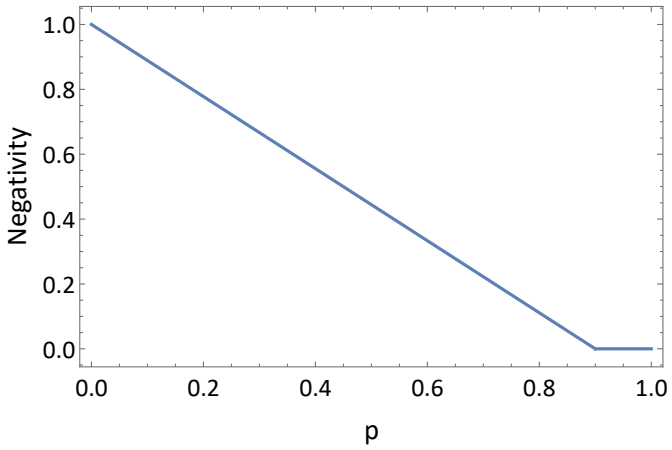

FIGURE 5.1: Bipartite negativity for the antisymmetric, GHZ and W state as a function of the noise parameter p.

The characterisation of biseparability may not be carried out in the terms we discussed separability for the class of states (5.47). We may however investigate in which regime the states are a PPT-mixture in terms of the decomposable witness discussed in section 1.1.2. We may apply the SDP in (5.19) in order to obtain a quantification of genuine multipartite negativity (GMN) for the totally antisymmetric state and compare it with that of the better known GHZ and W states. When the SDP returns a nonzero value for the GMN the state is certified to be genuinely multipartite entangled, however if it returns zero we may not exclude that the state is biseparable, only that it is not a PPT-mixture.

The noise threshold for detection of bi-PPT-ness does not coincide in the three states, yielding values of $p = p_{\mathcal{A}}^{\mathrm{GMN}} = 0.8$ for the antisymmetric state, $p = p_{\mathrm{GHZ}}^{\mathrm{GMN}} = 0.75$ for the GHZ state and $p = p_{W}^{\mathrm{GMN}} = 0.77$ for the W state. A comparison of the values of GMN for the three cases as a function of the noise parameter is reported in Figure 5.2. Albeit for a small amount, the totally antisymmetric state shows a better robustness to white noise for detection of genuine multipartite entanglement, a feature which may be crucial in attempts to push the limits of application of multipartite quantum states. It is interesting to notice that there is a difference between the noise threshold for bipartite and genuinely multipartite entanglement, that is in the range $[p_x^{\mathrm{GMN}}, p_E]$, for $x = \mathcal{A}, \mathrm{GHZ}, W$, where the state is entangled but can be written as a PPT-mixture. Furthermore, it is remarkable of these states to exhibit genuine entanglement between

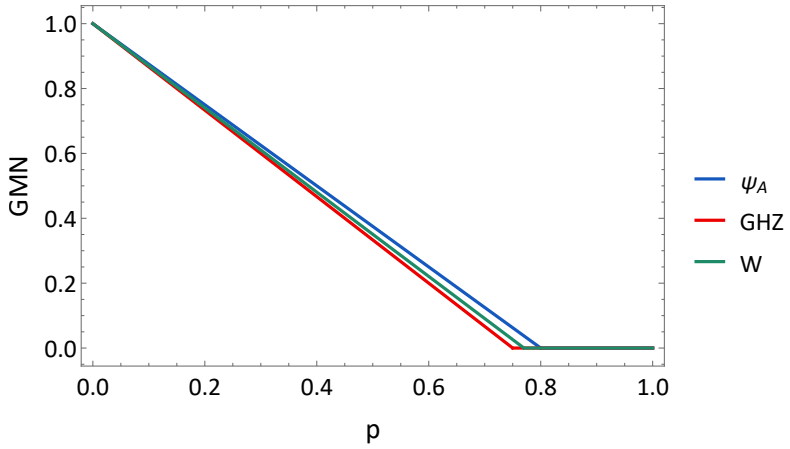

FIGURE 5.2: Genuine multipartite negativity for the antisymmetric, GHZ and W state as a function of the noise parameter p.

all three parties for noise levels up to 80%.

5.5 Multipartite Steering and Noise Robustness Lower Bounds

We wish to study the steering properties of the totally antisymmetric tripartite state with added white noise, as a function of the noise parameter p. In particular, we are interested in uncovering the maximum level of noise the system may endure and still exhibit steering.

To do so we need to choose the set of measurements $\{M_{a|x}\}_{a,x}$ acting on $\mathcal{H}_A$ which generate the assemblage. A typical choice is given by *mutually-unbiased bases* (MUBs), which are the optimal measurements for detecting correlations in many settings [35]. Two orthonormal bases $\{|a_i\rangle\}_{i=1}^d$ and $\{|b_j\rangle\}_{j=1}^d$ are called *mutually unbiased* if

$$|\langle a_i|b_j\rangle|^2 = \frac{1}{d} \quad \forall i,j = 1,...,d. \tag{5.49}$$

The name *mutually unbiased* is owed to the fact that when a measurement is carried out in a basis unbiased to that in which the state was prepared, its outcome is random.

5.5.1 Multipartite and genuinely multipartite steering of the noisy totally antisymmetric state with one untrusted party

In this section we compare the multipartite steering properties for the totally antisymmetric, generalised GHZ and W states.

We begin by studying the steering properties in the simple two-qubit case. The two-qubit totally antisymmetric noisy state is given by

$$\rho(p) = \frac{p}{4}\mathbb{1} + (1-p)\left|\phi^-\right\rangle\!\left\langle\phi^-\right|, \tag{5.50}$$

where $|\phi^-\rangle = (|0\rangle|1\rangle - |1\rangle|0\rangle)/\sqrt{2}$. In the two-qubit case, this is also the equivalent of a GHZ and W state. In [176] it is shown for this state to be steerable when $p < 1/2$. For two qubits steering and entanglement coincide, but this may be shown not to be the case for bipartite scenarios with larger local dimension [177].

In the tripartite case of three qutrits, we construct the assemblages based on measurements in mutually unbiased bases, of which there are four with a local Hilbert space of dimension 3. The assessment of the membership of the assemblages is carried out by means of the SDP in (5.28) for multipartite steering and of the SDP in (5.29) for genuine multipartite steering. As mentioned in Section 5.2.2 the formulation in terms of SDPs may only test for the membership of assemblages based on the *k-symmetric extension* criteria. However, we have shown in the analysis of multipartite entanglement in section 5.4, that the noise threshold for PPT-ness and separability coincides for the states under consideration. Therefore, increasing k does not bring about any differences in the membership of the steering assemblages. We will thus present the results of SDPs for the case $k = 1$.

The comparison of the steering noise robustness for the antisymmetric, GHZ and W states is reported in Figure 5.3 and Table 5.1. The first feature we may observe is that the noise thresholds in the fully-separable case are larger than those of the biseparable case for any number of measurements and for all states. The gap between the two values reflects the ability of the Bob-Charlie composite subsystem to exclude that their assemblage comes from a fully separable state but without certifying genuine multipartite entanglement. It is a showcase example of the difference in the multipartite scenario between entanglement and genuine entanglement certification. With our choices for Alice's measurements, entanglement may still be certified for noise levels up to 83%, in the case of the antisymmetric state, whereas genuine entanglement goes undetected at consistently lower levels of noise, with a maximum of 65%. Another interesting feature is that the biseparable threshold is strongly more affected by the number of measurements than the fully-separable case. Whereas in the fully separable case going from two to four measurements brings about a maximum increase of at most 5%, in the biseparable case the differences are more pronounced. Passing from two to four measurements, in fact, increases the noise threshold by about 20%. The antisymmetric state appears to be the choice with the overall best robustness to noise, albeit not by more than 10%, both in

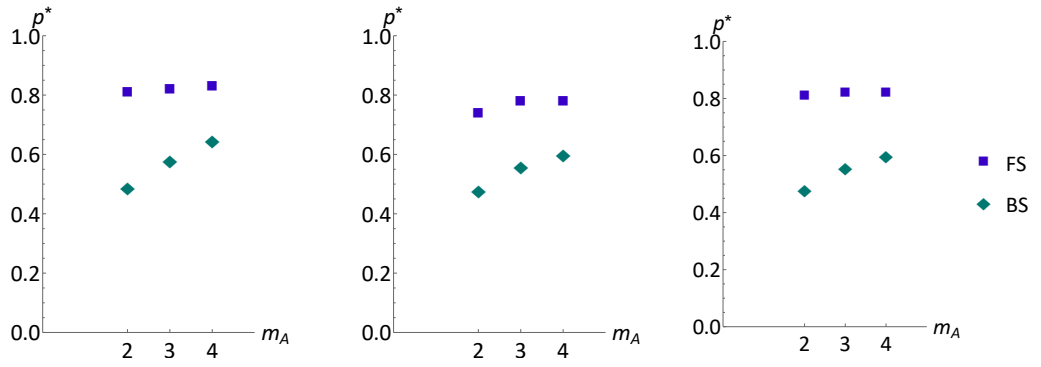

(A) $\psi_{\mathcal{A}}$ (B) GHZ (C) W

FIGURE 5.3: Noise robustness p^* of entanglement certification in the fully-separable (FS, squares) and biseparable (BS, diamonds) cases versus number of measurements by the untrusted party for the totally antisymmetric $\psi_{\mathcal{A}}$ (A), GHZ (B) and W (C) states. The number of measurements strongly affects the certification in the biseparable case, which exhibits overall weaker noise robustness compared to the fully-separable case. The antisymmetric state is the best performing in both schemes.

FS				BS			
m_A	$\psi_{\mathcal{A}}$	GHZ	W	m_A	$\psi_{\mathcal{A}}$	GHZ	W
2	0.81	0.74	0.81	2	0.49	0.48	0.48
3	0.82	0.78	0.82	3	0.58	0.56	0.56
4	0.83	0.78	0.82	4	0.65	0.6	0.6

TABLE 5.1: Tabulated values of noise robustness p^* for the totally antisymmetric $\psi_{\mathcal{A}}$, GHZ and W state for different number of measurements of the untrusted party m_A in the fully-separable (FS) and biseparable (BS) cases.

the fully-separable and bi-separable case. This confirms it as a very promising candidate for bringing about significant quantum enhancements in quantum information tasks.

Additional insight that we may infer from these results is the dramatic increase in noise robustness moving from the two qubit case to the three qutrit one. The noise threshold moves from 50% to 80% in the fully-separable case, and even the more delicate genuine multipartite entanglement outperforms to the two-qubit case with three or more measurements.

5.5.2 Multipartite steering of the noisy totally antisymmetric state with two untrusted parties

In the two-untrusted party scenario we will focus on the fully-separable case and compare the noise robustness for the different states and increasing number of measurement settings. The results obtained by applying the SDP in 5.30 are reported in Figure 5.4 and Table 5.2.

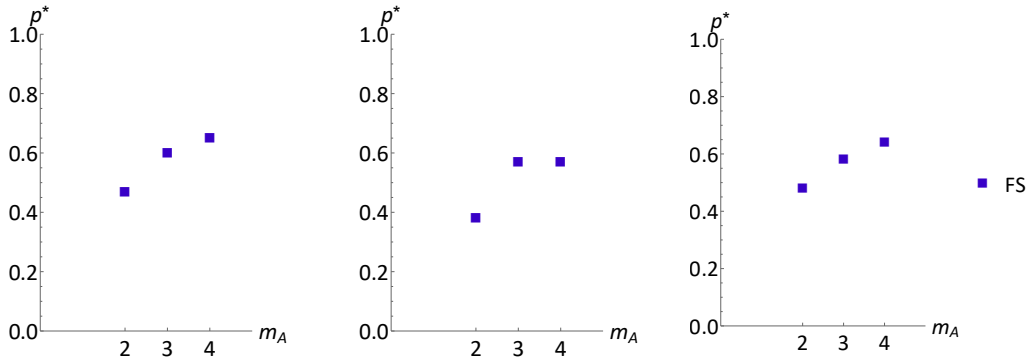

(A) $\psi_{\mathcal{A}}$ (B) GHZ (C) W

FIGURE 5.4: Noise robustness of entanglement certification in the fully-separable case versus number of measurements by the two untrusted parties for the totally antisymmetric, GHZ and W states. In this case the number of measurements strongly affects the certification in the fully-separable case too. Again, the antisymmetric state achieves the highest noise robustness.

m_A	$\psi_{\mathcal{A}}$	GHZ	W
2	0.47	0.38	0.48
3	0.6	0.57	0.58
4	0.65	0.57	0.64

TABLE 5.2: Tabulated values of noise robustness p^* for the totally antisymmetric $\psi_{\mathcal{A}}$, GHZ and W state for different number of measurements of the untrusted parties m_A in the fully-separable (FS) case with two untrusted parties.

The results show different trends for the three states. The totally antisymmetric and W states show an increase in noise robustness by increasing the number of measurements, whereas the GHZ state saturates at three measurements. The best noise robustness (0.65) is achieved by the antisymmetric state with four measurement settings, whereas the GHZ state does not improve the threshold of 0.57 passing between

three and four measurements. The W state has a similar trend to the totally antisymmetric one, albeit with slightly lower noise thresholds.

The noise robustness is consistently lower than the fully-separable case with one untrusted party, however, by comparing Tables 5.2 and 5.1, the calculated values for the fully-separable case with two untrusted parties bear a striking resemblance to the biseparable case with one untrusted party. Similar noise thresholds are required for the certification of genuine multipartite entanglement with one uncharacterised measurement device and bipartite entanglement with two uncharacterised measurements, for the exchange-symmetric states under consideration.

5.6 Bell Nonlocality of the Noisy Antisymmetric State

The certification of entanglement for the noisy totally antisymmetric state in the fully-device-independent scenario may be assessed by applying the coincidence Bell inequality reviewed in Section 5.2.4. Consider a state ρ for the three parties Alice, Bob and Charlie, each acting with the measurement operator $M(\bar{\varphi})$ defined in equation (5.41) on the single subsystem Hilbert space spanned by the ONB $\{|0\rangle, |1\rangle, |2\rangle\}$. The probability of obtaining an outcome (a, b, c) is given by

$$p(a,b,c) = \\ \mathrm{Tr}\Big[|abc\rangle\langle abc| \left(M(\bar{\varphi}_A) \otimes M(\bar{\varphi}_B) \otimes M(\bar{\varphi}_C)\right)\rho\big(M(\bar{\varphi}_A)^\dagger \otimes M(\bar{\varphi}_B)^\dagger \otimes M(\bar{\varphi}_C)^\dagger\big)\Big], \quad (5.51)$$

where $|abc\rangle\langle abc| = |a\rangle\langle a| \otimes |b\rangle\langle b| \otimes |c\rangle\langle c|$, for each of the measurement settings $\bar{\varphi}_A$, $\bar{\varphi}_B$ and $\bar{\varphi}_C$. The obtained behaviours may be inserted in the coincidence inequality (5.37) for the device-independent certification of the entanglement of ρ. We obtain a Bell parameter S in (5.37) which is dependent on the phase settings $\bar{\varphi}_j$, for $j = A, B, C$. In order to assess the best performance for entanglement certification for behaviours generated with the measurements (5.41), we maximise the Bell parameter S over all variables ϕ_j, ϕ'_j characterising $\bar{\varphi}_j$ for all $j = A, B, C$.

We extract two parameters for each of the states under analysis: the maximum noise threshold p^* within which the Bell inequality is violated and the maximum violation $S_{\max}$ of the inequality, i.e. the maximum value of the Bell parameter S. The calculated values for such parameters for the totally antisymmetric, GHZ and W state are reported in Table 5.3.

The three states have similar values for maximum Bell violation and noise robustness, the GHZ, with $S_{\max} = 4.33$ and $p^* = 0.4$ slightly outperforming the totally

	$\psi_{\mathcal{A}}$	GHZ	W
$S_{\max}$	4.28	4.33	4.28
p^*	0.39	0.4	0.39

TABLE 5.3: Maximum violation $S_{\max}$ and noise robustness p^* for the totally antisymmetric, GHZ and W state.

antisymmetric and W states, which instead return the same values at $S_{\max} = 4.28$ and $p^* = 0.39$.

5.7 Hierarchy of Quantum Correlations

Having investigated the entanglement certification for all numbers of untrusted parties we may now establish a hierarchy of quantum correlations, with focus on the robustness to white noise. Figure 5.5 reports the robustness to white noise as a function of number of untrusted parties in the fully separable and biseparable case, confronting the antisymmetric 5.5a, GHZ 5.5b and W 5.5c states. Certification of entanglement is possible for higher noise levels than genuine multipartite entanglement in all cases under investigation. The antisymmetric and W state provide a better robustness than the GHZ in the steering scenarios that we considered, applying a maximum number of 4 measurements in mutually unbiased bases. The GHZ state, however, is better performing in the nonlocality scenario, where it provides the best noise robustness and maximum violation of the coincidence Bell inequality with tritter measurements.

The bottom line is that states with permutation symmetry have an overall good robustness to noise for the task of entanglement certification. We investigate three notable examples of exchange symmetric states and compare the performance of the task for different device-independent scenarios and for different notions of multipartite entanglement.

Our work applies a device-independent entanglement certification approach to a class of states of interest to quantum information processing uncovering the structure of the quantum correlations available. We quantify and compare the noise robustness of entanglement certification tasks for different experimentally feasible setups providing benchmarks for the thresholds associated with each task. The results set bounds for the feasibility of the tasks and identify the best performing state among the totally antisymmetric, generalised GHZ and W states. In particular we find that the totally antisymmetric state, often less studied than the GHZ and W states, outperforms or is equivalent to the latter in certain scenarios.

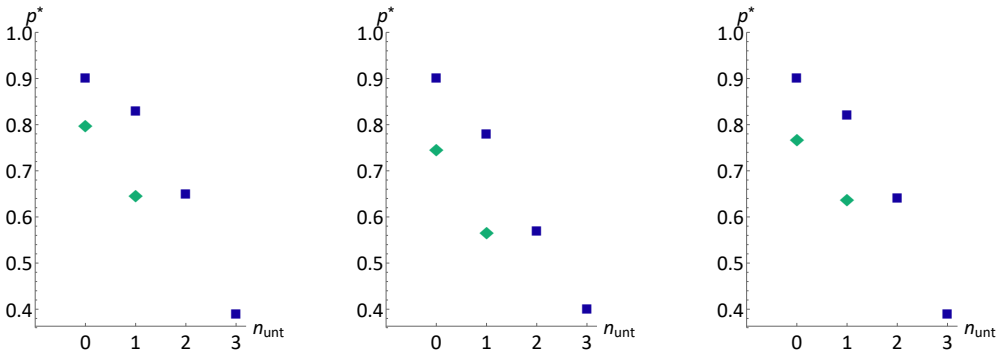

(A) $\psi_{\mathcal{A}}$ (B) GHZ (C) W

FIGURE 5.5: Noise robustness versus number of untrusted parties for the totally antisymmetric, GHZ and W states. The square markers represent the noise threshold in the fully separable case, and the diamond markers those of the biseparable case.

Finally, we characterise the intricate structure of quantum correlations in a multipartite setting and its interplay with the exchange symmetry of the states. States with a fixed permutation symmetry may be obtained as ground states of appropriately engineered hamiltonians and are proven to exhibit an overall high degree of quantum correlations, highlighting their potential usefulness in quantum information tasks.

Chapter 6

Conclusions and Outlook

The work presented in this thesis investigates the relationship between quantum correlations and symmetry within physical systems associated with the exchange of subsystems. In the first instance, a novel approach to entanglement quantification in systems of identical particles was put forward. The proposed entanglement measures, covering both systems of fermions and bosons, are based on a well-argued and established separability criteria for identical particles. Both measures may be thought of in terms of semidefinite programs, allowing for an efficient numerical evaluation and, in the simpler fermionic case, the detection of entanglement was proven to imply a violation of the separability criteria.

Our efforts provide new insight into the open debate involving identical particle entanglement. It overcomes the difficulties in quantifying entanglement resulting from the spin-statistics connection by effectively removing the symmetrization prescription which brings about misleading results for identical-particle entanglement quantification. Furthermore, it's formulation allows it to be directly applicable to the outcomes of measurements identical particle systems, an example of which we covered in Chapter 3.

The entanglement measure called antisymmetric negativity, covering the fermionic case, was shown to have a direct application for the estimation of entanglement based on real measurements. The data was given by joint measurements in position and momentum space of a system of two identical fermionic atoms in a double-well potential. An outstanding feature of our measure is the ability to provide a lower bound to the entanglement between the identical fermions even when the measurements are insufficient for full tomographic reconstruction of the system's state. In fact, its formulation as a semidefinite program, which is a minimization instance, provides an estimate of the minimum entanglement consistent with the experimental data and associated confidence intervals. Such approach can be applied to distinguishable particle systems as well, consisting of an attractive strategy for entanglement estimation without full quantum tomography.

Moreover, a comparison of antisymmetric negativity with standard mode and particle entanglement measures for a Hubbard dimer with RF coupling terms identifies two regimes: one where the quantification of the entanglement between the modes equals that of the entanglement between the identical particles, and one where this is not the case. Because of the connection between entanglement and quantum enhancements in many quantum information tasks, such a result is of significant conceptual and practical interest. Being able to identify what states appear to be strongly entangled in the mode partitioning, but have weak particle entanglement, allows to better select the best state for a given task. There is strong interest in establishing the connection between particle entanglement and sensitivity enhancements in atom interferometers [203], and our approach consists of a step in such direction.

Our identical particle entanglement measure, in fact, admits a straightforward generalization to the multipartite case, albeit the possibility of its evaluation is limited by the large number of degrees of freedom involved in the optimization underlying its formulation as a semidefinite program. Advances in the numerical algorithms for the solution of semidefinite programs may open up the applicability to multipartite systems of three or more particles, the latter being of great relevance to quantum computation and simulation.

By investigating the structure of the bipartite symmetric and antisymmetric subspaces, a novel class of bound entangled states was defined. Numerical prescriptions were put forward for the random or deterministic generation of states with bound entanglement in systems with any local dimension. Furthermore, a simple two-parameter class comprising Werner, Isotropic and bound entangled states was first introduced and its separability and PPT regions were outlined in detail. Simply parametrised families of bound entangled states versatile tools, being both useful in theorem proofs and in experimental scenarios, such as those involving superactivation.

Finally, the quantum correlation structure of a family of three-particle states with exchange symmetry was exposed. The primary objective was the study of the totally antisymmetric state, whose quantum correlation structure has not been studied in the literature, to the best of our knowledge. The entanglement, steering and nonlocality of the totally antisymmetric tripartite state were studied with the device-independent approach and compared to those of generalised GHZ and W states.

The usefulness of the three states for the task of device-independent entanglement certification, in the presence of different numbers of untrusted parties, was compared by finding the maximum noise threshold within which the task is successful, assuming commonly employed measurement configurations. The collection of results for zero, one, two and three untrusted parties enabled the outline of a hierarchy of quantum

correlations for the three states with exchange symmetry under investigation. Certain aspects of the quantum correlation structure of the totally antisymmetric state remain to be investigated, especially the device-independent certification of genuine tripartite entanglement with two and three untrusted parties. Furthermore, the noise thresholds we identify may in principle be improved by considering more general classes of measurements.

Appendix A

Discretized space model for momentum correlations fitting

The discretized-space simulation of the measured momentum correlations for a system of two identical fermions in a double-well (Chapter 4) is described in section 3.1.2. Here, we show how the simulated momentum correlations may be fitted to the measured data for quantum state estimation. We focus on the case of opposite spins to illustrate the method.

The first step is given by the diagonalization of $N^2 \times N^2$ Hamiltonian (3.11) and characterization of its lowest energy states

$$H_N^{(12)} |E_i(\bar{\mu})\rangle = E_i(\bar{\mu}) |E_i(\bar{\mu})\rangle \quad \forall i = 1, ..., N^2, \tag{A.1}$$

where the eigenvalues $E_i(\bar{\mu})$ and eigenvectors $|E_i(\bar{\mu})\rangle$ are functions of the model variables $V_{\max}$ (potential barrier), a (well separation) and g (interaction coupling constant) incorporated in the vector variable $\bar{\mu} = (V_{\max}, a, g)$. The experimental preparation of the system to simulate will determine a parametrization of the representation of the prepared state, to be fitted, alongside the parameters of the Hamiltonian, to the measured data. Let us call the model state $\rho_N(\bar{\omega})$, where $\bar{\omega}$ is the collection of parameters describing the $N^2 \times N^2$ state. In its discretized-space representation, $\rho_N(\bar{\omega})$ may be written as

$$\rho_N(\bar{\omega}) = \sum_{i,j=1}^{N^2} \lambda_{ij}(\bar{\nu}) |E_i(\bar{\mu})\rangle\langle E_j(\bar{\mu})| , \tag{A.2}$$

where the structure of the $\lambda_{ij}(\bar{\nu})$ coefficients is given by the state preparation and is determined by parameters $\bar{\nu}$.

We opt for a discretized momentum representation with the same number of *bins* as the position space, so that the momentum space is spanned by a basis $\{|\varphi_i\rangle\}_{i=1}^N$ which may be obtained by applying a unitary transformation matrix $U_N = e^{i\bar{p}^T \cdot \bar{x}}$,

where $\bar{p}$ and $\bar{x}$ are discretized momenta and positions, to the position basis vectors $\{|i\rangle\}_{i=1}^{N}$. The momentum representation of the state is therefore given by $\tilde{\rho}_N(\bar{\omega}) = (U_N \otimes U_N)\rho_N(\bar{\omega})(U_N^\dagger \otimes U_N^\dagger)$. The momentum correlations are thus represented as an $N \times N$ matrix with elements given by the expectation value

$$[G_N(\bar{\omega})]_{pq} = \mathrm{Tr}\Big[\big(|\varphi_p\rangle\langle\varphi_p| \otimes |\varphi_q\rangle\langle\varphi_q|\big)\tilde{\rho}_N(\bar{\omega})\Big], \quad \forall p, q = 1, .., N. \tag{A.3}$$

Provided the number of bins of the measured momentum correlations is large enough for the discretization to provide an accurate representation of the system, equation (A.3) may be directly compared to the measured momentum correlation matrix. If this is not the case, a finer sampling is required to generate the simulated correlations, which are then re-scaled and interpolated to match the measurement binning. It was verified that for values of $N > 70$ the sampling does not affect the accuracy of the representation with relative differences larger than 10^{-3}, which is within the experimental error margins.

A.1 Characterization of the Double-Well

As a first application of the discretized model we tackle the characterisation of the double-well potential. Typically, the interwell distance a is a known experimental design parameter, but the potential barrier V_{max} is not directly accessible. However, in the Fermi-Hubbard regime for non-interacting fermions, the relationship

$$J = \frac{1}{2}(E_2(\bar{\mu}) - E_1(\bar{\mu})), \tag{A.4}$$

between the experimentally measurable tunneling parameter J and the first energy gap $E_2(\bar{\mu}) - E_2(\bar{\mu})$ allows to constrain V_{max}. In fact, V_{max} is the only free parameter in the noninteracting case, assuming the well separation is known. We report in Figure A.1 the relationship between tunneling parameter and potential barrier (both measured in Hz in natural units where $\hbar = c = 1$) calculated with the discretized model. A measured value of $J = 269 \pm 50\,\mathrm{Hz}$ results in $V_{\mathrm{max}} = 2 \pm 0.3 \times 10^4\,\mathrm{Hz}$. Provided the potential preparation is the same throughout data acquisition in different interacting regimes, we may constrain the potential barrier parameter in the above indicated confidence interval, thus improving the fit performance.

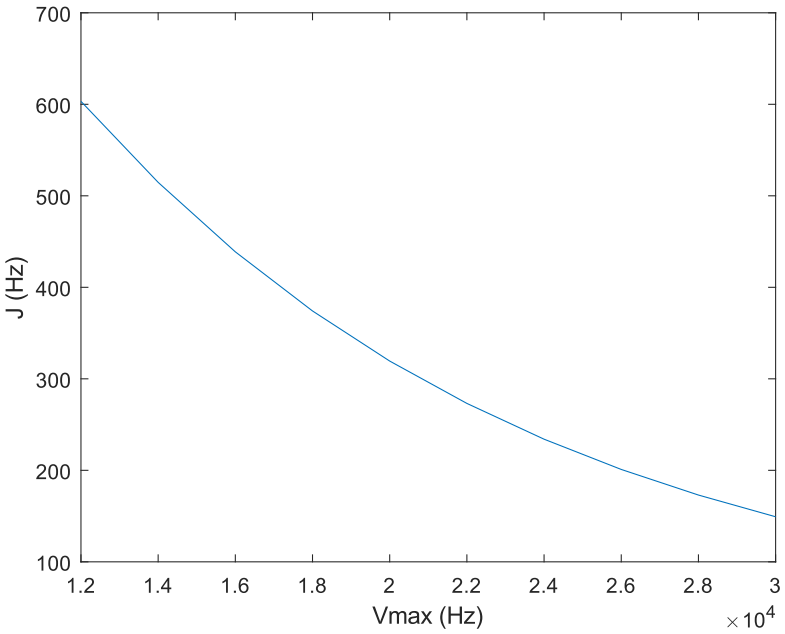

FIGURE A.1: Tunnel parameter $J = (E_2 - E_1)/2$ as a function of potential barrier $V_{\max}$ calculated with the discretized-space model in the non-interacting Fermi-Hubbard regime.

A.2 Fit Interface

The simulated momentum correlation matrix $G_N(\bar{\omega})$ may be compared element-wise to the measured correlation matrix with a nonlinear least-squares fit. In order to control which of the model parameters $\bar{\omega}$ are fixed or constrained by additional information about the system preparation, I developed a graphical user interface in Matlab's GUIDE environment for a simple initialization of the fit and visualization of the fit results and goodness of fit parameters, here taken to be the sum of squared errors (SSE) and root mean square error (RMSE), described in the Matlab documentation for the *fit* algorithm. An example of the interface for the non-interacting case fitted by a pure ground state is illustrated in Figure A.2. Because of the many features in the correlation data and the many parameters $\bar{\omega}$ of the state preparation (see section 3.5.1), the fit algorithm tends to converge to local minima, suggesting a more broad investigation of confidence intervals.

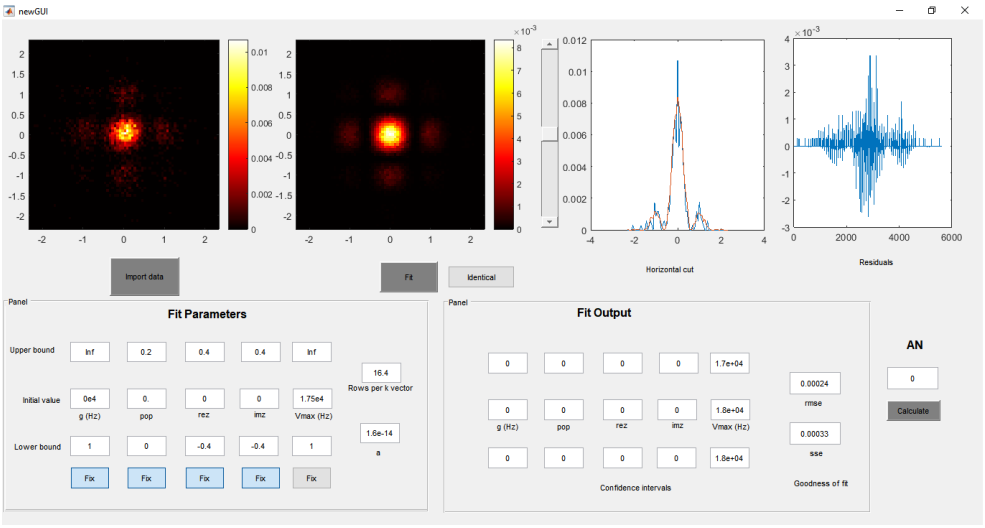

FIGURE A.2: Graphical user interface for the fitting of measured momentum correlations. Inputs are initial guesses for the parameters and corresponding bounds for the fit algorithm to span. Outputs are the parameter optimal values and confidence intervals, goodness of fit figures (RMSE and SSE) and the associated antisymmetric negativity of the optimal state. The graphics from left to right display the measured correlations, the simulated correlations, a horizontal cut comparing data with the simulation and the residuals between the linearised data and simulation. The data was provided by the Ultracold Quantum Gases Group at the Physikalisches Institut of Heidelberg University [147].

A.3 Confidence Intervals

In order to prevent the convergence in local minima for the fit algorithm from misrepresenting the data, we may investigate the parameter landscape associated with a goodness of fit indicator. In Figure A.3 we plot the RMSE between the $\rho_D^{(2)}$ model in section 3.5.1 and the momentum correlations reported in Figure 3.1b as a function of the excited state population p and the interaction constant g. By fixing a ratio $\Delta_R = R/R_{\min} = c_R$ between the RMSE R and the minimum calculated value $R_{\min}$, we identify a confidence surface around the optimal fit (or hypersurface if more parameters are assessed) and corresponding intervals for the fit parameters. These may be used to bound the corresponding values of estimated entanglement measure, by identifying the set of values corresponding to the parameter confidence intervals and computing the maximum and minimum of the set. An example is provided in Figure A.4 for the antisymmetric negativity associated with model states parametrized analogously to Figure A.3.

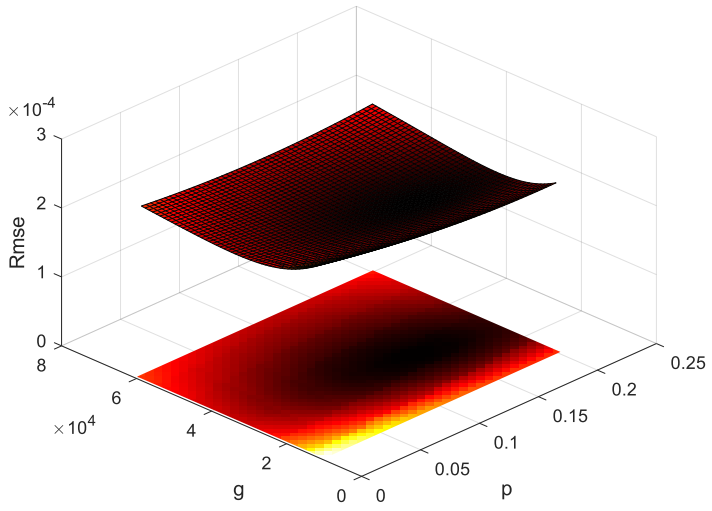

FIGURE A.3: Root mean square error (RMSE) as a function of excited state population p and the interaction constant g from the $\rho_D^{(2)}$ model (sec. 3.1).

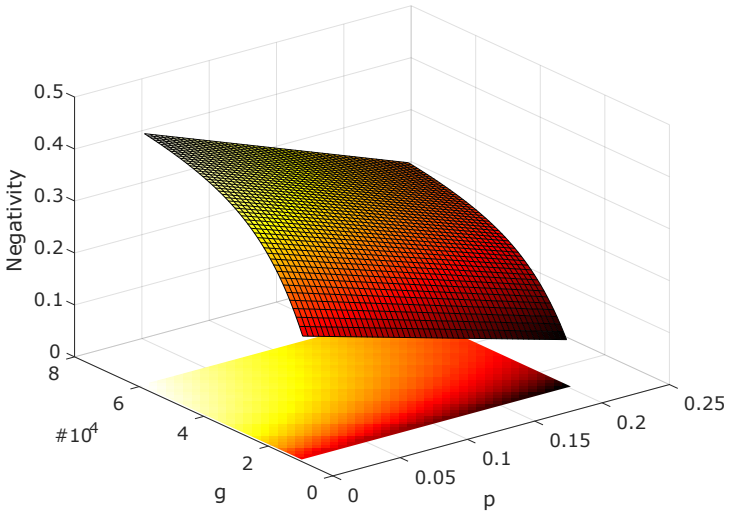

FIGURE A.4: Antisymmetric negativity $N_{\mathcal{A}}^{L}(\rho_{D\mathcal{A}}^{(2)})$ as a function of excited state population p and the interaction constant g from the $\rho_D^{(2)}$ model (sec. 3.1).

Bibliography

[1] M. F. Riedel, D. Binosi, R. Thew, and T. Calarco, "The european quantum technologies flagship programme," *Quantum Science and Technology*, vol. 2, no. 3, p. 030501, 2017.

[2] M. Riedel, M. Kovacs, P. Zoller, J. Mlynek, and T. Calarco, "Europe's quantum flagship initiative," *Quantum Science and Technology*, vol. 4, no. 2, p. 020501, 2019.

[3] L. Lydersen, C. Wiechers, C. Wittmann, D. Elser, J. Skaar, and V. Makarov, "Hacking commercial quantum cryptography systems by tailored bright illumination," *Nature Photonics*, vol. 4, no. 10, pp. 686–689, 2010.

[4] S. Danilin, A. V. Lebedev, A. Vepsäläinen, G. B. Lesovik, G. Blatter, and G. S. Paraoanu, "Quantum-enhanced magnetometry by phase estimation algorithms with a single artificial atom," *npj Quantum Information*, vol. 4, no. 1, 2018.

[5] D. Budker and M. Romalis, "Optical magnetometry," *Nature Physics*, vol. 3, no. 4, pp. 227–234, 2007.

[6] J. Rudolph, W. Herr, C. Grzeschik, T. Sternke, A. Grote, M. Popp, D. Becker, H. Müntinga, H. Ahlers, A. Peters, C. Lämmerzahl, K. Sengstock, N. Gaaloul, W. Ertmer, and E. M. Rasel, "A high-flux BEC source for mobile atom interferometers," *New Journal of Physics*, vol. 17, no. 6, p. 065001, 2015.

[7] V. Ménoret, P. Vermeulen, N. L. Moigne, S. Bonvalot, P. Bouyer, A. Landragin, and B. Desruelle, "Gravity measurements below 10-9 g with a transportable absolute quantum gravimeter," *Scientific Reports*, vol. 8, no. 1, 2018.

[8] P. Cheiney, L. Fouché, S. Templier, F. Napolitano, B. Battelier, P. Bouyer, and B. Barrett, "Navigation-compatible hybrid quantum accelerometer using a kalman filter," *Phys. Rev. Applied*, vol. 10, p. 034030, 2018.

[9] M. Genovese, "Real applications of quantum imaging," *Journal of Optics*, vol. 18, no. 7, p. 073002, 2016.

[10] G. M. Gibson, B. Sun, M. P. Edgar, D. B. Phillips, N. Hempler, G. T. Maker, G. P. A. Malcolm, and M. J. Padgett, "Real-time imaging of methane gas leaks using a single-pixel camera," *Optics Express*, vol. 25, no. 4, p. 2998, 2017.

[11] A. Lyons, G. C. Knee, E. Bolduc, T. Roger, J. Leach, E. M. Gauger, and D. Faccio, "Attosecond-resolution hong-ou-mandel interferometry," *Science Advances*, vol. 4, no. 5, p. eaap9416, 2018.

[12] A. D. King, J. Carrasquilla, J. Raymond, I. Ozfidan, E. Andriyash, A. Berkley, M. Reis, T. Lanting, R. Harris, F. Altomare, K. Boothby, P. I. Bunyk, C. Enderud, A. Fréchette, E. Hoskinson, N. Ladizinsky, T. Oh, G. Poulin-Lamarre, C. Rich, Y. Sato, A. Y. Smirnov, L. J. Swenson, M. H. Volkmann, J. Whittaker, J. Yao, E. Ladizinsky, M. W. Johnson, J. Hilton, and M. H. Amin, "Observation of topological phenomena in a programmable lattice of 1, 800 qubits," *Nature*, vol. 560, no. 7719, pp. 456–460, 2018.

[13] S. Boixo, S. Isakov, V. Smelyanskiy, R. Babbush, N. Ding, Z. Jiang, M. J. Bremner, J. Martinis, and H. Neven, "Characterizing quantum supremacy in near-term devices," *Nature Physics*, vol. 14, p. 595–600, 2018.

[14] B. K. Behera, S. Seth, A. Das, and P. K. Panigrahi, "Demonstration of entanglement purification and swapping protocol to design quantum repeater in IBM quantum computer," *Quantum Information Processing*, vol. 18, no. 4, 2019.

[15] I. M. Georgescu, S. Ashhab, and F. Nori, "Quantum simulation," *Rev. Mod. Phys.*, vol. 86, pp. 153–185, 2014.

[16] A. Steane, "Quantum computing," *Reports on Progress in Physics*, vol. 61, no. 2, pp. 117–173, 1998.

[17] J. P. Dowling and G. J. Milburn, "Quantum technology: the second quantum revolution," *Philosophical Transactions of the Royal Society of London. Series A: Mathematical, Physical and Engineering Sciences*, vol. 361, no. 1809, pp. 1655–1674, 2003.

[18] R. F. Streater and A. S. Wightman, *PCT, spin and statistics, and all that*. Princeton University Press, 2016.

[19] M. A. Nielsen and I. L. Chuang, *Quantum Computation and Quantum Information*. Cambridge University Press, 2009.

[20] L. Marinatto and T. Weber, "Teleportation with indistinguishable particles," *Physics Letters A*, vol. 287, no. 1-2, pp. 1–6, 2001.

[21] G. Ghirardi and L. Marinatto, "Entanglement and properties," *Fortschritte der Physik: Progress of Physics*, vol. 51, no. 4-5, pp. 379–387, 2003.

[22] U. Marzolino, "Entanglement in dissipative dynamics of identical particles," *EPL (Europhysics Letters)*, vol. 104, no. 4, p. 40004, 2013.

[23] U. Marzolino and A. Buchleitner, "Performances and robustness of quantum teleportation with identical particles," *Proc. R. Soc. A*, vol. 472, no. 2185, p. 20150621, 2016.

[24] J. Schliemann, J. I. Cirac, M. Kuś, M. Lewenstein, and D. Loss, "Quantum correlations in two-fermion systems," *Phys. Rev. A*, vol. 64, p. 022303, 2001.

[25] H. M. Wiseman and J. A. Vaccaro, "Entanglement of indistinguishable particles shared between two parties," *Phys. Rev. Lett.*, vol. 91, p. 097902, 2003.

[26] R. Lo Franco, "Quantum entanglement of identical particles by standard information-theoretic notions," *Sci. Rep.*, vol. 6, p. 20603, 2016.

[27] F. Benatti, R. Floreanini, and U. Marzolino, "Sub-shot-noise quantum metrology with entangled identical particles," *Annals of Physics*, vol. 325, no. 4, pp. 924–935, 2010.

[28] R. Paškauskas and L. You, "Quantum correlations in two-boson wave functions," *Physical Review A*, vol. 64, no. 4, p. 042310, 2001.

[29] P. Zanardi, "Quantum entanglement in fermionic lattices," *Phys. Rev. A*, vol. 65, p. 042101, 2002.

[30] A. Plastino, D. Manzano, and J. Dehesa, "Separability criteria and entanglement measures for pure states of n identical fermions," *EPL (Europhysics Letters)*, vol. 86, no. 2, p. 20005, 2009.

[31] A. Reusch, J. Sperling, and W. Vogel, "Entanglement witnesses for indistinguishable particles," *Physical Review A*, vol. 91, no. 4, p. 042324, 2015.

[32] J. Watrous, *The Theory of Quantum Information*. Cambridge University Press, 2018.

[33] S. Boyd and L. Vandenberghe, *Convex Optimization*. Cambridge University Press, 2004.

[34] O. Gühne and G. Tóth, "Entanglement detection," *Physics Reports*, vol. 474, no. 1-6, pp. 1–75, 2009.

[35] D. Cavalcanti and P. Skrzypczyk, "Quantum steering: a review with focus on semidefinite programming," *Reports on Progress in Physics*, vol. 80, no. 2, p. 024001, 2016.

[36] H. Barnum, M. Saks, and M. Szegedy, "Quantum query complexity and semidefinite programming," in *18th IEEE Annual Conference on Computational Complexity, 2003. Proceedings.*, IEEE Comput. Soc.

[37] J. Sikora and A. Varvitsiotis, "Linear conic formulations for two-party correlations and values of nonlocal games," *Mathematical Programming*, vol. 162, no. 1-2, pp. 431–463, 2016.

[38] C. V. Kraus, M. Lewenstein, and J. I. Cirac, "Ground states of fermionic lattice hamiltonians with permutation symmetry," *Physical Review A*, vol. 88, no. 2, 2013.

[39] D. Baguette, F. Damanet, O. Giraud, and J. Martin, "Anticoherence of spin states with point-group symmetries," *Physical Review A*, vol. 92, no. 5, 2015.

[40] C. Wu, Y. Wang, C. Guo, Y. Ouyang, G. Wang, and X.-L. Feng, "Initializing a permutation-invariant quantum error-correction code," *Physical Review A*, vol. 99, no. 1, 2019.

[41] J. Kempe, D. Bacon, D. A. Lidar, and K. B. Whaley, "Theory of decoherence-free fault-tolerant universal quantum computation," *Physical Review A*, vol. 63, no. 4, 2001.

[42] G. Tóth and O. Gühne, "Entanglement and permutational symmetry," *Phys. Rev. Lett.*, vol. 102, p. 170503, 2009.

[43] M. Horodecki, P. Horodecki, and R. Horodecki, "Mixed-state entanglement and distillation: Is there a "bound" entanglement in nature?," *Physical Review Letters*, vol. 80, no. 24, pp. 5239–5242, 1998.

[44] T. Moroder, O. Gittsovich, M. Huber, and O. Gühne, "Steering bound entangled states: A counterexample to the stronger peres conjecture," *Phys. Rev. Lett.*, vol. 113, p. 050404, 2014.

[45] T. Vértesi and N. Brunner, "Disproving the peres conjecture by showing bell nonlocality from bound entanglement," *Nature Communications*, vol. 5, no. 1, 2014.

[46] P. G. Kwiat, "Experimental verification of decoherence-free subspaces," *Science*, vol. 290, no. 5491, pp. 498–501, 2000.

[47] J. F. Poyatos, J. I. Cirac, and P. Zoller, "Quantum reservoir engineering with laser cooled trapped ions," *Phys. Rev. Lett.*, vol. 77, pp. 4728–4731, 1996.

[48] V. Scarani, *The device-independent outlook on quantum physics*. Acta physica Slovaca, Inst. of Physics, Slovak Acad. of Sciences, 2012.

[49] N. Brunner, D. Cavalcanti, S. Pironio, V. Scarani, and S. Wehner, "Bell nonlocality," *Reviews of Modern Physics*, vol. 86, no. 2, pp. 419–478, 2014.

[50] E. Sindici and M. Piani, "Simple class of bound entangled states based on the properties of the antisymmetric subspace," *Phys. Rev. A*, vol. 97, p. 032319, 2018.

[51] J. J. Sakurai and E. D. Commins, "Modern quantum mechanics, revised edition," *American Journal of Physics*, vol. 63, no. 1, pp. 93–95, 1995.

[52] C. Cohen-Tannoudji, B. Diu, and F. Laloe, *Quantum Mechanics*. No. v. 1 in Quantum Mechanics, Wiley, 1991.

[53] A. Messiah, *Quantum Mechanics*. No. v. 1-2 in Dover books on physics, Dover Publications, 1999.

[54] D. J. Griffiths and D. F. Schroeter, *Introduction to Quantum Mechanics*. Cambridge University Press, 2018.

[55] B. M. Terhal and P. Horodecki, "Schmidt number for density matrices," *Phys. Rev. A*, vol. 61, p. 040301, 2000.

[56] R. Horodecki, P. Horodecki, M. Horodecki, and K. Horodecki, "Quantum entanglement," *Reviews of Modern Physics*, vol. 81, no. 2, pp. 865–942, 2009.

[57] A. Peres, "Separability criterion for density matrices," *Phys. Rev. Lett.*, vol. 77, pp. 1413–1415, 1996.

[58] M. Horodecki, P. Horodecki, and R. Horodecki, "Separability of mixed states: necessary and sufficient conditions," *Physics Letters A*, vol. 223, no. 1-2, pp. 1–8, 1996.

[59] G. Vidal and R. Tarrach, "Robustness of entanglement," *Phys. Rev. A*, vol. 59, pp. 141–155, 1999.

[60] P. W. Shor, "Polynomial-time algorithms for prime factorization and discrete logarithms on a quantum computer," *SIAM Review*, vol. 41, no. 2, pp. 303–332, 1999.

[61] R. Jozsa and N. Linden, "On the role of entanglement in quantum-computational speed-up," *Proceedings of the Royal Society of London. Series A: Mathematical, Physical and Engineering Sciences*, vol. 459, no. 2036, pp. 2011–2032, 2003.

[62] J. S. Bell, "On the einstein podolsky rosen paradox," *Physics Physique Fizika*, vol. 1, pp. 195–200, 1964.

[63] J. F. Clauser, M. A. Horne, A. Shimony, and R. A. Holt, "Proposed experiment to test local hidden-variable theories," *Phys. Rev. Lett.*, vol. 23, pp. 880–884, 1969.

[64] D. Salart, A. Baas, C. Branciard, N. Gisin, and H. Zbinden, "Testing the speed of 'spooky action at a distance'," *Nature*, vol. 454, no. 7206, pp. 861–864, 2008.

[65] I. Marcikic, H. de Riedmatten, W. Tittel, H. Zbinden, M. Legré, and N. Gisin, "Distribution of time-bin entangled qubits over 50 km of optical fiber," *Phys. Rev. Lett.*, vol. 93, p. 180502, 2004.

[66] M. B. Plbnio and S. Virmani, "An introduction to entanglement measures," *Quantum Info. Comput.*, vol. 7, no. 1, pp. 1–51, 2007.

[67] C. H. Bennett, D. P. DiVincenzo, C. A. Fuchs, T. Mor, E. Rains, P. W. Shor, J. A. Smolin, and W. K. Wootters, "Quantum nonlocality without entanglement," *Phys. Rev. A*, vol. 59, pp. 1070–1091, 1999.

[68] C. H. Bennett, H. J. Bernstein, S. Popescu, and B. Schumacher, "Concentrating partial entanglement by local operations," *Phys. Rev. A*, vol. 53, pp. 2046–2052, 1996.

[69] I. Bengtsson and K. Zyczkowski, *Geometry of Quantum States.* Cambridge University Press, 2006.

[70] C. E. Shannon, "Communication theory of secrecy systems," *Bell System Technical Journal*, vol. 28, no. 4, pp. 656–715, 1949.

[71] R. Horodecki, P. Horodecki, M. Horodecki, and K. Horodecki, "Quantum entanglement," *Rev. Mod. Phys.*, vol. 81, pp. 865–942, 2009.

[72] B. Jungnitsch, T. Moroder, and O. Gühne, "Taming multiparticle entanglement," *Physical Review Letters*, vol. 106, no. 19, 2011.

[73] M. Hofmann, T. Moroder, and O. Gühne, "Analytical characterization of the genuine multiparticle negativity," *Journal of Physics A: Mathematical and Theoretical*, vol. 47, no. 15, p. 155301, 2014.

[74] C. Eltschka and J. Siewert, "Quantifying entanglement resources," *Journal of Physics A: Mathematical and Theoretical*, vol. 47, no. 42, p. 424005, 2014.

[75] L. Vandenberghe and S. Boyd, "Semidefinite programming," *SIAM Review*, vol. 38, no. 1, pp. 49–95, 1996.

[76] I. CVX Research, "CVX: Matlab software for disciplined convex programming, version 2.0." http://cvxr.com/cvx, Aug. 2012.

[77] N. Killoran, M. Cramer, and M. Plenio, "Extracting entanglement from identical particles," *Physical Review Letters*, vol. 112, no. 15, 2014.

[78] A. Caulton, "Discerning "indistinguishable" quantum systems," *Philosophy of Science*, vol. 80, no. 1, pp. 49–72, 2013.

[79] A. Caulton, "Is mereology empirical? composition for fermions," *T. Bigaj and C. Wüthrich*, pp. 293–322, 2015.

[80] A. Caulton, "Physical entanglement in permutation-invariant quantum mechanics," *arXiv preprint arXiv:1409.0246*, 2014.

[81] A. Caulton, *Issues of identity and individuality in quantum mechanics*. PhD thesis, University of Cambridge, 2015.

[82] P. Debye, "Der wahrscheinlichkeitsbegriff in der theorie der strahlung," *Annalen der Physik*, vol. 338, no. 16, pp. 1427–1434, 1910.

[83] Bose, "Plancks gesetz und lichtquantenhypothese," *Zeitschrift für Physik*, vol. 26, no. 1, pp. 178–181, 1924.

[84] W. Pauli, "Über den einfluß der geschwindigkeitsabhängigkeit der elektronenmasse auf den zeemaneffekt," *Zeitschrift für Physik*, vol. 31, no. 1, pp. 373–385, 1925.

[85] W. Pauli, "The connection between spin and statistics," *Phys. Rev.*, vol. 58, pp. 716–722, 1940.

[86] R. C. Hilborn and C. L. Yuca, "Identical particles in quantum mechanics revisited," *The British journal for the philosophy of science*, vol. 53, no. 3, pp. 355–389, 2002.

[87] S. D. Bartlett and H. M. Wiseman, "Entanglement constrained by superselection rules," *Physical Review Letters*, vol. 91, no. 9, 2003.

[88] R. H. Stolt and J. R. Taylor, "Correspondence between the first- and second-quantized theories of paraparticles," *Nuclear Physics B*, vol. 19, no. 1, pp. 1–19, 1970.

[89] A. Einstein, B. Podolsky, and N. Rosen, "Can quantum-mechanical description of physical reality be considered complete?," *Phys. Rev.*, vol. 47, pp. 777–780, 1935.

[90] G. Ghirardi and L. Marinatto, "Criteria for the entanglement of composite systems with identical particles," *Fortschritte der Physik*, vol. 52, no. 11-12, pp. 1045–1051, 2004.

[91] G. Ghirardi, L. Marinatto, and T. Weber *Journal of Statistical Physics*, vol. 108, no. 1/2, pp. 49–122, 2002.

[92] M. M. Wilde, *Quantum Information Theory.* Cambridge University Press, 2013.

[93] R. Bhatia, *Matrix Analysis.* Springer New York, 1997.

[94] A. Peres, ed., *Quantum Theory: Concepts and Methods.* Springer Netherlands, 2002.

[95] B. J. Dalton, J. Goold, B. M. Garraway, and M. D. Reid, "Quantum entanglement for systems of identical bosons: I. general features," *Physica Scripta*, vol. 92, no. 2, p. 023004, 2017.

[96] B. J. Dalton, J. Goold, B. M. Garraway, and M. D. Reid, "Quantum entanglement for systems of identical bosons: II. spin squeezing and other entanglement tests," *Physica Scripta*, vol. 92, no. 2, p. 023005, 2017.

[97] N. Schuch, F. Verstraete, and J. I. Cirac, "Quantum entanglement theory in the presence of superselection rules," *Phys. Rev. A*, vol. 70, p. 042310, 2004.

[98] F. Benatti, R. Floreanini, and U. Marzolino, "Bipartite entanglement in systems of identical particles: The partial transposition criterion," *Annals of Physics*, vol. 327, no. 5, pp. 1304 – 1319, 2012.

[99] F. Benatti, R. Floreanini, and U. Marzolino, "Entanglement and squeezing with identical particles: ultracold atom quantum metrology," *Journal of Physics B: Atomic, Molecular and Optical Physics*, vol. 44, no. 9, p. 091001, 2011.

[100] F. Benatti, R. Floreanini, and U. Marzolino, "Bipartite entanglement in systems of identical particles: The partial transposition criterion," *Annals of Physics*, vol. 327, no. 5, pp. 1304–1319, 2012.

[101] F. Benatti, R. Floreanini, and U. Marzolino, "Entanglement in fermion systems and quantum metrology," *Phys. Rev. A*, vol. 89, p. 032326, 2014.

[102] F. Benatti, R. Floreanini, and U. Marzolino, "Entanglement robustness and geometry in systems of identical particles," *Phys. Rev. A*, vol. 85, p. 042329, 2012.

[103] F. Benatti, R. Floreanini, F. Franchini, and U. Marzolino, "Remarks on entanglement and identical particles," *Open Systems & Information Dynamics*, vol. 24, no. 03, p. 1740004, 2017.

[104] A. P. Balachandran, T. R. Govindarajan, A. R. de Queiroz, and A. F. Reyes-Lega, "Entanglement and particle identity: A unifying approach," *Phys. Rev. Lett.*, vol. 110, p. 080503, 2013.

[105] H. Barnum, E. Knill, G. Ortiz, R. Somma, and L. Viola, "A subsystem-independent generalization of entanglement," *Phys. Rev. Lett.*, vol. 92, p. 107902, 2004.

[106] H. Barnum, G. Ortiz, R. Somma, and L. Viola, "A generalization of entanglement to convex operational theories: Entanglement relative to a subspace of observables," *International Journal of Theoretical Physics*, vol. 44, no. 12, pp. 2127–2145, 2005.

[107] F. D. Cunden, S. Di Martino, P. Facchi, and G. Florio, "Spatial separation and entanglement of identical particles," *International Journal of Quantum Information*, vol. 12, no. 02, p. 1461001, 2014.

[108] L. Heaney, J. Anders, D. Kaszlikowski, and V. Vedral, "Spatial entanglement from off-diagonal long-range order in a bose-einstein condensate," *Physical Review A*, vol. 76, no. 5, 2007.

[109] K. Eckert, J. Schliemann, D. Bruß, and M. Lewenstein, "Quantum correlations in systems of indistinguishable particles," *Annals of Physics*, vol. 299, no. 1, pp. 88–127, 2002.

[110] J. Schliemann, D. Loss, and A. H. MacDonald, "Double-occupancy errors, adiabaticity, and entanglement of spin qubits in quantum dots," *Phys. Rev. B*, vol. 63, p. 085311, 2001.

[111] Y. S. Li, B. Zeng, X. S. Liu, and G. L. Long, "Entanglement in a two-identical-particle system," *Phys. Rev. A*, vol. 64, p. 054302, 2001.

[112] R. L. Franco and G. Compagno, "Quantum entanglement of identical particles by standard information-theoretic notions," *Scientific Reports*, vol. 6, no. 1, 2016.

[113] D. Braun, G. Adesso, F. Benatti, R. Floreanini, U. Marzolino, M. W. Mitchell, and S. Pirandola, "Quantum-enhanced measurements without entanglement," *Rev. Mod. Phys.*, vol. 90, p. 035006, 2018.

[114] M. C. Tichy, F. Mintert, and A. Buchleitner, "Essential entanglement for atomic and molecular physics," *Journal of Physics B: Atomic, Molecular and Optical Physics*, vol. 44, no. 19, p. 192001, 2011.

[115] M. Tichy, F. de Melo, M. Kuś, F. Mintert, and A. Buchleitner, "Entanglement of identical particles and the detection process," *Fortschritte der Physik*, vol. 61, no. 2-3, pp. 225–237, 2012.

[116] M. Tichy, *Entanglement and interference of identical particles*. PhD thesis, 2011.

[117] R. F. Werner, "Quantum states with einstein-podolsky-rosen correlations admitting a hidden-variable model," *Phys. Rev. A*, vol. 40, pp. 4277–4281, 1989.

[118] C. H. Bennett, G. Brassard, S. Popescu, B. Schumacher, J. A. Smolin, and W. K. Wootters, "Purification of noisy entanglement and faithful teleportation via noisy channels," *Phys. Rev. Lett.*, vol. 76, pp. 722–725, 1996.

[119] E. M. Rains, "A semidefinite program for distillable entanglement," *IEEE Transactions on Information Theory*, vol. 47, no. 7, pp. 2921–2933, 2001.

[120] M. A. Nielsen, "Conditions for a class of entanglement transformations," *Physical Review Letters*, vol. 83, pp. 436–439, July 1999.

[121] T. Eggeling and R. F. Werner, "Separability properties of tripartite states with $u \bigotimes u \bigotimes u$ symmetry," *Phys. Rev. A*, vol. 63, p. 042111, 2001.

[122] J. Quintanilla and C. Hooley, "The strong-correlations puzzle," *Physics World*, vol. 22, no. 6, pp. 32–37, 2009.

[123] J. Cardy and E. Tonni, "Entanglement hamiltonians in two-dimensional conformal field theory," *Journal of Statistical Mechanics: Theory and Experiment*, vol. 2016, no. 12, p. 123103, 2016.

[124] U. Schneider, *Interacting Fermionic Atoms in Optical Lattices - A Quantum simulator for Condensed Matter Physics*. PhD thesis, 2010.

[125] R. P. Feynman, "Simulating physics with computers," *International Journal of Theoretical Physics*, vol. 21, no. 6, pp. 467–488, 1982.

[126] H. J. Metcalf and P. van der Straten, *Laser Cooling and Trapping*. Springer New York, 1999.

[127] W. Ketterle and N. V. Druten, "Evaporative cooling of trapped atoms," in *Advances In Atomic, Molecular, and Optical Physics*, pp. 181–236, Elsevier, 1996.

[128] M. H. Anderson, J. R. Ensher, M. R. Matthews, C. E. Wieman, and E. A. Cornell, "Observation of bose-einstein condensation in a dilute atomic vapor," *Science*, vol. 269, no. 5221, pp. 198–201, 1995.

[129] C. C. Bradley, C. A. Sackett, J. J. Tollett, and R. G. Hulet, "Evidence of bose-einstein condensation in an atomic gas with attractive interactions," *Phys. Rev. Lett.*, vol. 75, pp. 1687–1690, 1995.

[130] C. J. Pethick and H. Smith, *Bose–Einstein Condensation in Dilute Gases*. Cambridge University Press, 2 ed., 2008.

[131] L. Pitaevskii and S. Stringari, *Bose-Einstein Condensation and Superfluidity*. Oxford University Press, 2016.

[132] A. J. Leggett, "What DO we know about high tc?," *Nature Physics*, vol. 2, no. 3, pp. 134–136, 2006.

[133] S. S. Hodgman, R. I. Khakimov, R. J. Lewis-Swan, A. G. Truscott, and K. V. Kheruntsyan, "Solving the quantum many-body problem via correlations measured with a momentum microscope," *Phys. Rev. Lett.*, vol. 118, p. 240402, 2017.

[134] B. Fang, A. Johnson, T. Roscilde, and I. Bouchoule, "Momentum-space correlations of a one-dimensional bose gas," *Phys. Rev. Lett.*, vol. 116, p. 050402, 2016.

[135] T. Schweigler, V. Kasper, S. Erne, I. Mazets, B. Rauer, F. Cataldini, T. Langen, T. Gasenzer, J. Berges, and J. Schmiedmayer, "Experimental characterization of

a quantum many-body system via higher-order correlations," *Nature*, vol. 545, no. 7654, pp. 323–326, 2017.

[136] R. H. Brown and R. Q. Twiss, "A test of a new type of stellar interferometer on sirius," *Nature*, vol. 178, no. 4541, pp. 1046–1048, 1956.

[137] C. Sabín, B. Peropadre, M. del Rey, and E. Martín-Martínez, "Extracting past-future vacuum correlations using circuit qed," *Phys. Rev. Lett.*, vol. 109, p. 033602, 2012.

[138] A. Pozas-Kerstjens and E. Martín-Martínez, "Harvesting correlations from the quantum vacuum," *Phys. Rev. D*, vol. 92, p. 064042, 2015.

[139] M. C. Tichy, F. Mintert, and A. Buchleitner, "Limits to multipartite entanglement generation with bosons and fermions," *Phys. Rev. A*, vol. 87, p. 022319, 2013.

[140] J. Audretsch, *Entangled Systems: New Directions in Quantum Physics*. Physics Textbook, Wiley-VCH, wiley-vch ed., 2007.

[141] S. Sachdev, "Quantum magnetism and criticality," *Nature Physics*, vol. 4, no. 3, pp. 173–185, 2008.

[142] A. M. Läuchli and C. Kollath, "Spreading of correlations and entanglement after a quench in the one-dimensional bose–hubbard model," *Journal of Statistical Mechanics: Theory and Experiment*, vol. 2008, no. 05, p. P05018, 2008.

[143] R. G. Unanyan, D. Muth, and M. Fleischhauer, "Short-time versus long-time dynamics of entanglement in quantum lattice models," *Phys. Rev. A*, vol. 81, p. 022119, 2010.

[144] C. Kollath, A. M. Läuchli, and E. Altman, "Quench dynamics and nonequilibrium phase diagram of the bose-hubbard model," *Phys. Rev. Lett.*, vol. 98, p. 180601, 2007.

[145] A. J. Daley, H. Pichler, J. Schachenmayer, and P. Zoller, "Measuring entanglement growth in quench dynamics of bosons in an optical lattice," *Phys. Rev. Lett.*, vol. 109, p. 020505, 2012.

[146] C. Chin, R. Grimm, P. Julienne, and E. Tiesinga, "Feshbach resonances in ultracold gases," *Rev. Mod. Phys.*, vol. 82, pp. 1225–1286, 2010.

[147] A. Bergschneider, V. M. Klinkhamer, J. H. Becher, R. Klemt, L. Palm, G. Zürn, S. Jochim, and P. M. Preiss, "Experimental characterization of two-particle entanglement through position and momentum correlations," *Nature Physics*, 2019.

[148] D. C. McKay and B. DeMarco, "Cooling in strongly correlated optical lattices: prospects and challenges," *Reports on Progress in Physics*, vol. 74, no. 5, p. 054401, 2011.

[149] H. Ott, "Single atom detection in ultracold quantum gases: a review of current progress," *Reports on Progress in Physics*, vol. 79, no. 5, p. 054401, 2016.

[150] P. A. Murthy, D. Kedar, T. Lompe, M. Neidig, M. G. Ries, A. N. Wenz, G. Zürn, and S. Jochim, "Matter-wave fourier optics with a strongly interacting two-dimensional fermi gas," *Phys. Rev. A*, vol. 90, p. 043611, 2014.

[151] A. Bergschneider, V. M. Klinkhamer, J. H. Becher, R. Klemt, G. Zürn, P. M. Preiss, and S. Jochim, "Spin-resolved single-atom imaging of ^{6}Li in free space," *Phys. Rev. A*, vol. 97, p. 063613, 2018.

[152] L. Amico, R. Fazio, A. Osterloh, and V. Vedral, "Entanglement in many-body systems," *Reviews of Modern Physics*, vol. 80, no. 2, pp. 517–576, 2008.

[153] R. Islam, R. Ma, P. M. Preiss, M. E. Tai, A. Lukin, M. Rispoli, and M. Greiner, "Measuring entanglement entropy in a quantum many-body system," *Nature*, vol. 528, no. 7580, pp. 77–83, 2015.

[154] J. Hubbard, "Electron correlations in narrow energy bands," *Proceedings of the Royal Society of London. Series A. Mathematical and Physical Sciences*, vol. 276, no. 1365, pp. 238–257, 1963.

[155] T. Esslinger, "Fermi-hubbard physics with atoms in an optical lattice," *Annu. Rev. Condens. Matter Phys.*, vol. 1, no. 1, pp. 129–152, 2010.

[156] T. B. Boykin and G. Klimeck, "The discretized schrödinger equation and simple models for semiconductor quantum wells," *European Journal of Physics*, vol. 25, no. 4, pp. 503–514, 2004.

[157] V. Jelic and F. Marsiglio, "The double-well potential in quantum mechanics: a simple, numerically exact formulation," *European Journal of Physics*, vol. 33, no. 6, pp. 1651–1666, 2012.

[158] A. Bergschneider, "Strong correlations in few-fermion systems," 2017.

[159] M. Paris and J. Řeháček, eds., *Quantum State Estimation*. Springer Berlin Heidelberg, 2004.

[160] K. Banaszek, M. Cramer, and D. Gross, "Focus on quantum tomography," *New Journal of Physics*, vol. 15, no. 12, p. 125020, 2013.

[161] C. H. Bennett, H. J. Bernstein, S. Popescu, and B. Schumacher, "Concentrating partial entanglement by local operations," *Phys. Rev. A*, vol. 53, pp. 2046–2052, 1996.

[162] G. Smith and J. Yard, "Quantum communication with zero-capacity channels," *Science*, vol. 321, no. 5897, pp. 1812–1815, 2008.

[163] P. Horodecki, "Separability criterion and inseparable mixed states with positive partial transposition," *Physics Letters A*, vol. 232, no. 5, pp. 333–339, 1997.

[164] C. H. Bennett, D. P. DiVincenzo, T. Mor, P. W. Shor, J. A. Smolin, and B. M. Terhal, "Unextendible product bases and bound entanglement," *Phys. Rev. Lett.*, vol. 82, pp. 5385–5388, 1999.

[165] F. Benatti, R. Floreanini, and M. Piani, "Non-decomposable quantum dynamical semigroups and bound entangled states," *Open Systems & Information Dynamics*, vol. 11, no. 04, pp. 325–338, 2004.

[166] M. Piani and C. E. Mora, "Class of positive-partial-transpose bound entangled states associated with almost any set of pure entangled states," *Phys. Rev. A*, vol. 75, p. 012305, 2007.

[167] G. Sentís, C. Eltschka, and J. Siewert, "Quantitative bound entanglement in two-qutrit states," *Phys. Rev. A*, vol. 94, p. 020302, 2016.

[168] J.-Å. Larsson, "Loopholes in bell inequality tests of local realism," *Journal of Physics A: Mathematical and Theoretical*, vol. 47, no. 42, p. 424003, 2014.

[169] J. L. Park, "The concept of transition in quantum mechanics," *Foundations of Physics*, vol. 1, no. 1, pp. 23–33, 1970.

[170] D. Mayers and A. Yao, "Self testing quantum apparatus," *Quantum Info. Comput.*, vol. 4, no. 4, pp. 273–286, 2004.

[171] S. Pironio, A. Acín, S. Massar, A. B. de la Giroday, D. N. Matsukevich, P. Maunz, S. Olmschenk, D. Hayes, L. Luo, T. A. Manning, and C. Monroe, "Random numbers certified by bell's theorem," *Nature*, vol. 464, no. 7291, pp. 1021–1024, 2010.

[172] A. K. Ekert, "Quantum cryptography based on bell's theorem," *Phys. Rev. Lett.*, vol. 67, pp. 661–663, 1991.

[173] J.-D. Bancal, N. Brunner, N. Gisin, and Y.-C. Liang, "Detecting genuine multipartite quantum nonlocality: A simple approach and generalization to arbitrary dimensions," *Physical Review Letters*, vol. 106, no. 2, 2011.

[174] J.-D. Bancal, *On the Device-Independent Approach to Quantum Physics*. Springer International Publishing, 2014.

[175] A. Acín, J. L. Chen, N. Gisin, D. Kaszlikowski, L. C. Kwek, C. H. Oh, and M. Żukowski, "Coincidence bell inequality for three three-dimensional systems," *Phys. Rev. Lett.*, vol. 92, p. 250404, 2004.

[176] H. M. Wiseman, S. J. Jones, and A. C. Doherty, "Steering, entanglement, nonlocality, and the einstein-podolsky-rosen paradox," *Physical Review Letters*, vol. 98, no. 14, 2007.

[177] M. T. Quintino, T. Vértesi, D. Cavalcanti, R. Augusiak, M. Demianowicz, A. Acín, and N. Brunner, "Inequivalence of entanglement, steering, and bell nonlocality for general measurements," *Physical Review A*, vol. 92, no. 3, 2015.

[178] R. Augusiak, M. Demianowicz, J. Tura, and A. Acín, "Entanglement and nonlocality are inequivalent for any number of parties," *Physical Review Letters*, vol. 115, no. 3, 2015.

[179] M. Lewenstein, B. Kraus, J. I. Cirac, and P. Horodecki, "Optimization of entanglement witnesses," *Phys. Rev. A*, vol. 62, p. 052310, 2000.

[180] B. M. Terhal, "Bell inequalities and the separability criterion," *Physics Letters A*, vol. 271, no. 5-6, pp. 319–326, 2000.

[181] D. Bruß, J. I. Cirac, P. Horodecki, F. Hulpke, B. Kraus, M. Lewenstein, and A. Sanpera, "Reflections upon separability and distillability," *Journal of Modern Optics*, vol. 49, no. 8, pp. 1399–1418, 2002.

[182] R. F. Werner, "Quantum states with einstein-podolsky-rosen correlations admitting a hidden-variable model," *Phys. Rev. A*, vol. 40, pp. 4277–4281, 1989.

[183] R. Augusiak, M. Demianowicz, and A. Acín, "Local hidden–variable models for entangled quantum states," *Journal of Physics A: Mathematical and Theoretical*, vol. 47, no. 42, p. 424002, 2014.

[184] S. Popescu and D. Rohrlich, "Quantum nonlocality as an axiom," *Foundations of Physics*, vol. 24, no. 3, pp. 379–385, 1994.

[185] S. Pironio, "Lifting bell inequalities," *Journal of Mathematical Physics*, vol. 46, no. 6, p. 062112, 2005.

[186] S. Gerke, W. Vogel, and J. Sperling, "Numerical construction of multipartite entanglement witnesses," *Phys. Rev. X*, vol. 8, p. 031047, 2018.

[187] R. U. et al., "Quantum steering," *arXiv*, vol. quant-ph:1903.06663, 2019.

[188] A. C. Doherty, P. A. Parrilo, and F. M. Spedalieri, "Distinguishing separable and entangled states," *Phys. Rev. Lett.*, vol. 88, p. 187904, 2002.

[189] A. Máttar, P. Skrzypczyk, G. H. Aguilar, R. V. Nery, P. H. S. Ribeiro, S. P. Walborn, and D. Cavalcanti, "Experimental multipartite entanglement and randomness certification of the w state in the quantum steering scenario," *Quantum Science and Technology*, vol. 2, no. 1, p. 015011, 2017.

[190] M. Navascués, S. Pironio, and A. Acín, "A convergent hierarchy of semidefinite programs characterizing the set of quantum correlations," *New Journal of Physics*, vol. 10, no. 7, p. 073013, 2008.

[191] S. Pironio, J.-D. Bancal, and V. Scarani, "Extremal correlations of the tripartite no-signaling polytope," *Journal of Physics A: Mathematical and Theoretical*, vol. 44, no. 6, p. 065303, 2011.

[192] G. Svetlichny, "Distinguishing three-body from two-body nonseparability by a bell-type inequality," *Phys. Rev. D*, vol. 35, pp. 3066–3069, 1987.

[193] N. D. Mermin, "Extreme quantum entanglement in a superposition of macroscopically distinct states," *Phys. Rev. Lett.*, vol. 65, pp. 1838–1840, 1990.

[194] J. L. Cereceda, "Three-particle entanglement versus three-particle nonlocality," *Phys. Rev. A*, vol. 66, p. 024102, 2002.

[195] P. Mitchell, S. Popescu, and D. Roberts, "Conditions for the confirmation of three-particle nonlocality," *Phys. Rev. A*, vol. 70, p. 060101, 2004.

[196] M. Żukowski, A. Zeilinger, and M. A. Horne, "Realizable higher-dimensional two-particle entanglements via multiport beam splitters," *Physical Review A*, vol. 55, no. 4, p. 2564, 1997.

[197] D. Kaszlikowski, D. Gosal, E. J. Ling, L. C. Kwek, M. Żukowski, and C. H. Oh, "Three-qutrit correlations violate local realism more strongly than those of three qubits," *Physical Review A*, vol. 66, no. 3, 2002.

[198] I. Jex, G. Alber, S. Barnett, and A. Delgado, "Antisymmetric multi-partite quantum states and their applications," *Fortschritte der Physik*, vol. 51, no. 23, pp. 172–178, 2003.

[199] Y.-C. Ou, "Violation of monogamy inequality for higher-dimensional objects," *Physical Review A*, vol. 75, no. 3, 2007.

[200] A. Cabello, "n-particle n-level singlet states: Some properties and applications," *Phys. Rev. Lett.*, vol. 89, p. 100402, 2002.

[201] T. Eggeling, *On multipartite symmetric states in Quantum Information Theory.* PhD thesis, 2003.

[202] D. Kaszlikowski, P. Gnaciński, M. Żukowski, W. Miklaszewski, and A. Zeilinger, "Violations of local realism by two entangled N-dimensional systems are stronger than for two qubits," *Phys. Rev. Lett.*, vol. 85, pp. 4418–4421, 2000.

[203] G. Tóth, "Multipartite entanglement and high-precision metrology," *Physical Review A*, vol. 85, no. 2, p. 022322, 2012.